

**Biochemical Characterization of an Intermediate  
Membrane Subfraction in Cyanobacteria Involved in an  
Assembly Network for Photosystem II**

DISSERTATION

zur Erlangung des Grades eines Doktors der Naturwissenschaften  
an der Fakultät für Biologie  
der Ludwig-Maximilians-Universität München

vorgelegt von

**Birgit Rengstl**

München, 06. November 2012

Erstgutachter: Prof. Jörg Nickelsen  
Zweitgutachter: Prof. Jürgen Soll  
Tag der mündlichen Prüfung: 12. Dezember 2012

**TABLE OF CONTENTS**

<b>TABLE OF CONTENTS</b> .....	<b>3</b>
<b>SUMMARY</b> .....	<b>4</b>
<b>ZUSAMMENFASSUNG</b> .....	<b>5</b>
<b>1 INTRODUCTION</b> .....	<b>7</b>
<b>1.1 OXYGENIC PHOTOSYNTHESIS – A PROCESS CONVERTING LIGHT ENERGY INTO CHEMICAL ENERGY</b> ...	<b>7</b>
<b>1.2 <i>SYNECHOCYSTIS</i> SP. PCC 6803 – A MODEL ORGANISM TO STUDY OXYGENIC PHOTOSYNTHESIS</b> .....	<b>8</b>
<b>1.3 PHOTOSYSTEM II</b> .....	<b>10</b>
<b>1.3.1 Assembly of cyanobacterial PSII</b> .....	<b>11</b>
1.3.1.1 Assembly of PSII protein subunits and involved factors.....	11
1.3.1.2 Incorporation of inorganic cofactors in the PSII water-oxidizing complex.....	15
1.3.1.3 Synthesis of chlorophyll and pigment insertion into PSII.....	17
<b>1.3.2 Subcellular localization of PSII assembly</b> .....	<b>20</b>
<b>2 AIMS OF THIS WORK</b> .....	<b>24</b>
<b>3 RESULTS</b> .....	<b>25</b>
<b>3.1 THE ARABIDOPSIS THYLAKOID PROTEIN PAM68 IS REQUIRED FOR EFFICIENT D1 BIOGENESIS AND PHOTOSYSTEM II ASSEMBLY</b> .....	<b>25</b>
<b>3.2 AN INTERMEDIATE MEMBRANE SUBFRACTION IN CYANOBACTERIA IS INVOLVED IN AN ASSEMBLY NETWORK FOR PHOTOSYSTEM II BIOGENESIS</b> .....	<b>49</b>
<b>3.3 INITIAL STEPS OF PHOTOSYSTEM II <i>DE NOVO</i> ASSEMBLY AND PRELOADING WITH MANGANESE TAKE PLACE IN BIOGENESIS CENTERS IN <i>SYNECHOCYSTIS</i></b> .....	<b>58</b>
<b>3.4 CHARACTERIZATION OF A <i>SYNECHOCYSTIS</i> DOUBLE MUTANT LACKING THE PHOTOSYSTEM II ASSEMBLY FACTORS YCF48 AND SLL0933</b> .....	<b>76</b>
<b>4 DISCUSSION</b> .....	<b>87</b>
<b>4.1 ROLE OF PRATA-DEFINED MEMBRANES IN ASSEMBLY OF PHOTOSYNTHETIC COMPLEXES</b> .....	<b>87</b>
4.1.1 Involvement of PDMs in assembly of PSII .....	87
4.1.2 Coordination of protein and pigment synthesis/assembly in PDMs.....	88
4.1.3 Involvement of PDMs in assembly of PSI.....	90
<b>4.2 MEDIATION OF PSII ASSEMBLY BY A NETWORK OF FACILITATING FACTORS</b> .....	<b>91</b>
<b>4.3 INVOLVEMENT OF PRATA IN MANGANESE DELIVERY TO PSII</b> .....	<b>94</b>
<b>4.4 SPATIAL ORGANIZATION OF INITIAL STEPS OF PSII ASSEMBLY</b> .....	<b>96</b>
<b>4.5 CORRELATION BETWEEN PSII <i>DE NOVO</i> ASSEMBLY AND PSII REPAIR</b> .....	<b>98</b>
<b>4.6 PSII ASSEMBLY IN CHLOROPLASTS OF GREEN ALGAE AND PLANTS</b> .....	<b>102</b>
<b>4.7 CONCLUSIONS AND FUTURE PROSPECTS</b> .....	<b>105</b>
<b>5 REFERENCES</b> .....	<b>107</b>
<b>6 APPENDIX</b> .....	<b>117</b>
<b>LIST OF ABBREVIATIONS</b> .....	<b>155</b>
<b>CURRICULUM VITAE</b> .....	<b>156</b>
<b>LIST OF PUBLICATIONS</b> .....	<b>157</b>
<b>DANKSAGUNG</b> .....	<b>158</b>
<b>EIDESSTATTLICHE ERKLÄRUNG</b> .....	<b>159</b>

## SUMMARY

Oxygenic photosynthesis converts light energy into chemical energy and is responsible for generating most of our atmosphere's oxygen and biomass on earth. Several multimeric protein complexes are involved in the underlying photosynthetic electron transfer chain with photosystem II (PSII) representing the initial complex mediating the extraction of electrons from water molecules, thus generating molecular oxygen as a by-product. During recent years, the structural details and components of the PSII complex, including its inorganic and organic cofactors, have been elucidated in great detail. However, little is known about the assembly pathway of this at least 20 protein subunits containing machinery. Previous work indicated that PSII assembly occurs in a step-wise fashion and requires a number of facilitating factors, which interact transiently with nascent PSII complexes. Earlier studies of one of those assembly factors, the cyanobacterial PrtA protein, suggested that PSII biogenesis does not only underlie a temporal order but is also organized at the spatial level, as PrtA was shown to mark a special intermediate membrane subfraction (PDMs), hypothesized to represent regions for initial steps of PSII biogenesis.

The presented work focused on a more detailed characterization of PDMs, clearly supporting their significance not only with regard to early protein assembly, but also concerning pigment synthesis and integration into the PSII precomplexes. The PDMs could further be allocated to special membrane regions, named biogenesis centers, at sites where thylakoid membranes converge to the plasma membrane, thus demonstrating the spatial organization of PSII assembly at the cellular level. Moreover, a novel function of PrtA in preloading of PSII with  $Mn^{2+}$  ions, necessary for construction of the water-splitting complex, was discovered. Concomitantly with progression of the assembly, the nascent PSII complexes are transported from the PDMs to the thylakoid membrane system, where Sll0933 – a novel PSII assembly factor identified in this thesis – mediates the integration of the PSII inner antenna proteins followed by completion of the assembly process. Additionally, it could be shown that many of the so far identified facilitating factors interact with each other and, thus, form a complex network for PSII assembly. Especially the interaction between the two assembly factors YCF48 and Sll0933 was characterized in more detail, revealing a successive mode of action with YCF48 operating upstream of Sll0933. Taken together, the presented results enable the development of an extended and elaborated model of PSII assembly, which is a concerted process connecting protein and cofactor synthesis/integration in a spatiotemporal manner, and thus contribute to a more profound understanding of photosynthesis itself.

## ZUSAMMENFASSUNG

Oxygene Photosynthese ermöglicht die Umwandlung von Lichtenergie in chemische Energie. Aufgrund der bei den zugrunde liegenden Reaktionen gebildeten molekularen Sauerstoffs ( $O_2$ ) stellt sie die Basis für den in unserer Atmosphäre angesammelten Sauerstoff und somit die Grundlage für höheres Leben auf der Erde dar. Die Entstehung von  $O_2$  wird von Photosystem II (PSII) katalysiert, dem ersten Komplex in einer Reihe von aus verschiedenen Bestandteilen aufgebauten Proteinkomplexen, welche den Transport von Elektronen zur Energiegewinnung vermitteln. Während die Zusammensetzung von PSII aus mindestens 20 verschiedenen Protein-Untereinheiten und diversen Co-Faktoren in den letzten Jahren weitgehend aufgeklärt wurde, ist das Wissen über den zugrunde liegenden Assemblierungsweg verhältnismäßig beschränkt. Bislang konnte gezeigt werden, dass dieser Ablauf schrittweise erfolgt und eine Reihe von Assemblierungsfaktoren erfordert. Dass die Biogenese von PSII neben ihrer zeitlichen Abfolge auch auf räumlicher Ebene organisiert ist, lässt sich aus früheren Studien eines dieser Assemblierungsfaktoren, des cyanobakteriellen PrtA-Proteins schließen, welches eine spezielle Membranfraktion (PDMs) kennzeichnet, die offenbar an den frühen Schritten der PSII-Biogenese beteiligt ist.

Die hier gezeigten Ergebnisse einer detaillierteren Charakterisierung der PDMs unterstreichen ihre Bedeutung nicht nur im Hinblick auf die frühen Schritte der Assemblierung der Proteinuntereinheiten, sondern auch auf die Pigmentsynthese und deren Integration in PSII-Präkomplexe. Strukturell konnten PDMs sogenannten Biogenesezentren zugeordnet werden, welche sich an Stellen, an denen sich die Thylakoidmembranen der Plasmamembran annähern, befinden. Somit wurde die Frage der subzellulären Lokalisierung der PSII-Assemblierung beantwortet. Außerdem konnte eine Beteiligung von PrtA an der Beladung von PSII mit  $Mn^{2+}$ -Ionen zum Aufbau des Wasserspaltungsapparates gezeigt werden. Weitere Daten weisen darauf hin, dass mit zunehmender Assemblierung ein Transport der entstehenden PSII-Komplexe von den PDMs in Richtung der Thylakoidmembranen erfolgt. Unmittelbar nach Erreichen der Thylakoide scheint dann Sll0933 – ein neuer, in dieser Arbeit identifizierter PSII-Assemblierungsfaktor – die Integration der inneren PSII-Antennenproteine zu vermitteln. Der Abschluss der Assemblierung von PSII erfolgt ebenfalls im Thylakoidmembransystem. Es wurden außerdem Hinweise dafür erhalten, dass sich viele der bisher identifizierten Assemblierungsfaktoren gegenseitig beeinflussen und somit ein komplexes Netzwerk bilden. Insbesondere die Interaktion zwischen den beiden Assemblierungsfaktoren YCF48 und Sll0933 wurde detaillierter untersucht und führte zur

Schlussfolgerung, dass YCF48 an früheren Schritten als Sll0933 an der PSII-Assemblierung beteiligt ist. Alles in allem handelt es sich bei der Assemblierung von PSII also um einen Prozess mit einer auf räumlicher und zeitlicher Ebene organisierten Verknüpfung von Integration der Protein-Untereinheiten und Synthese/Insertion der Co-Faktoren. Die dargestellten Ergebnisse ermöglichen eine deutliche Ausweitung des bisher geltenden Modells der PSII-Assemblierung und tragen somit zu einem besseren Gesamtverständnis des Prozesses der oxygenen Photosynthese an sich bei.

# 1 INTRODUCTION

## 1.1 OXYGENIC PHOTOSYNTHESIS – A PROCESS CONVERTING LIGHT ENERGY INTO CHEMICAL ENERGY

Oxygenic photosynthesis is one of the most important processes on earth, since it is responsible for generation of our atmosphere's oxygen. It is thought to have developed approximately 3.5 billion years ago and nowadays it is spread throughout plants, algae and cyanobacteria, which are therefore able to absorb and use sunlight as energy source (Nelson, 2011). For this purpose, these organisms developed a specialized intracellular membrane system – the so-called thylakoid membranes (TMs) – in which the four large photosynthetic protein complexes, photosystem II (PSII), the cytochrome  $b_6f$  complex (cyt $b_6f$ ), photosystem I (PSI) and the ATP synthase, are embedded (Figure 1; Nelson and Ben-Shem, 2004; Nelson and Yocum, 2006).

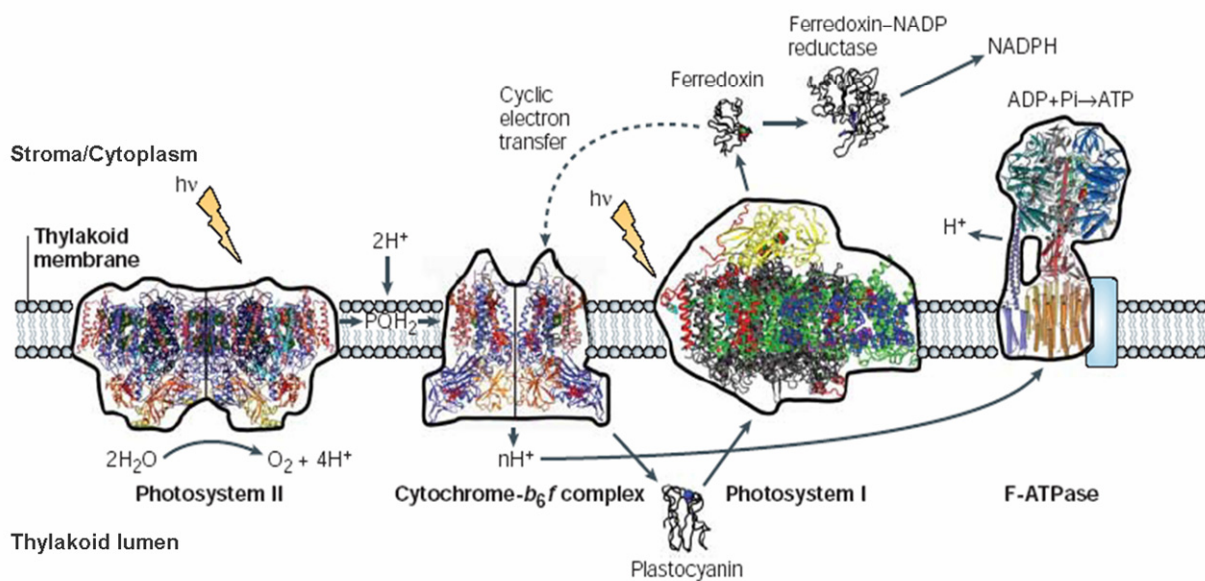


**Figure 1: The photosynthetic electron transfer chain.** Depicted are the contours and structures of the involved complexes and proteins as well as the electron and proton transfer pathways (arrows). Cyclic electron transport is indicated by a dashed line;  $h\nu$  denotes excitation of the photosystems by photons;  $PQH_2$ , plastoquinol (adapted from Nelson and Ben-Shem, 2004). For further details, see text.

In a first step, absorption of light energy by PSII antenna complexes and subsequent transfer to the PSII reaction center causes the release of an electron of the chlorophyll molecule P680. This electron is transferred to the initial electron acceptor pheophytin. The consequential electron gap at P680 is refilled by action of the manganese cluster ( $Mn_4Ca$  cluster) at the

lumenal side of PSII, providing electrons resulting from water oxidation. As a by-product in this water-splitting reaction, molecular oxygen ( $O_2$ ) is released. The electron of pheophytin is further transferred to a tightly bound plastoquinone A, which reduces a loosely bound plastoquinone B ( $Q_B$ ) molecule and therefore ends up in translocation of the electron to the stromal (in chloroplasts) or cytoplasmic (in cyanobacteria) side of the TM. Upon acceptance of two electrons,  $Q_B$  takes up two protons from the stroma/cytoplasm and moves as plastoquinol ( $PQH_2$ ) to its lumenal binding side at the  $cytb_6f$  complex (Kurusu et al., 2003; Stroebel et al., 2003). Protons are released to the thylakoid lumen and electrons cycle around the  $cytb_6f$  complex, mediating the pumping of two additional protons across the membrane before they are transferred to the soluble, lumenal, single electron carrier plastocyanin (or in some cases cytochrome  $c_6$ ), which then diffuses to PSI. In a second, light-dependent step, an electron of P700, a chlorophyll molecule located in the reaction center of PSI, is transferred via a number of cofactors to ferredoxin, localized at the stromal/cytoplasmic side of PSI (Saenger et al., 2002; Golbeck, 2003). Subsequently, the oxidized  $P700^+$  becomes re-reduced by plastocyanin or cytochrome  $c_6$ , respectively. Altogether, for generation of one molecule  $O_2$ , four electrons resulting from two water molecules have to be transferred to four ferredoxin molecules. Due to the involved transport of protons across the TM, an electrochemical gradient is built up, which powers the synthesis of ATP by the ATP synthase. The electrons of reduced ferredoxin can either be used for reduction of  $NADP^+$  to create NADPH catalyzed by the enzyme ferredoxin- $NADP^+$ -oxidoreductase (FNR), or they flow back to the  $cytb_6f$  complex to further contribute to the proton motive force and, therefore, to increase ATP production without generation of NADPH (called cyclic electron flow). This enables to balance ATP and NADPH levels according to the requirements (Lehtimäki et al., 2010).

In summary, the absorbed light energy is converted to reduction equivalents (reduced ferredoxin, NADPH) and ATP used to drive the organism's numerous catabolic reactions.

## **1.2 *SYNECHOCYSTIS* SP. PCC 6803 – A MODEL ORGANISM TO STUDY OXYGENIC PHOTOSYNTHESIS**

*Synechocystis* sp. PCC 6803 (hereafter *Synechocystis* 6803) is a unicellular representative of the group of cyanobacteria with spherical cells of  $\sim 1.5$ - $2 \mu\text{m}$  in diameter. As in other Gram-negative bacteria, the cell envelope consists of an outer membrane (OM) and a plasma membrane (PM), separated by the peptidoglycan containing periplasmic space (PP; Figure 2). The cell interior harbors the TMs, which are organized in concentric layers around the

periphery of the cell. Due to this internal membrane system and its therein located protein complexes – the photosynthetic protein machineries – cyanobacteria are able to perform oxygenic photosynthesis. According to the endosymbiotic theory, they are therefore considered to be closely related to the ancestor of nowadays chloroplasts found in plants and green algae (Deusch et al., 2008; Falcon et al., 2010). In contrast to chloroplasts, however, cyanobacterial thylakoids are not divided into grana stacks and stroma thylakoids, but they also develop a highly connected network formed by multiple membrane layers (Nevo et al., 2007). Furthermore, cyanobacteria use the TM system not only for photosynthetic reactions but also for respiration, making the coordination of the biochemical reactions even more complex (Vermaas, 1994; Peschek et al., 2004).

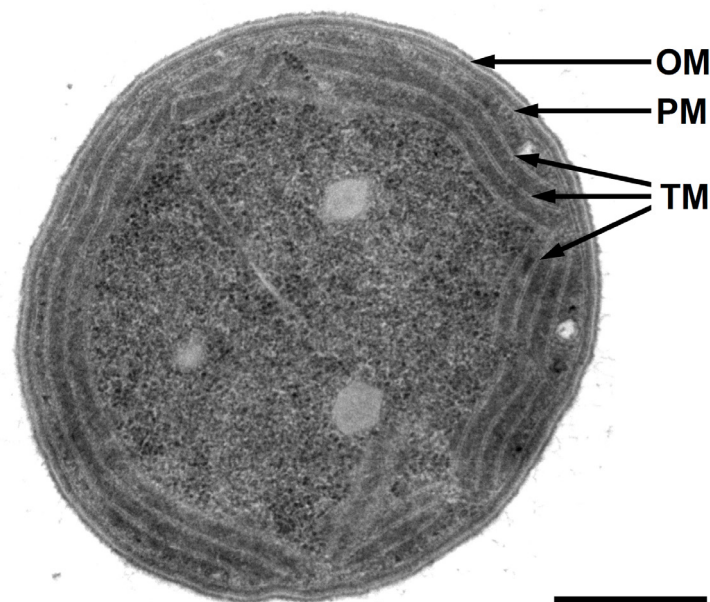


**Figure 2: Electron microscopic picture of a cross section of a typical *Synechocystis* 6803 wild-type cell (kindly provided by I. Gügel).** The different membrane systems are marked by arrows. OM, outer membrane; PM, plasma membrane; TM, thylakoid membrane. Bar: 500 nm.

*Synechocystis* 6803 is an advantageous model organism since its genome has been fully sequenced, transformation occurs spontaneously and it integrates foreign DNA into its genome by double-homologous recombination (Kaneko et al., 1996). Thus, this organism provides an ideal tool for targeted mutagenesis. However, it has to be taken into account that *Synechocystis* 6803 contains up to 200 genome copies per cell, which demands thorough segregation before analysis of the phenotype can be performed (Griese et al., 2011). Furthermore, when the growth medium is supplemented with glucose, *Synechocystis* 6803 can be cultivated even without a functional photosynthetic apparatus and therefore presents an

ideal organism to analyze the function of photosynthesis-related proteins and membrane dynamics.

### 1.3 PHOTOSYSTEM II

The structure and composition of PSII, the photosynthetic complex required for water-splitting and thus oxygen generation, has been studied in great detail during recent years. In crystal structures of PSII from the cyanobacterium *Thermosynechococcus elongatus*, at least 17 transmembrane proteins, 3 soluble proteins, 35 chlorophyll *a* molecules, 12 carotenoids and other additional cofactors could be assigned per PSII monomer (PSII [1]; Ferreira et al., 2004; Loll et al., 2005; Guskov et al., 2009). The structure of the water splitting  $Mn_4Ca$  cluster has been resolved at high resolution as well (Umena et al., 2011). It is generally thought that PSII *in vivo* functions as a dimer (PSII [2]), however this assumption is still discussed (Ferreira et al., 2004; Takahashi et al., 2009).

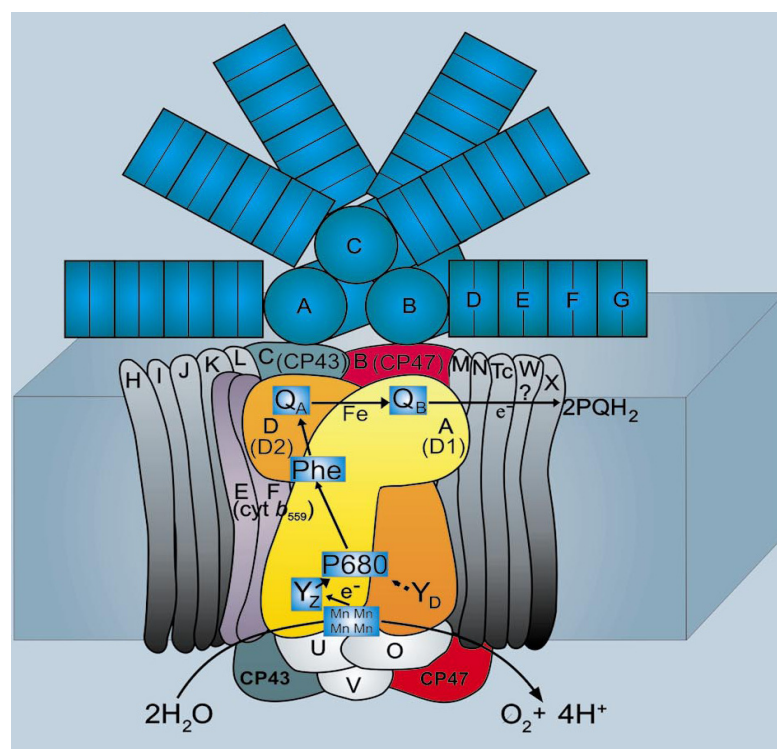


**Figure 3: Model of cyanobacterial PSII (Hankamer et al., 2001).** The different subunits are labeled according to the upper case letter of their gene nomenclature (e.g. PsbA = A). At the cytoplasmic side, a phycobilisome is depicted (blue). A, B and C indicate allophycocyanin rods; D-G discs of other phycobiliproteins. Arrows mark the electron transfer chain from water oxidation to quinone reduction. Phe = pheophytin;  $Y_Z$  and  $Y_D$  = tyrosin residues of D1 and D2, respectively. For further details, see text.

The center of PSII comprises a heterodimer composed of the subunits D1 (encoded by *psbA*) and D2 (encoded by *psbD*). Despite a symmetrical arrangement, the light-induced charge separation involves almost exclusively cofactors bound to the D1 protein (Figure 3). D1 and D2 are surrounded by the two inner antenna proteins CP43 (PsbC) and CP47 (PsbB), each containing 6 transmembrane domains and 13 or 16 chlorophyll molecules, respectively (Figure 3). The remaining PSII subunits are arranged around the core complex of D1, D2, CP43 and CP47. At the luminal side of the PSII complex, D1 and CP43 provide the amino acid ligands required for coordination of the Mn<sub>4</sub>Ca cluster (D1-Asp 170, D1-Glu 189, D1-His 332, D1-Glu 333, D1-Asp 342, D1-Ala 344 and CP43-Glu 354), which is further shielded by the C-terminus of D2 and the three extrinsic PSII proteins PsbO, PsbU and PsbV (Ferreira et al., 2004; Umena et al., 2011). The Mn<sub>4</sub>Ca cluster exhibits the ability of water oxidation and therefore production of O<sub>2</sub>.

As peripheral antenna system cyanobacteria possess so-called phycobilisomes – in contrast to the membrane-intrinsic light harvesting complexes which can be found in TMs of chloroplasts. Phycobilisomes are associated to the cytoplasmic side of TMs and transfer absorbed energy to both, PSII as well as PSI complexes (Mullineaux, 1992). Dependent on light quantity and light quality, these extrinsic antenna complexes are able to adapt their positions between PSI and PSII to balance the ratio of by PSI and PSII absorbed light energy under different light conditions (Mullineaux and Allen, 1990).

### **1.3.1 Assembly of cyanobacterial PSII**

#### 1.3.1.1 Assembly of PSII protein subunits and involved factors

During biogenesis of PSII, all protein subunits, pigments, lipids and ions have to be assembled very accurately and, therefore, a number of different cofactors is required to mediate this coordination (Figure 4; Mulo et al., 2008; Nixon et al., 2010; Komenda et al., 2012a).

The assembly process occurs in a stepwise manner and starts with generation of small precomplexes containing the reaction center core proteins D2 and D1, respectively (for recent reviews see Nixon et al., 2010; Komenda et al., 2012a): D2 is bound to cytochrome b<sub>559</sub> (cyt b<sub>559</sub>), and D1, which is synthesized in a precursor form (pD1), probably builds up a subcomplex together with PsbI (Figure 4; Komenda et al., 2004; Dobáková et al., 2007; Komenda et al., 2008). In the next step, the assembly of these two precomplexes results in formation of the PSII reaction center (RC) complexes (Figure 4; Komenda et al., 2008). Three different types of RC complexes have been detected in TMs, which seem to differ in their

composition of attached PSII assembly factors; one of them has been characterized in more detail and is marked by the presence of the YCF48 protein (see below; Komenda et al., 2008). The RC core complexes are able to perform charge separation, which indicates that the required pigments are already properly inserted (Keren et al., 2005a).

As mentioned, the D1 protein is synthesized in a precursor form with a C-terminal extension comprising 16 amino acids in *Synechocystis* 6803. Hence, a processing step is necessary to enable correct assembly of the Mn<sub>4</sub>Ca cluster and the extrinsic PSII subunits for subsequent PSII biogenesis (Nixon et al., 1992; Roose and Pakrasi, 2004). This cleavage is carried out by the protease CtpA (carboxyl-terminal processing protease) and occurs in a two-step fashion with the intermediate form (iD1) mainly detectable at the level of RC complexes (Anbudurai et al., 1994; Shestakov et al., 1994; Komenda et al., 2007).

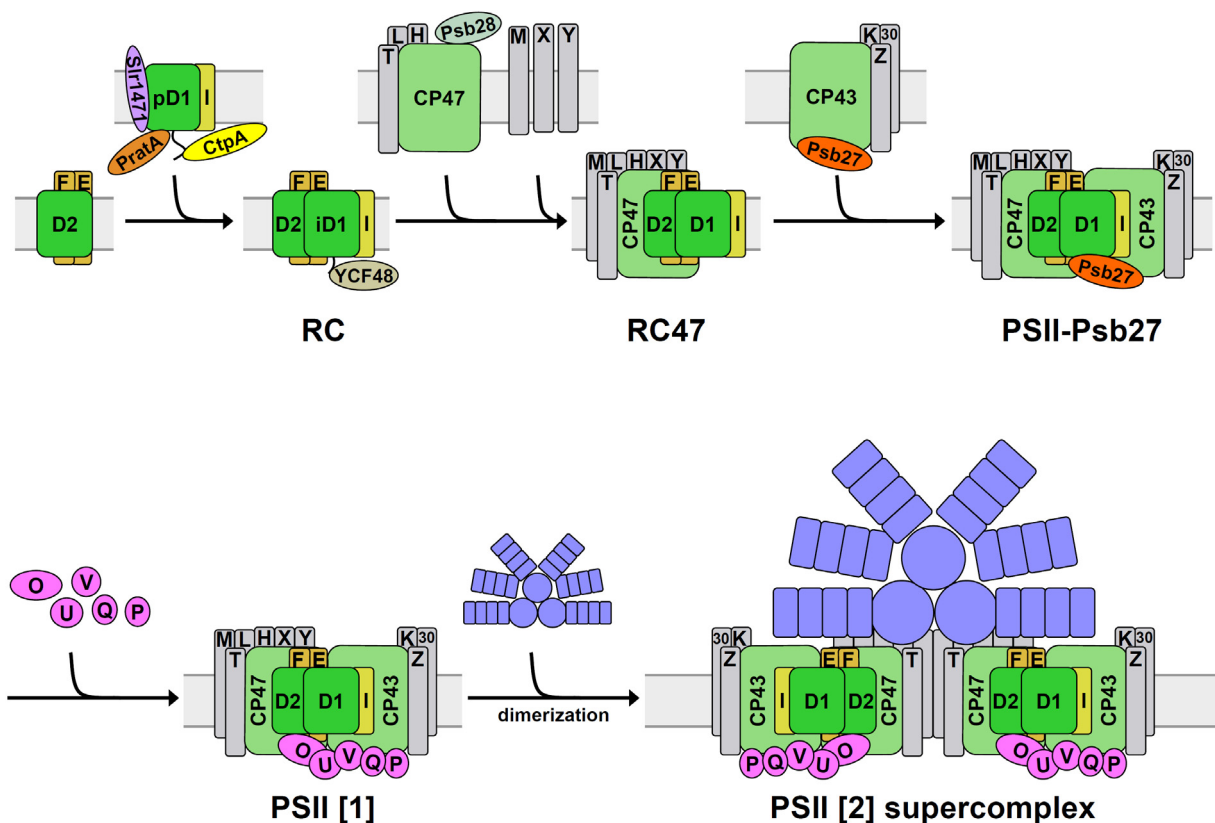


**Figure 4: Assembly of PSII in *Synechocystis* 6803.** Various intermediate complexes are formed during PSII assembly and several assembly factors (ovals) have been described to mediate this process. For details see text. For reduction of complexity, only subunits for which data regarding their integration into complexes is available are depicted. Chlorophyll binding subunits are shown in green, low molecular mass subunits in grey, extrinsic proteins in pink and phycobilisomes in blue. Designation of complexes: RC, reaction center complex lacking CP43 and CP47; RC47, PSII core complex lacking CP43; PSII-Psb27, PSII core monomer with Psb27 bound at the luminal side; PSII [1], PSII monomer; PSII [2], PSII dimer. According to Nickelsen and Rengstl, submitted (see appendix).

In the next step of PSII assembly, CP47 is attached to the RC complex together with the low molecular mass subunits PsbH, PsbL and PsbT and probably concomitantly with PsbM, PsbX and PsbY, which ends up in formation of the so-called RC47 complex (Figure 4; Boehm et al.). Following the correct insertion of CP47, PSII biogenesis is continued by attachment of a CP43 precomplex composed of at least CP43, PsbK, Psb30 and PsbZ (Figure 4; Boehm et al., 2011). After binding of the residual PSII subunits, formation of PSII [1] is completed (Komenda et al., 2004; Rokka et al., 2005; Nixon et al., 2010). The final steps of PSII assembly include the dimerization process as well as attachment of the peripheral antennae, i.e. the phycobilisomes (Figure 4; Nixon et al., 2010).

A number of different factors have been described to facilitate this well-coordinated process. Insertion of pD1, for example, is dependent on Slr1471, which is the only cyanobacterial representative of the Alb3/Oxa1/YidC protein family of insertases assisting membrane integration and assembly of different target proteins. Slr1471 was found to be involved in cell division as well as membrane biogenesis and until now, no fully segregated mutant could be obtained, suggesting an essential function of Slr1471 (Fulgosi et al., 2002; Spence et al., 2004). Further analyses revealed an interaction of Slr1471 with full-length D1 in co-immunoprecipitation experiments and a function of Slr1471 as membrane bound chaperone necessary for correct membrane integration, folding and assembly of the pD1 protein (Figure 4; Ossenbühl et al., 2006).

After insertion of pD1 into the membrane, one of the first facilitating factors in *Synechocystis* 6803 interacting with pD1 is probably represented by the soluble PratA protein, which belongs to the so-called tetratricopeptide repeat (TPR) protein family (Figure 4; Klinkert et al., 2004). In general, proteins of the TPR family are characterized by a repetitive degenerate motif of 34 amino acids forming two anti-parallel  $\alpha$ -helices with the potential to mediate protein-protein interactions including the assembly of multiprotein complexes (D'Andrea and Regan, 2003). Consistently, PratA directly binds to the C-terminus of the D1 protein and was found to be involved in its processing via CtpA (Klinkert et al., 2004; Schottkowski et al., 2009b).

Besides D1, the D2 protein has to be assembled properly as well. With *slr2013*, one cyanobacteria-specific gene was mapped to which a D2-related PSII assembly function was ascribed (Kufryk and Vermaas, 2003). However, since *slr2013* is not completely dispensable – even under photoheterotrophic conditions, i.e. growth in the presence of glucose – it seems to exhibit, in addition to its regulatory function in photosynthesis, other important roles in the cell (Kufryk and Vermaas, 2003).

YCF48 is the cyanobacterial homologue of HCF136 in *Arabidopsis thaliana* and – as mentioned above – was found to be part of a complex composed of D2, D1, cyt b<sub>559</sub> and PsbI, thus mediating the assembly of RC complexes (Figure 4; Komenda et al., 2008). Similarly, HCF136 in *A. thaliana* was shown to associate with a precomplex containing D2 and cyt b<sub>559</sub>, and in a *hcf136* T-DNA insertion line the accumulation of PSII subunits is severely affected resulting in the loss of photosynthetic activity (Meurer et al., 1998; Plücker et al., 2002).

A factor involved in regulation of RC47 generation is represented by Psb28 that was found in isolated RC47 complexes, although it is not part of fully assembled PSII complexes (Dobáková et al., 2009). Besides its association with RC47, smaller amounts of Psb28 could also be detected bound to PSII monomers (PSII [1]) and non-assembled CP47 (Figure 4). For binding of Psb28 to the stromal/cytoplasmic surface of CP47, PsbH, a small subunit of PSII bound to CP47, seems to be required, since loss of PsbH causes a striking reduction of Psb28 levels (Dobáková et al., 2009). Deletion of *psb28*, however, results in limited availability of CP47, of the PSI subunits PsaA/PsaB and in a reduced cellular content of chlorophyll. Therefore, Psb28 was suggested to be involved in efficient chlorophyll synthesis as well as biogenesis of chlorophyll binding proteins (Dobáková et al., 2009).

Moreover, Psb29 was shown to function as a facilitating factor that interacts transiently with PSII, however its exact function in the dynamic processes of PSII biogenesis still has to be dismantled (Kashino et al., 2002). Possibly, this protein plays a role during accurate assembly of the PSII inner antennae (Keren et al., 2005b).

A so far still unanswered question is the order of events during assembly of components at the lumenal side of the PSII complex. Crucial for this process seems to be the binding of the Psb27 protein to PSII assembly intermediates (PSII-Psb27) to enable proper Mn<sub>4</sub>Ca cluster integration by preventing premature association of extrinsic PSII subunits (Figure 4; Roose and Pakrasi, 2008; Liu et al., 2011a). Cyanobacterial Psb27 is a lumenal lipoprotein, its structure from *Synechocystis* 6803 and *T. elongatus* has been resolved and further analyses successfully demonstrated direct binding of Psb27 to CP43 (Cormann et al., 2009; Mabbitt et al., 2009; Liu et al., 2011b; Komenda et al., 2012b; Michoux et al., 2012). The main function of Psb27, however, seems not to be related to PSII *de novo* synthesis but rather to PSII repair, mediating the selective exchange of photodamaged D1 subunits (Aro et al., 1993; Nowaczyk et al., 2006; Grasse et al., 2011). Interestingly, Psb27 and CP43 were found to interact with the PSI subunit PsaB, suggesting that PSI may be linked to biogenesis/repair of PSII via these two proteins (Komenda et al., 2012b).

In summary, the so far described functions of different facilitating factors point to a well-

organized and complex network during biogenesis of PSII, which probably is also interconnected with PSI dynamics and pigment synthesis.

### 1.3.1.2 Incorporation of inorganic cofactors in the PSII water-oxidizing complex

Besides the binding of numerous protein subunits, also the incorporation of inorganic cofactors has to occur in an ordered manner during PSII biogenesis. To enable the function of PSII, the water-oxidizing complex at the luminal side of PSII has to be built up properly, which includes the abovementioned  $Mn_4Ca$  cluster as well as  $Cl^-$  and  $Ca^{2+}$  ions and the surrounding protein environment (Figure 5; Kawakami et al., 2011; Umena et al., 2011; Dau et al., 2012).

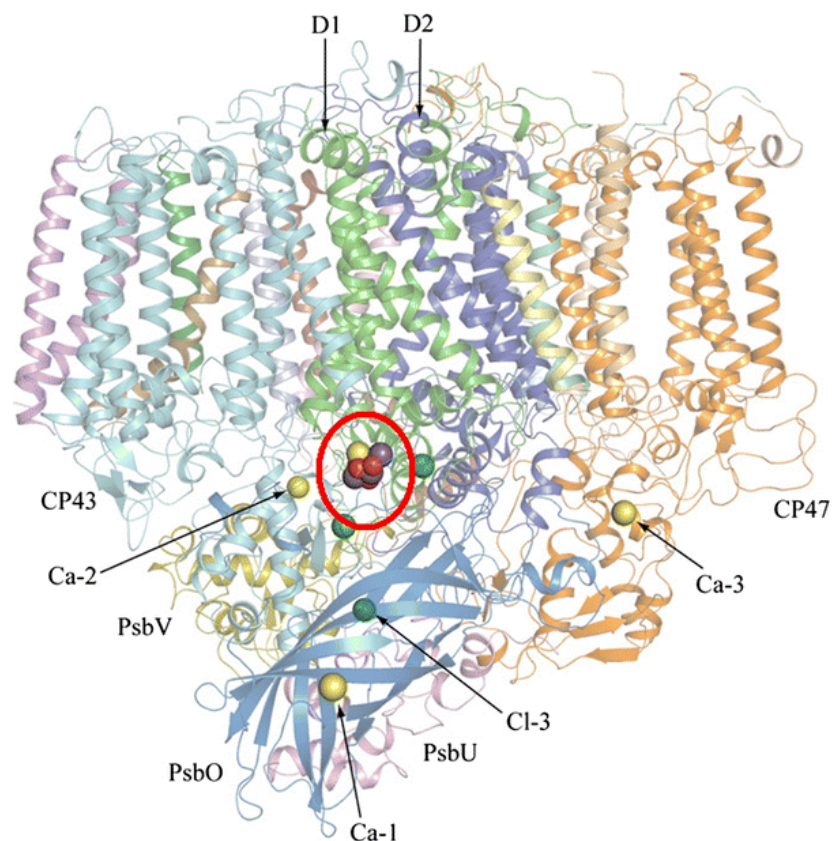


**Figure 5: Inorganic cofactors at the luminal side of PSII (adapted from Najafpour et al., 2012).** Structure of a PSII monomer from *Thermosynechococcus vulcanus*, where the core reaction center proteins (D1, D2, CP43, CP47) and the extrinsic proteins (PsbO, PsbV, PsbU) are depicted. The  $Mn_4Ca$  cluster is marked by a red circle.  $Ca^{2+}$  and  $Cl^-$ -binding sites in addition to the Ca atom of the  $Mn_4Ca$  cluster and the two  $Cl^-$  ions located near the cluster are indicated. Purple, manganese; yellow, calcium; red; oxygen; green, chloride.

Until now, not only the integration mechanisms, but also the exact transport routes of the inorganic cofactors to the PSII complex have remained elusive (for a review see Becker et al.,

2011). Concerning the uptake of manganese (Mn) into the cells, two distinct pathways have been described: the MntABC system, an ABC (ATP binding cassette) transporter for Mn, which is induced under Mn starvation conditions and a second pathway consisting of yet unidentified components (Bartsevich and Pakrasi, 1996; Ogawa et al., 2002). The uptake of Mn in form of  $Mn^{2+}$  from the medium into *Synechocystis* 6803 cells is known to occur very rapidly, and it can subsequently be stored in the PP (Keren et al., 2002). Interestingly, this uptake requires a functional photosynthetic electron transfer chain and, thus, is light-dependent (Bartsevich and Pakrasi, 1996; Keren et al., 2002). In addition, one periplasmic Mn-binding protein has been identified, named MncA, which could be involved in this Mn accumulation (Tottey et al., 2008). However, the exact role of MncA remains to be elucidated as well as the pathway of Mn transport from the periplasmic pool to the water-oxidizing complex.

Moreover, many questions need to be solved regarding the uptake and transport of the  $Ca^{2+}$  and  $Cl^-$  ions required for construction of the water-splitting machinery including the  $Mn_4Ca$  cluster (Becker et al., 2011). In 2001, Kufryk and Vermaas described a *Synechocystis* 6803 mutant showing a clearly reduced affinity of  $Ca^{2+}$  to its binding site at the water-splitting complex. Therefore, the lacking protein, Slr0286, was suggested to play a role in the functional assembly and stability of the  $Mn_4Ca$  cluster, however, no details of its putative mode of action have been elucidated yet (Kufryk and Vermaas, 2001). The  $Cl^-$  ions of the water oxidizing complexes have been suggested to function in maintaining the coordination environment of the  $Mn_4Ca$  cluster (Umena et al., 2011), but  $Cl^-$  uptake and transport to PSII remain to be investigated (Becker et al., 2011).

To become functional, the  $Mn_4Ca$  cluster has to be photoactivated. This process includes on the one hand the incorporation of the inorganic cofactors and on the other hand the light-driven oxidation of  $Mn^{2+}$  to  $Mn^{\geq 3+}$ . To date, the precise order of events during formation and activation of the  $Mn_4Ca$  cluster is not completely uncovered. The binding of the first two Mn ions is assumed to occur in a sequential manner, with the second  $Mn^{2+}$  requiring a proper bound and oxidized  $Mn^{3+}$  ion.  $Ca^{2+}$  seems to be involved in these early steps of  $Mn_4Ca$  cluster assembly as well (Zaltsman et al., 1997; Hwang and Burnap, 2005). Furthermore, it was shown that bicarbonate functions as additional inorganic cofactor, which influences the binding of the first Mn to the apo-water oxidizing complex (Baranov et al., 2000; Baranov et al., 2004; Dasgupta et al., 2007). However, the subsequent assembly of the two remaining Mn ions as well as chloride still has to be dismantled.

Interestingly, the assembly of the Mn<sub>4</sub>Ca cluster does not only affect the luminal side of PSII. Evidence suggests an additional influence of the Mn<sub>4</sub>Ca cluster's assembly state on the coupling of phycobilisomes to the complex at the cytoplasmic side. In this regard, it was hypothesized that phycobilisome association is regulated allosterically by Mn<sub>4</sub>Ca cluster assembly, even though both are located on different sides of the TM. This interaction might represent a mechanism to avoid photodamage on only partially assembled PSII reaction centers (Hwang et al., 2008).

#### 1.3.1.3 Synthesis of chlorophyll and pigment insertion into PSII

The energy driving the splitting of water is provided by sunlight. For its absorption, photosynthetic organisms have developed a variety of pigments differing in the wavelength of their maximal absorption range. Cyanobacteria contain three major groups of pigments: bilins, carotenoids and chlorophylls. Bilins are light-absorbing linear tetrapyrroles bound to phycobiliproteins, hence representing an important part of the water-soluble extrinsic cyanobacterial antenna system (see section 1.3; Brown et al., 1990). The ability of the highly abundant phycobiliproteins to absorb light in the range between 450 nm to 660 nm is responsible for the blue-green and blue-red colors of cyanobacteria (Samsonoff and MacColl, 2001).

Colors in the light-yellow to orange-red spectrum can be ascribed to carotenoids, which belong to the isoprenoid pigments. Their system of conjugated double bonds enables them to absorb light energy and dissipate it as heat. Therefore, they play a crucial role in quenching of triplet chlorophyll and singlet oxygen, and thus in protection against photoinhibition and oxidative stress (Frank and Brudvig, 2004). A similar function has also been described to xanthophylls, i.e. oxygenated carotenoids (Zhu et al., 2010). However, besides their photoprotective function, carotenoids are also involved in light harvesting and subsequent energy transfer to chlorophyll molecules (Figure 6; Maresca et al., 2008).

Chlorophylls are the most important pigments in oxygenic photosynthetic organisms, since they are – beside their role in light-harvesting – responsible for charge separation and electron transport inside the reaction centers of photosynthetic complexes (Figure 6; see section 1.1). Chemically, they are magnesium-coordinating tetrapyrroles with a five-membered ring structure and a phytol tail (Figure 7).

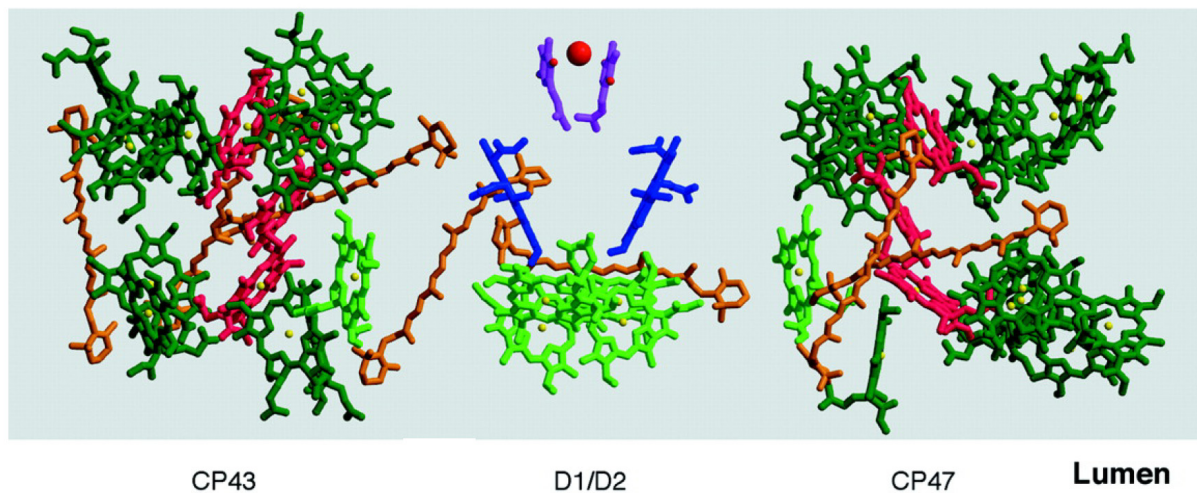


**Figure 6: Pigment cofactors of PSII membrane proteins (adapted from Ferreira et al., 2004).** Chlorophyll molecules bound to the reaction center proteins are depicted in light green; chlorophyll molecules of the antenna proteins in dark green and red and  $\beta$ -carotenes are shown in orange. For clarity, protein structures as well as phytol chains of chlorophyll molecules are omitted. Blue, pheophytines; purple, quinones; red ball, non-heme iron.

Synthesis of chlorophyll was shown to be a complex, highly regulated metabolic pathway (Masuda, 2008). As starting product, 5-aminolevulinic acid (5-ALA) is generated, which is synthesized from glutamate (Figure 7; for an overview see Eckhardt et al., 2004). Fusion of two molecules of 5-ALA leads to one molecule porphobilinogen; four porphobilinogen molecules are further combined to result in one molecule hydroxymethylbilan, a linear tetrapyrrole. This intermediate is subsequently modified in various steps to generate protoporphyrin IX, in which a magnesium ion is incorporated, a reaction catalyzed by the magnesium chelatase. After esterification, cyclization and subsequent reduction, monovinyl protochlorophyllide *a* is produced (Figure 7). The following reaction, which leads to generation of chlorophyllide *a*, can be mediated by two different enzymes (Reinbothe et al., 2010): on the one hand by a light-dependent protochlorophyllide-oxidoreductase (POR; Schoefs and Franck, 2003) and on the other hand by a light-independent protochlorophyllide-oxidoreductase (LiPOR; Armstrong, 1998). This light-independent enzyme enables organisms like cyanobacteria and green algae to synthesize chlorophyll even in the dark, whereas chlorophyll synthesis is strictly light-dependent in angiosperms since they lack LiPOR (Reinbothe et al., 2010). In a last step, chlorophyllide *a* is further esterified with phytol by the chlorophyll synthase, thus generating chlorophyll *a* (Figure 7).

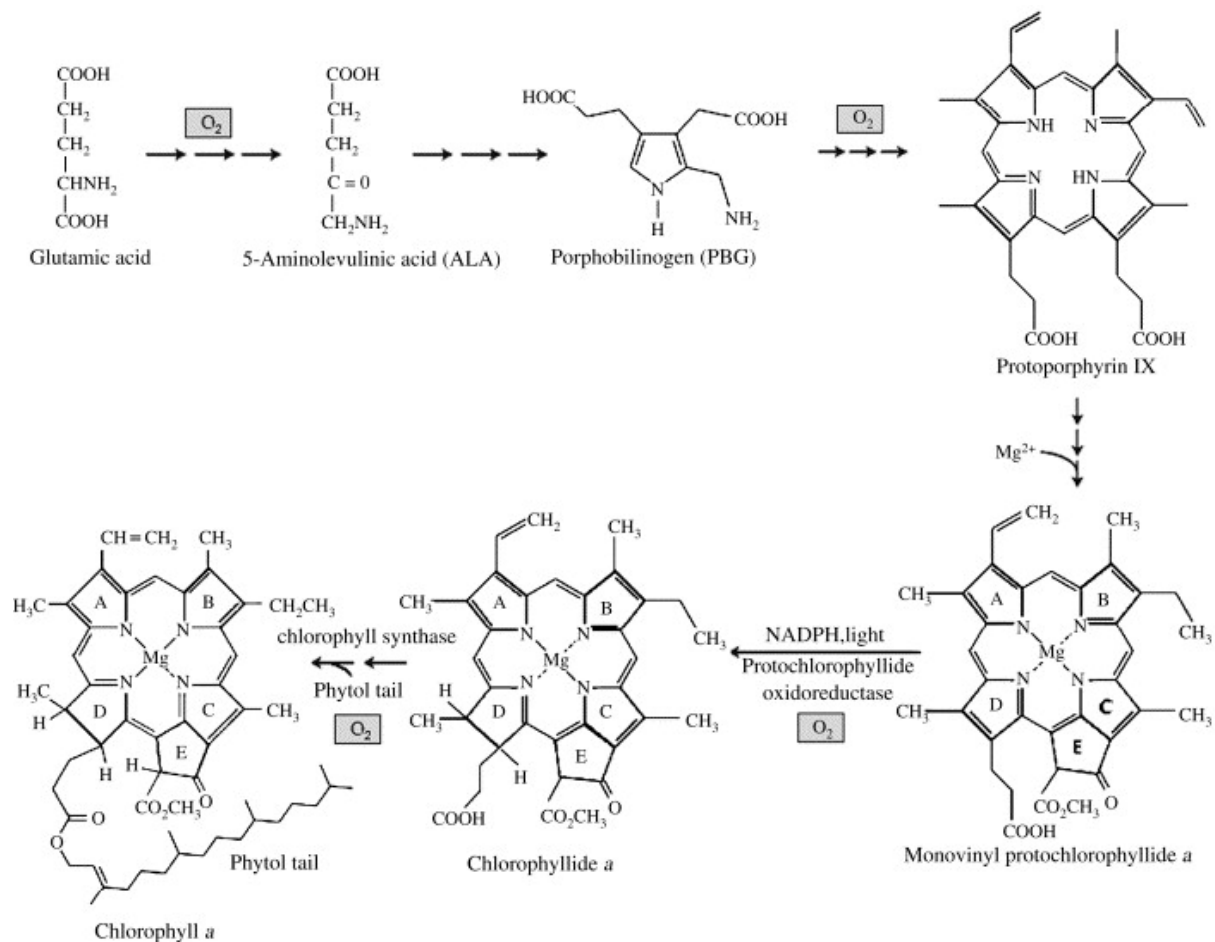


**Figure 7: Synthesis of chlorophyll *a*.** Pathway of major steps of chlorophyll synthesis (adapted from Zhang et al., 2007). The conversion step from monovinyl protochlorophyllide *a* to chlorophyllide *a* can be performed by the light-dependent POR (as depicted in the scheme) or by the LiPOR enzyme. For further description see text.

During assembly of the PSII complex, not only the different protein subunits, but also carotenoids and chlorophylls have to be integrated. Since accumulation of unbound pigments can cause formation of harmful reactive oxygen species, it is likely that pigment synthesis is tightly coupled to their integration into apoproteins (Domanskii et al., 2003; Krieger-Liszkay et al., 2008). Several indications suggest that pigment integration already occurs during early steps of PSII assembly: (i) Photosynthetic precomplexes including the early RC complex were described to contain chlorophyll molecules and can undergo light induced charge separation (Keren et al., 2005a). (ii) Synthesis of the D1 protein was shown to be affected by the availability of chlorophyll molecules on the level of initiation of translation as well as maturation. For the latter one, a conformational change of the D1 protein triggered by chlorophyll insertion was speculated to be required (He and Vermaas, 1998). Additionally, studies with barley led to the assumption that chlorophyll *a* binding apoproteins (for example

CP47, CP43, D2 and D1) are stabilized by direct interaction with chlorophyll (Kim et al., 1994; Eichacker et al., 1996). (iii) HCF136 – the *A. thaliana* homolog of the assembly factor YCF48 – was hypothesized to assist in the binding of chlorophyll *a* to PSII RC precomplexes (Plücker et al., 2002).

Besides the abovementioned assembly factor Psb28, other proteins have been identified which were ascribed to the integration of pigments during assembly of photosynthetic complexes. GUN4 (genome uncoupled) is a protein activating the magnesium chelatase, an enzyme of the chlorophyll synthesis pathway (Larkin et al., 2003; Davison et al., 2005). Furthermore, it was shown to stabilize the interaction of the magnesium chelatase subunit ChlH with chloroplast membranes in pea (Adhikari et al., 2009). Consequently, lack of GUN4 causes a strong reduction in chlorophyll synthesis, preventing photoautotrophical growth (Sobotka et al., 2008).

An additional protein connected to pigment synthesis/insertion into PSII is the POR-interacting TPR protein Pitt. Pitt was shown to be involved in photosynthetic complex formation and, due to its ability to interact with POR, it is linked to the light-dependent synthesis of chlorophyll molecules (Schottkowski et al., 2009a).

The majority of chlorophyll and carotenoid pigments required for capturing light energy are attached to the PSII inner antenna proteins: CP47 harbors 16 chlorophyll *a* and 5 carotenoid molecules, whereas 13 chlorophyll *a* and 3 carotenoids are bound to CP43 (Figure 6; Loll et al., 2005; Umena et al., 2011). Therefore, it is not surprising that availability of chlorophyll influences the accumulation of CP47 (Sobotka et al., 2005; Sobotka et al., 2008). Furthermore, mutation of amino acids responsible for binding of chlorophyll to CP47 and CP43 leads to a destabilization of these proteins causing defects in PSII function (Shen and Vermaas, 1994; Manna and Vermaas, 1997). Hence, pigment synthesis and insertion seem to be tightly coordinated with synthesis and assembly of the respective PSII subunits. Moreover, binding of pigments to their apoproteins is thought to already take place during early stages of PSII assembly and, most likely, might even occur while the translation of their acceptor proteins is still ongoing.

### 1.3.2 Subcellular localization of PSII assembly

Besides the question of the temporal sequence of events during PSII assembly, the subcellular localization of this process is a still unresolved issue as well. It was suggested that biogenesis of photosystems in cyanobacteria does not exclusively take place in the TMs, but starts at the PM due to the following findings: (i) Core protein subunits of PSI as well as PSII complexes

were detected in PM preparations (Smith and Howe, 1993; Zak et al., 2001). In contrast to this, the inner antenna proteins CP47 and CP43 were solely found in TMs (Zak et al., 2001; Bergantino et al., 2003). (ii) The CtpA protease required for C-terminal processing of the D1 protein has been exclusively found in association with the PM (Zak et al., 2001) and (iii) the PSII assembly factor PrtA is located in the PP, thus not having direct access to the main parts of the TM system (Klinkert et al., 2004).

Hence, a model was developed in which early steps of PSII biogenesis take place at the PM followed by transport of the precomplexes to the TM, where the assembly is completed by attachment of the remaining subunits. However, the transfer pathway of the nascent protein complexes from PM to TMs is still unclear, although two different mechanisms are conceivable (Liberton and Pakrasi, 2008): Transport occurs either using direct connections between the two membrane systems, or is mediated by a vesicle system bridging the gap between PM and TMs (Figure 8).

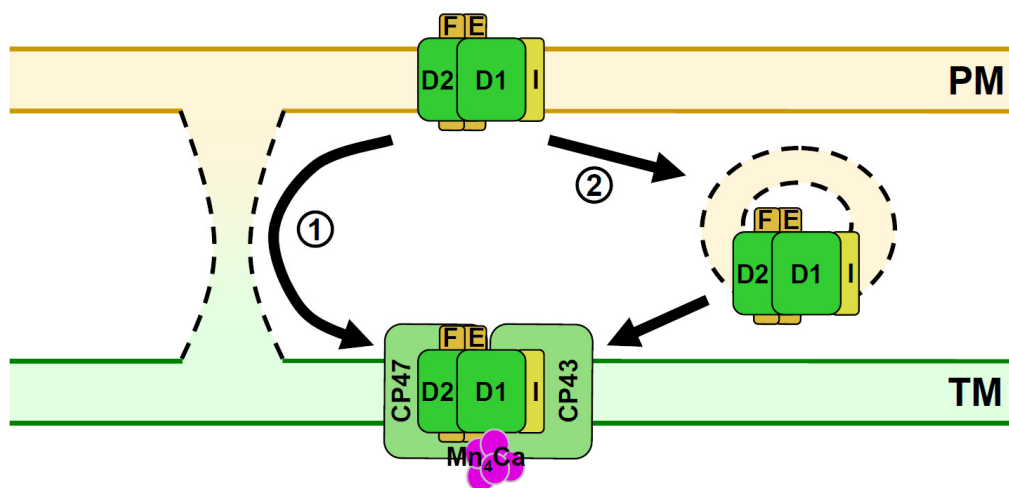


**Figure 8: Spatial organization of PSII biogenesis.** Early assembly steps are thought to occur in the plasma membrane (PM) and PSII precomplexes are then transported to the thylakoid membrane system (TM), where the inner antenna proteins CP47 and CP43 are attached and the assembly is completed. The transport of PSII from PM to TM is speculated to occur either via direct connections (1) or via vesicle transport (2). For simplification, low molecular mass subunits and phycobilisomes are omitted.

Indications supporting the second possibility were obtained by studies in chloroplasts of *A. thaliana*, which described the involvement of the VIPP1 protein (vesicle-inducing protein in plastids 1) in formation of TMs (Kroll et al., 2001). The corresponding homolog in *Synechocystis* 6803 seems to be essential for viability, as complete loss of the encoding gene could not be achieved (Westphal et al., 2001). However, analysis of these knock-down

mutants revealed a severe defect in development of ordered thylakoid structures, suggesting a role of VIPP1 in TM biogenesis also in *Synechocystis* 6803. Additional experiments favoring non-contiguous PM and TMs used a fluorescent dye, which stains the OM and PM of *Synechocystis* 6803 and is unable to cross membranes (Schneider et al., 2007). Since no staining of TMs could be detected, the absence of connections between PM and TMs was suggested, because in case of directly connected TM and PM, diffusion of the dye to the TM system had been expected. However, after continuous application of the dye, formation of fluorescent bodies was observed within the cells, indicating the existence of a transport system. The properties of these structures have not been characterized in more detail, but they were hypothesized to represent lipid bodies or membrane vesicles (Schneider et al., 2007).

On the other hand, direct connections between PM and TMs have been proposed and discussed controversially due to several electron microscopic studies of *Synechocystis* 6803 cells that gave rise to contradictory conclusions: Whereas van de Meene et al. depicted the existence of direct connections, Liberton and co-workers disapproved continuity between the PM and TM system (Liberton et al., 2006; van de Meene et al., 2006; van de Meene et al., 2012). Moreover, proteomic studies of PM and TM preparations obtained by sucrose density centrifugation and aqueous two-phase partitioning suggested the presence of common translocon sites at connecting regions between PM and TMs (Pisareva et al., 2011). These sites are characterized by the presence of protein insertion machineries mediating the insertion of integral membrane proteins followed by their correct lateral sorting. Nevertheless, the hypothesized membrane connections are thought to be dynamic, i.e. transiently connected instead of being permanently fused (Pisareva et al., 2011).

Regarding the biogenesis of TMs and potential connection sites between TM and PM, the presence and involvement of so-called thylakoid centers (TC) was discussed (Hinterstoisser et al., 1993; van de Meene et al., 2006). These are cylindrical structures which can be found at sites where thylakoids converge to the PM. Initially, they were described in four different cyanobacterial species, *Anabaena cylindrica*, *Dermocarpa violaceae*, *Gleocapsa alpicola* and *Pleurocapsa minor* and they were assumed to be directly linked to TMs (Kunkel, 1982). Three-dimensional analysis of the cell structure of *Synechocystis* 6803 using electron microscopy could not identify a clear continuity of TCs and TMs, although a connection between TCs and PM or PP seems to exist (van de Meene et al., 2006).

Another indication for the involvement of specialized membrane regions in early assembly steps of PSII was obtained by localization of the PSII biogenesis factor PrtA. About 80-90% of PrtA can be found in a soluble complex in the PP, whereas the remaining 10-20% are

membrane-bound via interaction with the D1 protein (Fulda et al., 2000; Klinkert et al., 2004; Schottkowski et al., 2009b). By using two sequential steps of sucrose density gradient centrifugation, the membrane-bound part of PrtA was detected in a specific fraction that was clearly separated from TMs (Schottkowski et al., 2009b). Additional to PrtA, pD1 as well as the mature D1 protein were found – aside from their TM localization – in these PrtA-defined fractions (PDMs, PrtA-defined membranes). Interestingly, upon deletion of *prtaA*, pD1 accumulates in PDMs and also D1 shows a slight shift towards these lighter fractions (Schottkowski et al., 2009b). This indicates that PrtA plays a considerable role in membrane organization required for proper and efficient PSII assembly.

Moreover, PDMs were not only suggested to represent the site of early steps of PSII protein assembly, but also seem to be involved in pigment synthesis/insertion, which was proposed by investigation of the Pitt protein (see section 1.3.1.3). Both, Pitt and its interaction partner POR display a more pronounced accumulation in PDMs in *prtaA*<sup>-</sup> cells, whereas in wild-type cells, they are mainly found in fractions representing TMs (Schottkowski et al., 2009a).

Furthermore, other studies point to a spatial organization of chlorophyll synthesis in cyanobacteria as well, as *Synechococcus elongatus* 7942 was found to accumulate the chlorophyll precursors protochlorophyllide *a* and chlorophyllide *a* exclusively in the PM, but not in TMs (Peschek et al., 1989). Similar analyses of *Synechocystis* 6803 membranes revealed the presence of a special membrane subfraction containing an extremely high accumulation of chlorophyll precursor molecules, concomitantly with reduced amounts of chlorophyll as compared to TMs. Therefore, this membrane fraction was suggested to play a distinctive role in chlorophyll biosynthesis, possibly resembling the TCs described above (Hinterstoisser et al., 1993).

In conclusion, the subcellular localization of PSII assembly is a still unresolved question. Nevertheless, there is growing evidence that – at least the early steps – take place in specialized membrane regions probably resembling TCs and/or PDMs (Hinterstoisser et al., 1993; Schottkowski et al., 2009b). In parallel, this process is coordinated with pigment synthesis and insertion into their apoproteins. This is speculated to occur via close integration of the PSII assembly and chlorophyll synthesis machineries, enabling a coordinated and efficient assembly of the PSII complex (Komenda et al., 2012a).

## 2 AIMS OF THIS WORK

Assembly of PSII is a complex process combining the integration of its protein subunits and cofactors in a well-organized pathway. Despite the identification and characterization of several facilitating factors as well as isolation of specific assembly intermediates and precomplexes during recent years, the understanding of the molecular details of the PSII assembly pathway is still in its beginning.

The aim of this work is to shed light on this process, particularly regarding early steps of PSII biogenesis and its subcellular localization. First, using the model cyanobacterium *Synechocystis* 6803, the earlier described PDM fractions were biochemically characterized in more detail, including the presence of PSII assembly factors as well as pigment and lipid composition, to elucidate their proposed function during PSII biogenesis. Second, morphological investigations using electron microscopic analyses were carried out to identify the localization of PrtA and the cellular structures corresponding to PDMs and, thus, the sites of early steps of PSII assembly within a *Synechocystis* 6803 cell. Third, studies using different PSII assembly mutants were performed to unravel the working mode of the corresponding facilitating factors as well as potential interdependencies. In particular, a more detailed characterization of the PrtA function as well as of the newly identified PAM68/SII0933 protein was addressed in this study.

The results of this work should contribute to develop a more elaborate model of PSII assembly, not only in terms of the temporal order of events and assembly factor actions, but also in regard to the spatial organization of this process.

### 3 RESULTS

This part consists of four chapters with each representing an independent study that is either published in or accepted by an international peer-reviewed journal. At the beginning of each chapter, the main results and conclusions of the respective paper are summarized and the contribution of the author is stated.

#### 3.1 THE ARABIDOPSIS THYLAKOID PROTEIN PAM68 IS REQUIRED FOR EFFICIENT D1 BIOGENESIS AND PHOTOSYSTEM II ASSEMBLY

Armbruster, U., Zühlke, J., **Rengstl, B.**, Kreller, R., Makarenko, E., Rühle, T., Schünemann, D., Jahns, P., Weisshaar, B., Nickelsen, J., and Leister, D. (2010) *Plant Cell* **22**, 3439-3460

The focus of this study was the identification and characterization of the *photosynthesis affected mutant 68* (*pam68*) of *A. thaliana*. The mutant contained only 65% of chlorophyll compared to the wild-type and showed severely reduced growth rates. This phenotype was found to be attributed to a strong decrease in accumulation of PSII core subunits and a perturbed assembly of PSII complexes, especially due to an increased instability of the D1 protein. PAM68 was described to be an integral membrane protein located in the TM system, with its N- and C-termini exposed to the chloroplast stroma. For co-localization of PAM68 with different PSII assembly intermediates, thylakoidal protein complexes were separated by sucrose density gradient centrifugation and analyzed for their protein components. PAM68 was found to co-migrate with the PSII subunits CP43, PsbE and PsbH as well as small amounts of pD1 and D2, and, interestingly, with the chloroplast-specific PSII assembly factor LPA1. An interrelationship between PAM68 and LPA1 was furthermore supported by analogous analyses of isolated TMs from *pam68* and *lpa1* mutant plants, in which the distribution of the respective other protein was altered. In summary, PAM68 was proposed to be part of a low molecular weight complex that might contain pD1 and D2, and which is thus involved in early steps of PSII assembly. Furthermore, PAM68 possibly displaces LPA1 during PSII biogenesis to mediate proper progression of the assembly process.

Sequence homologs of PAM68 are found in all photosynthetic eukaryotes as well as cyanobacteria. The function of the homologous protein in *Synechocystis* 6803, SII0933, was additionally examined in this study. The effects of a knock-out of SII0933 did not cause a severe phenotype as observed in *A. thaliana*, as the mutant strain nearly displayed wild-type characteristics in terms of growth and photosynthetic activity. However, molecular and

biochemical analyses revealed the presence of Sll0933 in smaller protein complexes and a clear reduction of the amount of RC complexes in the *sll0933*<sup>-</sup> mutant. This suggests a role of Sll0933 in early steps of PSII biogenesis as well, although other proteins are able to at least partially take over its function in *Synechocystis* 6803, in contrast to its counterpart in higher plants, which seems more crucial for plant viability.

I contributed to this study by analyzing the function of Sll0933 in *Synechocystis* 6803. This comprised construction of the *sll0933*<sup>-</sup> mutant as well as cloning and production of recombinant Sll0933 peptides required for antiserum generation. Moreover, measurements of growth curves, oxygen evolution and fluorescence emission spectra at 77 K of wild-type and *sll0933*<sup>-</sup> cells were performed for determining the effect of Sll0933 loss on photosynthetic activity. Furthermore, I performed immunoblot experiments including protein accumulation and solubilization studies as well as BN/SDS-PAGE for detection of PSII and Sll0933 complexes.

# The *Arabidopsis* Thylakoid Protein PAM68 Is Required for Efficient D1 Biogenesis and Photosystem II Assembly<sup>W</sup>

Ute Armbruster,<sup>a</sup> Jessica Zühlke,<sup>a</sup> Birgit Rengstl,<sup>b</sup> Renate Kreller,<sup>a</sup> Elina Makarenko,<sup>a</sup> Thilo Rühle,<sup>a</sup> Danja Schünemann,<sup>c</sup> Peter Jahns,<sup>d</sup> Bernd Weisshaar,<sup>e</sup> Jörg Nickelsen,<sup>b</sup> and Dario Leister<sup>a,1</sup>

<sup>a</sup> Lehrstuhl für Molekularbiologie der Pflanzen (Botanik), Department Biologie I, Ludwig-Maximilians-Universität, 82152 Martinsried, Germany

<sup>b</sup> Molekulare Pflanzenwissenschaften, Department Biologie I, Ludwig-Maximilians-Universität, 82152 Martinsried, Germany

<sup>c</sup> AG Molekularbiologie Pflanzlicher Organellen, Ruhr-Universität-Bochum, 44801 Bochum, Germany

<sup>d</sup> Institute of Plant Biochemistry, Heinrich-Heine University Düsseldorf, 40225 Düsseldorf, Germany

<sup>e</sup> Lehrstuhl für Genomforschung, Fakultät für Biology, Universität Bielefeld, 33615 Bielefeld, Germany

**Photosystem II (PSII) is a multiprotein complex that functions as a light-driven water:plastoquinone oxidoreductase in photosynthesis. Assembly of PSII proceeds through a number of distinct intermediate states and requires auxiliary proteins. The *photosynthesis affected mutant 68 (pam68)* of *Arabidopsis thaliana* displays drastically altered chlorophyll fluorescence and abnormally low levels of the PSII core subunits D1, D2, CP43, and CP47. We show that these phenotypes result from a specific decrease in the stability and maturation of D1. This is associated with a marked increase in the synthesis of RC (the PSII reaction center-like assembly complex) at the expense of PSII dimers and supercomplexes. PAM68 is a conserved integral membrane protein found in cyanobacterial and eukaryotic thylakoids and interacts in split-ubiquitin assays with several PSII core proteins and known PSII assembly factors. Biochemical analyses of thylakoids from *Arabidopsis* and *Synechocystis* sp PCC 6803 suggest that, during PSII assembly, PAM68 proteins associate with an early intermediate complex that might contain D1 and the assembly factor LPA1. Inactivation of cyanobacterial PAM68 destabilizes RC but does not affect larger PSII assembly complexes. Our data imply that PAM68 proteins promote early steps in PSII biogenesis in cyanobacteria and plants, but their inactivation is differently compensated for in the two classes of organisms.**

## INTRODUCTION

Photosystem II (PSII) is a multiprotein-pigment complex that functions as a light-driven water:plastoquinone oxidoreductase in the thylakoid membranes of cyanobacteria and chloroplasts (Wollman et al., 1999; Iwata and Barber, 2004; Nelson and Yocum, 2006). The reaction center of PSII is composed of the subunits D1 and D2, which bind the pigment cofactors chlorophyll, pheophytin, and plastoquinone, the  $\alpha$  and  $\beta$  subunits of cytochrome (Cyt)  $b_{559}$  (hereafter designated as PsbE and PsbF, the E and F subunits of PSII), and PsbI. Peripherally attached are CP43 and CP47, which bind chlorophyll  $a$  and  $\beta$ -carotene; CP43 and D1 together provide ligands for the  $\text{CaMn}_4$  cluster that is involved in water oxidation (Ferreira et al., 2004; Guskov et al., 2009). Surrounding these subunits are several low molecular weight subunits of PSII (Shi and Schröder, 2004), and extrinsic subunits on the luminal side of PSII stabilize the  $\text{CaMn}_4$  cluster (reviewed in Roose et al., 2007; Enami et al., 2008). Moreover, the extrinsic phycobilisomes (in cyanobacteria) and the intrinsic chlorophyll  $a/b$  binding light-harvesting complex of PSII (LHCII)

(in chloroplasts) operate as distal, pigment-containing, light-harvesting complexes of PSII.

In cyanobacteria and chloroplasts, assembly of PSII occurs in a stepwise manner (Baena-Gonzalez and Aro, 2002; Rokka et al., 2005; Mulo et al., 2008; Nixon et al., 2010). In chloroplasts, this process is modulated by a combination of translational auto- and transregulation of PSII subunit synthesis (Choquet et al., 2001; Choquet and Wollman, 2002). Radioactive pulse-chase experiments, together with sucrose gradient and native gel analyses, provided initial support for the stepwise assembly of the chloroplast PSII complex, involving a number of discrete PSII subcomplexes and processing of the D1 protein (van Wijk et al., 1995, 1996, 1997). On the basis of two-dimensional analysis of radioactively labeled thylakoid proteins, Rokka et al. (2005) described the sequential appearance of distinct PSII assembly states in chloroplasts. First, the precursor of the D1 subunit (pD1) is assembled into the receptor complex (consisting of D2, PsbE, PsbF, and PsbI) to form RC, the PSII reaction center-like assembly complex. Next, CP47 attaches to RC to generate the so-called CP47-RC complex. In two further steps, the PsbH, PsbM, PsbT<sub>C</sub>, and PsbR subunits are added to form CP43-free PSII monomers (or CP43-PSII). Addition of CP43 and other subunits then generates PSII core monomers, which in turn form PSII core dimers and PSII supercomplexes, the native forms of functional PSII units that in vivo collect light energy, convert it into electro-chemical energy, and drive electron transfer from water to plastoquinone (Minagawa and Takahashi, 2004). In the

<sup>1</sup> Address correspondence to leister@lrz.uni-muenchen.de.

The author responsible for distribution of material integral to the findings presented in this article in accordance with the policy described in the Instructions for Authors (www.plantcell.org) is: Dario Leister (leister@lrz.uni-muenchen.de).

<sup>W</sup>Online version contains Web-only data.

www.plantcell.org/cgi/doi/10.1105/tpc.110.077453

PSII supercomplexes, LHCII trimers are attached to PSII core dimers (Boekema et al., 1995; Hankamer et al., 1997), probably via the proteins CP29, CP26, and CP24 that serve as linkers (Nelson and Yocum, 2006). During the biogenesis of PSII, subsequent to the insertion of pD1 in RC, the C-terminal extension of pD1 is cleaved by the C-terminal peptidase (CtpA) on the luminal side of the thylakoid membrane to form mature D1 (mD1) (Diner et al., 1988; Taylor et al., 1988; Anbudurai et al., 1994; Shestakov et al., 1994). The processing of assembled pD1 is a prerequisite for the ligation of the catalytic manganese cluster and, thus, for the formation of PSII complexes capable of splitting water (Diner et al., 1988; Nixon et al., 1992; Hatano-Iwasaki et al., 2000; Roose and Pakrasi, 2004).

In addition to the structural subunits of PSII, several auxiliary proteins are involved in PSII biogenesis (reviewed in Mulo et al., 2008; Nixon et al., 2010). Moreover, many of the auxiliary proteins involved in the de novo biogenesis of PSII also participate in the PSII repair cycle, which involves the replacement of damaged subunits, mainly the D1 subunit, by a newly synthesized copy and occurs much more frequently than does de novo biogenesis in mature chloroplasts (Adir et al., 2003; Aro et al., 2005; Nixon et al., 2005; Edelman and Mattoo, 2008; Mulo et al., 2008; Kato and Sakamoto, 2009). Some, but not all, PSII assembly factors are conserved in cyanobacteria and chloroplasts. These include HIGH CHLOROPHYLL FLUORESCENCE 136 (HCF136)/HYPOTHETICAL CHLOROPLAST OPEN READING FRAME 48 (YCF48) (Meurer et al., 1998; Komenda et al., 2008), ALBINO3 (ALB3)/Slr1471 (Sundberg et al., 1997; Spence et al., 2004), Psb27 (Kashino et al., 2002; Roose and Pakrasi, 2004; Chen et al., 2006; Nowaczyk et al., 2006; Wei et al., 2010), Psb28 (Kashino et al., 2002; Dobakova et al., 2009), Psb29 (Kashino et al., 2002; Keren et al., 2005), YCF39 (Ermakova-Gerdes and Vermaas, 1999), as well as immunophilins like CYCLOPHILIN38/THYLAKOID LUMEN PEPTIDYL-PROLYL ISOMERASE OF 40 kD (Sirpiö et al., 2008). Presumably, therefore, their roles in PSII biogenesis or maintenance have been retained during evolution. Other factors are specific to cyanobacteria (for instance, PROCESSING ASSOCIATED TPR PROTEIN [PratA] [Klinkert et al., 2004; Schottkowski et al., 2009a], Slr0286 [Kufryk and Vermaas, 2001], and Slr2013 [Kufryk and Vermaas, 2003]) or to chloroplasts (such as LOW PSII ACCUMULATION1 [LPA1]/PSII REPAIR 27 [REP27] [Peng et al., 2006; Park et al., 2007] and LPA2 [Ma et al., 2007]) and may represent evolutionary adaptations to specific environments.

HCF136, LPA1, LPA2, and ALB3 are the best studied PSII assembly factors in *Arabidopsis thaliana*. ALB3 performs auxiliary functions during the assembly of several thylakoid protein complexes, and ALB3 gene inactivation in *Arabidopsis*, *Chlamydomonas reinhardtii*, and *Synechocystis* sp. PCC 6803 results in severe phenotypes (Sundberg et al., 1997; Bellafiore et al., 2002; Spence et al., 2004). In chloroplasts, ALB3 proteins have been shown to interact with D1, D2, and CP47, as well as with subunits from photosystem I (PSI) and the ATP synthase (Ossenbühl et al., 2004; Pasch et al., 2005; Göhre et al., 2006), whereas the *Synechocystis* ALB3 ortholog has been proposed to play a role in the integration of pD1 into the membrane (Ossenbühl et al., 2006). The gene for HCF136 was identified in the *Arabidopsis* high chlorophyll fluorescence mutant *hcf136*, which contains

only traces of PSII but synthesizes PSII subunits at normal rates (Meurer et al., 1998). HCF136 predominantly associates with a very early PSII assembly complex containing D2, PsbE, and PsbF (Plücker et al., 2002), and YCF48, the *Synechocystis* HCF136 homolog, has been detected in RC, where it interacts with unassembled pD1 (Komenda et al., 2008). In *Arabidopsis*, LPA1 binds to D1 during de novo biogenesis of PSII (Peng et al., 2006), whereas its *Chlamydomonas* ortholog, REP27, has also been suggested to play a role in D1 synthesis, albeit during PSII repair rather than during assembly (Park et al., 2007; Dewez et al., 2009). The *Arabidopsis* LPA2, which has no counterpart in cyanobacteria or *Chlamydomonas*, interacts specifically with CP43 and ALB3 (Ma et al., 2007).

In this study, we describe the identification and characterization of PAM68, a protein required for normal accumulation of PSII in *Arabidopsis*. The thylakoid protein PAM68, like HCF136 and ALB3, is conserved in cyanobacteria and photosynthetic eukaryotes. PAM68 also interacts with these two proteins, as well as with several structural subunits of PSII and further PSII assembly factors. Our data imply that PAM68 is a previously undiscovered PSII assembly factor that acts at the level of D1 maturation and stability, promoting the transition from the RC assembly state to larger PSII assembly complexes. In *Synechocystis*, inactivation of the homolog of PAM68, SlI0933, has less severe effects on photosynthesis and prevents accumulation of RC to detectable levels under steady state conditions, indicating that lack of PAM68 is differently compensated for in plants and cyanobacteria.

## RESULTS

### Mutations in PAM68 Severely Affect Growth Rate and PSII Function

Screening of the *Arabidopsis* GABI-KAT T-DNA insertion collection (Rosso et al., 2003) for lines that show alterations in  $\Phi_{II}$ , the effective quantum yield of PSII, resulted in the recovery of a set of mutants with defects in photosynthesis (Varotto et al., 2000a, 2000b). In the line GABI\_152D07, renamed as the *photosynthesis affected mutant 68-1* (*pam68-1*),  $\Phi_{II}$  was drastically reduced (Table 1), and this character segregated as a recessive trait. Moreover, homozygous *pam68-1* mutant plants had pale-green cotyledons and leaves (Figure 1A). Analysis of chlorophyll a fluorescence showed a clear increase in the minimum fluorescence ( $F_0$ ; Figure 1A) and a dramatic decrease in maximum quantum yield of PSII ( $F_v/F_m$ ; Figure 1A, Table 1). This combination is characteristic for mutants with abnormally low levels of PSII, such as *hcf136* (Meurer et al., 1998), *lpa1* (Peng et al., 2006; see Supplemental Figure 1 online), and *lpa2* (Ma et al., 2007) mutants. Closer inspection of the chlorophyll a fluorescence induction curves employed to determine  $F_v/F_m$  and  $\Phi_{II}$  showed that, in *pam68-1*, chlorophyll a fluorescence transiently dropped below  $F_0$  after the initial rise induced by exposure to actinic light (Figure 1B). This too is typical of mutants in which the ratio PSII/PSI is reduced (Meurer et al., 1998; Peng et al., 2006; Ma et al., 2007; see Supplemental Figure 1 online for *lpa1-2*) and can be attributed to the higher initial activity of PSI relative to PSII.

**Table 1.** Parameters of Chlorophyll *a* Fluorescence in Mutant (*pam68-1*, *pam68-2*, and *lpa1-2*) and Corresponding Wild-Type (Col-0 and *Ler*) Leaves

Parameter	<i>pam68-1</i>	<i>pam68-2</i>	Col-0	<i>lpa1-2</i>	<i>Ler</i>
$F_v/F_m$	0.44 ± 0.01	0.45 ± 0.02	0.83 ± 0.01	0.56 ± 0.01	0.83 ± 0.01
$\Phi_{II}$	0.28 ± 0.01	0.29 ± 0.02	0.72 ± 0.00	0.42 ± 0.02	0.72 ± 0.01
1-qP	0.24 ± 0.03	0.23 ± 0.02	0.09 ± 0.01	0.13 ± 0.03	0.09 ± 0.01
NPQ	0.13 ± 0.02	0.14 ± 0.01	0.18 ± 0.03	0.11 ± 0.00	0.21 ± 0.01

At least five leaves from different plants were measured. Actinic light intensity was 80  $\mu\text{mol photons m}^{-2} \text{s}^{-1}$ .  $F_v/F_m$ , maximum quantum yield of PSII;  $\Phi_{II}$ , effective quantum yield of PSII; 1-qP, excitation pressure; NPQ, nonphotochemical quenching. Mean values  $\pm$  SD are provided.

DNA gel blot analysis of a population of 30 plants segregating for the *pam68-1* mutation using the 5'-end of the AC106 T-DNA as a probe revealed the presence of only one T-DNA copy, which cosegregated with the *pam68-1* phenotype. A DNA fragment flanking the left border of the T-DNA was isolated and was found to be identical to the second exon of the *At4g19100* gene (Figure 1C). A second line with a T-DNA insertion in this gene, *pam68-2*, was obtained from the SALK T-DNA insertion collection (Alonso et al., 2003). The *pam68-2* plants behaved like the *pam68-1* line with respect to growth, leaf coloration, and chlorophyll *a* fluorescence parameters (Table 1) and induction curve characteristics (Figures 1A and 1B), confirming that disruption of *At4g19100* is responsible for the observed *pam68* phenotypes.

The effect of the T-DNA insertions on the expression of *PAM68* was monitored by RNA gel blot analysis. In *pam68-1*, few *PAM68/At4g19100* transcripts with increased size were detected, whereas transcripts were undetectable in the *pam68-2* allele (Figure 1D). To quantify the effect of loss of *PAM68* function on growth behavior, we compared mutant and wild-type plants using noninvasive image analysis (Leister et al., 1999). Even under optimal greenhouse conditions, the leaf area of the mutants was reduced by  $\sim 90\%$  relative to the wild type at 28 d after germination (Figure 1E). Because the two *pam68* alleles behaved very similarly in all analyses, the *pam68-2* allele was used in the following experiments. To evaluate quantitatively the altered coloration of *pam68-2* leaves, leaf pigments were analyzed by HPLC. As expected, the mutant contained only 65% of wild-type levels of total chlorophyll (chlorophyll *a* + *b*) (*pam68-2*, 1339  $\pm$  123; Columbia-0 [Col-0], 2060  $\pm$  180 nmol/g fresh weight). The chlorophyll *a/b* ratio was slightly decreased (*pam68-2*, 2.7; wild type, 3.1), indicating either a higher PSII/PSI ratio or, more probably in light of the chlorophyll *a* fluorescence analyses described above, an increase in the size of the peripheral antenna relative to the chlorophyll *a* binding reaction centers.

Taken together, the data suggest that disruption of *PAM68/At4g19100* affects photosynthetic electron flow, particularly at the level of PSII, resulting in severely reduced growth rates and altered leaf pigment composition.

#### Relative Levels of PSII Subunits Are Perturbed in *pam68-2* Plants

To determine whether the defect in PSII activity found in the *pam68* mutants reflects a reduction in the abundance of PSII subunits, and to assess the levels of representative members of other thylakoid multiprotein complexes, immunoblot analyses were performed on total protein extracts from leaves. Marked

reductions in the levels of the PSII core subunits D1, D2, CP43, CP47, and PsbE, to about  $\sim 10$ ,  $\sim 10$ ,  $\sim 15$ ,  $\sim 15$ , and  $\sim 30\%$  of those seen in the wild type, respectively, were indeed observed on the basis of estimating the intensity of mutant signals relative to the ones of different dilutions of wild-type samples (Figure 2A). PsbO (a subunit of the oxygen-evolving complex) was reduced to  $\sim 40\%$  of wild-type levels, Lhcb1 (a subunit of LHCII) to 80%, and the B subunit of PSI (PsaB) and Cyt *f* (part of the Cyt *b<sub>6</sub>/f* complex) to  $\sim 70\%$ . Only the chloroplast ATPase  $\beta$ -subunit appeared to show an increase relative to the wild type (Figure 2A). Interestingly, in *pam68-2*, two distinct D1 bands were obtained, representing the precursor (pD1) and mature (mD1) forms of the protein (Figure 2A). To clarify whether pD1 is indeed overrepresented in *pam68-2* thylakoids, total protein extracts containing similar amounts of total D1 protein were compared (wild type, 8 and 4  $\mu\text{g}$ ; *pam68-2*, 40 and 80  $\mu\text{g}$  of total leaf protein) and signal intensities quantified (see Methods) (Figure 2B). In the wild type, the pD1/mD1 ratio was  $\sim 0.15$ , but in *pam68-2*, it was  $\sim 0.85$ , indicating that processes which trigger conversion of pD1 into mD1 are affected in the mutant.

Taken together, our results imply that the phenotype of *pam68-2* plants is attributable primarily to changes in steady state concentrations of PSII proteins. In particular, levels of PSII core subunits are much lower than in the wild type, while the pD1/mD1 ratio is much higher.

#### Absence of *PAM68* Affects the Maturation and Stability of Newly Synthesized D1

To investigate whether the fall in steady state levels of PSII proteins in *pam68-2* is caused by a decrease in de novo synthesis of its plastid-encoded subunits, rates of synthesis of thylakoid membrane proteins were analyzed by in vivo pulse labeling experiments. The results for *pam68-2* leaves were compared with those obtained for another PSII mutant, *lpa1-2* (see Supplemental Figure 1 online). The labeling experiments with [ $^{35}\text{S}$ ]Met were performed under low light (20  $\mu\text{mol photons m}^{-2} \text{s}^{-1}$ ) on leaves from greenhouse-grown plants to avoid activating the PSII repair cycle, which would lead to preferential labeling of the D1 protein (Figure 3A). In the presence of cycloheximide to block synthesis of nucleus-encoded proteins, newly translated chloroplast-encoded proteins were labeled for 20 min and thylakoid proteins were isolated. In both mutant genotypes, rates of synthesis of the PSII core proteins CP43 and CP47, as well as the  $\alpha$ - and  $\beta$ -subunits of the cpATPase, were almost unchanged relative to the respective wild-type rates. However, incorporation of [ $^{35}\text{S}$ ]Met into D1 + D2 was reduced to  $\sim 60$  and

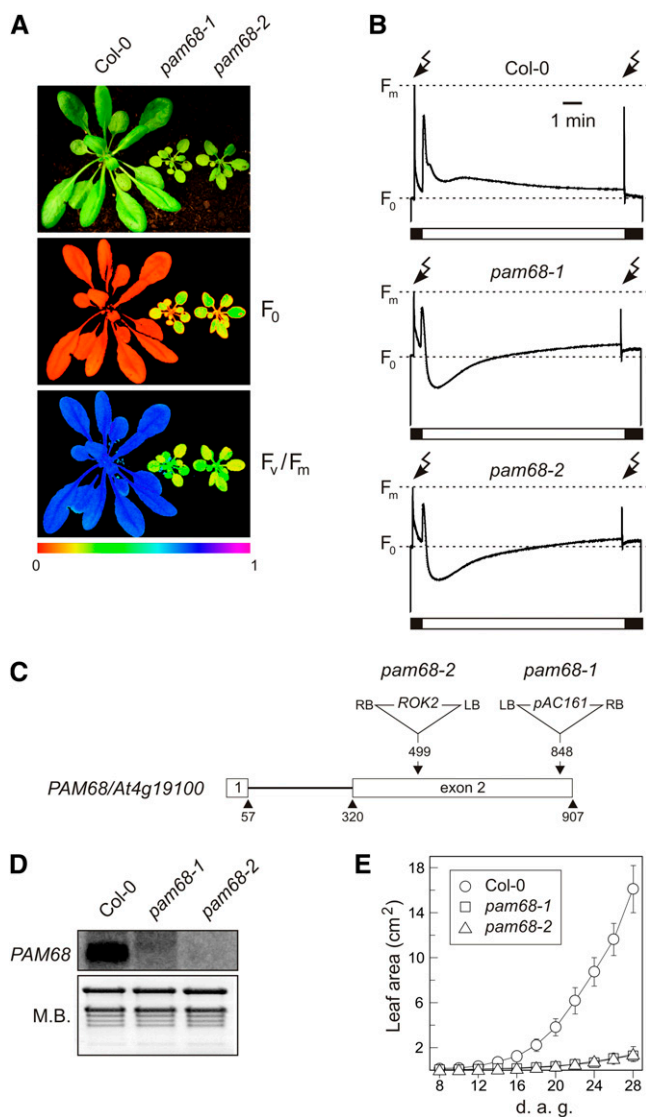


**Figure 1.** Identification and Characterization of the Mutants *pam68-1* and *pam68-2*.

**(A)** Five-week-old wild type (Col-0) and mutant (*pam68-1* and *pam68-2*) plants were grown in the greenhouse (top panel), and the photosynthetic parameters  $F_0$  (minimum chlorophyll a fluorescence) and  $F_v/F_m$  (maximum quantum yield of PSII) were measured as described in Methods. Signal intensities for  $F_0$  and  $F_v/F_m$  are indicated in accordance with the color scale at the bottom of the figure.

**(B)** Chlorophyll a fluorescence induction curves of wild-type (Col-0) and mutant (*pam68-1* and *pam68-2*) leaves. The white bar indicates exposure to actinic light ( $80 \mu\text{mol photons m}^{-2} \text{s}^{-1}$ ) and the lightning symbols the application of saturation light pulses ( $0.8 \text{ s}$ ;  $5000 \mu\text{mol photons m}^{-2} \text{s}^{-1}$  white light).  $F_0$  and  $F_m$  are indicated for each genotype.

**(C)** T-DNA tagging of the *PAM68/At4g19100* locus. Exons are numbered and shown as white boxes and the intron as a black line. Locations and orientations of T-DNA insertions are indicated. The *pam68-1* allele was found in the GABI-KAT line GABI\_152D07; *pam68-2* corresponds to the SALK\_044323 line from the SALK collection. Note that the T-DNAs are not drawn to scale.

**(D)** Effect of the T-DNA insertions on steady state levels of *PAM68* RNA.

35% of wild-type levels in *pam68-2* and *lpa1-2* mutant plants, respectively, on the basis of quantification of signal intensities (see Methods) (Figure 3A). Moreover, and in contrast with *lpa1-2*, in *pam68-2*, the D1 + D2 band was slightly shifted toward higher molecular weight products (Figure 3A). In fact, immunoblot analysis (see Supplemental Figure 2 online) allowed the conclusion that the position of the upper band in *pam68-2* corresponds to the position of the signals for pD1 and D2, whereas the lower signal should exclusively derive from mD1. To clarify whether the drop in the accumulation of labeled D1 + D2 was caused by a decrease in synthesis or by rapid degradation of newly synthesized D1 proteins, shorter pulse times (5 and 15 min) were applied (Figure 3B). In all cases, markedly less radioactivity was incorporated into D1 + D2 in *pam68-2* plants relative to the wild type. These results imply either that D1 + D2 synthesis is impaired or that newly synthesized D1 + D2 polypeptides are very rapidly degraded.

To minimize further any secondary effects on chloroplast translation due to the reduction in photosynthesis in the *pam68-2* mutants, labeling experiments were performed under very low light ( $5 \mu\text{mol photons m}^{-2} \text{s}^{-1}$ ) on leaves from heterotrophically grown Col-0 and *pam68-2* plants (Figure 3C). Labeling was performed for 60 min to visualize better the synthesis of thylakoid proteins other than D1. Whereas rates of synthesis of the PSI reaction center PsaA/B proteins and PSII core proteins CP43 and CP47, as well as the  $\alpha$ - and  $\beta$ -subunits of the cpATPase, were at most barely affected, incorporation of [<sup>35</sup>S] Met into the PSII subunit D1 + D2 was reduced to  $\sim 70\%$  of wild-type levels in the *pam68-2* mutant on the basis of quantification of signal intensities (Figure 3C). Once again, in *pam68-2*, but not in Col-0, a prominent signal for pD1 + D2 was detected. To quantify unambiguously the effect of the *pam68-2* mutation on the rate of D1 synthesis, immunoprecipitation of the translation products employing a D1-specific antibody was performed. This experiment confirmed that D1 synthesis in *pam68-2* was severely reduced and corresponded to  $\sim 50\%$  of wild-type levels, based on quantification of signal intensities (Figure 3D). This also implies that the upper band in Figures 3A and 3C mostly derives from pD1.

The drop in accumulation of newly synthesized D1 in the *pam68-2* mutant could be due to a defect in translation, in posttranslational processing of pD1 and/or a decrease in the stability of D1. To distinguish between these possibilities, levels of total and polysome-associated chloroplast transcripts encoding PSII subunits were analyzed. RNA gel blot analysis revealed that the *psbA* transcript encoding the D1 protein was present at wild-type levels in *pam68-2* leaves (Figure 3E). The levels of the polycistronic *psbEFJL* transcript and the *psbC* transcript

Aliquots ( $30 \mu\text{g}$ ) of total leaf RNA were fractionated on a denaturing agarose gel, transferred to a positively charged nylon membrane, and hybridized with a *PAM68* cDNA probe. rRNA was stained with methylene blue (M.B.) as a loading control.

**(E)** Growth kinetics of wild type (Col-0) and mutant (*pam68-1* and *pam68-2*) plants ( $n \geq 10$ ). Leaf area was measured during the period from 8 to 28 d after germination (d.a.g.). Bars indicate SD.

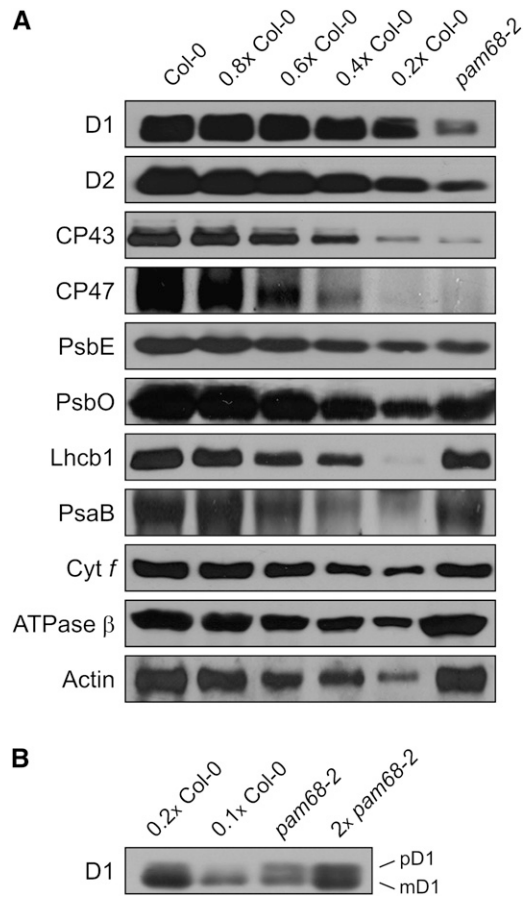


**Figure 2.** Immunoblot Analysis of Representative Thylakoid Proteins.

**(A)** Total leaf proteins from *pam68-2* and wild-type (Col-0) plants were fractionated by SDS-PAGE, and blots were probed with antibodies raised against individual subunits of PSII (D1, D2, CP43, CP47, PsbE, and PsbO), LHCII (Lhcb1), PSI (PsaB), the Cyt *b<sub>6</sub>/f* complex (Cyt *f*) and the chloroplast ATP synthase ( $\beta$ -subunit). Decreasing levels of wild-type proteins were loaded in the lanes marked 0.8x Col-0, 0.6x Col-0, 0.4x Col-0, and 0.2x Col-0. Actin served as loading control.

**(B)** Total leaf protein extracts containing similar amounts of total D1 protein were loaded (wild type, 4 and 8  $\mu$ g; *pam68-2*, 40 and 80  $\mu$ g of protein), fractionated and treated as in **(A)**. pD1, precursor D1; mD1, mature D1.

resembled those in the wild type, whereas the amounts of *psbB* mRNA encoding CP47 were increased and the polycistronic *psbCD* transcript was slightly decreased (Figure 3E). The effects of the *pam68-2* mutation on the translation of the *psbA* transcript were further examined by analyzing the association of *psbA* mRNA with ribosomes. To this end, whole-cell extracts from Col-0 and *pam68-2* plants leaves were fractionated in sucrose gradients under conditions that keep polysomes intact. Efficiently translated RNAs are almost all associated with ribosomes and migrate deep into the gradient. Plastidic and cytosolic rRNAs in wild-type and *pam68-2* polysome gradients showed an equal distribution, as determined by methylene blue staining and quantification of signals, indicating that there is no general

difference in the distribution of ribosomes between the two genotypes (Figure 3F). Specific mRNAs were localized in the gradients by performing RNA gel blot hybridizations with RNA purified from gradient fractions. In both genotypes, the distribution of *psbA* mRNA within the gradient was very similar. For the *psbCD* polycistronic transcript also, no difference in degree of association with polysomes was detected between the two genotypes (Figure 3F).

Therefore, our data suggest that the reduction in synthesis of D1 does not result from a decrease in the availability of *psbA* transcripts or from altered translation initiation in terms of their loading onto polysomes. Instead, (1) stability of the D1 protein is specifically affected in the *pam68-2* mutant; (2) the defect in D1 accumulation in *pam68-2* is less pronounced than that found in the *lpa1-2* mutant, which is impaired in the synthesis of D1 and D2 (Peng et al., 2006); and (3) the drastic accumulation of pD1 is characteristic for *pam68-2* but not for *lpa1*.

### Formation and Stability of PSII Assembly Complexes Are Perturbed in *pam68-2* Plants

To investigate the effects of altered D1 levels on the biogenesis of PSII, Blue-Native PAGE (BN-PAGE) analysis was performed. Thylakoids were prepared from equal amounts of leaf material and solubilized with *n*-dodecyl  $\beta$ -D-maltoside ( $\beta$ -DM) (Schägger et al., 1988), and proteins were separated in the presence of Coomassie blue G 250. Nine prominent bands were resolved and assigned to thylakoid multiprotein complexes based on earlier reports (Granvogl et al., 2006; Schwenkert et al., 2006; Peng et al., 2008) as follows: PSI-NDH supercomplex (band I), PSII supercomplexes (bands II and III), PSI monomers and PSII core dimers (band IV), PSII core monomers and Cyt *b<sub>6</sub>/f* dimers (band V), multimeric LHCII (band VI), CP43-free PSII monomers (band VII), and trimeric (band VIII) and monomeric (band IX) LHCII (Figure 4A). Only the signals for LHCII monomers and trimers, and for the PSI-NDH supercomplex, showed similar intensities in wild-type and *pam68-2* mutant plants. All other bands were markedly weaker in the mutant (Figure 4A).

The complexes resolved by BN-PAGE were then separated into their subunits in the second dimension by electrophoresis on SDS-PAGE gels and stained with Coomassie blue G 250 (Figure 4B). In *pam68-2* plants, levels of the chloroplast ATP synthase, Cyt *b<sub>6</sub>/f*, and LHCII were equivalent to those in the wild type; amounts of PSI-forming proteins were slightly lower (Figure 4B). As expected (Figure 2A), the amounts of the PSII core subunits D1, D2, CP43, and CP47 were drastically reduced in the mutant. CP43-free PSII monomers (band VII), as well as PSII monomers (band V) and dimers (band IV), were still detectable, but PSII supercomplexes (bands II and III) were not found in *pam68-2* plants (Figures 4A and 4B). The two-dimensional (2D) BN/SDS-PAGE analysis also revealed that *pam68-2* plants contain a stable PSI-LHCII supercomplex (designated as band IIa), which migrates in the same region as band III. This PSI-LHCII supercomplex can be formed when the plastoquinone pool becomes overreduced (Pesaresi et al., 2002, 2009; Ilnatowicz et al., 2008). Although 1-qP, a standard measure for the reduction state of plastoquinone, was indeed found to be increased in *pam68-2* plants (Table 1), it is more likely that the plastoquinone pool is

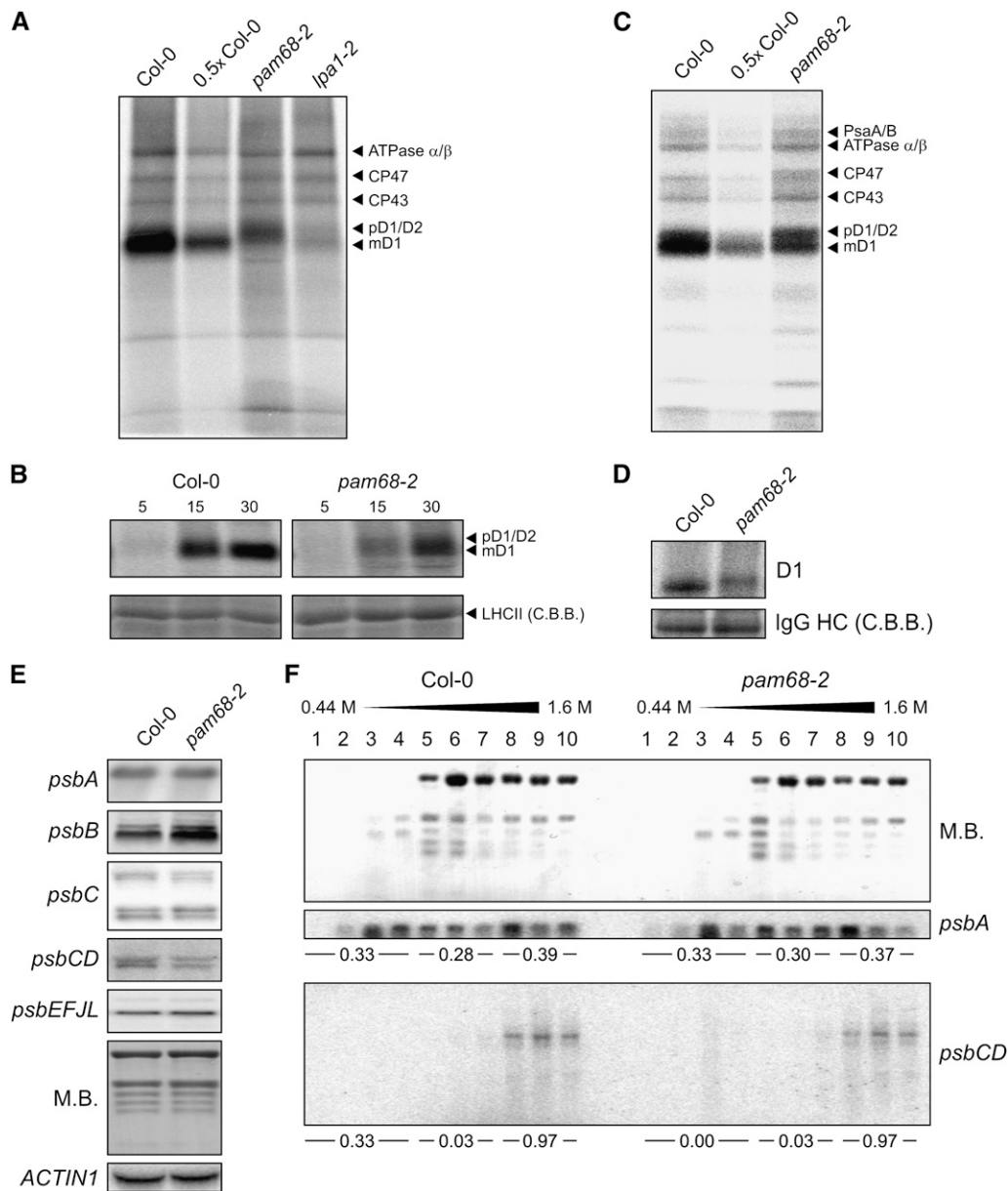


**Figure 3.** Translation Profiling of Chloroplast-Encoded Proteins.

**(A)** Incorporation of [ $^{35}\text{S}$ ]Met into thylakoid membrane proteins of 4-week-old greenhouse-grown wild-type (Col-0) and mutant (*pam68-2* and *lpa1-2*) plants at low light ( $20 \mu\text{mol photons m}^{-2} \text{s}^{-1}$ ). After pulse labeling of leaves with [ $^{35}\text{S}$ ]Met for 20 min in the presence of cycloheximide, thylakoid membranes were isolated, and proteins were fractionated by SDS-PAGE and detected by autoradiography. In *pam68-2* and *lpa1-2*, incorporation of [ $^{35}\text{S}$ ]Met into D1 was reduced to  $61\% \pm 3\%$  and  $35\% \pm 7\%$  of wild-type levels, respectively, as determined by quantification of the intensity of signals shown here and of three further repetitions of the experiment. Note that *Ler*, the genetic background of *lpa1-2*, behaved like Col-0.

**(B)** Incorporation of [ $^{35}\text{S}$ ]Met into thylakoid membrane proteins of 4-week-old wild-type (Col-0) and mutant (*pam68-2*) plants as in **(A)**, except that pulses of 5, 15, and 30 min were applied. As loading control, nonlabeled LHCII was visualized by staining with Coomassie blue (C.B.B.).

**(C)** Incorporation of [ $^{35}\text{S}$ ]Met into thylakoid membrane proteins of 4-week-old wild-type (Col-0) and mutant (*pam68-2*) plants grown heterotrophically (see Methods) under very low light levels ( $5 \mu\text{mol photons m}^{-2} \text{s}^{-1}$ ). Pulse labeling for 60 min and signal detection were performed as in **(A)**.

**(D)** SDS-solubilized membrane proteins with the equivalent of 200,000 incorporated cpm were used for immunoprecipitation with a D1-specific antibody (see Methods). As loading control, IgG heavy chains (HC) were visualized by staining with Coomassie blue. Incorporation of [ $^{35}\text{S}$ ]Met into D1 was reduced to  $53\% \pm 4\%$  of wild-type levels, as determined by quantification of the intensity of signals shown here and of two further repetitions of the experiment.

**(E)** Transcript analysis in wild-type (Col-0) and mutant (*pam68-2*) plants. Ten-microgram aliquots of total leaf RNA from 4-week-old plants were fractionated by denaturing agarose gel electrophoresis, blotted onto nylon membrane, and hybridized with probes specific either for the first 500 bp of

more oxidized because of the marked drop in PSII abundance relative to PSI in the mutant (Figure 2A). Therefore, it appears plausible that the relative abundance of LHCII with respect to PSII (Figures 2A, 4A, and 4B) should favor increased docking of LHCII to PSI.

To investigate further the changes in the PSII assembly process in the *pam68-2* mutant, immunoblot analysis with antibodies directed against several PSII core subunits (D1, D2, PsbE, PsbI, CP47, and CP43) was performed on replicate 2D BN/SDS-PAGE gels (Figure 4C), and signals were quantified (Figure 4D). This analysis confirmed that PSII supercomplexes were virtually absent and PSII dimers were drastically reduced in amount, relative to PSII monomers and CP43-free PSII monomers. In addition, an increase in free PSII proteins was observed. Moreover, the PSII assembly intermediate RC, which comprises pD1, D2, PsbE, PsbF, and PsbI (Rokka et al., 2005), was detected, migrating just below the LHCII trimers (band VIII). Compared with the wild type, about twice as much pD1, D2, PsbE, and PsbI was present in the *pam68-2* RC complex (Figures 4C and 4D). Interestingly, in the *lpa1-2* mutant, PSII monomers and CP43-free PSII monomers are the predominant PSII assembly states, and RC does not accumulate to the same degree as in *pam68-2* (see Supplemental Figure 1 online; Figure 4D). Moreover, PSII supercomplexes are detectable in the *lpa1-2* line, but not in *pam68-2* (see Supplemental Figure 1 online; Figure 4D).

To study the kinetics of PSII assembly, thylakoid membrane proteins from Col-0, *pam68-2*, and *lpa1-2* plants were separated by 2D BN/SDS-PAGE after labeling with [<sup>35</sup>S]Met for 20 min (Figure 5A), as well as after a subsequent 30-min chase with unlabeled Met (Figure 5B). The various PSII assembly intermediates, RC, CP43-free PSII monomers (CP43-PSII), PSII monomers, dimers, and supercomplexes, as well as free PSII proteins, were visualized autoradiographically (Figures 5A and 5B) and quantified (Figure 5C). After pulse labeling, in Col-0 and *lpa1-2*, most of the assembled radiolabeled D1 was found in PSII monomers and CP43-PSII, and the two genotypes differed only with respect to free unassembled D1 protein, the level of which was about sevenfold higher in *lpa1-2*. Strikingly, the *pam68-2* mutant exhibited a sixfold increase (relative to the wild type) in newly synthesized RC, which clearly contained pD1 instead of mD1 (Figures 5A and 5C). After the chase, the relative abundance of CP43-PSII and PSII monomers and dimers was increased in *pam68-2* plants at the expense of RC, suggesting that the mutant RC complex was assembled into larger PSII intermediates (Figure 5C). When the relative accumulation of PSII

intermediates under steady state conditions was also considered (Figure 4D), it became clear that the PSII assembly in *pam68-2* plants is delayed. Thus, directly after pulse labeling, radiolabeled D1 was found predominantly in the RC complex in *pam68-2* plants, whereas Col-0 and *lpa1-2* showed labeling in PSII monomers and CP43-PSII. After the chase, *pam68-2* plants showed labeled D1 mostly in CP43-less monomers, while Col-0 and *lpa1-2* had mostly labeled PSII monomers and CP43-PSII. Under steady state conditions, the predominant PSII intermediates, as determined by immunoblot analyses (Figures 4C and 4D), were PSII monomers and CP43-PSII in *pam68-2* plants, PSII monomers and dimers in Col-0, and PSII monomers and CP43-PSII in *lpa1-2* (Figure 5C).

The discrepancy between the sixfold increase in the synthesis of RC and the only twofold increase under steady state conditions on one side (Figures 4D and 5C) and between the rate of D1 synthesis of 60% of wild-type levels versus only 10% of wild-type accumulation under steady state conditions on the other side (Figures 2A and 3A) clearly suggests a decrease in the stability of pD1 or D1 in *pam68-2* plants. In fact, quantification of the signals of D1 + D2 obtained in pulse-chase experiments as shown in Figures 5A and 5B indicated that D1 degradation already occurs during 30 min of chase (see Supplemental Figure 3A online). Moreover, the half-life of D1 in *pam68-2* plants is much shorter than that of wild-type D1, as determined by time-course experiments with plants treated with lincomycin (see Supplemental Figure 3B online).

Taken together, our results imply that in *pam68-2* plants, the assembly of PSII is delayed. The assembly step leading from RC to larger PSII assembly intermediates seems to be impaired in *pam68-2*, as RC accumulates together with pD1 (see Figures 5A to 5C). However, the finding that CP43-less PSII monomers and PSII monomers, and not RC, are the predominant forms of PSII under steady state conditions (Figures 4C and 4D), along with the decreased stability of D1 in the mutant (see Supplemental Figure 3 online), leads to the conclusion that a fraction of the RC complex becomes disassembled and degraded in *pam68-2*. This interpretation is corroborated by the observation that the accumulation of free PSII proteins is increased. The marked drop in steady state levels of PSII dimers and PSII supercomplexes observed in *pam68-2* (Figures 4C and 4D) follows their lowered synthesis rates, as determined by *in vivo* labeling (Figure 5). This effect on late steps in PSII assembly is most likely the consequence of the decreased availability of the early assembly states due to delayed transition of RC into later assembly intermediates.

**Figure 3.** (continued).

the coding region (*psbA*, *psbB*, *psbC*, and *psbD*) or the complete sequence (*psbE*) of the transcript. Note that the *psbC* probe recognizes both *psbC* (bottom bands) and *psbCD* (top bands) transcripts, the *psbD* probe detects the bicistronic *psbCD* transcripts (corresponding to the top two bands of the *psbC* probed membrane), and *psbE* labels *psbEFJL* transcripts. To control for loading, replicate blots were stained with methylene blue (M.B.) and hybridized with a probe specific for *ACTIN1*.

**(F)** Association of *psbA* and *psbD* mRNAs with polysomes. Whole-cell extracts from Col-0 and *pam68-2* plants were fractionated in linear 0.44 to 1.6 M (15 to 55%) sucrose gradients by ultracentrifugation. Gradients were divided into 10 fractions, and RNA was isolated from equal volumes. RNA gel blots were stained with methylene blue (M.B.) to visualize the distribution of rRNAs and then hybridized with probes specific for *psbA* and *psbD* (recognizing *psbCD* polycistronic transcripts). Signals were quantified (see Methods), and relative values of fractions 1 to 4, 5 to 7, and 8 to 10 calculated and given below the *psbA* and *psbCD* panels.

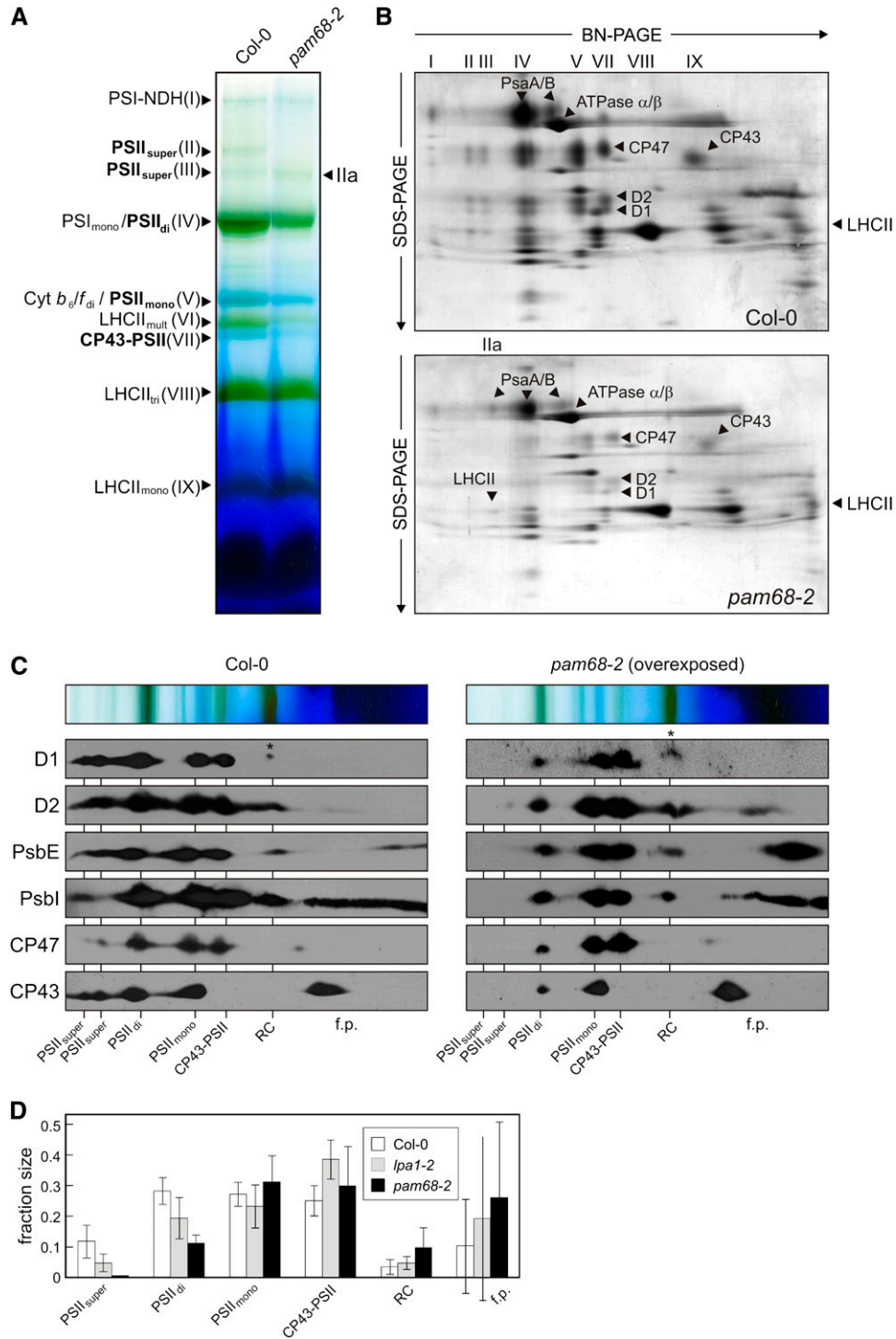


**Figure 4.** Accumulation of PSII Assembly Complexes under Steady State Conditions.

**(A)** BN-PAGE analysis of thylakoid multiprotein complexes. Thylakoids were isolated from equal amounts of fresh leaf material (100 mg) obtained from wild-type (Col-0) and mutant (*pam68-2*) plants and solubilized with 1.5% (w/v)  $\beta$ -DM. The extracts were then fractionated by BN-PAGE. The bands detected were identified with specific protein complexes in accordance with previously published profiles (Granvogl et al., 2006; Schwenkert et al., 2006; Peng et al., 2008): PSI-NDH supercomplex (PSI-NDH; band I), PSII supercomplexes (PSII<sub>super</sub>; bands II and III), PSI-LHCII complex (band Ila), PSI monomers and PSII dimers (PSI<sub>mono</sub> and PSII<sub>di</sub>; band IV), PSII monomers and dimeric Cyt *b<sub>6</sub>/f* (PSII<sub>mono</sub> and Cyt *b<sub>6</sub>/f<sub>d</sub>*; band V), multimeric LHCII (LHCII<sub>mult</sub>; band VI), CP43-free PSII monomers (CP43-PSII; band VII), trimeric LHCII (LHCII<sub>tri</sub>; band VIII), and monomeric LHCII (LHCII<sub>mono</sub>; band IX). PSII

Furthermore, because the *lpa1-2* mutant, which shows a more pronounced drop in levels of newly synthesized D1 than does *pam68-2* (Figure 3A), does not display a *pam68*-like increase in RC accumulation (Figure 5C), it can be concluded that PAM68 and LPA1 exert different functions on the assembly of D1 into PSII.

### PAM68 Is Conserved in Photosynthetic Eukaryotes and Cyanobacteria

PAM68 encodes a protein of 214 amino acids with a predicted molecular mass of 24.3 kD. The ChloroP program (see Methods) predicts a chloroplast targeting signal of 35 amino acids, resulting in a mature protein of 20.3 kD (Figure 6). Orthologs of PAM68 exist in all sequenced photosynthetic eukaryotes and cyanobacteria. For instance, the mature *Arabidopsis* PAM68 protein and its cyanobacterial orthologs in *Synechocystis* and *Synechococcus* share 42/61% and 38/55% amino acid sequence identity/similarity, respectively. Even higher levels of homology were found between *Arabidopsis* PAM68 and its orthologs in photoautotrophic eukaryotes, ranging from 43/67% identity/similarity in *C. reinhardtii* to 76/89% identity/similarity in *Ricinus communis*. In addition, the product of the *At5g52780* gene in *Arabidopsis* shares 38/58% sequence identity/similarity with PAM68.

All PAM68 proteins contain two transmembrane domains (TMs), as predicted by the TMHMM program (see Methods) (Figure 6; amino acids 126 to 145 and 155 to 177 for PAM68). In addition, the PAM68 proteins in vascular plants contain an N-terminal stretch composed of acidic amino acids only, which is referred to in the following as the acidic domain. The PAM68 sequences of *Physcomitrella*, *Synechocystis*, *Synechococcus*, and the *Arabidopsis* At5g52780 homolog at least partially lack this acidic domain.

Two lines of evidence argue against the idea that PAM68 and At5g52780 have redundant functions in *Arabidopsis*. First, the acidic domain is not conserved in At5g52780 (see above) and, second, PAM68 and At5g52780 do not derive from a recent segmental duplication in the genome of the *Arabidopsis* lineage (*Arabidopsis* Paralogon database; <http://wolfe.gen.tcd.ie/athal/dup>; Blanc et al., 2003). To clarify unambiguously whether At5g52780 and PAM68 encode proteins with overlapping functions, the At5g52780 T-DNA insertion mutant SALK\_143426, designated *at5g52780-1*, was identified in the SALK collection

and characterized (see Supplemental Figure 4 online). The *at5g52780-1* mutant plants totally lacked the At5g52780 protein, as revealed by immunoblot analysis with an antibody specific for the protein, and displayed wild-type-like growth rate and leaf coloration. Moreover, *at5g52780-1* chloroplasts showed wild-type-like levels of the D1 protein. A *pam68-2 at5g52780-1* double mutant was generated by crossing and found to behave like *pam68-2* plants with respect to growth rate, leaf coloration, and accumulation of the D1 protein (see Supplemental Figure 4 online). This clearly indicates that PAM68 and At5g52780 do not exercise redundant functions.

### *Synechocystis* PAM68 Also Promotes Early Steps in PSII Biogenesis

To test whether the function of PAM68 was conserved during evolution, *SII0933*, the PAM68 ortholog from *Synechocystis* sp PCC 6803 (hereafter, *Synechocystis*), was disrupted by insertion of a kanamycin resistance cassette (see Supplemental Figure 5A online). The resulting mutant *ins0933* showed complete segregation of the mutated gene (see Supplemental Figure 5B online), and the absence of the SII0933 protein was verified by immunoblot analysis using an SII0933-specific antibody (see Supplemental Figure 5C online). The *ins0933* mutant grew like the wild type under both mixotrophic and photoautotrophic conditions (see Supplemental Figure 5D online). No differences between the wild type and *ins0933* were observed in fluorescence emission spectra at low temperature (77K); immunoblot analyses likewise revealed no changes in levels of PSII and PSI subunits (see Supplemental Figures 5C and 5E online). Furthermore, light-dependent oxygen evolution was very similar in *ins0933* and the wild type (*ins0933*,  $1490 \pm 54 \mu\text{mol O}_2 \text{ mg Chl}^{-1} \cdot \text{h}^{-1}$ ; wild type,  $1440 \pm 55 \mu\text{mol O}_2 \text{ mg Chl}^{-1} \cdot \text{h}^{-1}$ ). This indicates that SII0933 is less important for efficient photosynthesis than is its plant counterpart PAM68. In *ins0933*, late PSII assembly complexes were present in normal amounts, but the PSII reaction center complexes RCa and RCb, which in wild-type cells contain pD1, mD1, D2, PsbE, PsbF, and PsbI and probably different associated assembly factors (reviewed in Nixon et al., 2010), were not detectable by 2D BN/SDS-PAGE analysis (Figure 7). Moreover, in wild-type cells, the SII0933 protein was detected in complexes corresponding in molecular weight to early PSII assembly intermediates (Figure 7).

#### Figure 4. (continued).

assembly complexes are highlighted in bold.

(B) 2D BN/SDS-PAGE separation of thylakoid protein complexes. Individual lanes from BN-PA gels as in (A) were analyzed in the presence of SDS by electrophoresis on 10 to 16% PA gradient gels, which were then stained with colloidal Coomassie blue (G 250). The identity of relevant proteins is indicated by arrows.

(C) Detection of PSII assembly complexes by immunoblot analyses of 2D BN/SDS gels as in (B) with antibodies against D1, D2, PsbE, PsbI, CP47, and CP43. The positions of PSII assembly complexes (PSII<sub>super</sub>, PSII supercomplexes; PSII<sub>di</sub>, PSII dimers; PSII<sub>mono</sub>, PSII monomers; CP43-PSII, CP43-free PSII monomers; RC, reaction center-like complex) and free proteins (f.p.) are indicated. Signals were obtained by chemiluminescence. Exposure times were ~2 min (wild type) and ~10 min (mutant). Accumulation of pD1 is indicated by asterisks.

(D) Signals obtained for D1, D2, PsbE, PsbI, CP43, and CP47 in (C), and for the same proteins from the *lpa1-2* mutant (see Supplemental Figure 1 online), were quantified for each PSII assembly complex and for free proteins. The relative amounts of all PSII assembly complexes were calculated for each protein (summing to 1 for each protein), and mean values and standard deviations for each PSII assembly complex were determined from three replicates. Note that *Ler*, the genetic background of *lpa1-2*, behaved similar to Col-0.

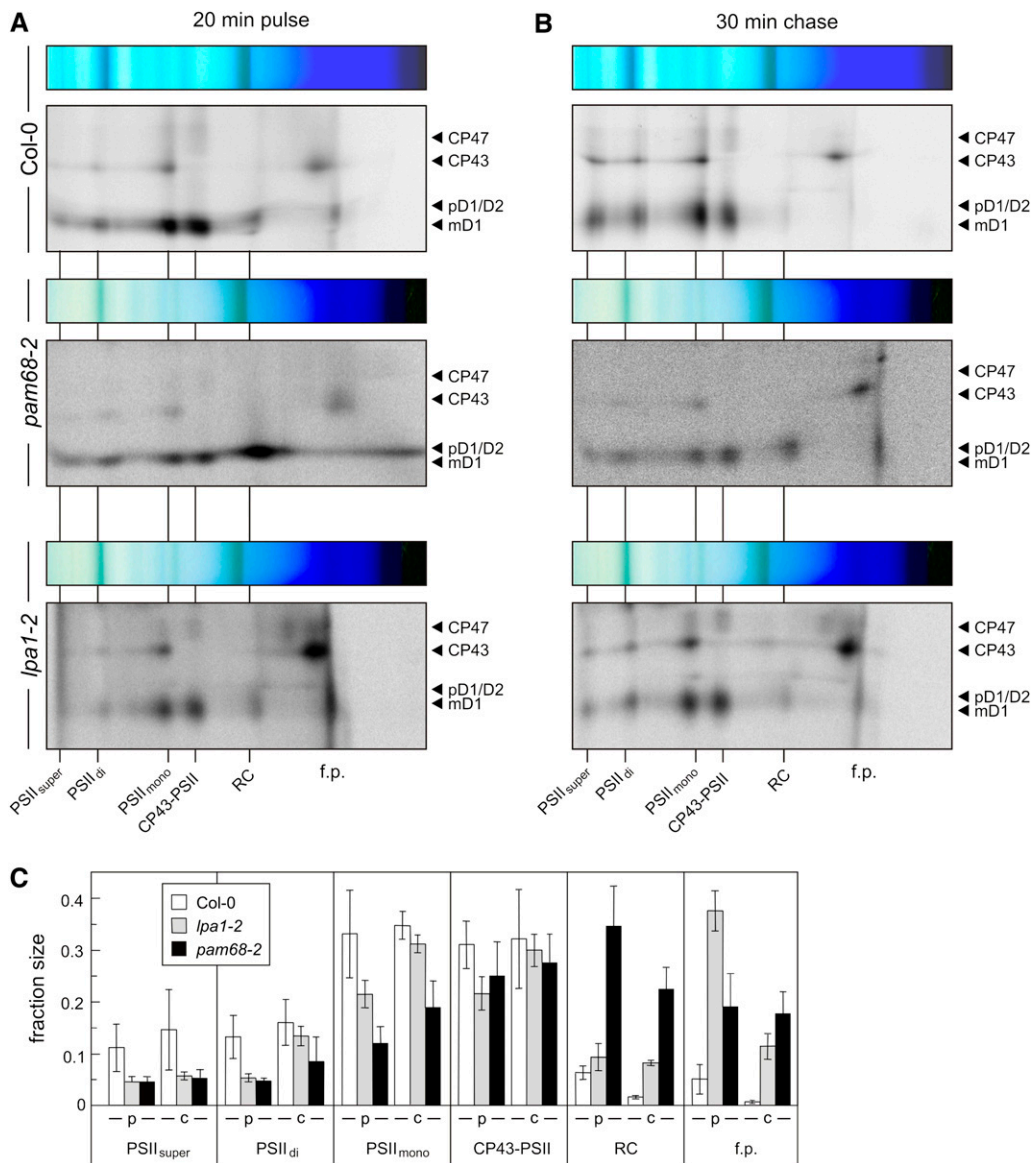


**Figure 5.** Rates of Synthesis of PSII Assembly Complexes as Detected by Pulse-Chase Analysis.

**(A)** and **(B)** 2D BN/SDS-PAGE analysis of [<sup>35</sup>S]Met incorporation into thylakoid membrane protein complexes. After pulse labeling of 4-week-old leaves with [<sup>35</sup>S]Met for 20 min in the presence of cycloheximide **(A)**, a chase of unlabeled Met for 30 min was applied **(B)**. After thylakoid membrane isolation, proteins were fractionated by 2D BN/SDS-PAGE and complexes visualized by autoradiography. The positions of the different PSII assembly complexes and free proteins (f.p.) are indicated as in Figure 4C.

**(C)** Signals obtained for D1 + D2 in **(A)** and **(B)** were quantified for each PSII assembly complex as in Figure 4D. p, pulse; c, chase.

Taken together, the data indicate that PAM68 and its cyanobacterial counterpart are involved in early step(s) in PSII biogenesis. However, defects in this early step lead to very different effects in the two species: levels of RC and pD1 increase in *pam68-2*, whereas RCa and RCb, as well as pD1, become undetectable in *ins0933*. Furthermore, while absence of PAM68 has marked effects on the accumulation of PSII dimers and supercomplexes and, thus, on the photosynthesis rate, *ins0933* mutants behave like the wild type with respect to photosynthesis and growth.

### PAM68 Is an Integral Thylakoid Protein

Several attempts were made to generate an antibody that specifically recognized PAM68 (see Methods), but only an antibody raised against an epitope located in the acidic stretch of PAM68 was able to detect minimal traces of PAM68 in wild-type plants. However, this antibody also recognized multiple additional proteins in the *pam68-2* mutant and was therefore unsuitable for conventional immunoblot analyses (see Supplemental Figure 6 online). Therefore, plants that overexpressed the PAM68

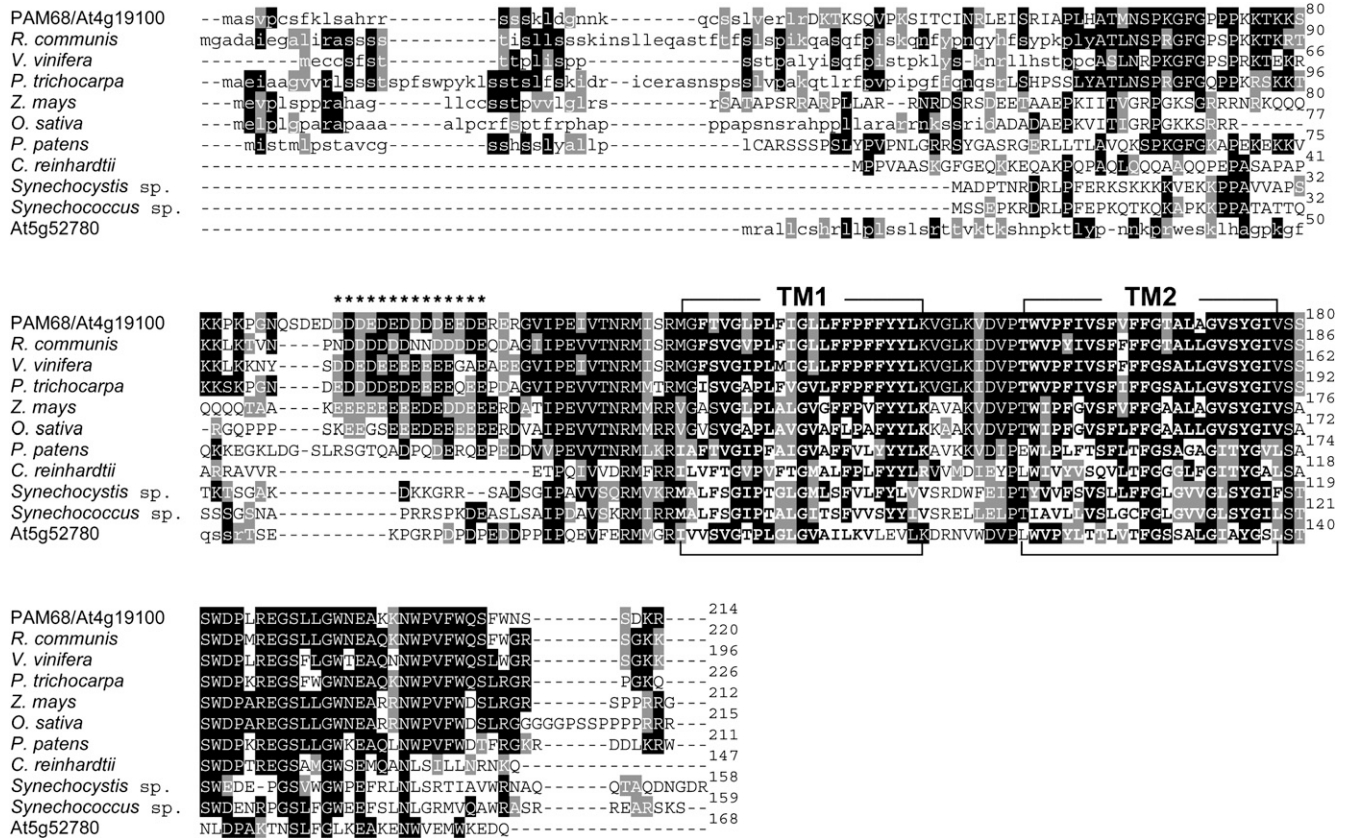


**Figure 6.** Sequence Alignment of *Arabidopsis* PAM68 and Its Homologs from Other Species.

The sequence of the PAM68 protein was compared with related sequences from *R. communis*, *Vitis vinifera*, *Populus trichocarpa*, *Zea mays*, *Oryza sativa*, *Physcomitrella patens* subsp. *patens*, *C. reinhardtii*, *Synechocystis* sp PCC 6803 and *Synechococcus* sp PCC 7002, and the *Arabidopsis* homolog At5g52780. The sequences were aligned using ClustalW and BoxShade (see Methods). Transit peptide sequences predicted by ChloroP are shown in lowercase letters. The two TM domains (TM1 and TM2) of each protein predicted by TMHMM (see Methods) are highlighted in bold; residues comprising the acidic domains are indicated by asterisks. Identical and closely related amino acids that are conserved in at least 30% of the aligned sequences are highlighted by black and gray shading, respectively.

protein were constructed for subcellular localization experiments (see Methods). The *PAM68* overexpressor (*35S:PAM68* in the *pam68-2* background, referred to as *oePAM68*) plants showed an ~30-fold increase in PAM68 levels, which reversed the effects of the *pam68-2* mutation with respect to growth, pigmentation, and D1 accumulation (see Supplemental Figure 6 online). Chloroplasts from *oePAM68* plants were fractionated into stroma and thylakoid fractions. Both fractions were subjected to immunoblot analysis, and the purity of fractions was tested by monitoring the stromal CSP41a and thylakoid D2 proteins (Figure 8A). The PAM68 protein was exclusively detected in the thylakoid fraction. To clarify whether PAM68 constitutes an integral or peripheral thylakoid protein, thylakoids from *oePAM68* plants were treated with alkaline and chaotropic salts to release membrane-associated proteins (Figure 8B). In this assay, PAM68 behaved like the integral protein Lhcb1 and not like the peripheral PsaD1, indicating that PAM68 represents an integral membrane protein, as already suggested by the presence of two predicted TMs (Figure 6). As expected, fractionation and solubilization experiments similar to those presented in

Figures 8A and 8B revealed that *Synechocystis* SII0933 too is an integral thylakoid protein (see Supplemental Figures 5F and 5G online).

To determine the topology of PAM68 in the thylakoid membrane, thylakoids were subjected to mild digestion with trypsin, such that only the stroma-exposed face was accessible to the protease. If the N and C termini of PAM68 faced the stroma (Topology 1 in Figure 8C), tryptic digestion should generate a 2-kD peptide detectable with the PAM68 antibody raised against the acidic domain. Tryptic digestion of an oppositely oriented PAM68 (with the N and C termini facing the lumen; Topology 2 in Figure 8C) at two sites within the inter-TM region is expected to result in a 13-kD fragment. As expected, PsbO on the lumen side of the thylakoid membrane was not affected by trypsin, whereas PAM68 was efficiently digested without leaving any detectable proteolytic fragment sized between 8 and 20 kD (Figure 8D). The missing detection of the 2-kD fragment can be explained by failed precipitation with acetone, which was used for trypsin inactivation, or inefficient membrane transfer of the small fragment during electroblotting. Nevertheless, the absence

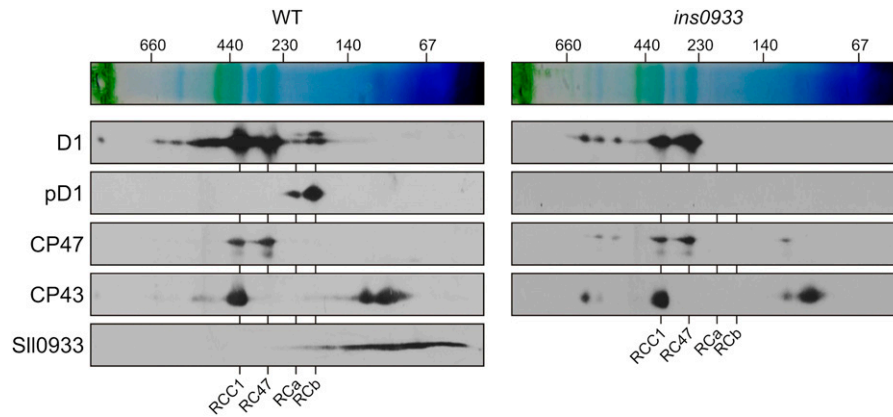


**Figure 7.** 2D BN/SDS-PAGE Analysis of PSII Complexes from *Synechocystis* Wild-Type and *ins0933* Cells.

Membrane samples (each equivalent to 20  $\mu\text{g}$  of chlorophyll) were solubilized with  $\beta$ -DM, subjected to 2D BN/SDS-PAGE, and blotted onto a nitrocellulose membrane. The PSII proteins D1, pD1, CP47, CP43, and SII0933 (the *Synechocystis* PAM68 homolog) were detected using appropriate antibodies. Designation of complexes: RCC1, PSII core monomers; RC47, PSII core complex lacking CP43; RCa and RCb, reaction center complexes a and b, respectively. Positions of size marker bands are indicated at the top.

of the 13-kD fragment clearly implies that Topology 1 depicted in Figure 8C represents the actual topology of PAM68.

#### PAM68 Forms Part of a Small Multiprotein Complex That Requires LPA1 for Its Stability

The above results suggest that *Arabidopsis* PAM68 promotes early steps in PSII biogenesis and that the *Synechocystis* PAM68 ortholog is present in low molecular weight complexes corresponding to early PSII assembly intermediates. Because our PAM68 antibodies were not suitable for detection of PAM68 on 2D BN/SDS gels in which only limited amounts of thylakoid complexes can be loaded and separated (see above), we used sucrose gradient centrifugation to fractionate increased amounts of assembly intermediates in *Arabidopsis*. To this end, thylakoids were isolated from Col-0 and *pam68-2* plants and solubilized with  $\beta$ -DM. Thylakoid complexes were then separated by ultracentrifugation on a linear 0.1 to 1 M sucrose gradient. After centrifugation, 19 fractions were collected (numbered from top to bottom), and proteins were precipitated and subjected to immunoblot analysis. Several additional unspecific bands of various sizes were detected with the PAM68 antibody, as expected from the PAM68 immunoblot experiments with total thylakoid fractions (see Supplemental Figure 6 online), but these signals were distributed throughout the gradient and much weaker than the distinct PAM68 signal present in Col-0 but not in *pam68-2*. Thus, in Col-0, but not in *pam68-2*, a distinct signal for PAM68 was identified in fraction 8 (Figure 9). Fraction 8 from both the wild type and *pam68-2* also contained CP43, PsbE, PsbH, and LPA1, together with traces of pD1 and D2, but no CP47 (Figure 9). In *pam68-2*, traces of pD1 and D2, but no CP43, were also detected in fraction 7, possibly indicating that loss of PAM68 affects a complex that contains pD1 and D2, but not CP43. Interestingly, the distribution of LPA1 was shifted toward denser fractions in *pam68-2* (fractions 7 to 19) compared with the wild type (fractions 7 to 14).

Because Col-0 LPA1 and PAM68 were found in the same fraction of the sucrose gradient, thylakoid complexes from *lpa1-2* plants were also analyzed. In the corresponding wild type (*Landsberg erecta* [Ler]), as in Col-0 (Figure 9, top panel), the PAM68 protein was found in fraction 8, again together with traces of D1 and D2 (see Supplemental Figure 7 online). In *lpa1-2* mutants, however, the distribution of PAM68 was shifted toward less dense fractions (fractions 6 to 8). In addition, pD1 and D2 also shifted to fraction 7 in the *lpa1-2* mutant. The distribution of CP43, which was also present in fraction 8 from wild-type (Col-0 and Ler) plants, remained unchanged in *lpa1-2*.

Taken together, these data are consistent with the idea that *Arabidopsis* PAM68, like *Synechocystis* SII0933 (Figure 7), is associated with a low molecular weight complex formed at an early step in the PSII assembly process. This complex might contain pD1 and D2, but it seems to lack CP47 or CP43. Because LPA1 is found in more dense fractions when PAM68 is absent, whereas PAM68 is found in less dense fractions when LPA1 is missing, one may speculate that PAM68 displaces LPA1 during PSII biogenesis. Thus, in the absence of LPA1, the PAM68 protein might bind to a smaller complex than usual. Conversely, in the absence of PAM68, the LPA1 protein remains associated with PSII or even larger complexes, such as ribosome-associated nascent chains at later assembly steps.

#### PAM68 Interacts with Several PSII Core Subunits and Assembly Factors

To test further for associations between PAM68 and structural or auxiliary PSII proteins, we examined the interaction of PAM68 with several thylakoid proteins using the split-ubiquitin system (Pasch et al., 2005). In this assay, the mature form of PAM68 (PAM68<sub>36-214</sub>; Figure 10A) failed to interact with representative components of PSI (PsaA, PsaB, ferredoxin [Fd], and the ferredoxin-NADP<sup>+</sup> oxidoreductase [FNR]), subunit IV of the cpATPase (AtpI), or components of the signal recognition particle (FtsY;

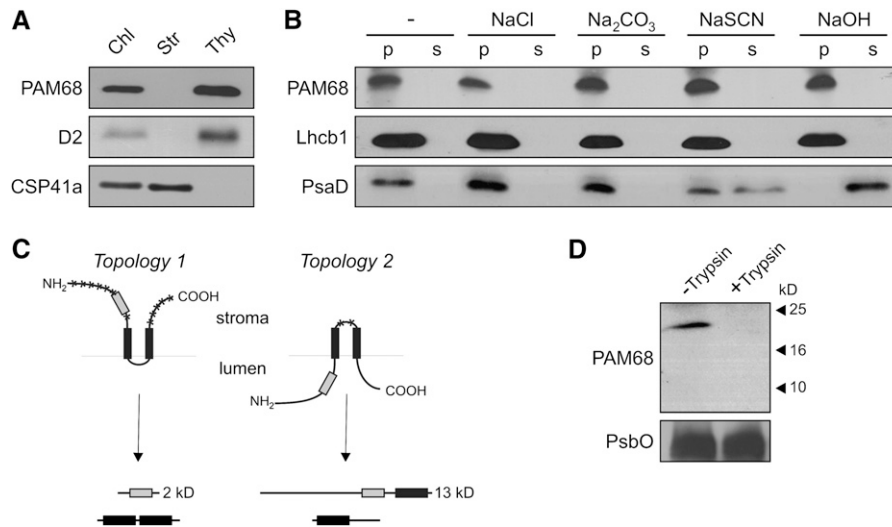


**Figure 8.** Subcellular Localization and Topology of PAM68.

**(A)** Suborganellar localization of PAM68. Chloroplasts, stroma, and thylakoids were isolated from *oePAM68* (35S:PAM68 *pam68-2*) plants, fractionated by SDS-PAGE, transferred to poly(vinylidene difluoride) membrane, and visualized using antibodies raised against the acidic domain of PAM68, CSP41a (as a control for stromal proteins), or D2 (as a control for thylakoid proteins).

**(B)** Extraction of thylakoid-associated proteins with chaotropic salt solutions or alkaline pH. Thylakoid membranes from *oePAM68* plants were resuspended at 0.5 mg chlorophyll/mL in 10 mM HEPES/KOH, pH 7.5, containing either 2 M NaCl, 0.1 M Na<sub>2</sub>CO<sub>3</sub>, 2 M NaSCN, 0.1 M NaOH, or no additive. After incubation for 30 min on ice, supernatants containing the extracted proteins (s) and membrane fractions (p) were separated by SDS-PAGE and immunolabeled with antibodies raised against the acidic domain of PAM68, PsaD (as a control for peripheral membrane proteins), or Lhcb1 (as a control for integral membrane proteins).

**(C)** Schematic representation of the two possible topologies of PAM68, with the two TMs indicated by black boxes, the acidic domain as a gray box, and the trypsin cleavage sites depicted by asterisks. In the bottom half of the panel, relevant proteolytic fragments are indicated.

**(D)** Immunoblot analysis of thylakoid membrane preparations with antisera specific for the acidic domain of PAM68 or PsbO (as a control for luminal thylakoid proteins) before (–Trypsin) and after (+Trypsin) treatment with trypsin. In intact thylakoids, only stroma-exposed polypeptides are accessible to the enzyme.

Kogata et al., 1999) or secretory (Sec) (SecY; Laidler et al., 1995; Roy and Barkan, 1998) thylakoid targeting pathways (Figure 10B). Strikingly, in the same assay, mature PAM68 interacted with most PSII core proteins tested (D1, D2, CP43, CP47, PsbH, and PsbI) but not with PsbE, PsbF, or PsbO. We next tested whether PAM68 interacts with known PSII assembly factors. Here, PAM68 was found to interact with HCF136, LPA1, LPA2, and ALB3 (Figure 10B).

To investigate whether the multiple interactions of PAM68 with PSII proteins and assembly factors depend on specific domains, deletion derivatives of PAM68 were analyzed for their interaction capacity. The PAM68 fragments tested were PAM68<sub>36-146</sub> (representing the N-terminal region of the mature protein including TM1) and PAM68<sub>122-214</sub>, consisting of both TMs and the C terminus of PAM68 (Figures 10A and 10C). The deletion products interacted with most of the proteins that interacted with the full-length construct, and three different interaction domains could be identified, with the N terminus responsible for interaction with PsbI, the region including TM1 for interaction with D2, PsbH, LPA1, LPA2, and ALB3, and the C terminus required for interaction with D1 and CP43 (Figure 10A). The deletion derivatives failed to interact with CP47 and HCF136, indicating that multiple domains of PAM68 might be required for these interactions.

In summary, the interactions of PAM68 with D1, D2, HCF136, and LPA1 are compatible with the requirement for PAM68 for

efficient D1 maturation and stability. Moreover, the multiple interactions of PAM68 with PSII subunits that are added later in PSII biogenesis might also provide an explanation for the decreased formation of PSII dimers and supercomplexes in *pam68-2* plants (Figure 4), in the event that this is not simply a secondary effect of the delay in early PSII assembly steps.

## DISCUSSION

### Absence of *Arabidopsis* PAM68 Has Multiple Effects on PSII Assembly

Loss of PAM68 has drastic effects on PSII function and plant growth (Figure 1). These effects are similar to those seen in *lpa1* (Peng et al., 2006; see Supplemental Figure 1 online) or *lpa2* (Ma et al., 2007) mutants, but less severe than the seedling-lethal phenotype of the *hcf136* mutant (Meurer et al., 1998). At the protein level, the abundance of PSII core subunits, particularly D1, D2, CP43, and CP47, was markedly decreased (Figures 2 and 4), and the maturation (Figure 2) and stability (Figure 3; see Supplemental Figure 3 online) of D1 are both impaired. Conversely, there is a clear increase in the accumulation of the RC assembly intermediate and free nonassembled proteins at the expense of PSII dimers and supercomplexes (Figure 4). In the

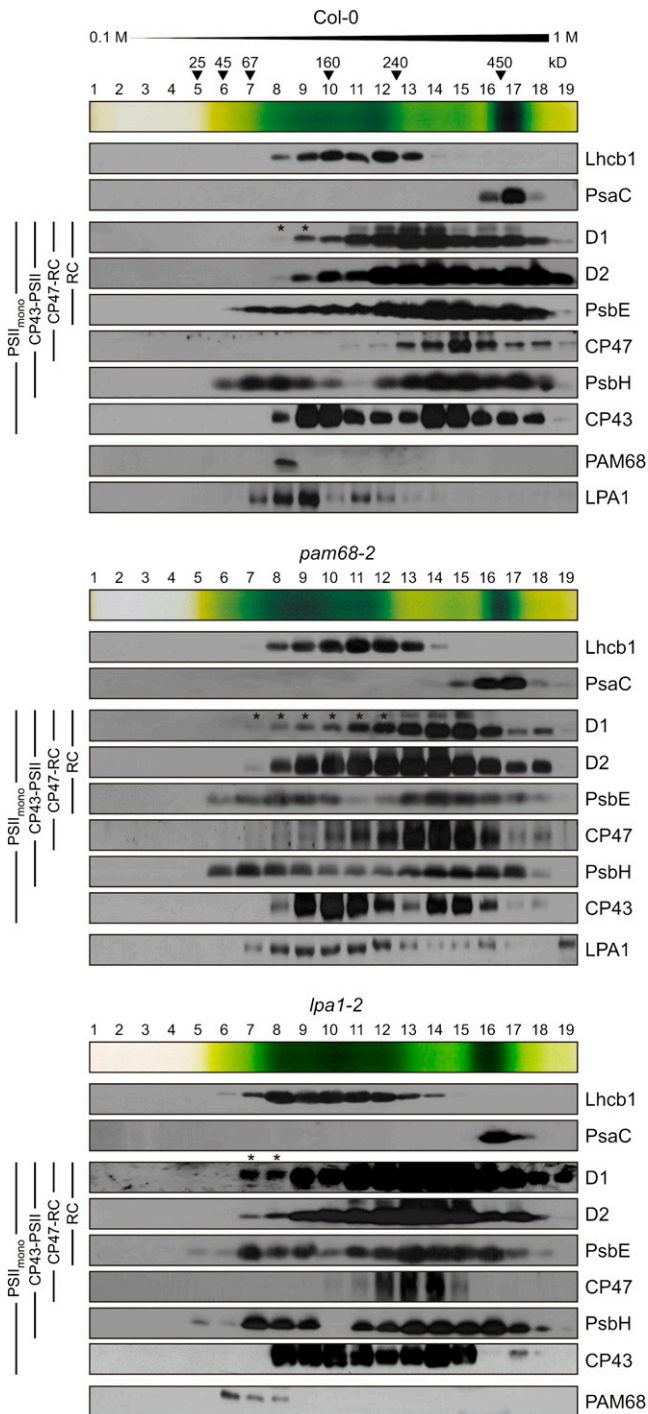


**Figure 9.** Analysis of PAM68-Containing Complexes by Sucrose Gradient Sedimentation.

Thylakoids (1 mg chlorophyll/mL) from wild-type (Col-0) and mutant (*pam68-2* and *lpa1-2*) plants were solubilized with 1% (w/v)  $\beta$ -DM and separated by centrifugation in a linear 0.1 to 1 M sucrose gradient. Note that because chlorophyll (*a + b*) levels in *pam68-2* plants are equivalent to 65% of wild-type chlorophyll levels, the *pam68-2* sample contained ~50% more protein. Nineteen fractions were collected (numbered from top to bottom) from two wild-type and four *pam68-2* and *lpa1-2* gradi-

*lpa1* mutant, levels of newly synthesized D1 and D2 are even lower, but this has much less effect on PSII assembly (Figures 5A and 5B) and stability (Figures 4C and 4D). Hence, it can be concluded that the perturbation of PSII biogenesis in *pam68* mutants cannot be attributed solely to the reduction in D1 abundance. The absence of PAM68, unlike that of LPA1, appears to have multiple effects on (1) maturation and stability of the D1 protein and (2) conversion of the RC complex into larger PSII intermediates. In addition, (3) the accumulation of PSII dimers and supercomplexes is highly reduced in *pam68* plants under steady state conditions (Figure 4D), probably as a consequence of the delayed assembly of earlier PSII states, although it cannot be totally excluded that PAM68 might also play a role in the assembly of PSII dimers and supercomplexes (see below).

### Cyanobacterial and Plant PAM68 Proteins Are Involved in Early PSII Biogenesis

*Arabidopsis* PAM68 (Figure 10) and LPA1 (Peng et al., 2006) interact with D1, and LPA2 binds CP43 (Ma et al., 2007). In all three cases, inactivation of the assembly factor by mutation is accompanied by a specific reduction in the synthesis of its binding partner. This implies that physical interaction of these assembly factors with specific PSII subunits is necessary for normal synthesis or stability of the latter. A dramatic increase in accumulation of pD1, like that seen in *pam68-2* plants, has also been observed in *hcf136* plants (Meurer et al., 1998), but not in *lpa1* (Peng et al., 2006; Figure 3) or *lpa2* (Ma et al., 2007) mutants. Comparison of the kinetics of the synthesis/processing of D1 and its incorporation into PSII showed that pD1 processing occurs early in PSII assembly (van Wijk et al., 1997), and in *Synechocystis*, an increase in pD1 has been noted when either PsbH or CP47 is absent, suggesting that the formation of the CP47-RC complex facilitates the maturation of D1 (Komenda et al., 2005). YCF48, the cyanobacterial HCF136, plays a role in the stabilization of newly synthesized pD1 and in its subsequent binding to D2-PsbE-PsbF; thus, absence of YCF48 dramatically decreases the level of pD1 (Komenda et al., 2008). The increase in pD1 observed in *Arabidopsis hcf136* plants appears at first sight to be at variance with the *ycf48* phenotype but can be explained by the fact that, in contrast with *ycf48*, the *hcf136* mutant accumulates only trace amounts of D1 and PsbE/PsbF, while D2, CP43, and CP47 are undetectable (Meurer et al., 1998). Therefore, the formation of CP47-RC, which, by analogy to the situation in cyanobacteria, should be required for pD1 maturation, is

ents, and fractions from the same genotype were pooled. Proteins were precipitated from each fraction, separated by SDS-PAGE, blotted onto poly(vinylidene difluoride) membranes, and detected with antibodies against D1, D2, PsbE, CP47, PsbH, CP43, PAM68, and LPA1, as well as PsaC and Lhcb1. At the top of each blot, an image of the sucrose gradient is shown, and the positions of molecular mass markers in the gradient are indicated. Note that *Ler*, which serves as wild-type control for *lpa1-2*, behaved very similarly to Col-0 (see Supplemental Figure 7 online) and that PAM68 and LPA1 were not detected in *pam68-2* and *lpa1-2* samples, respectively. Accumulation of pD1 is indicated by asterisks.

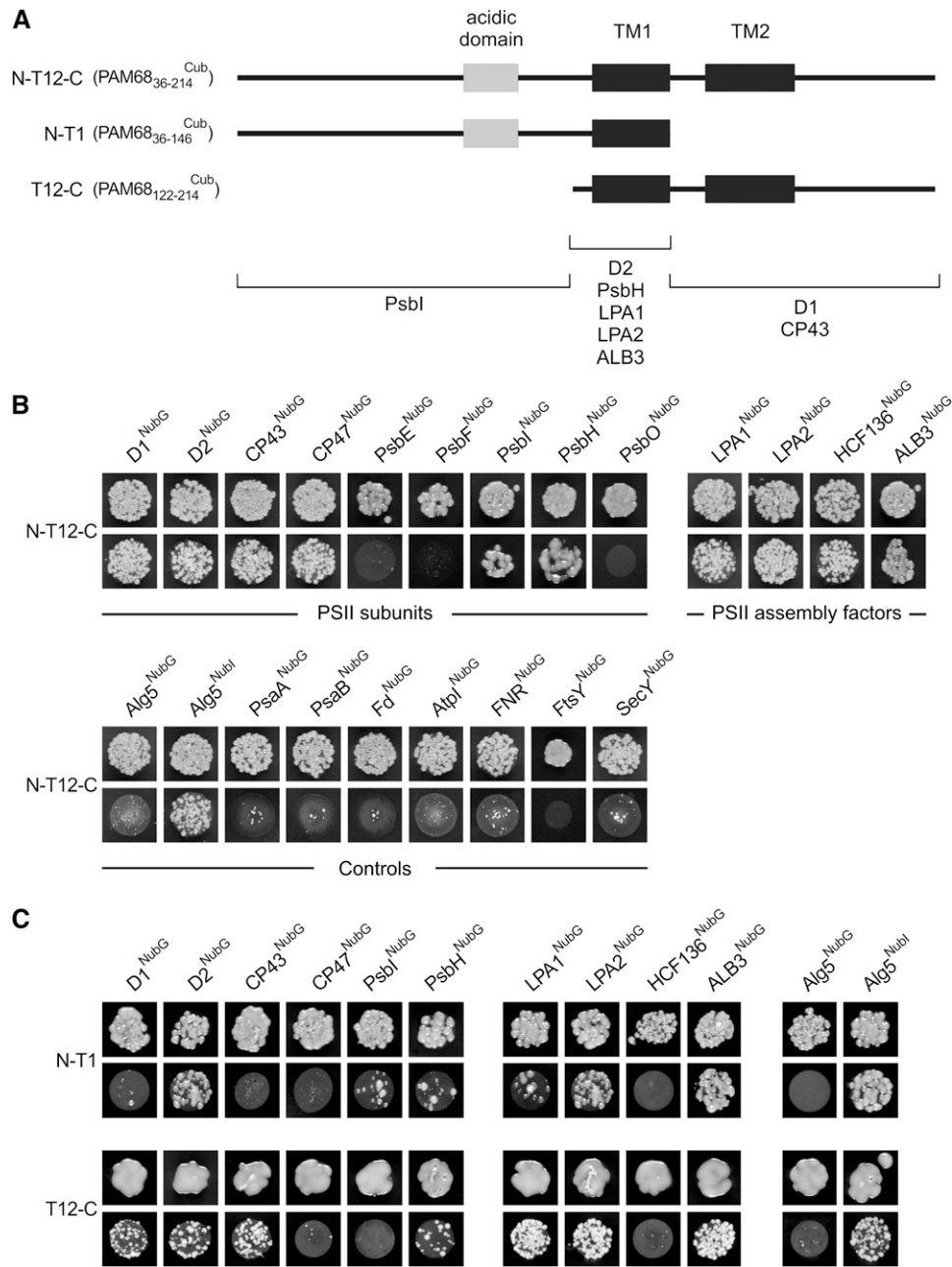


**Figure 10.** Interaction of PAM68 with Other Thylakoid Proteins.

**(A)** Schematic presentation of the fragments of PAM68 used to identify interaction domains. The acidic domain is shown as a gray box and the two TMs as black boxes. In the bottom half of the panel, the three interaction domains and the corresponding interacting proteins are shown.

**(B)** Split-ubiquitin assays for interactions between full-length PAM68 and selected thylakoid proteins. Assays were performed employing fusions to the C- (Cub) and N- (NubG) terminal halves of ubiquitin. Alg5<sup>Nubi</sup> (the unrelated endoplasmic reticulum membrane protein Alg5 fused to the wild-type Nub) served as a positive control. Alg5 fused to NubG (Alg5<sup>NubG</sup>) was used as the negative control. To test for interactions involving the PAM68 protein, the mature PAM68 protein was fused to Cub (N-T12-C or PAM68<sub>36-214</sub><sup>Cub</sup>), and the selected thylakoid proteins were fused to NubG. Yeast colonies were first plated on permissive (-LT, top panels) and then on selective medium (-LTH, bottom panels) (see Methods).

**(C)** Interaction mapping to distinct domains of PAM68. Two different fragments as shown in **(A)** were employed to detect interactions between domains of PAM68 and selected thylakoid proteins. Split-ubiquitin assays were performed as in **(B)**.

prevented in the *hcf136* genotype (Plücken et al., 2002). Why then does *pam68* exhibit an increase in accumulation of pD1? This can be explained by assuming either a direct involvement of PAM68 in pD1 maturation or indirect effects caused by perturbations in the formation of CP47-RC in *pam68-2*, similar to the situation in *hcf136*. Although the accumulation of CP47-RC has not been determined here, the delayed assembly of RC into larger PSII intermediates in *pam68-2* argues in favor of the latter scenario.

Inactivation of the *Synechocystis* gene for the SII0933 protein prevents accumulation of both the RC complex and pD1 under steady state conditions, whereas the accumulation of later PSII assembly intermediates was unaltered (Figure 7). This clearly implies that, in contrast with the *pam68-2* mutant, in the *Synechocystis* mutant the assembly of RC into larger intermediates is not delayed; instead, the transition from RC to CP47-RC might be even more efficient in the mutant so that both RC and pD1 are not detectable under steady state conditions. Assuming that PAM68 and its cyanobacterial homolog exert similar functions at the molecular level in both organisms, how can their absence lead to such contrasting effects? A general explanation for the more severe phenotype of the *Arabidopsis pam68-2* mutation compared with the *Synechocystis sII0933* mutation (and correspondingly for *hcf136* in *Arabidopsis* and *ycf48* in *Synechocystis*; see above) might be provided by the more effective elimination of nonassembled proteins and abnormal complexes by the proteolytic quality control system in chloroplasts (reviewed in Nixon et al., 2010). Alternatively, the delay in the assembly of RC into larger complexes evident in the *Arabidopsis pam68-2* mutant might be bypassed in *Synechocystis* by pathways that have been lost during the evolution of the plant lineage. A third explanation could be that PAM68 contributes also to the PSII repair cycle, such that the contrasting mutant phenotypes in *Synechocystis* and *Arabidopsis* might result from the different consequences of perturbations in PSII repair in the two species.

At what stage in the assembly process do *Arabidopsis* and *Synechocystis* PAM68 proteins come into play? *Synechocystis* SII0933 was detected in small complexes that might represent RC or even earlier assembly states (Figure 7). The sucrose gradient analysis of the *Arabidopsis* PAM68 protein (Figure 9) indicates that PAM68 may form a relatively small complex with LPA1, D1, and D2. This complex might again correspond to RC or earlier steps in PSII assembly. So whereas PAM68 proteins appear to associate with early assembly states, further analyses will be required for their unambiguous identification.

### Do Assembly Factors Associate Only Transiently with PSII?

Our results indicate that PAM68 interacts with LPA1, LPA2, HCF136, and ALB3 in the split-ubiquitin assay (Figure 10), and the interaction with LPA1 is supported by sucrose gradient analysis (Figure 9). Because PSII assembly factors are generally thought to associate transiently with intermediates during PSII biogenesis, the action of PAM68 in early PSII biogenesis (see above) on one side, and its multiple interactions with other assembly factors thought to act on various PSII assembly complexes on the other side, is unexpected. However, although

YCF48 has been found only in RC complexes (Komenda et al., 2008), its eukaryotic counterpart HCF136 has also been detected in larger PSII assembly complexes (Plücken et al., 2002). LPA2 is thought to promote CP43 assembly within PSII to form PSII core monomers, but it also interacts with ALB3 (Ma et al., 2007), which is thought to be involved in D1 biogenesis. Indeed, inspection of mRNA expression databases indicates that HCF136, ALB3, LPA1, and PAM68 are more or less constitutively expressed, whereas DEG1 (Kapri-Pardes et al., 2007; Sun et al., 2010) and VAR2 (Zaltsman et al., 2005), as examples for factors involved in PSII turnover and repair, vary markedly in their expression under different light conditions (see Supplemental Table 1 online). Therefore, PSII assembly factors might operate on more than one assembly state during PSII biogenesis. Alternatively, PAM68 might participate in complexes that contain other assembly factors but lack PSII subunits. Indeed, PAM68 (see Supplemental Figure 6 online) and HCF136 (P. Westhoff, personal communication) can accumulate many fold when overexpressed, implying that they do not require their PSII interaction partners for stability.

### Conclusions

The PAM68 protein is involved in the assembly of PSII and appears to interact with early assembly intermediates. Intriguingly, its absence delays certain assembly steps in *Arabidopsis*, such that the RC complex accumulates, whereas in *Synechocystis* the transition from RC to later PSII intermediates seems to be accelerated. Moreover, PAM68 interacts in split-ubiquitin assays with some PSII proteins and assembly factors that appear at later stages of PSII assembly, and much lower levels of PSII dimers and supercomplexes accumulate under steady state conditions in *pam68-2* than in the *lpa1-2* mutant, which has a comparable synthesis rate of PSII dimers and supercomplexes (Figures 4D and 5C). Although the decrease in PSII dimer and supercomplex formation might be attributed, as a secondary effect, to the perturbation in early PSII assembly, it cannot be excluded that PAM68 might also support later assembly steps through transient interaction with the proteins identified by the split-ubiquitin assay, although PAM68 was detected only in smaller complexes (Figures 7 and 9). Future experiments have to clarify whether PAM68 might be sufficiently abundant for such an additional role in later PSII assembly steps and provide independent experimental evidence for its multiple interactions identified by the split-ubiquitin assay. Moreover, further experiments are needed to explain the different effects of the absence of PAM68 on PSII assembly in cyanobacteria and flowering plants.

### METHODS

#### Plant Material, Propagation, and Growth Measurement

The *pam68-1* mutant (GABI\_152D07) is from the GABI-KAT collection (Rosso et al., 2003), and *pam68-2* (SALK\_044323) and *at5g52780-1* (SALK\_143426) are from the SALK T-DNA collection (<http://signal.salk.edu/>; Alonso et al., 2003). All three mutants have the Col-0 genetic background. The *lpa1-2* mutant (CSHL\_ET6851) originates from the Cold

Spring Harbor Laboratory collection and carries a *Dissociation* element insertion in the *Ler* background (Martienssen, 1998).

Plants overexpressing PAM68 (*oePAM68*) were generated by introducing the *PAM68* coding region (for primers, see Supplemental Table 2 online) into the Gateway plant expression vector pH2GW7 (Karimi et al., 2002) under the control of the 35S promoter of *Cauliflower mosaic virus* and then transforming flowers of *pam68-2* mutant plants with the *PAM68* overexpression construct as described (Clough and Bent, 1998). The plants were then transferred to the greenhouse, and seeds were collected after 3 weeks. Individual transgenic plants were selected on the basis of their resistance to hygromycin. The presence and expression of the transgene was confirmed by PCR, RNA gel blot, and protein immunoblot analyses.

*Arabidopsis thaliana* plants were grown on potting soil (Stender) under controlled greenhouse conditions (daylight supplemented with illumination from HQI Powerstar 400W/D, giving  $\sim 180 \mu\text{mol photons m}^{-2} \text{s}^{-1}$  on leaf surfaces,  $\sim 14/10$  h light/dark cycle). Wuxal Super fertilizer (8% N, 8%  $\text{P}_2\text{O}_5$ , and 6%  $\text{K}_2\text{O}$ ; MANNA) was used according to the manufacturer's instructions. For in vivo translation assays, plants were grown on Murashige and Skoog medium (Duchefa) supplemented with 1% (w/v) sucrose. The screen for mutants exhibiting an altered photosynthetic performance was performed on 4-week-old, greenhouse-grown plants. Methods used for measurement of growth have been described previously (Leister et al., 1999).

### Construction and Cultivation of Cyanobacterial Strains

*Synechocystis* sp PCC 6803 (referred to as the wild type) and mutant strains were grown under continuous irradiation ( $30 \mu\text{mol}$  of photons  $\text{m}^{-2} \text{s}^{-1}$ ) at  $30^\circ\text{C}$  on solid or in liquid BG 11 medium containing 5 mM glucose. To generate the *sll0933* insertion mutant (*ins0933*), the *Sll0933* coding sequence including its 5'- and 3'-flanking regions was amplified using the primers *sll0933-5in* (5'-TCTATCTGCTCCTCCTGAC-3') and *sll0933-3in* (5'-TAAAGTCTGACAGTAAATGC-3') and subcloned into the pDrive vector (Qiagen). The fragment obtained after restriction with *Bam*HI and *Xho*I was ligated into the Bluescript pKS vector, and the *sll0933* gene was disrupted by insertion of a kanamycin resistance cassette of the plasmid pBSL15 into the single *Pst*I site located 77 bp downstream of the ATG start codon. Wild-type cells were transformed with this construct as described (Eaton-Rye, 2004). Complete segregation of the *ins0933* mutant was confirmed by PCR analysis using the primer pair *sll0933-5kom* (5'-AACATATGGCTGACCCACCAATC-3') and *sll0933-3kom* (5'-AAATCGATTCAACGATCGCCATTGTC-3').

### Chlorophyll Fluorescence Analysis

Mutants that show alterations in  $\Phi_{II}$ , the effective quantum yield of PSII [ $\Phi_{II} = (F_m' - F_0)/F_m'$ ] were identified using an automatic pulse amplitude modulation fluorometer system (Varotto et al., 2000a, 2000b). In vivo chlorophyll *a* fluorescence of leaves was measured using the Pulse Amplitude Modulation 101/103 as described (Varotto et al., 2000b). Five plants of each genotype were analyzed, and average values and standard deviations were calculated. Plants were dark adapted for 30 min and minimal fluorescence ( $F_0$ ) was measured. Then, pulses (0.8 s) of white light ( $5000 \mu\text{mol photons m}^{-2} \text{s}^{-1}$ ) were used to determine the maximum fluorescence ( $F_m$ ) and the ratio  $(F_m - F_0)/F_m = F_v/F_m$  (maximum quantum yield of PSII) was calculated. A 10-min exposure to actinic light ( $80 \mu\text{mol photons m}^{-2} \text{s}^{-1}$ ) served to drive electron transport between PSII and PSI. Then, steady state fluorescence ( $F_s$ ) was measured, and  $F_m'$  was determined after exposure to further saturation pulses (0.8 s,  $5000 \mu\text{mol photons m}^{-2} \text{s}^{-1}$ ). The effective quantum yield of PSII ( $\Phi_{II}$ ) was calculated, and the photosynthetic parameters *qP* [photochemical quenching  $(F_m' - F_s)/(F_m' - F_0)$ ] and nonphotochemical quenching  $[(F_m - F_m')/F_m']$  were determined. In vivo chlorophyll *a* fluorescence of whole plants

was recorded using an imaging chlorophyll fluorometer (Walz Imaging PAM) by exposing dark-adapted plants to a pulsed, blue measuring beam (1 Hz, intensity 4;  $F_0$ ) and a saturating light flash (intensity 4) to obtain  $F_v/F_m$ . The 77K fluorescence emission spectra of *Synechocystis* cells were measured after chlorophyll excitation at 435 nm as described previously (Klinkert et al., 2004).

### Nucleic Acid Analysis

*Arabidopsis* DNA was isolated (Ihnatowicz et al., 2004), and T-DNA insertion-junction sites were recovered by amplification of insertion-mutagenized sites according to Frey et al. (1998). For RNA analysis, total leaf RNA was extracted from fresh tissue using the TRIzol reagent (Invitrogen). RT-PCR was performed by synthesizing first-strand cDNA using SuperScript reverse transcriptase (Invitrogen) and dT oligomers, followed by PCR with specific primers (see Supplemental Table 2 online). RNA gel blot analyses were performed under stringent conditions, according to standard protocols. Blots were stained with 0.04% methylene blue in 0.5 M sodium acetate, pH 5.2. Probes complementary to *PAM68*, *ACTIN1*, *psbA*, *psbB*, *psbC*, *psbD*, and *psbE* amplified from cDNA (see Supplemental Table 2 online), labeled with  $^{32}\text{P}$ , were used for the hybridizations. Signals were quantified using a phosphor imager (Typhoon; GE Healthcare) and the program IMAGE QUANT for Macintosh (version 1.2; Molecular Dynamics).

Polysomes were isolated as described (Barkan, 1988). Leaf tissue (200 mg) was frozen with liquid nitrogen in a mortar and ground with a pestle. Subsequently, the microsomal membranes were solubilized with 1% (v/v) Triton X-100 and 0.5% (w/v) sodium deoxycholate. The solubilized material was layered onto 15/55% sucrose step gradients (corresponding to 0.44/1.6 M) and centrifuged at  $250,000g$  for 65 min at  $4^\circ\text{C}$ . The step gradient was fractionated and the mRNA associated with polysomes was then extracted with phenol/chloroform/isoamyl alcohol (25:24:1), followed by precipitation at room temperature with 95% ethanol. All samples were then subjected to RNA gel blot analysis.

### Leaf Pigment Analysis

Pigments were analyzed by reverse-phase HPLC as described (Färber et al., 1997). For pigment extraction, leaf discs were frozen in liquid nitrogen and disrupted with beads in microcentrifuge tubes in the presence of acetone. After a short centrifugation, pigment extracts were filtered through a membrane filter (pore size  $0.2 \mu\text{m}$ ) and either used directly for HPLC analysis or stored for up to 2 d at  $-20^\circ\text{C}$ .

### BN- and 2D-PAGE

Leaves were harvested from plants at the 12-leaf rosette stage, and thylakoids were prepared as described (Bassi et al., 1985). For BN-PAGE, thylakoid samples equivalent to 100 mg of fresh leaf material were solubilized in 750 mM 6-aminocaproic acid, 5 mM EDTA, pH 7, and 50 mM NaCl in the presence of 1.0% (w/v)  $\beta$ -DM for 10 min at  $4^\circ\text{C}$ . Following centrifugation (15 min,  $21,000g$ ), the solubilized material was fractionated using nondenaturing BN-PAGE at  $4^\circ\text{C}$  as described (Schägger et al., 1988). For 2D-PAGE, samples were subsequently fractionated by electrophoresis on denaturing gradient Tricine-SDS gels (10 to 16% acrylamide) supplemented with 4 M urea (Schägger and von Jagow, 1987). Second-dimension gels were either stained with colloidal Coomassie Brilliant Blue (Candiano et al., 2004) or subjected to immunoblot analysis with antibodies against D1, D2, CP43, CP47, PsbE, and PsbO as described below.

For 2D BN/SDS-PAGE of *Synechocystis* membranes, *Synechocystis* cells were harvested at  $OD_{750} \sim 2.2$ , and membranes were isolated according to Dühring et al. (2006). 2D BN/SDS-PAGE was performed as described previously (Schottkowski et al., 2009a, 2009b).

### Immunoblot Analyses

For 2D-PAGE analysis, proteins were prepared as described above. For SDS-PAGE analysis, total proteins were prepared from 4-week-old *Arabidopsis* leaves as reported (Martinez-Garcia et al., 1999), then fractionated on SDS-PAGE gradient gels (10 to 16% acrylamide) supplemented with 4 M urea (Schägger and von Jagow, 1987). Proteins were transferred to poly(vinylidene difluoride) membranes (Ihnatowicz et al., 2004), and replicate filters were incubated with antibodies specific for the PSII subunits D1 (obtained from Jürgen Soll, University of Munich), D2 (Agrisera), CP47 (obtained from Roberto Barbato, University of Alessandria), CP43 (Agrisera), PsbE (Agrisera), PsbI (Agrisera), PsbO (Agrisera), Cyt *f* (Agrisera), ATP synthase  $\beta$ -subunit and Lhcb1 (Agrisera), PsaB (PSI; Agrisera), LPA1 (obtained from Lixin Zhang, Chinese Academy of Sciences), CSP41a (obtained from David Stern, Boyce Thompson Institute for Plant Research, Cornell University), and actin (Dianova) as control. Signals were detected by enhanced chemiluminescence (GE Healthcare) and quantified using IMAGE QUANT for Macintosh (version 1.2; Molecular Dynamics).

### In Vivo Translation Assay and Immunoprecipitation of D1

Radioactive labeling of thylakoid proteins was performed essentially as described (Pesaresi et al., 2006). In short, leaves of plants at the 12-leaf rosette stage, grown either in the greenhouse or in sterile culture, were vacuum-infiltrated in a syringe containing 20  $\mu$ g/mL cycloheximide in 10 mL of 10 mM Tris, 5 mM MgCl<sub>2</sub>, 20 mM KCl, pH 6.8, and 0.1% (v/v) Tween 20 and incubated for 30 min to block cytosolic translation. Then leaves were again infiltrated with the same solution containing 1 mCi of [<sup>35</sup>S]Met, transferred into the light (5 to 20  $\mu$ mol m<sup>-2</sup> s<sup>-1</sup>), and collected after 5, 15, 20, 30, or 60 min. For a chase after pulse labeling, 10 mM of unlabeled Met was applied. Subsequently, thylakoid proteins were prepared. Immunoprecipitation of D1 was performed as described (Schult et al., 2007). Thylakoid proteins were either fractionated on denaturing gradient Tricine-SDS gels (10 to 16% acrylamide) supplemented with 4 M urea, or complexes were separated using 2D BN/SDS-PAGE as described. Signals were detected and quantified using a phosphor imager as described above.

### Computational Analyses

Protein sequences were retrieved from the National Center for Biotechnology Information (NCBI; <http://www.ncbi.nlm.nih.gov/>), the Joint Genome Initiative (<http://genome.jgi-psf.org/>), or the Cyanobase database (<http://genome.kazusa.or.jp/cyanobase/>). Putative chloroplast transit peptides were predicted by ChloroP (<http://www.cbs.dtu.dk/services/ChloroP/>; Emanuelsson et al., 1999) and transmembrane domains by the program TMHMM (<http://www.cbs.dtu.dk/services/TMHMM-2.0/>; Krogh et al., 2001). Amino acid sequences were aligned using the ClustalW program ([www.ebi.ac.uk/clustalw/](http://www.ebi.ac.uk/clustalw/); Chenna et al., 2003), and alignments were shaded according to sequence similarity using the Boxshade server 3.21 ([www.ch.embnet.org/software/BOX\\_form.html](http://www.ch.embnet.org/software/BOX_form.html)). Sequence identities and similarities were calculated using NCBI BLAST 2 sequences (Tatusova and Madden, 1999).

Expression analyses of target genes in response to different light qualities derive from the Genevestigator platform ([www.genevestigator.com](http://www.genevestigator.com)). These data originate from microarrays with The Arabidopsis Information Resource accession number 1007966126.

### Generation of Antibodies

For immunolocalization of At5g52780, an antibody against the specific peptide sequence RTSEKPGRPD was generated in rabbits. For immunolocalization of *Arabidopsis* PAM68, several antibodies against specific

peptide sequences (SKKPKPGNQSD and DEDDDDEDED: acidic stretch), or the hydrophilic N terminus (amino acids 54 to 143) expressed in *Escherichia coli*, were generated in rabbits. Peptide synthesis, generation of peptide antibodies in rabbits, and purification of monospecific antibodies were all performed by Biogenes. All antibodies were used in a 1:100 dilution.

For production of antibodies specific for SlI0933, the sequence encoding the soluble N-terminal part of SlI0933 (amino acid positions 1 to 63) was overexpressed as a glutathione S-transferase fusion protein in *E. coli* cells and purified. Polyclonal  $\alpha$ SlI0933 antiserum was raised in rabbit (Biogenes) and used in a 1:625 dilution.

### Determination of PAM68 Topology

Intact *Arabidopsis* chloroplasts were isolated and purified from leaves of 4- to 5-week-old plants as described (Aronsson and Jarvis, 2002). Intact chloroplasts were ruptured by mixing with 10 volumes of lysis buffer (20 mM HEPES/KOH, pH 7.5, and 10 mM EDTA) and incubated on ice for 30 min. To separate thylakoid and stroma phases, ruptured chloroplasts were centrifuged (42,000g, 30 min; 4°C).

For salt washes of thylakoids, according to Karnauchov et al. (1997), isolated thylakoids were resuspended in 50 mM HEPES/KOH, pH 7.5, at a chlorophyll concentration of 0.5 mg/mL. Extraction with 2 M NaCl, 0.1 M Na<sub>2</sub>CO<sub>3</sub>, 2 M NaSCN, or 0.1 M NaOH was performed for 30 min on ice, soluble and membrane proteins were separated by centrifugation for 10 min at 10,000g and 4°C, and immunoblot analysis was performed on both fractions using antibodies specific for PAM68, Lhcb1 (Agrisera), and PsaD (Agrisera).

For tryptic proteolysis experiments, thylakoid membranes were isolated as described above (omitting PMSF) and then resuspended in 50 mM HEPES/KOH, pH 8.0, and 300 mM sorbitol at a chlorophyll concentration of 1 mg/mL. Trypsin was added to a concentration of 10  $\mu$ g/mL. Samples were taken 10 min later, and proteins were precipitated with 10 volumes of acetone and resuspended in SDS loading dye containing 5 mM of the Ser endopeptidase inhibitor PMSF.

### Split-Ubiquitin Assay

In the split-ubiquitin assay, NubG and Cub are able to reconstitute ubiquitin only when brought into close proximity by two interacting test proteins that are expressed as fusion proteins with NubG and Cub. To test for interactions between PAM68 and other proteins, corresponding proteins or their fragments were fused to the C and N terminus of NubG and Cub, respectively. The coding sequences for the mature PAM68 protein and its respective fragments were cloned in the multiple cloning site of pAMBV4 (Dualsystems Biotech) and used as bait in interaction studies with prey proteins generated by cloning the coding sequences of mature thylakoid proteins (D1, D2, CP47, CP43, PsbI, PsbH, PsbE, PsbF, PsbO, LPA1, and LPA2; HCF136, Alb3, FtsY, SecY, PsaA, PsaB, Fd, Atpl, and FNR) into the multiple cloning site of pADSL (Dualsystems Biotech). Interaction studies were performed using the Dual-Membrane kit (Dualsystems Biotech) as described (Pasch et al., 2005). As negative controls, the plasmid pAlg5-NubG, which encodes the endoplasmic reticulum membrane protein Alg5 fused to NubG (Alg5<sup>NubG</sup>), and pADSL-Nx expressing soluble NubG were used for cotransformations. Because Nubl (the wild-type Nub) and Cub spontaneously reassemble to reconstitute ubiquitin, Alg5 fused to Nubl (Alg5<sup>Nubl</sup>) was used as positive control. The specificity of the pADSL-Nx constructs was confirmed by cotransformation with a control vector encoding Alg5 fused to Cub (Alg5<sup>Cub</sup>). Yeast colonies were first plated on permissive medium (synthetic medium lacking Leu and Trp; -LT); the same colonies were later tested for their ability to grow on selective medium also lacking His (-LTH).

### Sucrose Gradient Fractionation of Thylakoid Complexes

Thylakoids were washed twice with 5 mM EDTA, pH 7.8, and diluted in 20 mM Tricine/KOH, pH 7.5, to a chlorophyll concentration of 2 mg/mL. Solubilization of membrane complexes was performed by addition of an equal volume of 2%  $\beta$ -DM and incubation on ice for 10 min. Centrifugation at 16,000g for 5 min at 4°C removed nonsolubilized membranes. The supernatant was loaded onto a linear 0.1 to 1.0 M sucrose gradient in 20 mM Tricine/KOH, pH 7.5, and 0.06% (w/v)  $\beta$ -DM and centrifuged at 191,000g for 21 h at 4°C. The gradient was divided into 19 fractions (numbered from the top). Proteins were precipitated by extraction with methanol-chloroform (Wessel and Flügge, 1984) and separated on denaturing gradient Tricine-SDS gels (10 to 16% acrylamide) supplemented with 4 M urea. Immunoblot analyses were performed as described previously. The protein molecular mass standard contained proteins from 25 to 450 kD (Serva).

### Accession Numbers

Sequence data from this article can be found in the *Arabidopsis* Genome Initiative or GenBank/EMBL databases under the following accession numbers: At4g19100 (*Arabidopsis* PAM68), At5g52780 (*Arabidopsis* homolog of PAM68), and the PAM68 homologs in *Ricinus communis* (GI:255557684), *Vitis vinifera* (GI:225466098), *Populus trichocarpa* (GI:224138363), *Zea mays* (GI:226491093), *Oryza sativa* (Os06g21530.1), *Physcomitrella patens* subsp. *patens* (jgijPhypa1\_1|172321|estExt\_fggenes1\_pg.C\_3420021), *Chlamydomonas reinhardtii* (GI:159464826), *Synechocystis* sp PCC 6803 (SI10933), and *Synechococcus* sp PCC 7002 (SYNPCC7002\_A1824).

### Supplemental Data

The following materials are available in the online version of this article.

- Supplemental Figure 1.** Characteristics of the *lpa1-2* Mutant.
- Supplemental Figure 2.** Discrimination of Signals for D1 and D2 Proteins.
- Supplemental Figure 3.** Stability of the D1 Protein.
- Supplemental Figure 4.** Characterization of *at5g52780-1* Mutants and the Double Mutant *pam68-2 at5g52780-1*.
- Supplemental Figure 5.** *Synechocystis* SI10933: Generation and Characterization of Knockout Lines (*ins0933*) and Subcellular Localization and Topology.
- Supplemental Figure 6.** Overexpression of *PAM68* Complements the *pam68-2* Phenotype.
- Supplemental Figure 7.** Analysis of *PAM68* Complex Formation.
- Supplemental Table 1.** Relative Transcript Levels of PSII Assembly Factors, as well as *DEG1* and *VAR2*, under Different Light Conditions.
- Supplemental Table 2.** Primers Used in This Study.

### ACKNOWLEDGMENTS

We thank Norio Murata and Yoshitaka Nishiyama for providing the pD1 antibody. Further antisera were obtained from Jürgen Soll, Elisabeth Ankele, and Monique Benz (against D1), Roberto Barbato (CP47), Lixin Zhang (LPA1), and David Stern (CSP41a). We thank Peter Nixon and Josef Komenda for discussions and suggestions, Paul Hardy for critical reading of the manuscript, and Christine Hümmer and Angela Dietzmann for technical support.

Received June 17, 2010; revised September 4, 2010; accepted September 21, 2010; published October 5, 2010.

### REFERENCES

- Adir, N., Zer, H., Shochat, S., and Ohad, I. (2003). Photoinhibition - A historical perspective. *Photosynth. Res.* **76**: 343–370.
- Alonso, J.M., et al. (2003). Genome-wide insertional mutagenesis of *Arabidopsis thaliana*. *Science* **301**: 653–657.
- Anbudurai, P.R., Mor, T.S., Ohad, I., Shestakov, S.V., and Pakrasi, H.B. (1994). The *ctpA* gene encodes the C-terminal processing protease for the D1 protein of the photosystem II reaction center complex. *Proc. Natl. Acad. Sci. USA* **91**: 8082–8086.
- Aro, E.M., Suorsa, M., Rokka, A., Allahverdiyeva, Y., Paakkarinen, V., Saleem, A., Battchikova, N., and Rintamäki, E. (2005). Dynamics of photosystem II: A proteomic approach to thylakoid protein complexes. *J. Exp. Bot.* **56**: 347–356.
- Aronsson, H., and Jarvis, P. (2002). A simple method for isolating import-competent *Arabidopsis* chloroplasts. *FEBS Lett.* **529**: 215–220.
- Baena-González, E., and Aro, E.M. (2002). Biogenesis, assembly and turnover of photosystem II units. *Philos. Trans. R. Soc. Lond. B Biol. Sci.* **357**: 1451–1459, discussion 1459–1460.
- Barkan, A. (1988). Proteins encoded by a complex chloroplast transcription unit are each translated from both monocistronic and polycistronic mRNAs. *EMBO J.* **7**: 2637–2644.
- Bassi, R., dal Belin Peruffo, A., Barbato, R., and Ghisi, R. (1985). Differences in chlorophyll-protein complexes and composition of polypeptides between thylakoids from bundle sheaths and mesophyll cells in maize. *Eur. J. Biochem.* **146**: 589–595.
- Bellafiore, S., Ferris, P., Naver, H., Göhre, V., and Rochaix, J.D. (2002). Loss of Albino3 leads to the specific depletion of the light-harvesting system. *Plant Cell* **14**: 2303–2314.
- Blanc, G., Hokamp, K., and Wolfe, K.H. (2003). A recent polyploidy superimposed on older large-scale duplications in the *Arabidopsis* genome. *Genome Res.* **13**: 137–144.
- Boekema, E.J., Hankamer, B., Bald, D., Kruij, J., Nield, J., Boonstra, A.F., Barber, J., and Rögner, M. (1995). Supramolecular structure of the photosystem II complex from green plants and cyanobacteria. *Proc. Natl. Acad. Sci. USA* **92**: 175–179.
- Candiano, G., Bruschi, M., Musante, L., Santucci, L., Ghiggeri, G.M., Carnemolla, B., Orecchia, P., Zardi, L., and Righetti, P.G. (2004). Blue silver: A very sensitive colloidal Coomassie G-250 staining for proteome analysis. *Electrophoresis* **25**: 1327–1333.
- Chen, H., Zhang, D., Guo, J., Wu, H., Jin, M., Lu, Q., Lu, C., and Zhang, L. (2006). A Psb27 homologue in *Arabidopsis thaliana* is required for efficient repair of photodamaged photosystem II. *Plant Mol. Biol.* **61**: 567–575.
- Chenna, R., Sugawara, H., Koike, T., Lopez, R., Gibson, T.J., Higgins, D.G., and Thompson, J.D. (2003). Multiple sequence alignment with the Clustal series of programs. *Nucleic Acids Res.* **31**: 3497–3500.
- Choquet, Y., and Wollman, F.A. (2002). Translational regulations as specific traits of chloroplast gene expression. *FEBS Lett.* **529**: 39–42.
- Choquet, Y., Wostrickoff, K., Rimbault, B., Zito, F., Girard-Bascou, J., Drapier, D., and Wollman, F.A. (2001). Assembly-controlled regulation of chloroplast gene translation. *Biochem. Soc. Trans.* **29**: 421–426.
- Clough, S.J., and Bent, A.F. (1998). Floral dip: A simplified method for *Agrobacterium*-mediated transformation of *Arabidopsis thaliana*. *Plant J.* **16**: 735–743.
- Diner, B.A., Ries, D.F., Cohen, B.N., and Metz, J.G. (1988). COOH-terminal processing of polypeptide D1 of the photosystem II reaction center of *Scenedesmus obliquus* is necessary for the assembly of the oxygen-evolving complex. *J. Biol. Chem.* **263**: 8972–8980.
- Dewez, D., Park, S., García-Cerdán, J.G., Lindberg, P., and Melis, A. (2009). Mechanism of REP27 protein action in the D1 protein turnover and photosystem II repair from photodamage. *Plant Physiol.* **151**: 88–99.
- Dobáková, M., Sobotka, R., Tichý, M., and Komenda, J. (2009).

- Psb28 protein is involved in the biogenesis of the photosystem II inner antenna CP47 (PsbB) in the cyanobacterium *Synechocystis* sp. PCC 6803. *Plant Physiol.* **149**: 1076–1086.
- Dühring, U., Irrgang, K.D., Lünser, K., Kehr, J., and Wilde, A.** (2006). Analysis of photosynthetic complexes from a cyanobacterial *ycf37* mutant. *Biochim. Biophys. Acta* **1757**: 3–11.
- Eaton-Rye, J.J.** (2004). The construction of gene knockouts in the cyanobacterium *Synechocystis* sp. PCC 6803. *Methods Mol. Biol.* **274**: 309–324.
- Edelman, M., and Mattoo, A.K.** (2008). D1-protein dynamics in photosystem II: The lingering enigma. *Photosynth. Res.* **98**: 609–620.
- Emanuelsson, O., Nielsen, H., and von Heijne, G.** (1999). ChloroP, a neural network-based method for predicting chloroplast transit peptides and their cleavage sites. *Protein Sci.* **8**: 978–984.
- Enami, I., Okumura, A., Nagao, R., Suzuki, T., Iwai, M., and Shen, J.R.** (2008). Structures and functions of the extrinsic proteins of photosystem II from different species. *Photosynth. Res.* **98**: 349–363.
- Ermakova-Gerdes, S., and Vermaas, W.** (1999). Inactivation of the open reading frame *slr0399* in *Synechocystis* sp. PCC 6803 functionally complements mutations near the Q<sub>A</sub> niche of photosystem II. A possible role of Slr0399 as a chaperone for quinone binding. *J. Biol. Chem.* **274**: 30540–30549.
- Färber, A., Young, A.J., Ruban, A.V., Horton, P., and Jahns, P.** (1997). Dynamics of xanthophyll-cycle activity in different antenna subcomplexes in the photosynthetic membranes of higher plants. The relationship between zeaxanthin conversion and nonphotochemical fluorescence quenching. *Plant Physiol.* **115**: 1609–1618.
- Ferreira, K.N., Iverson, T.M., Maghlaoui, K., Barber, J., and Iwata, S.** (2004). Architecture of the photosynthetic oxygen-evolving center. *Science* **303**: 1831–1838.
- Frey, M., Stettner, C., and Gierl, A.** (1998). A general method for gene isolation in tagging approaches: amplification of insertion mutagenised sites (AIMS). *Plant J.* **13**: 717–721.
- Göhre, V., Ossenbühl, F., Crèvecoeur, M., Eichacker, L.A., and Rochaix, J.D.** (2006). One of two *alb3* proteins is essential for the assembly of the photosystems and for cell survival in *Chlamydomonas*. *Plant Cell* **18**: 1454–1466.
- Granvogel, B., Reisinger, V., and Eichacker, L.A.** (2006). Mapping the proteome of thylakoid membranes by de novo sequencing of intermembrane peptide domains. *Proteomics* **6**: 3681–3695.
- Guskov, A., Kern, J., Gabdulkhakov, A., Broser, M., Zouni, A., and Saenger, W.** (2009). Cyanobacterial photosystem II at 2.9-Å resolution and the role of quinones, lipids, channels and chloride. *Nat. Struct. Mol. Biol.* **16**: 334–342.
- Hankamer, B., Nield, J., Zheleva, D., Boekema, E., Jansson, S., and Barber, J.** (1997). Isolation and biochemical characterisation of monomeric and dimeric photosystem II complexes from spinach and their relevance to the organisation of photosystem II in vivo. *Eur. J. Biochem.* **243**: 422–429.
- Hatano-Iwasaki, A., Minagawa, J., Inoue, Y., and Takahashi, Y.** (2000). Characterization of chloroplast *psbA* transformants of *Chlamydomonas reinhardtii* with impaired processing of a precursor of a photosystem II reaction center protein, D1. *Plant Mol. Biol.* **42**: 353–363.
- Ihnatowicz, A., Pesaresi, P., Lohrig, K., Wolters, D., Müller, B., and Leister, D.** (2008). Impaired photosystem I oxidation induces STN7-dependent phosphorylation of the light-harvesting complex I protein Lhca4 in *Arabidopsis thaliana*. *Planta* **227**: 717–722.
- Ihnatowicz, A., Pesaresi, P., Varotto, C., Richly, E., Schneider, A., Jahns, P., Salamini, F., and Leister, D.** (2004). Mutants for photosystem I subunit D of *Arabidopsis thaliana*: Effects on photosynthesis, photosystem I stability and expression of nuclear genes for chloroplast functions. *Plant J.* **37**: 839–852.
- Iwata, S., and Barber, J.** (2004). Structure of photosystem II and molecular architecture of the oxygen-evolving centre. *Curr. Opin. Struct. Biol.* **14**: 447–453.
- Kapri-Pardes, E., Naveh, L., and Adam, Z.** (2007). The thylakoid lumen protease Deg1 is involved in the repair of photosystem II from photoinhibition in *Arabidopsis*. *Plant Cell* **19**: 1039–1047.
- Karimi, M., de Oliveira Manes, C.L., Van Montagu, M., and Gheysen, G.** (2002). Activation of a pollenin promoter upon nematode infection. *J. Nematol.* **34**: 75–79.
- Karnauchov, I., Herrmann, R.G., and Klösgen, R.B.** (1997). Transmembrane topology of the Rieske Fe/S protein of the cytochrome *b<sub>6</sub>/f* complex from spinach chloroplasts. *FEBS Lett.* **408**: 206–210.
- Kashino, Y., Lauber, W.M., Carroll, J.A., Wang, Q., Whitmarsh, J., Satoh, K., and Pakrasi, H.B.** (2002). Proteomic analysis of a highly active photosystem II preparation from the cyanobacterium *Synechocystis* sp. PCC 6803 reveals the presence of novel polypeptides. *Biochemistry* **41**: 8004–8012.
- Kato, Y., and Sakamoto, W.** (2009). Protein quality control in chloroplasts: A current model of D1 protein degradation in the photosystem II repair cycle. *J. Biochem.* **146**: 463–469.
- Keren, N., Ohkawa, H., Welsh, E.A., Liberton, M., and Pakrasi, H.B.** (2005). Psb29, a conserved 22-kD protein, functions in the biogenesis of photosystem II complexes in *Synechocystis* and *Arabidopsis*. *Plant Cell* **17**: 2768–2781.
- Klinkert, B., Ossenbühl, F., Sikorski, M., Berry, S., Eichacker, L., and Nickelsen, J.** (2004). PrtA, a periplasmic tetratricopeptide repeat protein involved in biogenesis of photosystem II in *Synechocystis* sp. PCC 6803. *J. Biol. Chem.* **279**: 44639–44644.
- Kogata, N., Nishio, K., Hirohashi, T., Kikuchi, S., and Nakai, M.** (1999). Involvement of a chloroplast homologue of the signal recognition particle receptor protein, FtsY, in protein targeting to thylakoids. *FEBS Lett.* **447**: 329–333.
- Komenda, J., Nickelsen, J., Tichý, M., Prášil, O., Eichacker, L.A., and Nixon, P.J.** (2008). The cyanobacterial homologue of HCF136/YCF48 is a component of an early photosystem II assembly complex and is important for both the efficient assembly and repair of photosystem II in *Synechocystis* sp. PCC 6803. *J. Biol. Chem.* **283**: 22390–22399.
- Komenda, J., Tichý, M., and Eichacker, L.A.** (2005). The PsbH protein is associated with the inner antenna CP47 and facilitates D1 processing and incorporation into PSII in the cyanobacterium *Synechocystis* PCC 6803. *Plant Cell Physiol.* **46**: 1477–1483.
- Krogh, A., Larsson, B., von Heijne, G., and Sonnhammer, E.L.** (2001). Predicting transmembrane protein topology with a hidden Markov model: Application to complete genomes. *J. Mol. Biol.* **305**: 567–580.
- Kufryk, G.I., and Vermaas, W.F.** (2001). A novel protein involved in the functional assembly of the oxygen-evolving complex of photosystem II in *Synechocystis* sp. PCC 6803. *Biochemistry* **40**: 9247–9255.
- Kufryk, G.I., and Vermaas, W.F.** (2003). Slr2013 is a novel protein regulating functional assembly of photosystem II in *Synechocystis* sp. strain PCC 6803. *J. Bacteriol.* **185**: 6615–6623.
- Laidler, V., Chaddock, A.M., Knott, T.G., Walker, D., and Robinson, C.** (1995). A SecY homolog in *Arabidopsis thaliana*. Sequence of a full-length cDNA clone and import of the precursor protein into chloroplasts. *J. Biol. Chem.* **270**: 17664–17667.
- Leister, D., Varotto, C., Pesaresi, P., Niwergall, A., and Salamini, F.** (1999). Large-scale evaluation of plant growth in *Arabidopsis thaliana* by non-invasive image analysis. *Plant Physiol. Biochem.* **37**: 671–678.
- Ma, J., Peng, L., Guo, J., Lu, Q., Lu, C., and Zhang, L.** (2007). LPA2 is required for efficient assembly of photosystem II in *Arabidopsis thaliana*. *Plant Cell* **19**: 1980–1993.
- Martienssen, R.A.** (1998). Functional genomics: Probing plant gene function and expression with transposons. *Proc. Natl. Acad. Sci. USA* **95**: 2021–2026.
- Martínez-García, J.F., Monte, E., and Quail, P.H.** (1999). A simple,

- rapid and quantitative method for preparing *Arabidopsis* protein extracts for immunoblot analysis. *Plant J.* **20**: 251–257.
- Meurer, J., Plücker, H., Kowallik, K.V., and Westhoff, P.** (1998). A nuclear-encoded protein of prokaryotic origin is essential for the stability of photosystem II in *Arabidopsis thaliana*. *EMBO J.* **17**: 5286–5297.
- Minagawa, J., and Takahashi, Y.** (2004). Structure, function and assembly of photosystem II and its light-harvesting proteins. *Photosynth. Res.* **82**: 241–263.
- Mulo, P., Sirpiö, S., Suorsa, M., and Aro, E.M.** (2008). Auxiliary proteins involved in the assembly and sustenance of photosystem II. *Photosynth. Res.* **98**: 489–501.
- Nelson, N., and Yocum, C.F.** (2006). Structure and function of photosystems I and II. *Annu. Rev. Plant Biol.* **57**: 521–565.
- Nixon, P.J., Barker, M., Boehm, M., de Vries, R., and Komenda, J.** (2005). FtsH-mediated repair of the photosystem II complex in response to light stress. *J. Exp. Bot.* **56**: 357–363.
- Nixon, P.J., Michoux, F., Yu, J., Boehm, M., and Komenda, J.** (2010). Recent advances in understanding the assembly and repair of photosystem II. *Ann. Bot. (Lond.)* **106**: 1–16.
- Nixon, P.J., Trost, J.T., and Diner, B.A.** (1992). Role of the carboxy terminus of polypeptide D1 in the assembly of a functional water-oxidizing manganese cluster in photosystem II of the cyanobacterium *Synechocystis* sp. PCC 6803: Assembly requires a free carboxyl group at C-terminal position 344. *Biochemistry* **31**: 10859–10871.
- Nowaczyk, M.M., Hebel, R., Schlodder, E., Meyer, H.E., Warscheid, B., and Rögner, M.** (2006). Psb27, a cyanobacterial lipoprotein, is involved in the repair cycle of photosystem II. *Plant Cell* **18**: 3121–3131.
- Ossenbühl, F., Göhre, V., Meurer, J., Krieger-Liszka, A., Rochaix, J.D., and Eichacker, L.A.** (2004). Efficient assembly of photosystem II in *Chlamydomonas reinhardtii* requires Alb3.1p, a homolog of *Arabidopsis* ALBINO3. *Plant Cell* **16**: 1790–1800.
- Ossenbühl, F., Inaba-Sulpice, M., Meurer, J., Soll, J., and Eichacker, L.A.** (2006). The *synechocystis* sp PCC 6803 *oxa1* homolog is essential for membrane integration of reaction center precursor protein pD1. *Plant Cell* **18**: 2236–2246.
- Park, S., Khamai, P., Garcia-Cerdan, J.G., and Melis, A.** (2007). REP27, a tetratricopeptide repeat nuclear-encoded and chloroplast-localized protein, functions in D1/32-kD reaction center protein turnover and photosystem II repair from photodamage. *Plant Physiol.* **143**: 1547–1560.
- Pasch, J.C., Nickelsen, J., and Schünemann, D.** (2005). The yeast split-ubiquitin system to study chloroplast membrane protein interactions. *Appl. Microbiol. Biotechnol.* **69**: 440–447.
- Peng, L., Ma, J., Chi, W., Guo, J., Zhu, S., Lu, Q., Lu, C., and Zhang, L.** (2006). LOW PSII ACCUMULATION1 is involved in efficient assembly of photosystem II in *Arabidopsis thaliana*. *Plant Cell* **18**: 955–969.
- Peng, L., Shimizu, H., and Shikanai, T.** (2008). The chloroplast NAD(P)H dehydrogenase complex interacts with photosystem I in *Arabidopsis*. *J. Biol. Chem.* **283**: 34873–34879.
- Pesaresi, P., Hertle, A., Pribil, M., Kleine, T., Wagner, R., Strissel, H., Ihnatowicz, A., Bonardi, V., Scharfenberg, M., Schneider, A., Pfanschmidt, T., and Leister, D.** (2009). *Arabidopsis* STN7 kinase provides a link between short- and long-term photosynthetic acclimation. *Plant Cell* **21**: 2402–2423.
- Pesaresi, P., Lunde, C., Jahns, P., Tarantino, D., Meurer, J., Varotto, C., Hirtz, R.D., Soave, C., Scheller, H.V., Salamini, F., and Leister, D.** (2002). A stable LHCII-PSI aggregate and suppression of photosynthetic state transitions in the *psae1-1* mutant of *Arabidopsis thaliana*. *Planta* **215**: 940–948.
- Pesaresi, P., Masiero, S., Eubel, H., Braun, H.P., Bhushan, S., Glaser, E., Salamini, F., and Leister, D.** (2006). Nuclear photosynthetic gene expression is synergistically modulated by rates of protein synthesis in chloroplasts and mitochondria. *Plant Cell* **18**: 970–991.
- Plücker, H., Müller, B., Grohmann, D., Westhoff, P., and Eichacker, L.A.** (2002). The HCF136 protein is essential for assembly of the photosystem II reaction center in *Arabidopsis thaliana*. *FEBS Lett.* **532**: 85–90.
- Rokka, A., Suorsa, M., Saleem, A., Battchikova, N., and Aro, E.M.** (2005). Synthesis and assembly of thylakoid protein complexes: multiple assembly steps of photosystem II. *Biochem. J.* **388**: 159–168.
- Roose, J.L., and Pakrasi, H.B.** (2004). Evidence that D1 processing is required for manganese binding and extrinsic protein assembly into photosystem II. *J. Biol. Chem.* **279**: 45417–45422.
- Roose, J.L., Wegener, K.M., and Pakrasi, H.B.** (2007). The extrinsic proteins of photosystem II. *Photosynth. Res.* **92**: 369–387.
- Rosso, M.G., Li, Y., Strizhov, N., Reiss, B., Dekker, K., and Weisshaar, B.** (2003). An *Arabidopsis thaliana* T-DNA mutagenized population (GABI-Kat) for flanking sequence tag-based reverse genetics. *Plant Mol. Biol.* **53**: 247–259.
- Roy, L.M., and Barkan, A.** (1998). A SecY homologue is required for the elaboration of the chloroplast thylakoid membrane and for normal chloroplast gene expression. *J. Cell Biol.* **141**: 385–395.
- Schägger, H., Aquila, H., and Von Jagow, G.** (1988). Coomassie blue-sodium dodecyl sulfate-polyacrylamide gel electrophoresis for direct visualization of polypeptides during electrophoresis. *Anal. Biochem.* **173**: 201–205.
- Schägger, H., and von Jagow, G.** (1987). Tricine-sodium dodecyl sulfate-polyacrylamide gel electrophoresis for the separation of proteins in the range from 1 to 100 kDa. *Anal. Biochem.* **166**: 368–379.
- Schottkowski, M., Gkalypoudis, S., Tzekova, N., Stelljes, C., Schünemann, D., Ankele, E., and Nickelsen, J.** (2009a). Interaction of the periplasmic PrtaA factor and the PsbA (D1) protein during biogenesis of photosystem II in *Synechocystis* sp. PCC 6803. *J. Biol. Chem.* **284**: 1813–1819.
- Schottkowski, M., Ratke, J., Oster, U., Nowaczyk, M., and Nickelsen, J.** (2009b). Pitt, a novel tetratricopeptide repeat protein involved in light-dependent chlorophyll biosynthesis and thylakoid membrane biogenesis in *Synechocystis* sp. PCC 6803. *Mol. Plant* **2**: 1289–1297.
- Schult, K., Meierhoff, K., Paradies, S., Töller, T., Wolff, P., and Westhoff, P.** (2007). The nuclear-encoded factor HCF173 is involved in the initiation of translation of the *psbA* mRNA in *Arabidopsis thaliana*. *Plant Cell* **19**: 1329–1346.
- Schwenkert, S., Umate, P., Dal Bosco, C., Volz, S., Mičochová, L., Zoryan, M., Eichacker, L.A., Ohad, I., Herrmann, R.G., and Meurer, J.** (2006). PsbI affects the stability, function, and phosphorylation patterns of photosystem II assemblies in tobacco. *J. Biol. Chem.* **281**: 34227–34238.
- Shestakov, S.V., Anbudurai, P.R., Stanbekova, G.E., Gadzhiev, A., Lind, L.K., and Pakrasi, H.B.** (1994). Molecular cloning and characterization of the *ctpA* gene encoding a carboxyl-terminal processing protease. Analysis of a spontaneous photosystem II-deficient mutant strain of the cyanobacterium *Synechocystis* sp. PCC 6803. *J. Biol. Chem.* **269**: 19354–19359.
- Shi, L.X., and Schröder, W.P.** (2004). The low molecular mass subunits of the photosynthetic supracomplex, photosystem II. *Biochim. Biophys. Acta* **1608**: 75–96.
- Sirpiö, S., Khrouchtchova, A., Allahverdiyeva, Y., Hansson, M., Fristedt, R., Vener, A.V., Scheller, H.V., Jensen, P.E., Haldrup, A., and Aro, E.M.** (2008). AtCYP38 ensures early biogenesis, correct assembly and sustenance of photosystem II. *Plant J.* **55**: 639–651.
- Spence, E., Bailey, S., Nenninger, A., Möller, S.G., and Robinson, C.** (2004). A homolog of Albino3/Oxal is essential for thylakoid biogenesis in the cyanobacterium *Synechocystis* sp. PCC6803. *J. Biol. Chem.* **279**: 55792–55800.
- Sun, X., Ouyang, M., Guo, J., Lu, C., Adam, Z., and Zhang, L.** (2010). The thylakoid protease Deg1 is involved in photosystem-II assembly in *Arabidopsis thaliana*. *Plant J.* **62**: 240–249.

- Sundberg, E., Slagter, J.G., Fridborg, I., Cleary, S.P., Robinson, C., and Coupland, G.** (1997). *ALBINO3*, an *Arabidopsis* nuclear gene essential for chloroplast differentiation, encodes a chloroplast protein that shows homology to proteins present in bacterial membranes and yeast mitochondria. *Plant Cell* **9**: 717–730.
- Tatusova, T.A., and Madden, T.L.** (1999). BLAST 2 Sequences, a new tool for comparing protein and nucleotide sequences. *FEMS Microbiol. Lett.* **174**: 247–250.
- Taylor, M.A., Packer, J.C.L., and Bowyer, J.R.** (1988). Processing of the D1 polypeptide of the photosystem II reaction centre and photoactivation of a low fluorescence mutant (LF-1) of *Scenedesmus obliquus*. *FEBS Lett.* **237**: 229–233.
- van Wijk, K.J., Andersson, B., and Aro, E.M.** (1996). Kinetic resolution of the incorporation of the D1 protein into photosystem II and localization of assembly intermediates in thylakoid membranes of spinach chloroplasts. *J. Biol. Chem.* **271**: 9627–9636.
- van Wijk, K.J., Bingsmark, S., Aro, E.M., and Andersson, B.** (1995). In vitro synthesis and assembly of photosystem II core proteins. The D1 protein can be incorporated into photosystem II in isolated chloroplasts and thylakoids. *J. Biol. Chem.* **270**: 25685–25695.
- van Wijk, K.J., Roobol-Boza, M., Kettunen, R., Andersson, B., and Aro, E.M.** (1997). Synthesis and assembly of the D1 protein into photosystem II: Processing of the C-terminus and identification of the initial assembly partners and complexes during photosystem II repair. *Biochemistry* **36**: 6178–6186.
- Varotto, C., Pesaresi, P., Maiwald, D., Kurth, J., Salamini, F., and Leister, D.** (2000a). Identification of photosynthetic mutants of *Arabidopsis* by automatic screening for altered effective quantum yield of photosystem 2. *Photosynthetica* **38**: 497–504.
- Varotto, C., Pesaresi, P., Meurer, J., Oelmüller, R., Steiner-Lange, S., Salamini, F., and Leister, D.** (2000b). Disruption of the *Arabidopsis* photosystem I gene *psaE1* affects photosynthesis and impairs growth. *Plant J.* **22**: 115–124.
- Wei, L., Guo, J., Ouyang, M., Sun, X., Ma, J., Chi, W., Lu, C., and Zhang, L.** (2010). LPA19, a Psb27 homolog in *Arabidopsis thaliana*, facilitates D1 protein precursor processing during PSII biogenesis. *J. Biol. Chem.* **285**: 21391–21398.
- Wessel, D., and Flügge, U.I.** (1984). A method for the quantitative recovery of protein in dilute solution in the presence of detergents and lipids. *Anal. Biochem.* **138**: 141–143.
- Wollman, F.A., Minai, L., and Nechushtai, R.** (1999). The biogenesis and assembly of photosynthetic proteins in thylakoid membranes. *Biochim. Biophys. Acta* **1411**: 21–85.
- Zaltsman, A., Feder, A., and Adam, Z.** (2005). Developmental and light effects on the accumulation of FtsH protease in *Arabidopsis* chloroplasts—Implications for thylakoid formation and photosystem II maintenance. *Plant J.* **42**: 609–617.

### 3.2 AN INTERMEDIATE MEMBRANE SUBFRACTION IN CYANOBACTERIA IS INVOLVED IN AN ASSEMBLY NETWORK FOR PHOTOSYSTEM II BIOGENESIS

**Rengstl, B.,** Oster, U., Stengel, A., and Nickelsen, J. (2011) J Biol Chem **286**, 21944-21951

In this study, PDMs, which were described to represent a special membrane subfraction where early steps of PSII biogenesis take place, were characterized in more detail with regard to their lipid, pigment and protein composition. Besides PratA, other facilitating factors involved in earlier steps of PSII assembly like Slr1471 and YCF48 could be detected – at least partially – in PDMs substantiating the important role of these membranes in PSII biogenesis. The finding, that in a *prata*<sup>-</sup> mutant the distribution of all tested PSII assembly factors was altered, further underlined the significance of the PratA protein in spatial organization of this process. Moreover, by analyzing the pigment composition of PDMs and TMs using thin layer chromatography and HPLC techniques, an accumulation of the chlorophyll *a* precursor chlorophyllide *a* in PDMs could be revealed. This supports the hypothesis that not only PSII protein subunit assembly but also pigment synthesis and probably also their insertion into apoproteins take place in PDMs.

In addition, examination of the accumulation as well as membrane distribution of different PSII-related proteins in various PSII mutant strains also gave insight into potential interdependencies between individual assembly factors. Indeed, the results suggest a complex regulatory network between PSII protein complex assembly factors as well as proteins involved in chlorophyll synthesis. The most obvious correlation was obtained for YCF48 and Sll0933, whose interrelation was furthermore confirmed by co-migration in blue-native gels as well as co-immunoprecipitation studies. Since membrane fractionation experiments revealed a localization of Sll0933 exclusively in TMs of wild-type cells, whereas YCF48 was also detected in the PDMs, interaction of YCF48 and Sll0933 was discussed to occur at the interface between PDMs and TMs, probably mediating the correct attachment of CP47 to RC complexes and, thus, formation of RC47.

All experiments were carried out by myself with exception of HPLC analyses including preceding pigment extraction, which was performed by U. Oster. The manuscript was written by J. Nickelsen and me and revised by A. Stengel.

# An Intermediate Membrane Subfraction in Cyanobacteria Is Involved in an Assembly Network for Photosystem II Biogenesis<sup>\*S</sup>

Received for publication, March 7, 2011, and in revised form, April 20, 2011. Published, JBC Papers in Press, April 29, 2011, DOI 10.1074/jbc.M111.237867

Birgit Rengstl<sup>‡</sup>, Ulrike Oster<sup>§</sup>, Anna Stengel<sup>‡</sup>, and Jörg Nickelsen<sup>†1</sup>

From <sup>‡</sup>Molekulare Pflanzenwissenschaften and <sup>§</sup>Biochemie und Physiologie der Pflanzen, Biozentrum, Ludwig-Maximilians-Universität München, Grosshaderner Strasse 2-4, 82152 Planegg-Martinsried, Germany

Early steps in the biogenesis of Photosystem II (PSII) in the cyanobacterium *Synechocystis* sp. PCC 6803 are thought to occur in a specialized membrane fraction that is characterized by the specific accumulation of the PSII assembly factor PrataA and its interaction partner pD1, the precursor of the D1 protein of PSII. Here, we report the molecular characterization of this membrane fraction, called the PrataA-defined membrane (PDM), with regard to its lipid and pigment composition and its association with PSII assembly factors, including YCF48, Slr1471, Sll0933, and Pitt. We demonstrate that YCF48 and Slr1471 are present and that the chlorophyll precursor chlorophyllide *a* accumulates in the PDM. Analysis of PDMs from various mutant lines suggests a central role for PrataA in the spatial organization of PSII biogenesis. Moreover, quantitative immunoblot analyses revealed a network of interdependences between several PSII assembly factors and chlorophyll synthesis. In addition, formation of complexes containing both YCF48 and Sll0933 was substantiated by co-immunoprecipitation experiments. The findings are integrated into a refined model for PSII biogenesis in *Synechocystis* 6803.

Cyanobacteria are Gram-negative bacteria that perform oxygenic photosynthesis. They contain three types of membranes: the outer membrane, the plasma membrane (PM),<sup>2</sup> and the thylakoid membrane (TM) system. The outer membrane and PM form the cell envelope and delimit the periplasmic space, whereas TMs are localized within the cell and house the large pigment-protein complexes of the photosynthetic electron transfer chain, *i.e.* Photosystem (PS) II, PSI, the cytochrome *b<sub>6</sub>f* complex, and the ATP synthase (1). It is not clear whether direct connections exist between the different membrane systems and, in particular, where synthesis of TMs is initiated (2–4). In the cyanobacterium *Synechocystis* sp. PCC 6803, an intermediate membrane subfraction (PDM) was recently identified, which is defined by the presence of a membrane-bound

form of the PSII assembly factor PrataA (5). PrataA is a periplasmic tetratricopeptide repeat protein that has been shown to interact with the C-terminal segment of pD1, the precursor of the PSII reaction center core protein D1 and to affect its maturation (5, 6). In *Synechocystis* 6803, pD1 contains a C-terminal extension of 16 amino acids that has to be processed by the endoprotease CtpA to allow proper assembly of the oxygen-evolving complex on the luminal side of PSII (7–10). Because substantial amounts of pD1 accumulate in PDMs, these were hypothesized to represent a specialized membrane region close to the PM where early steps in the *de novo* assembly of PSII take place (4, 5). Several intermediates in this early assembly process have been detected, including the so-called reaction center (RC) complex containing pD1 and D2, as well as subunits PsbI, PsbE, and PsbF (11). Successive attachment of the inner antennal proteins CP47 and CP43 yields complexes RC47 and RCC1, respectively. RCC1 represents the monomeric PSII core complex, which is capable of oxygen evolution (11).

In addition to PrataA, several other D1-associated factors have been suggested to function during the early steps of PSII biogenesis not only in cyanobacteria but also in higher plants (for a recent review, see Ref. 11). Thus, the cyanobacterial YidC/Oxa1/Alb3 homolog Slr1471 has been shown to interact directly with the D1 protein during its integration into the membrane (12). Similarly, a direct interaction has been revealed between pD1 and YCF48, the *Synechocystis* homolog of HCF136 from *Arabidopsis thaliana*, which seems to be involved in facilitating formation of PSII RC intermediates (13, 14). The *A. thaliana* protein PAM68 and its *Synechocystis* homolog Sll0933 have also been shown to be required for proper assembly of PSII, and a direct interaction of PAM68 with D1 was suggested in yeast two-hybrid analyses (15).

As the assembly of photosynthetic protein complexes has to be coordinated with the integration of pigments to form functional photosystems, it appears likely that chlorophyll synthesis is synchronized with the expression of chlorophyll-binding proteins. This would not only ensure the availability of sufficient pigments to build up the photosynthetic apparatus but would also prevent the accumulation of free and potentially harmful chlorophyll and/or chlorophyll precursor molecules (16, 17). Such coordination may be favored by co-localization of the machineries required for protein and pigment synthesis, as suggested by studies of the Pitt protein, which interacts with the light-dependent protochlorophyllide oxidoreductase (POR), an enzyme involved in the conversion of protochlorophyllide *a*

<sup>\*</sup> This work was supported by Deutsche Forschungsgemeinschaft Grant SFB TR1 TPC10 (to J. N.) and a Bayerische Gleichstellungsförderung (BGF) scholarship from the Ludwig-Maximilians-Universität München (to A. S.).

<sup>‡</sup> The on-line version of this article (available at <http://www.jbc.org>) contains supplemental Figs. 1 and 2.

<sup>†</sup> To whom correspondence should be addressed. Tel.: 49-89-2180-74773; Fax: 49-89-2180-9974773; E-mail: joerg.nickelsen@lrz.uni-muenchen.de.

<sup>2</sup> The abbreviations used are: PM, plasma membrane; TM, thylakoid membrane; PS, Photosystem; PDM, PrataA-defined membrane; RC, reaction center; POR, protochlorophyllide oxidoreductase.

into chlorophyllide *a* (4, 11, 18, 19), a precursor of chlorophyll *a*. Intriguingly, both Pitt and POR are present in PDM fractions of wild-type cells, suggesting a role for PDMs not only in protein synthesis and assembly but also in pigment synthesis and insertion (4, 18).

Here, we present a comprehensive characterization of the distribution of membrane-associated D1 assembly factors in the PDM subfraction from *Synechocystis* 6803. Additionally, we looked at qualitative differences in the lipid and pigment composition of PDMs and TMs to uncover correlations between pigment and protein synthesis and assembly. The results reveal a PDM-localized network for pigment-protein complex assembly and underline the importance of the PrtA factor for the spatial organization of the assembly process. Moreover, further evidence for a direct link between YCF48 and Sll0933 was obtained. Together, they appear to mediate crucial steps at the PDM/TM interface.

## EXPERIMENTAL PROCEDURES

**Growth Conditions and Construction of Cyanobacterial Strains**—Glucose-tolerant wild-type *Synechocystis* 6803 and relevant mutant strains were grown under continuous irradiation with 30  $\mu\text{mol}$  of photons  $\text{m}^{-2} \text{s}^{-1}$  at 30 °C in BG11 medium containing 5 mM glucose (20). For construction of a *ctpA*<sup>−</sup> mutant strain, the coding region was amplified by PCR using the primer pair THctpAa (GAATTCATGGGTAACCGACAAGGCGGTTT) and THctpAb (CTCGAGTTAGTTAGTTGGGCTTGTGAGCCG). The *ctpA* gene was disrupted by insertion of a kanamycin resistance cassette into the single MunI restriction site, and wild-type cells were transformed with this construct as described (21). Complete segregation of the mutated gene was confirmed by PCR analysis (data not shown). Mutant strains *pratA*<sup>−</sup>, *pitt*<sup>−</sup>, *ins0933*, *ycf48*<sup>−</sup>, and *psbB*<sup>−</sup> and *psbA* deletion strain *TD41* were constructed as described previously (6, 7, 14, 15, 18, 22).

**Antibody Production**—For generation of specific antibodies, the sequence encoding amino acid residues 275–342 of YCF48 was amplified using primers 2034-5 (AAGGATCCGAAGAA-GTATGGGTAGCGGG) and 2034-3 (AACTCGAGCTAGG-GAACCATTGCCACCT). The subcloned PCR fragment was inserted into the BamHI and XhoI sites of expression vector pGEX-4T-1. Overexpression of the GST fusion proteins in *Escherichia coli* BL21(DE3) cells and subsequent purification using glutathione-Sepharose 4B (GE Healthcare) were carried out according to the manufacturer's instructions. Polyclonal antisera were raised in rabbits (BioGenes GmbH, Berlin, Germany). Generation of antibodies against *Synechocystis* 6803 PrtA, Pitt, and Sll0933 has been described previously (6, 15, 18). Antibodies specific for CP47 (global), *A. thaliana* CP43, *Chlamydomonas reinhardtii* PsaA, and RbcL (global) were obtained from Agrisera (Vännäs, Sweden).

**Protein Extraction, Membrane Fractionation, and Immunoblot Analysis**—Protein extraction, two-step membrane fractionation on sucrose gradients, and subsequent immunoblot analysis were carried out as described previously (5, 18). For quantification, proteins of different strains were isolated, separated by SDS-PAGE, blotted, and probed with various antibodies. After densitometric scanning, quantification of signals was

performed using AIDA software (version 3.52.046), and the levels of mutant strains were compared with those of the wild-type strain (set to 100%). Means  $\pm$  S.D. were calculated from three independently inoculated cultures.

**Two-dimensional Blue Native/SDS-PAGE**—*Synechocystis* membranes were isolated as described (23), and two-dimensional Blue native/SDS-PAGE was performed as described previously (5).

**Co-immunoprecipitation**—For co-immunoprecipitation experiments, 50 ml of wild-type cells were harvested by centrifugation (4000  $\times$  *g*, 10 min, 4 °C), resuspended in 750  $\mu\text{l}$  of thylakoid buffer (50 mM HEPES/NaOH (pH 7.0), 5 mM MgCl<sub>2</sub>, 25 mM CaCl<sub>2</sub>, and 10% glycerol), and broken with glass beads (0.4–0.6 mm) using a Mini-BeadBeater (Glen Mills). Unbroken cells were removed by a short centrifugation step (20,000  $\times$  *g*, 45 s) before membranes were sedimented (20,000  $\times$  *g*, 30 min, 4 °C) and washed twice with thylakoid buffer. The sediment was subsequently resuspended in 50  $\mu\text{l}$  of Tris/NaCl buffer (50 mM Tris-HCl (pH 8) and 150 mM NaCl) and solubilized for 30 min on ice with 1.3%  $\beta$ -dodecyl maltoside. After another centrifugation step (20,000  $\times$  *g*, 30 min, 4 °C), the supernatant was diluted 1:10 with Tris/NaCl and incubated overnight at 4 °C in the presence of 10  $\mu\text{l}$  of anti-YCF48 antiserum or preimmune serum. Protein A-agarose was added (5 mg; Roche Applied Science), and incubation was continued for another hour at room temperature. The agarose beads were sedimented by centrifugation and washed five times, and bound proteins were eluted by incubation with 30  $\mu\text{l}$  of 2 $\times$  Roti<sup>®</sup>-Load 1 (Roth, Karlsruhe, Germany) for 5 min at 95 °C.

**Pigment and Lipid Analyses**—Pigments were extracted from concentrated membrane subfractions (5) by vortexing in the presence of added chloroform (2 ml) and methanol (1 ml). After the addition of 3 ml of chloroform and 3 ml of water, tubes were inverted, and the two phases were separated by centrifugation (3000  $\times$  *g*, 5 min, 4 °C). The organic phase was dried, and pigments/lipids were redissolved in 100  $\mu\text{l}$  of chloroform and subjected to TLC on silica gel plates (SIL G-25 UV<sub>254</sub>, Macherey-Nagel, Düren, Germany) in a mixture of acetone, toluene, and water (91:30:8). For visualization of lipids, the plates were sprayed with a staining solution (36 mM FeSO<sub>4</sub>, 5.7 mM KMnO<sub>4</sub>, and 3% (v/v) H<sub>2</sub>SO<sub>4</sub>) and incubated for 10 min at 120 °C.

Prior to analysis by HPLC, pigments were extracted from concentrated membrane subfractions with acetone. The analysis was performed on a Flux instrument equipped with a C<sub>18</sub> column (Grom Sil 120 ODS-5, 3- $\mu\text{m}$  particle size, 150-mm length, 2-mm inner diameter). Elution was carried out for 3 min with a 60:40 acetone/water mixture (pH 3.5), followed by a linear gradient to 100% acetone applied over a period of 20 min. The column was then rinsed for 20 min with 100% acetone. Absorption spectra were measured with a Thermo diode array detector in the 350–750-nm range. Pigments were identified based on their retention times and absorption spectra.

## RESULTS

**Pigments in PDMs and TMs**—PDMs have recently been suggested to represent a special membrane subcompartment where early steps in TM biogenesis take place (4, 5). As a first step toward a comprehensive characterization of PDMs, we

## Characterization of PDMs

examined the main pigments and lipids in PDMs and TMs. Membranes of wild-type *Synechocystis* 6803 cells were separated into PDM and TM fractions by two rounds of sucrose density gradient centrifugation (first on a step and then on a linear gradient), and the distribution of marker proteins was analyzed using antibodies (5). The inner antennal proteins of PSII, *i.e.* CP47 and CP43, serve as markers for TMs (10, 24) and were almost exclusively detected in fractions 7–11, hereafter referred to as TM fractions (see Fig. 2A) (5). In contrast, PDM fractions 1–6 were defined by the accumulation of Prata and pD1 (see Fig. 2A) (5). The majority of the PSII RC core protein D2 was located in TMs; however, a minor portion was detected in PDM fractions 4–6 (see Fig. 2A). Although it cannot be excluded that also minor amounts of CP43 and CP47 were present in the PDM fractions, it is obvious that this dual localization was more pronounced for D2 (see Fig. 2A). Hence, CP47 and CP43 can be regarded as suitable TM markers with the membrane fractionation method used. Subsequent TLC of membrane material from isolated fractions revealed no obvious qualitative differences in the main lipids between the two subfractions (supplemental Fig. 1).

Similarly, most of the lipophilic pigments, *i.e.* carotenoids and chlorophyll derivatives, were detectable in both PDMs (Fig. 1A, fractions 1–6) and TMs, although relatively more chlorophyll *a* was found in TMs (fractions 7–11). The only exception was a minor green band that was identified only in PDM fractions 5 and 6 of the wild-type material (Fig. 1A). HPLC-based analyses comparing the pigment compositions of PDM fraction 5 (Fig. 1D) and TM fraction 9 (Fig. 1E) revealed that the only pigment of green color that could exclusively be detected in PDM fraction 5 represents chlorophyllide *a*, a late intermediate in chlorophyll biosynthesis (Fig. 1D). Therefore, the PDM-specific band visible on thin-layer plates seems to be caused by chlorophyllide *a* accumulation (Fig. 1A, asterisks). This result is in agreement with earlier reports demonstrating that the highest concentrations of chlorophyllide *a* and its precursor, protochlorophyllide *a*, were detected in a membrane subfraction hypothesized to resemble contact sites between PMs and TMs called “thylakoid centers” (25). The PDM-specific accumulation of chlorophyllide *a* argues that PDMs represent a subcompartment in which not only protein complex assembly but also later steps in chlorophyll synthesis and probably insertion into polypeptides take place. This specific membrane localization of chlorophyllide *a* is independent of the presence of the PDM-specific Prata protein because it was not altered in a *prata*<sup>-</sup> mutant (Fig. 1B).

It was recently shown that lack of the POR-interacting protein Pitt causes a reduction in light-dependent chlorophyll synthesis (18). Therefore, we examined whether the accumulation and/or membrane localization of chlorophyllide *a* is affected in the *pitt*<sup>-</sup> mutant. Fig. 1C shows that the distribution of chlorophyll *a* and carotenoids in *pitt*<sup>-</sup> cells resembled that in the wild-type cells, whereas the putative chlorophyllide *a* band was completely absent. Therefore, loss of Pitt seems to affect synthesis of chlorophyllide *a* and, in particular, its accumulation in PDMs.

**Localization of PSII Assembly Factors in PDMs**—The accumulation of Prata and the pD1 precursor protein in PDMs

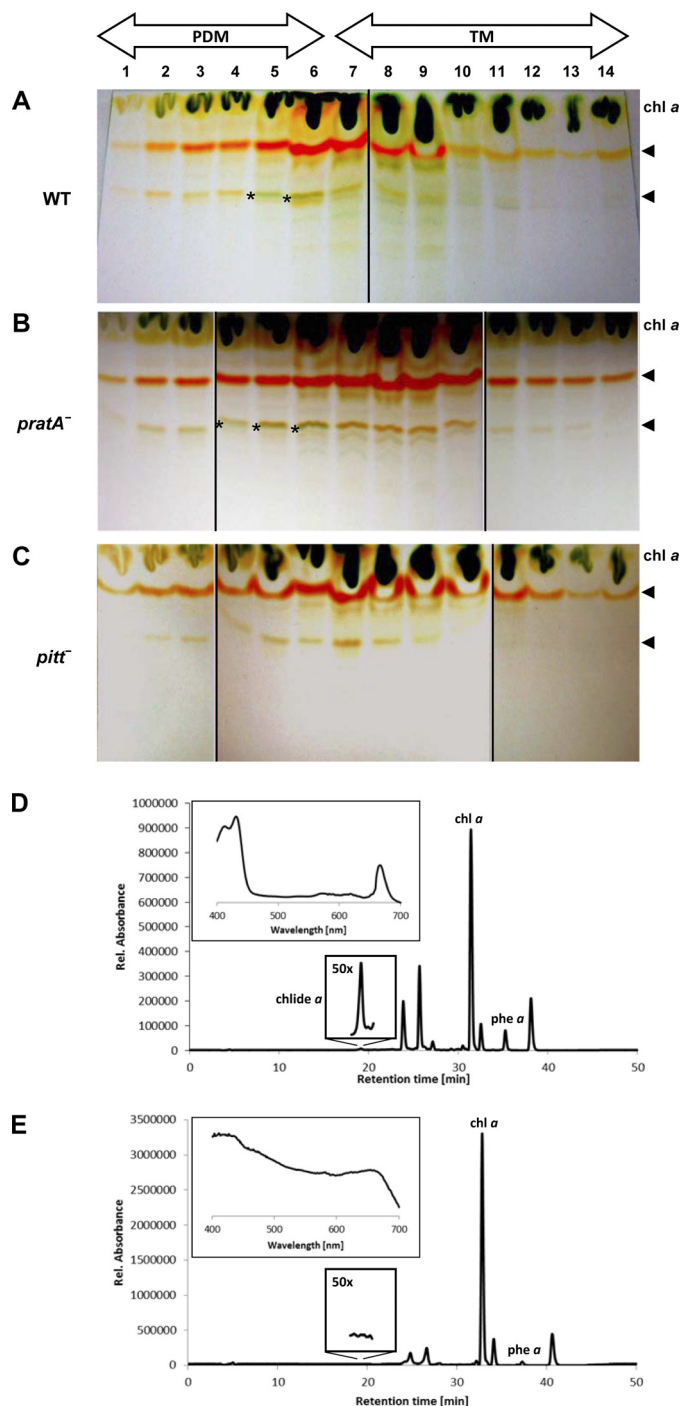


**FIGURE 1. Pigment analysis of PDM and TM fractions.** *Synechocystis* PDMs and TMs of wild-type (A), *prata*<sup>-</sup> (B), and *pitt*<sup>-</sup> (C) cells were obtained by two rounds of sucrose density gradient centrifugation. Equal volumes of hydrophobic pigments extracted from each fraction were then subjected to TLC. Asterisks mark a pigment accumulation in PDM fractions that seems to represent chlorophyllide *a*. Arrows indicate the positions of carotenoids. D and E, HPLC-based pigment analysis of PDM fraction 5 and TM fraction 9, respectively, of wild-type cells. The PDM-specific peak (shown also magnified  $\times 50$ ) was identified as chlorophyllide *a* (*chl* *a*) based on its retention time and absorption spectrum (*inset*). At the comparable retention time in TM fraction 9, no characteristic absorption spectrum for chlorophyll derivatives was detectable (*inset*). Due to their retention times and absorption spectra, other peaks were identified as chlorophyll *a* (*chl* *a*), pheophytin *a* (*phe* *a*), and carotenoids (all unlabeled peaks). Carotenoids were not further specified. *Rel.*, relative.

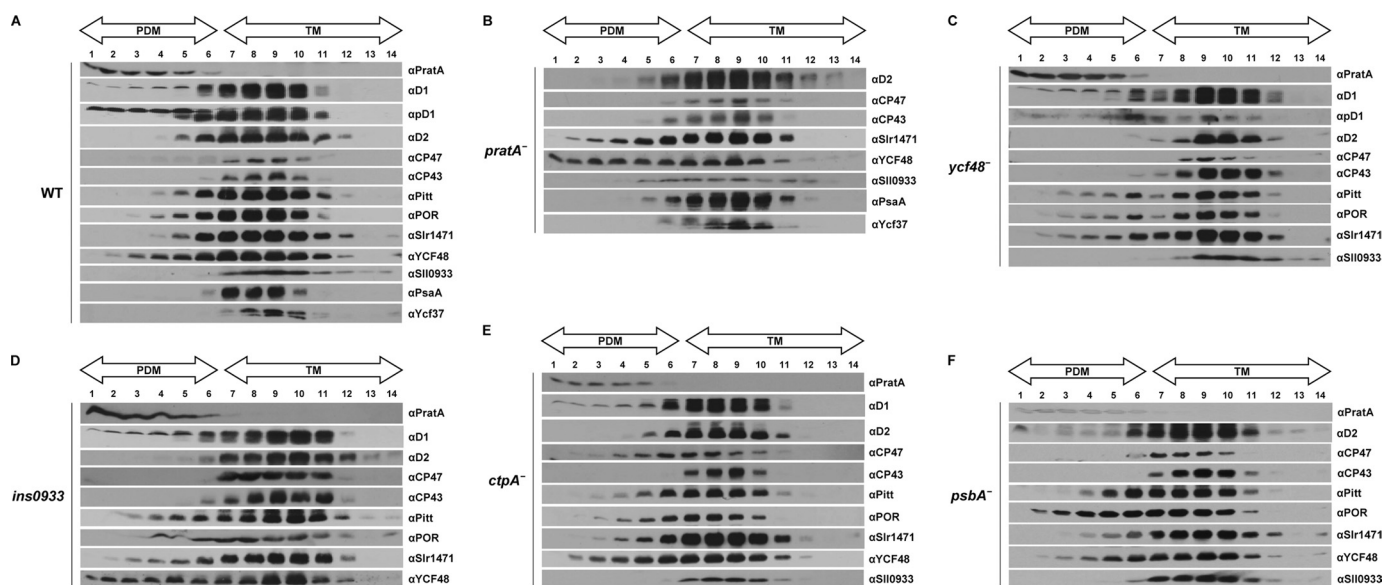


**FIGURE 2. Membrane sublocalization of different PSII assembly factors.** *Synechocystis* cell extracts of the wild-type strain (A) and *prata*<sup>-</sup> (B), *ycf48*<sup>-</sup> (C), *ins0933* (D), *ctpA*<sup>-</sup> (E), and *psbA*<sup>-</sup> (F) mutant strains were separated by two consecutive rounds of sucrose density gradient centrifugation (5). The second linear gradient from 20 to 60% sucrose was apportioned into 14 fractions, which were analyzed by immunoblotting using the indicated antibodies. Fractions 1–6 represent PDMs, and fractions 7–14 represent TMs. To facilitate comparison between gradients, sample volumes were normalized to the volume of fraction 7 that contained 40  $\mu$ g of protein. Due to the sharp fall in the levels of pD1-containing RC complexes in *ins0933*, no pD1 signal could be detected in this mutant (15). Because no mature D1 can accumulate in the *ctpA*<sup>-</sup> mutant, pD1 was detected using anti-D1 antiserum. For the pD1 signal of *prata*<sup>-</sup>, see Ref. 5.

implies that other factors involved in early steps in *de novo* PSII assembly might be located in the same membrane subfraction. To test this prediction, the accumulation of various assembly-related factors in membrane subfractions was monitored by immunoblotting. As described previously (18), the chlorophyll synthesis factors Pitt and POR were localized mainly in TMs, with only minor portions present in PDMs (Fig. 2A). The early PSII assembly factors Slr1471 and YCF48 accumulated predominantly in TMs, but substantial amounts of these proteins, especially YCF48, were also detected in PDM fractions, underlining a role of PDMs during early PSII assembly (Fig. 2A) (12, 14). Interestingly, Sll0933, a factor suggested to be involved in integration of CP47 into PSII subcomplexes, showed a different membrane localization (15). This protein was found solely in TM fractions (Fig. 2A), supporting the idea that the assembly of the inner PSII antenna takes place in TMs (10).

To determine whether PDMs are also involved in PSI assembly, the subcellular distribution of the PSI core protein PsaA and the PSI assembly factor YCF37 was investigated (23). Both proteins showed the same pattern as CP47/CP43 and therefore appear to be restricted to TMs (Fig. 1A). Thus, PDMs seem to represent a membrane subcompartment harboring factors involved in the early steps of PSII assembly only.

**Effects of Inactivation of Individual PSII-related Assembly Factors on Localization of Other PSII-associated Proteins**—We have previously shown that inactivation of *PratA* affects the distribution of pD1, the POR enzyme, and its interaction partner Pitt. In the absence of *PratA*, all three proteins are shifted toward lighter fractions of the sucrose gradient, *i.e.* they show a more pronounced accumulation in PDMs (5, 18). Hence, we tested whether the membrane localization of these and other photosynthesis-related proteins is affected in various mutant backgrounds.

In the *prata*<sup>-</sup> mutant, the PSII-associated proteins Slr1471 and YCF48 accumulated to higher levels in PDM fractions compared with wild-type cells (Fig. 2, A and B). In addition, the localization of Sll0933 was moderately affected upon inactivation of *prata*. In wild-type cells, this protein was found in TMs only, whereas in a *prata*<sup>-</sup> mutant background, it was also detected in PDM fractions 5 and 6 (Fig. 2, A and B). In contrast, the distribution of D2 remained unaltered (Fig. 2B). Similarly, the PSI-related proteins PsaA and Ycf37 continued to co-localize with TM markers CP43 and CP47 (Fig. 2B). Thus, the localization of the PSII assembly factors tested, but not of PSI-associated proteins, depends on the presence of *PratA*. For this reason, the distribution of PsaA and Ycf37 was not analyzed in other PSII mutants described below.

Because YCF48 had been postulated to play a role in the transfer of PSII precomplexes to TMs (14), we also investigated the distribution of PSII-associated proteins in PDM and TM fractions from *ycf48*<sup>-</sup> mutant cells. The data revealed a moderate shift of Pitt, POR, and Slr1471 toward PDM fractions, whereas the distribution of all other proteins tested was not affected (Fig. 2, A and C, compare fractions 2–4, respectively). Hence, although YCF48 might be involved in the membrane organization of selected PSII assembly factors, it is apparently not strictly required for directing PSII intermediates from PDMs to TMs.

Recently, the list of PSII assembly factors was further extended by the identification of PAM68 in *A. thaliana* (15). Its homolog in *Synechocystis*, Sll0933, was shown to affect accumulation of the RC complex (15). Here, a minor alteration in membrane organization was observed in the *sll0933*<sup>-</sup> mutant *ins0933*, as suggested by a slight shift of Slr1471 and YCF48 toward the top of the gradient. The distribution of other proteins tested did not change (Fig. 2D). This indicates some

## Characterization of PDMs

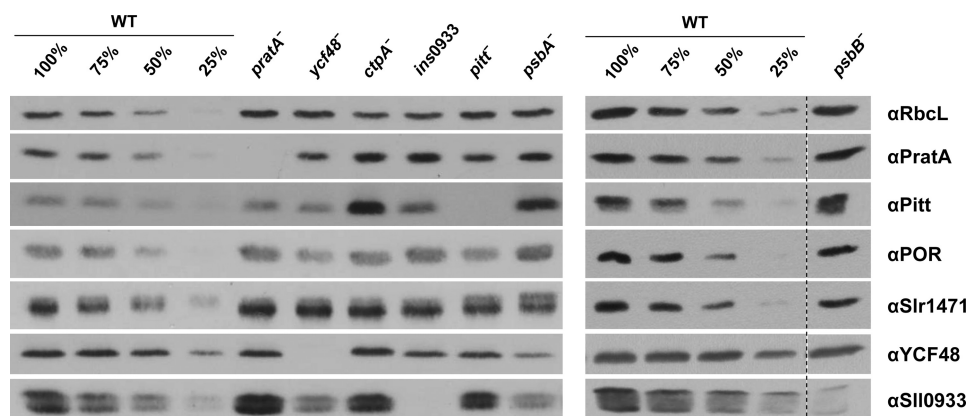


FIGURE 3. **Accumulation of PSII assembly factors in various mutants.** Whole cell extracts (30  $\mu$ g of protein) from wild-type cells and *pratA*<sup>-</sup>, *ycf48*<sup>-</sup>, *ctpA*<sup>-</sup>, *ins0933*, *pitt*<sup>-</sup>, *psbA*<sup>-</sup>, and *psbB*<sup>-</sup> mutants were fractionated by SDS-PAGE, blotted onto nitrocellulose membrane, and probed with the indicated antibodies. Representative results of three independent experiments are shown.

**TABLE 1**

**Summary of the effects of the indicated PSII mutants on membrane localization and relative levels of different PSII assembly factors**

The entries for proteins that differ in their membrane localization in certain mutants compared with wild-type cells are in *italic* (compare Fig. 2 and supplemental Fig. 2). The numbers refer to the levels of membrane-localized PSII assembly factors in the indicated mutants relative to those in wild-type cells (arbitrarily set to 100). Values are means  $\pm$  S.D. of three independent experiments. The clearest differences from wild-type levels are highlighted in boldface; examples of the underlying experiments are shown in Fig. 3.

Protein	Mutant						
	<i>pratA</i> <sup>-</sup> (5)	<i>pitt</i> <sup>-</sup> (18)	<i>ycf48</i> <sup>-</sup>	<i>ins0933</i>	<i>ctpA</i> <sup>-</sup>	<i>psbB</i> <sup>-</sup>	<i>psbA</i> <sup>-</sup>
PratA		113 $\pm$ 20	108 $\pm$ 33	105 $\pm$ 22	<b>149 <math>\pm</math> 17</b>	110 $\pm$ 55	138 $\pm$ 4
Slr1471	<i>103 <math>\pm</math> 25</i>	83 $\pm$ 28	<i>106 <math>\pm</math> 21</i>	<i>105 <math>\pm</math> 10</i>	109 $\pm$ 16	110 $\pm$ 38	89 $\pm$ 14
YCF48	99 $\pm$ 35	88 $\pm$ 16		<b>70 <math>\pm</math> 20</b>	104 $\pm$ 2	101 $\pm$ 17	49 $\pm$ 23
Sll0933	<i>108 <math>\pm</math> 31</i>	<b>82 <math>\pm</math> 11</b>	<b>51 <math>\pm</math> 8</b>		77 $\pm$ 17	<b>15 <math>\pm</math> 9</b>	48 $\pm$ 13
Pitt	101 $\pm$ 32		<i>103 <math>\pm</math> 21</i>	178 $\pm$ 32	<b>295 <math>\pm</math> 122</b>	<b>206 <math>\pm</math> 62</b>	<b>244 <math>\pm</math> 108</b>
POR	101 $\pm$ 15	<b>52 <math>\pm</math> 16</b>	<b>52 <math>\pm</math> 16</b>	104 $\pm$ 20	67 $\pm$ 25	107 $\pm$ 28	96 $\pm$ 35

involvement of Sll0933 in the spatial organization of early PSII assembly steps in the PDM.

Previous membrane fractionation studies on a *pitt*<sup>-</sup> mutant had revealed increased accumulation of POR and the pD1 precursor protein in PDMs (18). Therefore, it was postulated that Pitt plays a role in the spatial organization of early PSII assembly, in addition to its involvement in chlorophyll synthesis (18). However, it did not alter the membrane distribution of other PSII proteins or assembly factors additionally tested in this study (supplemental Fig. 2A).

In summary, various factors are required to coordinate the membrane localization of PSII intermediates and their associated proteins during the assembly of PSII. Inactivation of PratA leads to the most obvious changes in localization. Because PratA was initially found to affect the C-terminal maturation of pD1 (8, 26), we next tested whether inhibiting C-terminal processing by inactivation of CtpA, the endoprotease that removes the D1 extension, compromises PDM/TM membrane organization. Surprisingly, in this mutant, the localization of all proteins, including immature pD1, was similar to that seen in wild-type cells (Fig. 2, A and E) with one striking exception: the inner antennal protein CP47 was detected in fractions 4–11 in the *ctpA*<sup>-</sup> mutant but in fractions 7–11 in the wild-type cells (Fig. 2, A and E). In contrast, CP43 was not affected by the lack of mature D1 protein (Fig. 2, A and E). Hence, a defect in pD1 processing results in the accumulation of CP47 in PDMs, but cleavage of the C-terminal extension of D1 is not essential for the transport of PSII subcomplexes to TMs.

When D1 itself is lacking due to the inactivation of all three *psbA* gene copies in the *psbA*<sup>-</sup> mutant strain *TD41* (7), only POR showed a more pronounced abundance in PDM fractions; no effects on the distribution of other tested factors were noted (Fig. 2F). Finally, we analyzed factor localization in a *psbB*<sup>-</sup> mutant lacking CP47 (22). One major difference was observed relative to the wild-type cells, *i.e.* the absence of substantial amounts of pD1 in PDM fractions (supplemental Fig. 2B). This suggests that, in the absence of ongoing PSII assembly, PDM-localized pD1 is rapidly degraded or is quickly transferred to TMs.

**Accumulation of PSII Assembly Factors in Different PSII Assembly Mutants**—The membrane distribution of PSII assembly factors described above suggests at least a degree of interdependence between some of them. To determine whether their accumulation is affected in various PSII assembly mutants, whole cell protein extracts were prepared from the wild-type cells and mutants of interest and quantified by immunoblot analyses. No effects were observed in the case of the Oxa homolog Slr1471, which accumulated to wild-type levels in all mutants tested (Fig. 3 and Table 1). Intriguingly, the accumulation of PSII assembly factors was not altered in the *pratA*<sup>-</sup> mutant either, in contrast to the strong effects on their membrane localization observed upon inactivation of PratA (Figs. 2, A and B, and 3 and Table 1). The amounts of PratA itself increased to  $\sim$ 150% of wild-type levels in the *ctpA*<sup>-</sup> mutant (in which pD1 accumulates) and to  $\sim$ 140% in the D1-deficient strain *psbA*<sup>-</sup>. This suggests

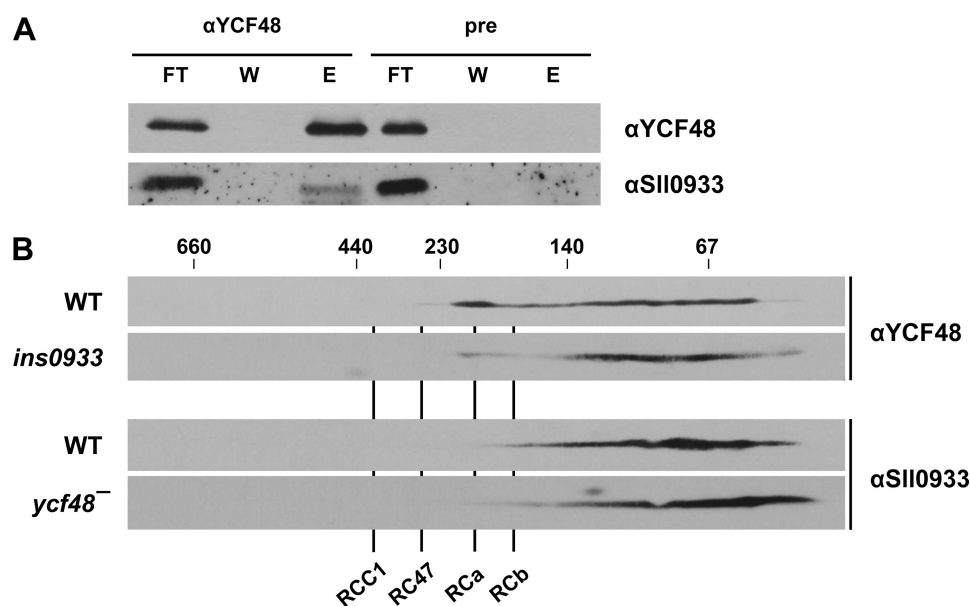


FIGURE 4. **Interaction of YCF48 and Sll0933.** *A*, membrane proteins from wild-type cells were solubilized with 1.3%  $\beta$ -dodecyl maltoside and co-immunoprecipitated using anti-YCF48 antiserum or preimmune serum (*pre*). *FT*,  $1/25$  of the flow-through containing unbound proteins; *W*,  $1/25$  of the supernatant from the last washing step; *E*, one-half of the eluted fraction containing co-immunoprecipitated proteins. *B*, two-dimensional Blue native/SDS-PAGE of wild-type, *ycf48*<sup>-</sup>, and *ins0933* membranes (each fraction is equivalent to 20  $\mu$ g of chlorophyll) was performed as described previously (5). *RCa* and *RCb* are RC complexes a and b (these complexes are not defined in text), *RC47* is the PSII core complex lacking CP43, and *RCC1* is the monomeric PSII core complex. The positions of size markers are indicated at the top. The indicated proteins were detected using the respective antibodies.

some feedback control of *prata* gene expression in the absence of functional D1.

Inactivation of *ctpA* has an even more pronounced effect on the POR interaction partner Pitt than on Prata. Steady-state levels of Pitt were 3-fold higher in the *ctpA*<sup>-</sup> mutant than in the wild-type cells, whereas a decrease in the amount of POR to ~70% and a slighter decrease in the amount of Sll0933 to ~80% were observed (Fig. 3 and Table 1). A similar increase in Pitt accumulation was noted in the *psbA*<sup>-</sup> mutant and, to a lesser extent, in the *psbB*<sup>-</sup> and *ins0933* mutants also (Fig. 3 and Table 1).

On the other hand, lack of the Pitt protein resulted in a minor decrease in Sll0933 to ~80% of wild-type amounts, in addition to the previously reported reduction in the level of POR (18). The level of POR was also reduced to ~50% in the *ycf48*<sup>-</sup> mutant. This suggests that Sll0933 and YCF48 represent additional candidates that might play a role in coordinating protein and cofactor synthesis during PSII assembly (Fig. 3 and Table 1).

Furthermore, the amounts of Sll0933 and YCF48 were found to be reduced by 50% relative to wild-type levels in the *psbA*<sup>-</sup> mutant, and the amount of Sll0933 was also reduced by half in the *ycf48*<sup>-</sup> mutant (Fig. 3 and Table 1). Conversely, lack of Sll0933 resulted in a 30% drop in the steady-state levels of YCF48, suggesting an interrelationship between YCF48 and Sll0933. However, one striking exception to the consistent coregulation of YCF48 and Sll0933 was the dramatic decrease in Sll0933 seen in the *psbB*<sup>-</sup> mutant, in which YCF48 levels were not affected. This argues for a close relationship between Sll0933 and CP47 (Fig. 3 and Table 1).

**Sll0933 and YCF48 Form Part of a Complex**—The interdependence between the levels of YCF48 and Sll0933 is compatible with a direct interaction between them. Indeed, this has

already been postulated based on yeast two-hybrid studies of their respective *A. thaliana* homologs HCF136 and PAM68 (15). To test this hypothesis further, solubilized membrane proteins of wild-type cells were subjected to co-immunoprecipitation analyses. The anti-YCF48 antiserum quantitatively precipitated the YCF48 factor, together with lesser but significant amounts of Sll0933 (Fig. 4A). Neither protein could be precipitated by the preimmune serum. Due to non-quantitative precipitation, no conclusive results were obtained when, in the reciprocal experiment, an anti-Sll0933 antiserum was used for co-immunoprecipitation. Nevertheless, the data suggest that YCF48 and Sll0933 are, at least transiently, components of the same complex. This is further supported by the fact that the two proteins co-migrated, at least to some extent, in the range between 150 kDa and the free proteins on two-dimensional Blue native/SDS gels (Fig. 4B). In the *ycf48*<sup>-</sup> mutant, a subtle effect on Sll0933 migration was observed: relatively more Sll0933 was associated with the smaller complexes than was the case in the wild-type cells (Fig. 4B). The more pronounced but still moderate accumulation of YCF48 in RC complexes was reduced in the *ins0933* mutant, with a concomitant increase in accumulation in the lower molecular mass range (Fig. 4B). We therefore conclude that subpopulations of YCF48 and Sll0933 molecules form a transient complex. Overall, the analysis of PSII-related assembly factors in the different mutant backgrounds reveals a complex regulatory network that links factors involved in chlorophyll synthesis and protein complex assembly.

## DISCUSSION

**Assignment of Stages in PSII Biogenesis to Specific Membrane Fractions**—Previous membrane fractionation studies have identified a PDM fraction in *Synechocystis* 6803 in which early

## Characterization of PDMs

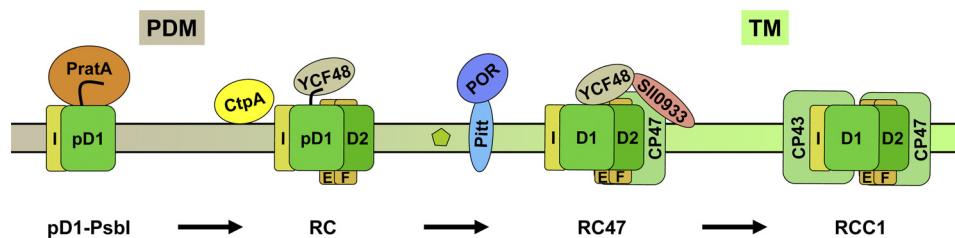


FIGURE 5. **Working model for PSII biogenesis in *Synechocystis* 6803.** PSII biogenesis begins in PDMs close to the PM with the interaction of PrtA-bound pD1 protein with Psbl. After the addition of D2 and PsbE/F subunits, RC complexes are formed. Insertion of chlorophyll *a* (small green pentagon) is probably mediated by the Pitt-POR and YCF48-Sll0933 complexes, with the concomitant insertion of CP47. The resulting RC47 complexes are transferred to the TM, where CP43 is attached to form RCC1 monomers. For further explanation, see "Discussion."

steps of PSII assembly were suggested to occur (4, 5). Here, we have demonstrated that PrtA itself plays an essential role in the spatial organization of PDMs as a PSII biogenesis platform because its inactivation (in contrast to that of other factors) severely affects the sublocalization of all other PSII assembly factors tested, *i.e.* Slr1471, YCF48, and Sll0933 (Fig. 2B). Additional support for a role of PDMs during the initial steps of PSII assembly is provided by the preferential accumulation of pD1 in this membrane subcompartment (5). In contrast, the inner antennal proteins CP47 and CP43, which are attached to PSII RC complexes during later steps in PSII biogenesis, are localized to TMs (Fig. 2A). The immediate assembly partner of D1, the D2 subunit of PSII, was found in both PDMs and TMs, suggesting that assembly proceeds from lighter to more dense membrane fractions in the order D1 + D2 + CP47/CP43. This is consistent with current models of PSII biogenesis based on the analysis of PSII assembly intermediates by two-dimensional Blue native/SDS-PAGE (11) and is further supported by the relative accumulation of the early PSII assembly factors Slr1471 and YCF48 in PDMs (Fig. 2A). Intriguingly, D2-containing PDM fractions 4–6, which probably mark the positions of RC complexes, represent the only membrane fractions in which the chlorophyll *a* precursor chlorophyllide *a* accumulates to detectable levels. However, the POR enzyme is localized mainly in TMs and only to smaller proportions in fractions 5 and 6 (Fig. 2A). Possibly, the chlorophyllide *a* synthesized in TMs is converted faster into chlorophyll *a*. In chloroplasts, the respective enzyme, the chlorophyll synthase, has been localized exclusively in TMs, whereas activity measurements in *Synechocystis* revealed its presence in both TMs and perhaps the PDMs resembling thylakoid centers (19, 25). As discussed previously (4), it also remains to be established whether the pool of chlorophyllide *a* in PDMs is synthesized by the light-dependent POR enzyme or the light-independent POR system in cyanobacteria (27). To answer this question, the ChlL subunit of light-independent POR was used for antiserum production, but due to unspecific binding of the antibody, no conclusions could be drawn (data not shown). Nevertheless, the strong reduction of chlorophyllide *a* accumulation in PDMs in the *pitt*<sup>-</sup> mutant suggests a direct involvement of POR in the synthesis of PDM-localized chlorophyll and, concomitantly, a more efficient conversion of residual childe *a* to chlorophyll *a* in the *pitt*<sup>-</sup> mutant. Thus, the data suggest that chlorophyll *a* synthesis/integration is correlated with RC complex formation. This is further evidenced by the finding that inactivation of the RC assembly factor YCF48 (14) clearly affects both the localization and accu-

mulation of POR (Figs. 2C and 3 and Table 1). Therefore, the chlorophyll synthesis enzyme POR and its interaction partner Pitt appear to be integrated into the assembly network. Moreover, Pitt levels are clearly increased in the *ins0933*, *ctpA*<sup>-</sup>, *psbB*<sup>-</sup>, and *psbA*<sup>-</sup> strains, suggesting that, in these mutants, regulatory pathways that are dedicated to the compensation of photosynthetic deficiencies are activated. Overall, the results obtained therefore substantiate a tight connection between membrane protein assembly and pigment insertion.

*A Network of Assembly Factors Mediates PSII Assembly*—The patterns of co-localization among assembly factors and their response to genetic perturbation point to certain interdependencies between them. This is most striking in the case of YCF48 and Sll0933. (i) Sll0933 inactivation shifts the distribution of YCF48 toward PDM fractions. (ii) Accumulation of each is decreased in the absence of the other. (iii) The levels of both proteins decline in the absence of D1. (iv) The two factors co-migrate, at least partially, in two-dimensional Blue native/SDS gels, and the absence of Sll0933 affects the migration behavior of YCF48. (v) Immunoprecipitation of YCF48 with a cognate antiserum also brings down Sll0933, demonstrating that the two factors form part of the same complex. Moreover, yeast two-hybrid assays have shown that the Sll0933 homolog from *A. thaliana*, PAM68, interacts directly with several PSII subunits and assembly factors, including the plant YCF48 homolog HCF136 (15). In addition, YCF48 has previously been shown to recognize the pD1 C-terminal extension, whereas Sll0933 has been implicated in the accumulation of PSII RC complexes that lack the inner antennal protein CP47 but contain YCF48 and pD1/D1 (14, 15). In the mutant *ins0933*, no stable accumulation of RC complexes and no pD1 precursor protein could be detected, suggesting rapid conversion of RC complexes into monomeric PSII core complexes (RCC) (15). Considering that the two factors localize to different membrane fractions and that Sll0933 is strongly dependent on the presence of CP47 (Figs. 2A and 3 and Table 1), the following scenario for the early steps of *de novo* PSII assembly can be envisaged (Fig. 5). In PDMs, the pD1 precursor protein first associates with the periplasmic PrtA protein. Following the addition of D2 to form the RC complex, YCF48 is then attached via the C terminus of pD1 (14). The resulting complex then moves to TMs, where Sll0933, possibly together with CP47, binds to YCF48, thereby facilitating the correct integration of CP47 into the RC to yield the RC47 complex. This process appears to be accelerated in the *ins0933* mutant strain because no RC complexes and pD1 accumulate in *ins0933* cells despite the presence of wild-

type levels of functional PSII complexes (15). This suggests rapid conversion of pD1 into D1 and formation of RC47 complexes.

The question arises as to the function of the Sll0933-mediated delay of PSII assembly. One possibility is that a slow down in PSII assembly might allow for more efficient integration of other factors, such as chlorophylls, into RC complexes. This idea is especially appealing in light of the relationship between YCF48 and the POR enzyme discussed above, as well as the accumulation of chlorophyllide *a* in fractions likely to contain RC complexes. Further evidence suggesting a connection between chlorophyll integration and YCF48/Sll0933 (and thus RC complex formation) is provided by the finding that Sll0933 levels fall upon Pitt inactivation (Fig. 3 and Table 1). In addition, inhibition of maturation of RC-localized pD1 in the *ctpA*<sup>-</sup> mutant is accompanied by a reduction in the levels of both POR and Sll0933 (Fig. 3 and Table 1) and aberrant accumulation of CP47 in PDM fractions.

Alternatively or in addition, it is conceivable that Sll0933 participates in a quality-control step during movement of RCs into TMs. Obviously, more detailed studies are required to elucidate the precise functions and interrelationships of assembly factors like PrtA, Pitt, and YCF48/Sll0933. All of them seem to interact at the interface between PDMs and TMs to coordinate early steps in the PSII maturation pathway.

One aspect that has not been addressed in this work concerns the reassembly of PSII during repair after photodamage to the D1 protein. It is still unclear whether D1 repair and *de novo* PSII assembly are spatially separated. In chloroplasts of *C. reinhardtii*, repair and *de novo* synthesis indeed take place in different TM subfractions, raising the possibility that the same holds for cyanobacteria (28). The factor Psb27 has recently been shown to be involved in facilitating the assembly of the manganese cluster of PSII during the repair process (29, 30). However, when we analyzed the membrane distribution of PSII assembly factors in a *psb27*<sup>-</sup> mutant, no alterations were observed (data not shown). Hence, the question remains open whether PSII reassembly in general (and Psb27 in particular) is integrated into the network responsible for the *de novo* assembly of PSII.

**Conclusions and Future Perspectives**—The emerging picture of TM biogenesis in cyanobacteria is dominated by a strict spatiotemporal organization, especially of the early steps in PSII assembly. Initially, the pD1 precursor protein is integrated into regions that contact the PM. Progressive maturation of PSII, with sequential formation of the intermediate complexes RC, RC47, and RCC1, then occurs in a subcompartment that is linked to the TMs. This physical and functional link is represented by the PDM. The maturation process also includes the insertion of chlorophyll *a* and probably other cofactors like carotenoids and the non-heme iron atom of PSII. Apparently, YCF48 and Sll0933 play a crucial role in this process at the interface between PDMs and TMs. It is tempting to speculate that the connecting PDMs are identical to previously described thylakoid centers that are located at the ends of converging TMs close to the PM (3, 4). Future work will have to determine the

precise location of PDMs within the cell using high resolution imaging of live cells and electron microscopy.

**Acknowledgments**—We thank A. Wilde, J. Soll, N. Murata, and Y. Nishiyama for providing anti-Ycf37, anti-Slr1471, anti-POR, and anti-pD1 antibodies and J. Komenda and P. Nixon for providing the *psbB*<sup>-</sup> and *psbA*<sup>-</sup> mutants, respectively.

## REFERENCES

- Vermaas, W. F. J. (2001) in *Encyclopedia of Life Sciences*, pp. 245–251, Nature Publishing Group, London
- Liberton, M., Howard Berg, R., Heuser, J., Roth, R., and Pakrasi, H. B. (2006) *Protoplasma* **227**, 129–138
- van de Meene, A. M., Hohmann-Marriott, M. F., Vermaas, W. F., and Roberson, R. W. (2006) *Arch. Microbiol.* **184**, 259–270
- Nickelsen, J., Rengstl, B., Stengel, A., Schottkowski, M., Soll, J., and Ankele, E. (2011) *FEMS Microbiol. Lett.* **315**, 1–5
- Schottkowski, M., Gkalypoudis, S., Tzekova, N., Stelljes, C., Schünemann, D., Ankele, E., and Nickelsen, J. (2009) *J. Biol. Chem.* **284**, 1813–1819
- Klinkert, B., Ossenbühl, F., Sikorski, M., Berry, S., Eichacker, L., and Nickelsen, J. (2004) *J. Biol. Chem.* **279**, 44639–44644
- Nixon, P. J., Trost, J. T., and Diner, B. A. (1992) *Biochemistry* **31**, 10859–10871
- Anbudurai, P. R., Mor, T. S., Ohad, I., Shestakov, S. V., and Pakrasi, H. B. (1994) *Proc. Natl. Acad. Sci. U.S.A.* **91**, 8082–8086
- Roose, J. L., and Pakrasi, H. B. (2004) *J. Biol. Chem.* **279**, 45417–45422
- Zak, E., Norling, B., Maitra, R., Huang, F., Andersson, B., and Pakrasi, H. B. (2001) *Proc. Natl. Acad. Sci. U.S.A.* **98**, 13443–13448
- Nixon, P. J., Michoux, F., Yu, J., Boehm, M., and Komenda, J. (2010) *Ann. Bot.* **106**, 1–16
- Ossenbühl, F., Inaba-Sulpice, M., Meurer, J., Soll, J., and Eichacker, L. A. (2006) *Plant Cell* **18**, 2236–2246
- Plücken, H., Müller, B., Grohmann, D., Westhoff, P., and Eichacker, L. A. (2002) *FEBS Lett.* **532**, 85–90
- Komenda, J., Nickelsen, J., Tichý, M., Prásil, O., Eichacker, L. A., and Nixon, P. J. (2008) *J. Biol. Chem.* **283**, 22390–22399
- Armbruster, U., Zühlke, J., Rengstl, B., Kreller, R., Makarenko, E., Rühle, T., Schünemann, D., Jahns, P., Weisshaar, B., Nickelsen, J., and Leister, D. (2010) *Plant Cell* **22**, 3439–3460
- Yaronskaya, E., Ziemann, V., Walter, G., Averina, N., Börner, T., and Grimm, B. (2003) *Plant J.* **35**, 512–522
- He, Q., and Vermaas, W. (1998) *Proc. Natl. Acad. Sci. U.S.A.* **95**, 5830–5835
- Schottkowski, M., Ratke, J., Oster, U., Nowaczyk, M., and Nickelsen, J. (2009) *Mol. Plant* **2**, 1289–1297
- Eckhardt, U., Grimm, B., and Hörtensteiner, S. (2004) *Plant Mol. Biol.* **56**, 1–14
- Rippka, R., Deruelles, J., Waterbury, J. B., Herdman, M., and Stanier, R. Y. (1979) *J. Gen. Microbiol.* **111**, 1–61
- Eaton-Rye, J. J. (2004) *Methods Mol. Biol.* **274**, 309–324
- Eaton-Rye, J. J., and Vermaas, W. F. (1991) *Plant Mol. Biol.* **17**, 1165–1177
- Dühring, U., Irrgang, K. D., Lünser, K., Kehr, J., and Wilde, A. (2006) *Biochim. Biophys. Acta* **1757**, 3–11
- Bergantino, E., Brunetta, A., Touloupakis, E., Segalla, A., Szabò, I., and Giacometti, G. M. (2003) *J. Biol. Chem.* **278**, 41820–41829
- Hinterstoisser, B., Chichna, M., Kuntner, O., and Peschek, G. A. (1993) *J. Plant Physiol.* **142**, 407–413
- Shestakov, S. V., Anbudurai, P. R., Stanbekova, G. E., Gadzhiev, A., Lind, L. K., and Pakrasi, H. B. (1994) *J. Biol. Chem.* **269**, 19354–19359
- Armstrong, G. A. (1998) *J. Photochem. Photobiol. B* **43**, 87–100
- Uniacke, J., and Zerges, W. (2007) *Plant Cell* **19**, 3640–3654
- Nowaczyk, M. M., Hebel, R., Schlodder, E., Meyer, H. E., Warscheid, B., and Rögner, M. (2006) *Plant Cell* **18**, 3121–3131
- Roose, J. L., and Pakrasi, H. B. (2008) *J. Biol. Chem.* **283**, 4044–4050

### 3.3 INITIAL STEPS OF PHOTOSYSTEM II *DE NOVO* ASSEMBLY AND PRELOADING WITH MANGANESE TAKE PLACE IN BIOGENESIS CENTERS IN *SYNECHOCYSTIS*

Stengel, A., Gügel, I.L., Hilger, D., **Rengstl, B.**, Jung, H., and Nickelsen, J. (2012) *Plant Cell* **24**, 660-675

The PSII assembly factor PrtA is part of two different complexes in *Synechocystis* 6803: on the one hand, it represents a component of a soluble complex of ~ 200 kDa present in the PP, on the other hand it is found membrane-associated via direct interaction with the D1 protein (Schottkowski et al., 2009b). Whereas the latter defines the PDMs (for a thorough analysis see section 3.2), here, the function of the soluble PrtA complex was investigated in more detail. Thereby, recombinant as well as native PrtA were found to possess  $Mn^{2+}$  binding activity based on circular dichroism measurements, electron paramagnetic resonance spectroscopy as well as affinity chromatography experiments using a column loaded with  $Mn^{2+}$ . PrtA is able to bind totally up to 8-9  $Mn^{2+}$  ions, of which one is specifically bound to a high-affinity site with a  $K_d = 73 \pm 31 \mu M$ , whereas the remaining  $Mn^{2+}$  ions are loosely attached and can be substituted by  $Ca^{2+}$  or  $Mg^{2+}$ . Lack of PrtA in *Synechocystis* 6803 resulted in clear reduction of  $Mn^{2+}$  levels in the PP, the cell compartment which was described to function as storage for  $Mn^{2+}$ , and which harbors the soluble PrtA complex (Keren et al., 2002). Furthermore, pulse-labeling of cells with  $^{54}Mn^{2+}$  followed by immunoprecipitation of PSII complexes using an  $\alpha D1$  antibody was performed to determine the rates of incorporation of freshly engulfed  $Mn^{2+}$  into PSII complexes. As the transport of  $^{54}Mn^{2+}$  to D1 was found to be clearly reduced in *prtaA*<sup>-</sup> compared to wild-type cells, a specific function of PrtA in delivery of  $Mn^{2+}$  to PSII can be postulated.

Additionally, ultrastructural analyses of wild-type and *prtaA*<sup>-</sup> cells were carried out to visualize the localization of PrtA and, concomitantly, PDMs inside the cell. In some wild-type cells biogenesis centers were observed at convergence sites of TMs, which were completely missing in *prtaA*<sup>-</sup>. These centers consist of a semicircle-like structure which surrounds electron dense material with approx. 60 nm in diameter. Immunogold labelling furthermore localized PrtA as well as pD1 at distinct clusters with a diameter of approx. 100 nm at the cell periphery. It was therefore assumed that these PrtA clusters correspond to the biogenesis centers and most probably represent the earlier biochemically characterized PDMs. The  $Mn^{2+}$  transport function of PrtA suggests that at these regions preloading of pD1 with periplasmic  $Mn^{2+}$  ions takes place, before the early PSII assembly intermediates are

further transferred towards the TMs, where assembly of PSII is completed and the  $Mn_4Ca$  cluster is photoactivated. Thus, an extended model for spatial organization of PSII assembly including the incorporation of  $Mn^{2+}$  could be developed.

I contributed to this work by performing the atomic absorption spectroscopy measurements for determination of Mn and iron contents in isolated PP of wild-type and *prata<sup>-</sup>* cells. Furthermore, I evaluated the ultrastructural data of *Synechocystis* 6803 cells together with I. Gügel for reliable statistics regarding the number of biogenesis centers in wild-type and *prata<sup>-</sup>*. The manuscript was written by A. Stengel and revised by J. Nickelsen and me.

# Initial Steps of Photosystem II de Novo Assembly and Preloading with Manganese Take Place in Biogenesis Centers in *Synechocystis*

Anna Stengel,<sup>a</sup> Irene L. Gügel,<sup>b</sup> Daniel Hilger,<sup>c</sup> Birgit Rengstl,<sup>a</sup> Heinrich Jung,<sup>c</sup> and Jörg Nickelsen<sup>a,1</sup>

<sup>a</sup> Molekulare Pflanzenwissenschaften, Biozentrum Ludwig-Maximilians-Universität München, 82152 Planegg-Martinsried, Germany

<sup>b</sup> Biochemie und Physiologie der Pflanzen, Biozentrum Ludwig-Maximilians-Universität München, 82152 Planegg-Martinsried, Germany

<sup>c</sup> Mikrobiologie, Biozentrum Ludwig-Maximilians-Universität München, 82152 Planegg-Martinsried, Germany

**In the cyanobacterium *Synechocystis* sp PCC 6803, early steps in thylakoid membrane (TM) biogenesis are considered to take place in specialized membrane fractions resembling an interface between the plasma membrane (PM) and TM. This region (the PrataA-defined membrane) is defined by the presence of the photosystem II (PSII) assembly factor PrataA (for processing-associated TPR protein) and the precursor of the D1 protein (pD1). Here, we show that PrataA is a Mn<sup>2+</sup> binding protein that contains a high affinity Mn<sup>2+</sup> binding site ( $K_d = 73 \mu\text{M}$ ) and that PrataA is required for efficient delivery of Mn<sup>2+</sup> to PSII in vivo, as Mn<sup>2+</sup> transport is retarded in *prataA*<sup>-</sup>. Furthermore, ultrastructural analyses of *prataA*<sup>-</sup> depict changes in membrane organization in comparison to the wild type, especially a semicircle-shaped structure, which appears to connect PM and TM, is lacking in *prataA*<sup>-</sup>. Immunogold labeling located PrataA and pD1 to these distinct regions at the cell periphery. Thus, PrataA is necessary for efficient delivery of Mn<sup>2+</sup> to PSII, leading to Mn<sup>2+</sup> preloading of PSII in the periplasm. We propose an extended model for the spatial organization of Mn<sup>2+</sup> transport to PSII, which is suggested to take place concomitantly with early steps of PSII assembly in biogenesis centers at the cell periphery.**

## INTRODUCTION

Oxygenic photosynthesis supplies the energy for production of most of the biomass on earth. The underlying light-driven photosynthetic electron transport is mediated by multiprotein/pigment complexes (i.e., photosystem II [PSII], the cytochrome b6f complex, and photosystem I), which reside within the thylakoid membrane (TM) system of cyanobacteria, algae, and plants. Electron flow is initiated at PSII, which serves as a light-driven water-plastoquinone oxidoreductase producing oxygen as a by-product of electron extraction from water. The structure of cyanobacterial PSII has been resolved at high resolution and is known to comprise 17 transmembrane protein subunits, three peripheral proteins, 35 chlorophylls, and several additional cofactors, including the catalytic machinery required for water splitting (Ferreira et al., 2004; Yano et al., 2006; Kern et al., 2007; Guskov et al., 2009; Umena et al., 2011). This machinery, the water-oxidizing complex (WOC), is localized on the luminal side of PSII and contains one calcium atom and four atoms of the transition metal Mn, which are complexed by the D1 and CP43 subunits of PSII (Ferreira et al., 2004; Barber, 2008; Umena et al., 2011). The five metal atoms were found to be linked by five

oxygen atoms, and four additional water molecules bind to the Mn<sub>4</sub>Ca cluster. It is proposed that some of these serve as substrates for the generation of dioxygen (Umena et al., 2011).

The question of how Mn is transported to PSII and assembled into the Mn<sub>4</sub>Ca cluster has been the subject of intensive research. In the cyanobacterium *Synechocystis* sp PCC 6803 (*Synechocystis* 6803), earlier studies have shed much light on the uptake of Mn (as Mn<sup>2+</sup>; Bartsevich and Pakrasi, 1995, 1996) and assembly/photoactivation of the Mn cluster (Cheniae and Martin, 1971; Tamura and Cheniae, 1987; Zaltsman et al., 1997; Hwang and Burnap, 2005). However, the mechanisms and components involved in transport of Mn to PSII have remained elusive. Two distinct systems for cellular Mn uptake have been described, the so-called MntABC transporter, and a second pathway whose components are yet unidentified (Bartsevich and Pakrasi, 1995, 1996). Moreover, *Synechocystis* 6803 can store Mn efficiently in the periplasmic space of the cell (Keren et al., 2002). Accumulation occurs rapidly upon transfer of cells to Mn-containing medium and is regulated by the rate of photosynthetic electron transport in an unknown manner (Bartsevich and Pakrasi, 1995, 1996; Keren et al., 2002). This pool may function as a reservoir to keep levels of intracellular Mn constant; however, it is still unknown how Mn is transported from this pool to PSII. Only one periplasmic Mn binding protein (MncA) has been described to date (Totter et al., 2008), but its precise function remains to be elucidated. In vascular plants, the extrinsic PSII proteins PsbP and PsbO have been reported to bind Mn (Abramowicz and Dismukes, 1984; Bondarava et al., 2007), but these proteins help to stabilize the Mn cluster and do not transport Mn to the WOC (Roose et al., 2007).

Compared with the detailed structural picture of functional PSII, less information is available on its biogenesis. Nevertheless,

<sup>1</sup> Address correspondence to joerg.nickelsen@lrz.uni-muenchen.de.

The author responsible for distribution of materials integral to the findings presented in this article in accordance with the policy described in the Instructions for Authors (www.plantcell.org) is: Jörg Nickelsen (joerg.nickelsen@lrz.uni-muenchen.de).

 Some figures in this article are displayed in color online but in black and white in the print edition.

 Online version contains Web-only data.

www.plantcell.org/cgi/doi/10.1105/tpc.111.093914

it is well established that early steps of assembly of PSII subunits include the formation of distinct transient precomplexes (Nixon et al., 2010). Assembly starts with the reaction center proteins D2 and D1, which, together with the PsbE, PsbF, and PsbI subunits, constitute the first detectable intermediate, the so-called RC complex. Upon successive attachment of the inner antennae proteins CP47 and CP43, RC47 and RCC1 core complexes are formed, respectively. At the RCC1 stage, the Mn cluster is photoactivated and thus represents the first assembly intermediate capable of oxygen evolution (Cheniae and Martin, 1971; Becker et al., 2011). Finally, PSII undergoes dimerization and higher order organization within the TM (Mullineaux, 2008).

Several factors have been identified that participate in PSII biogenesis in *Synechocystis* 6803, including YCF48, a homolog of HCF136 from *Arabidopsis thaliana* (Plücken et al., 2002; Nickelsen et al., 2007; Komenda et al., 2008; Mulo et al., 2008; Nixon et al., 2010). YCF48 assists in early PSII assembly steps, as it was found to interact directly with the pD1 protein (precursor of D1) and was suggested to be involved in stabilizing newly synthesized pD1 (Komenda et al., 2008). Another factor with a function during early steps of cyanobacterial PSII biogenesis is represented by PrtA (for processing-associated TPR protein), a member of the tetratricopeptide repeat (TPR) protein family (Klinkert et al., 2004; Schottkowski et al., 2009a). These proteins contain repetitive motifs of 34 amino acids and are known to mediate protein-protein interactions (Blatch and Lässle, 1999; Main et al., 2005). Consistent with this, PrtA was shown to bind directly to the C terminus of D1 and affects its processing by the endoprotease CtpA (Klinkert et al., 2004; Schottkowski et al., 2009a). PrtA occurs in two forms: (1) attached to the membrane via its interaction with D1, and (2) as a soluble complex of ~200 kD in the periplasm. Interestingly, although no obvious PrtA homologs can be found in vascular plants or green algae (Klinkert et al., 2004), recently, two proteins from *Arabidopsis* and *Chlamydomonas reinhardtii* have been characterized that possess similar properties as they were both found to interact directly with D1 and belong to the family of TPR proteins (Peng et al., 2006; Park et al., 2007). This raises the possibility that, despite the apparent lack of sequence similarity to PrtA, the role of PrtA in PSII biogenesis is conserved in plants and algae.

This periplasmic localization of PrtA raises the question on the spatial organization of the PSII assembly process. In cyanobacteria, TMs represent an internal membrane system that is distinct from the cellular envelope formed by the outer membrane and the plasma membrane (PM) enclosing the periplasmic space. Whereas this overall organization is well established, it is unclear how and where the biogenesis of the TM system takes place (Zak et al., 2001; Liberton and Pakrasi, 2008; Mullineaux, 2008; Nixon et al., 2010). Especially, the question of whether direct connections exist between the PM and the TM has been controversial for several years (Liberton et al., 2006; van de Meene et al., 2006; Nickelsen et al., 2011). Earlier membrane fractionation studies in *Synechocystis* 6803 led to the proposal that assembly of photosynthetic complexes (especially PSII) is initiated at PMs; subsequently, precomplexes are transported to TMs via vesicles or transient fusion of PMs and TMs (Zak et al., 2001; Schneider et al., 2007; Nickelsen et al., 2011). Furthermore, an intermediate membrane subfraction was described and

characterized, which is defined by the presence of PrtA and was therefore named PDM (for PrtA-defined membrane; Schottkowski et al., 2009a; Rengstl et al., 2011). It was speculated that PDMs might resemble PM/TM convergence sites and that they could additionally be identical to previously described thylakoid centers (Hinterstoisser et al., 1993; van de Meene et al., 2006; Nickelsen et al., 2011). Moreover, PDMs have been shown to accumulate the chlorophyll *a* precursor molecule chlorophyllide *a* as well as several other PSII assembly factors in a PrtA-dependent manner, suggesting that PDMs harbor a network for TM biogenesis where initial steps of PSII assembly take place (Rengstl et al., 2011).

Using *Synechocystis* 6803 as a model system, here, we focus on two questions: How is Mn delivered to PSII, and where does TM biogenesis originate? Our results demonstrate that both aspects are tightly coupled to the function and localization of PrtA. We found that PrtA participates in preloading D1 with Mn<sup>2+</sup> already during initial PSII assembly steps. Moreover, both markers for initial PSII biogenesis (i.e., PrtA and pD1) could be localized to distinct clusters where TMs converge. Taken together, our data allow the proposal of a model on the spatio-temporal organization of TM biogenesis.

## RESULTS

### The D1 Interaction Partner PrtA Influences Mn Homeostasis

A variety of factors have been characterized in recent years that are required for regulation of PSII assembly (Mulo et al., 2008; Nixon et al., 2010). One of these proteins is PrtA, which was previously found to interact directly with the core reaction center protein D1 that plays a major role in complexing the Mn cluster required for oxidation of water (Schottkowski et al., 2009a). This direct binding between PrtA and D1 had been shown by yeast two-hybrid and glutathione S-transferase (GST) pull-down experiments, revealing that recombinant PrtA (rPrtA) binds to the soluble parts of both mature (mD1) and precursor D1 (pD1) C-terminal regions (Schottkowski et al., 2009a). To substantiate further the PrtA-D1 interaction, we performed pull-down experiments using heterologously expressed mD1 and pD1 C termini coupled to GST-agarose as applied before (Schottkowski et al., 2009a), but incubated these with isolated periplasmic proteins from both the wild type and a *prtA*<sup>-</sup> mutant (Figure 1A). With this approach, native PrtA was successfully pulled down from wild-type periplasm by both D1 versions, whereas no PrtA signal was detected upon incubation with the *prtA*<sup>-</sup> periplasm or when an empty column without bound mD1/pD1 C termini was used (Figure 1A). This verifies the interaction between PrtA and D1 in a more physiological system (using native PrtA) than applied before.

Interestingly, after isolation and concentration of periplasm, the color of wild-type periplasm was found to be greenish, whereas the color of the *prtA*<sup>-</sup> periplasm appeared yellow (Figure 1B). Since putative pigments could not be extracted by organic solvents, we speculated that the alteration in color might be due to differences in transition metal composition. We were especially interested in Mn because the binding site for PrtA on

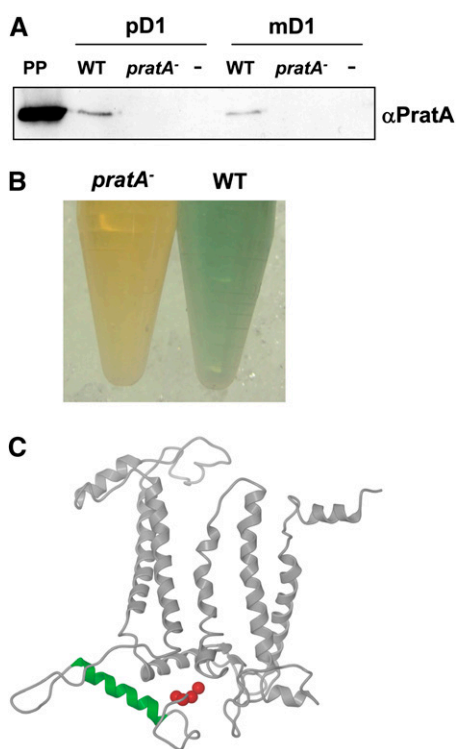


**Figure 1.** Native PrtA Binds to the Mature D1 C Terminus Near the Mn Cluster.

**(A)** Pull-down experiment of GST-mD1 (mature D1) and GST-pD1 (precursor of D1) bound to GST-agarose and incubation with isolated periplasm from *Synechocystis* wild-type (WT) and *prtA*<sup>-</sup> cells. Bound proteins were eluted (see Methods) and subjected to immunoblotting with  $\alpha$ PrtA. A negative control (-) without mD1/pD1 proteins bound to GST-agarose is included. The first lane includes 10  $\mu$ g isolated periplasm (PP) without further treatment.

**(B)** Periplasm samples from *Synechocystis* wild-type and *prtA*<sup>-</sup> cells.

**(C)** The binding site for PrtA on D1 (amino acids 314 to 328; green helix; Schottkowsky et al., 2009a) lies close to the residues that form the Mn cluster (His-332, Glu-333, His-337, Asp-342, and Ala-344; red balls; Ferreira et al., 2004; Barber, 2008). The three-dimensional structure of D1 was visualized with Pymol (<http://pymol.sourceforge.net>, version 0.99, based on the Protein Data Bank file 3BZ1).

D1 is located in close proximity to those amino acid residues of D1 that are involved in complexing the Mn cluster (Ferreira et al., 2004; Barber, 2008; Schottkowsky et al., 2009a; Figure 1C). Measurements of the amounts of Mn and Fe by atomic absorption spectrometry revealed that the level of Mn in *prtA*<sup>-</sup> periplasm was reduced by almost two-thirds to  $36 \pm 7\%$  (sd) relative to the wild type, whereas the Fe concentration was unaltered ( $99 \pm 18\%$ ; sd). Hence, the loss of PrtA affects the periplasmic concentration of Mn.

### PrtA Is a Mn Binding Protein

We next tested whether rPrtA itself has the capacity to bind Mn ions (see Supplemental Figure 1 online). We first performed

circular dichroism (CD) measurements of PrtA in the absence or presence of either 1 mM Mn<sup>2+</sup>, 1 mM Fe<sup>3+</sup>, 1 mM Fe<sup>2+</sup>, 1 mM Mg<sup>2+</sup>, or 1 mM Ca<sup>2+</sup>. The CD data obtained for rPrtA alone indicated a structure consisting of 72%  $\alpha$ -helices, 5%  $\beta$ -sheets, and 23% turns/coils (Figures 2A and 2B). The high amount of  $\alpha$ -helices reflects the nine helix-turn-helix-folded TPR motifs present in PrtA that constitute the majority of this protein (Klinkert et al., 2004; Main et al., 2005). When rPrtA was incubated with 1 mM Mn<sup>2+</sup> prior to the measurement, the  $\alpha$ -helical fraction fell from 72% (without Mn<sup>2+</sup>) to 62%, and a concomitant increase of turns/coils (from 23 to  $\sim 30\%$ ) was observed (Figures 2A and 2B). This could also be judged by the mean residue ellipticity at 222 nm ( $\Theta_{222}$ ) that was altered to  $\Theta_{222} = -18762.0$  in contrast with  $\Theta_{222} = -20955.4$  without Mn<sup>2+</sup>. These data indicate a conformational change of rPrtA in the presence of Mn<sup>2+</sup> and suggest that Mn<sup>2+</sup> might be directly bound by rPrtA. By contrast, no obvious changes in secondary structure were observed upon incubation with 1 mM Fe<sup>3+</sup>, 1 mM Fe<sup>2+</sup>, 1 mM Mg<sup>2+</sup>, or 1 mM Ca<sup>2+</sup> (Figures 2A and 2B).

To test directly whether rPrtA binds Mn<sup>2+</sup>, electron paramagnetic resonance (EPR) measurements were conducted. The room temperature (298.15K) spectra of 500  $\mu$ M Mn<sup>2+</sup> recorded in the presence or absence of 100  $\mu$ M rPrtA showed a six-line hyperfine pattern typical of Mn-(H<sub>2</sub>O)<sub>6</sub><sup>2+</sup> species. In the presence of rPrtA, a significantly smaller EPR signal amplitude was observed in comparison to a rPrtA-free sample containing identical Mn<sup>2+</sup> concentration in the same buffer (Figure 3A). The reduction of the signal amplitude of the Mn<sup>2+</sup> spectrum suggests decreased amounts of free Mn<sup>2+</sup> in solution due to Mn<sup>2+</sup> binding to the protein (Reed and Cohn, 1970; Reed and Markham, 1984; Sen et al., 2006; Hayden and Hendrich, 2010). This effect was abolished upon denaturation of rPrtA by 8M urea, indicating specific binding of Mn<sup>2+</sup>, as folding of the protein is crucial for Mn<sup>2+</sup> interaction (Figure 3B). To determine binding stoichiometry and affinities of rPrtA, Mn<sup>2+</sup> titration experiments were performed and the fraction of bound Mn<sup>2+</sup> was calculated from the amplitude of the lowest field transition and plotted against total Mn<sup>2+</sup> concentrations (Figure 3C). A maximum of eight Mn<sup>2+</sup> ions were found to bind per rPrtA molecule. The entire titration curve was shown to exhibit a sigmoid shape indicative of binding of Mn<sup>2+</sup> to multiple sites. The data suggest the existence of a high-affinity Mn<sup>2+</sup> binding site ( $K_{d1} \sim 90 \mu$ M; Figure 3C, detail) and multiple low-affinity sites ( $K_{d2} > 1$  mM; Figure 3C, overview). Because  $K_{d1}$  could not be precisely determined by the applied EPR method due to technical resolution limitations, we further analyzed it by filter binding assays. In this approach, rPrtA was incubated with 10 to 75  $\mu$ M <sup>54</sup>Mn<sup>2+</sup>, the amount of <sup>54</sup>Mn<sup>2+</sup> bound to rPrtA was counted, and the number of <sup>54</sup>Mn<sup>2+</sup> per rPrtA was calculated from the values obtained from <sup>54</sup>Mn<sup>2+</sup> in the absence of protein. This allowed us to determine  $K_{d1}$  to  $73 \pm 31 \mu$ M (Figure 3D).

To analyze the specificity of Mn<sup>2+</sup> binding, we performed competition experiments, in which 500  $\mu$ M CaCl<sub>2</sub> (equimolar amount) or 5 mM CaCl<sub>2</sub> (10-fold excess) were incubated together with 500  $\mu$ M MnCl<sub>2</sub> and 100  $\mu$ M rPrtA prior to EPR analysis. The results suggest that using equimolar amounts, only a minor fraction of Mn<sup>2+</sup> could be replaced by Ca<sup>2+</sup>, since 85.2% of Mn<sup>2+</sup> remained bound to PrtA (Figures 4A and 4C; fraction of bound Mn<sup>2+</sup> was calculated from the amplitude relative to that of total

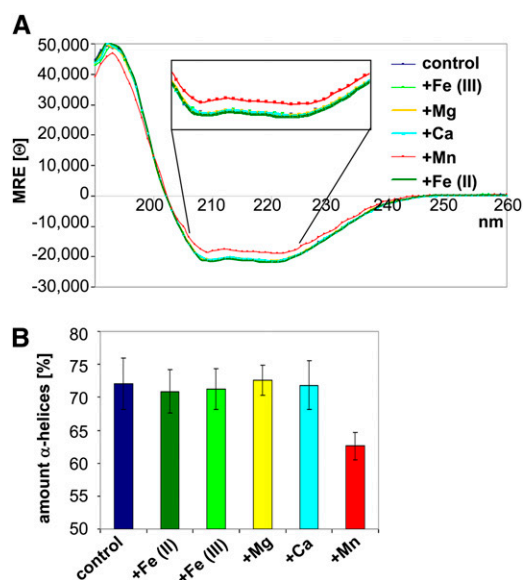


**Figure 2.** PrtA Undergoes Changes in Secondary Structure upon Incubation with Mn.

**(A)** CD spectroscopy of recombinant PrtA in the absence (dark-blue curve) and presence of 1 mM MnCl<sub>2</sub> (red), FeCl<sub>3</sub> (light green), MgCl<sub>2</sub> (yellow), CaCl<sub>2</sub> (light blue), or FeCl<sub>2</sub> (dark green). MRE [θ] represents mean residue ellipticity in degrees cm<sup>2</sup> dmol<sup>-1</sup> residue<sup>-1</sup>. The figure shows one representative graph of three independent experiments.

**(B)** Quantification of the α-helical content from the CD data using the CDSSTR program (protein reference set 7) obtained from the DichroWeb server (<http://dichroweb.cryst.bbk.ac.uk/html/home.shtml>). Values shown are means (±SD) of three independent experiments.

Mn<sup>2+</sup> bound without competitor). Considering that a maximum of eight Mn<sup>2+</sup> ions were found to bind per rPrtA, seven Mn<sup>2+</sup> molecules remain attached to rPrtA under these conditions. Even upon incubation with 10-fold excess of Ca<sup>2+</sup>, 16.2% of Mn<sup>2+</sup> stayed associated with rPrtA, which roughly corresponds to one out of the total eight Mn<sup>2+</sup> ions bound (Figures 4A and 4C). Similar effects were observed in competition experiments with MgCl<sub>2</sub>, although the competition effect was slightly more pronounced in this case (Figures 4B and 4C). Additionally, the same competition experiment was performed using 5 mM MnCl<sub>2</sub> (instead of 500 μM) and 5 mM CaCl<sub>2</sub> or MgCl<sub>2</sub> or 50 mM CaCl<sub>2</sub> or MgCl<sub>2</sub>, respectively. Comparable results were obtained with this approach, as nine Mn<sup>2+</sup> ions were found to be attached to one PrtA and 1 Mn<sup>2+</sup> ion remained bound to PrtA upon competition with 10-fold excess of Ca<sup>2+</sup> or Mg<sup>2+</sup> (percentage of Mn<sup>2+</sup> that stays attached: 1× CaCl<sub>2</sub>, 82.3%; 10× CaCl<sub>2</sub>, 6.7%; 1× MgCl<sub>2</sub>, 78.3%; 10× MgCl<sub>2</sub>, 16.6%; see Supplemental Figure 2 online). Based on these data, it is proposed that rPrtA specifically binds Mn<sup>2+</sup> with a higher affinity than Ca<sup>2+</sup> or Mg<sup>2+</sup> and that even with 10-fold excess of Ca<sup>2+</sup> or Mg<sup>2+</sup>, the high-affinity binding site seems to be specific for Mn<sup>2+</sup>, whereas the residual seven or eight Mn<sup>2+</sup> ions are loosely attached to the low-affinity binding sites and, hence, can easily be substituted. Furthermore, in good agreement with the CD spectroscopic data, no evidence for Fe<sup>3+</sup> binding to rPrtA was obtained in low-

temperature (104K) EPR spectra (Figure 4D). To exclude other possible reasons for the observed decay of the EPR signal amplitude (e.g., oxidation of paramagnetic Mn<sup>2+</sup>; Reaney et al., 2002), EPR measurements were performed on the same Mn<sup>2+</sup>/rPrtA sample before and after the addition of 100 mM CaCl<sub>2</sub>. To exclude dilution effects caused by addition of CaCl<sub>2</sub> to the Mn<sup>2+</sup>/PrtA sample, in parallel an equal amount of buffer was subjected to a second Mn<sup>2+</sup>/PrtA sample used for normalization purposes afterwards. Whereas in the presence of 100 μM rPrtA, the signal amplitude decayed to 78.4%, the subsequent addition of CaCl<sub>2</sub> returned the signal to 91.4% compared with the signal intensity of 5 mM MnCl<sub>2</sub> free in solution (using the amplitude of the first peak of the EPR spectrum for calculation; see Supplemental Figure 3A online). Although the amplitude was not completely restored by the addition of CaCl<sub>2</sub>, which is likely due to the higher affinity of rPrtA for Mn<sup>2+</sup> than for Ca<sup>2+</sup> (see above), the result suggests that the loss of EPR signal intensity in the presence of rPrtA is due to Mn<sup>2+</sup> binding rather than to changes in the oxidation state of Mn<sup>2+</sup>. In the latter case, the presence of CaCl<sub>2</sub> would not lead to an EPR signal recovery. As an additional control to determine whether the protein specifically determines the amount of Mn<sup>2+</sup> binding, we performed the PrtA/Mn<sup>2+</sup> binding experiment using 100 μM Mn<sup>2+</sup> and varying concentrations of PrtA (100, 50, and 25 μM). The results clearly show a linear increase of the amount of PrtA-bound Mn<sup>2+</sup> dependent on the protein concentration applied (29, 15, and 7 μM Mn<sup>2+</sup> attached to PrtA, respectively), demonstrating that in this range, the amount of bound Mn<sup>2+</sup> is directly proportional to the PrtA concentration applied (see Supplemental Figures 3B and 3C online).

To analyze whether Mn<sup>2+</sup> binding can also be observed for native PrtA, we used a Mn<sup>2+</sup>-loaded nitrilotriacetic acid column and isolated periplasmic Mn<sup>2+</sup> binding proteins via affinity chromatography. Indeed, PrtA could be extracted from periplasm by this method, but it did not bind to a Ni<sup>2+</sup>-containing column or a column not preloaded with metal ions, indicating that PrtA isolated from periplasm can specifically bind Mn<sup>2+</sup> (Figure 5). Quantification of the eluted PrtA in relation to the amount of total periplasmic PrtA used for the experiment revealed that 3.4% of PrtA was actually precipitated by our approach. Thus, it is likely that the majority of periplasmic PrtA might either be already bound to Mn<sup>2+</sup> or is involved in complex formation with additional proteins and is thus not accessible for the pull-down assay. Nevertheless, the control samples clearly show the specificity of PrtA binding to the Mn<sup>2+</sup> column. Taken together, these results indicate that Mn<sup>2+</sup> is directly and specifically bound by both recombinant and native PrtA.

### PrtA Functions in Transport of Mn<sup>2+</sup> to D1 in Vivo

The data obtained so far raised the possibility that PrtA might donate Mn<sup>2+</sup> to the D1 protein of PSII in vivo. To investigate this hypothesis, we pulse-labeled wild-type and *prtA*<sup>-</sup> cells with <sup>54</sup>Mn<sup>2+</sup> for 1 or 3 h. Subsequently, PSII assembly intermediates were isolated from solubilized protein extracts by immunoprecipitation using an αD1 antibody. Analysis of precipitated <sup>54</sup>Mn<sup>2+</sup> should then reflect the amount of Mn<sup>2+</sup> transported to and incorporated into de novo-synthesized PSII. When protein extracts from a *psbA*<sup>-</sup> mutant (*TD41*; Nixon et al., 1992) were used

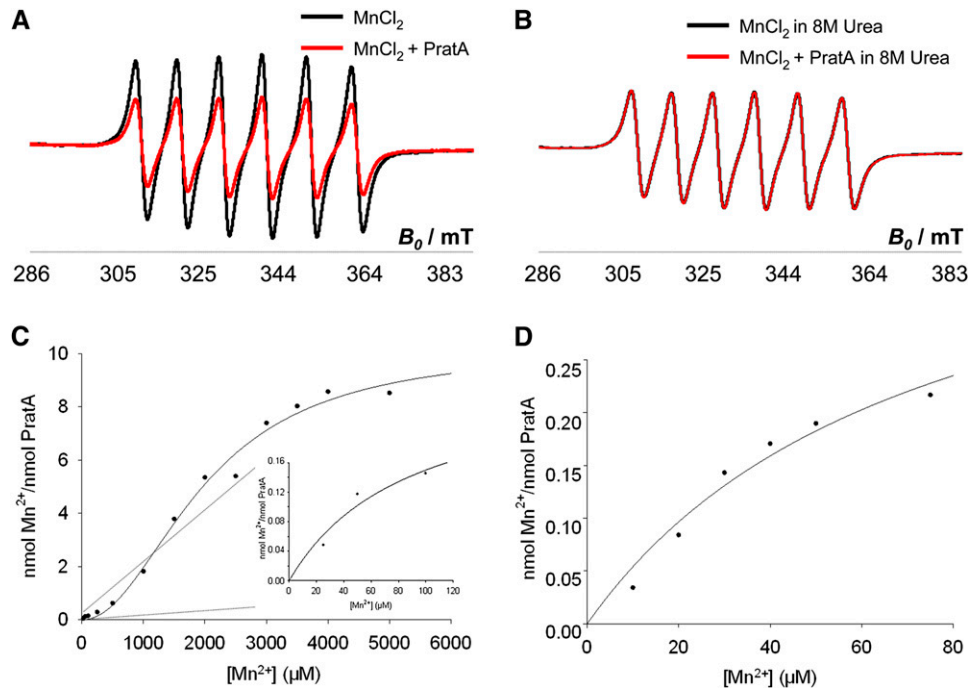


**Figure 3.** PrtA Is a Mn Binding Protein and Contains High- and Low-Affinity Binding Sites.

**(A)** and **(B)** EPR analyses of 500  $\mu\text{M}$   $\text{MnCl}_2 \pm 100 \mu\text{M}$  PrtA in 50 mM Tris, pH 8, and 150 mM NaCl **(A)** and 500  $\mu\text{M}$   $\text{MnCl}_2 \pm 100 \mu\text{M}$  PrtA in Tris/NaCl + 8 M urea **(B)**.

**(C)** EPR experiment for determination of stoichiometry and binding constant of PrtA-Mn. The data show two different binding modes of  $\text{Mn}^{2+}$  to PrtA, one high-affinity (detail), and several low-affinity binding sites (large graph). The data were fitted using SigmaPlot 11 software.

**(D)** Filter binding assay for exact determination of the high-affinity binding site. Recombinant PrtA was incubated with 10 to 75  $\mu\text{M}$   $^{54}\text{Mn}^{2+}$ , the amount of  $\text{Mn}^{2+}$  bound to PrtA was measured, and the number of  $\text{Mn}^{2+}$  per PrtA was calculated from the values obtained from  $^{54}\text{Mn}^{2+}$  without addition of protein.

as a negative control, only minute amounts of background radioactivity were detected in D1-specific precipitates, which were then subtracted from measured values in wild-type and *prata*<sup>-</sup> samples. Intriguingly, rates of incorporation of  $\text{Mn}^{2+}$  into PSII were clearly affected in *prata*<sup>-</sup> cells. After 1 h of incubation with  $^{54}\text{Mn}^{2+}$ , amounts of bound  $\text{Mn}^{2+}$  were reduced 4.0-fold compared with the wild type, and after 3 h, the effect was even more pronounced, resulting in an 8.8-fold reduction of precipitated radioactivity from the *prata*<sup>-</sup> material (Figure 6A). To exclude the possibility that this reduction was solely due to lower cellular  $\text{Mn}^{2+}$  uptake rates in *prata*<sup>-</sup>, in parallel, levels of radioactivity in whole cells were assessed after incubation with  $^{54}\text{Mn}^{2+}$ . After 3 h, the level of  $^{54}\text{Mn}^{2+}$  in the *psbA*<sup>-</sup> strain was 6.0-fold less than in the wild type (Figure 6B). This is consistent with earlier reports showing that cellular uptake of  $\text{Mn}^{2+}$  depends on photosynthetic activity (Bartsevich and Pakrasi, 1996; Keren et al., 2002). In *prata*<sup>-</sup> cells,  $^{54}\text{Mn}^{2+}$  levels decreased only 1.6-fold, which is likely to be a secondary effect due to lower photosynthesis rates in *prata*<sup>-</sup> (Bartsevich and Pakrasi, 1996; Klinkert et al., 2004; Figure 6B). To address this point further, we quantified the amount of D1 in *prata*<sup>-</sup> using immunodetection with a  $\alpha\text{D1}$  antibody in total protein extracts from wild-type and *prata*<sup>-</sup> cells. Previous analyses had revealed a severe reduction of D1 in *prata*<sup>-</sup> in the absence of precise protein quantifications (Klinkert et al., 2004). Here, three independent protein extractions from

*prata*<sup>-</sup> were analyzed together with dilution series of wild-type proteins, and the D1 level in *prata*<sup>-</sup> was calculated to be decreased to only  $72 \pm 8\%$  (= 1.4-fold reduction) of the wild-type level under the growth conditions applied (Figure 6C). Hence, this moderate reduction of D1 amount and, thus, of cellular  $\text{Mn}^{2+}$  uptake cannot explain the drastically diminished  $\text{Mn}^{2+}$  incorporation into PSII in *prata*<sup>-</sup> cells (8.8-fold reduction compared with the wild type), strongly suggesting that PrtA is directly involved in delivery of  $\text{Mn}^{2+}$  to PSII. Additionally, we investigated the amount of  $^{54}\text{Mn}^{2+}$  taken up by PrtA in the wild type compared with *psbA*<sup>-</sup>, proposing that if PrtA functions in transport of  $\text{Mn}^{2+}$  to D1, the metal ion should accumulate bound to PrtA when lacking the target. For this purpose, wild-type, *prata*<sup>-</sup>, and *psbA*<sup>-</sup> cells were incubated with  $^{54}\text{Mn}^{2+}$  as described before; however, after subsequent protein extraction, immunoprecipitation was performed using a  $\alpha\text{PrtA}$  instead of  $\alpha\text{D1}$  antibody. After 3 h of incubation with  $^{54}\text{Mn}^{2+}$ , indeed, an increase (twofold) of PrtA-bound  $^{54}\text{Mn}^{2+}$  was observed in *psbA*<sup>-</sup> compared with the wild type (Figure 6D; the background values obtained for *prata*<sup>-</sup> were subtracted from wild-type and *psbA*<sup>-</sup> values). This supports the hypothesis of PrtA functioning as a  $\text{Mn}^{2+}$  transport protein to D1. If and how PrtA also exchanges  $\text{Mn}^{2+}$  with the periplasmic Mn storage system remain to be determined (Keren et al., 2002).

As PrtA is involved in maturation/assembly of D1 (Klinkert et al., 2004; Schottkowski et al., 2009a), we further aimed to test

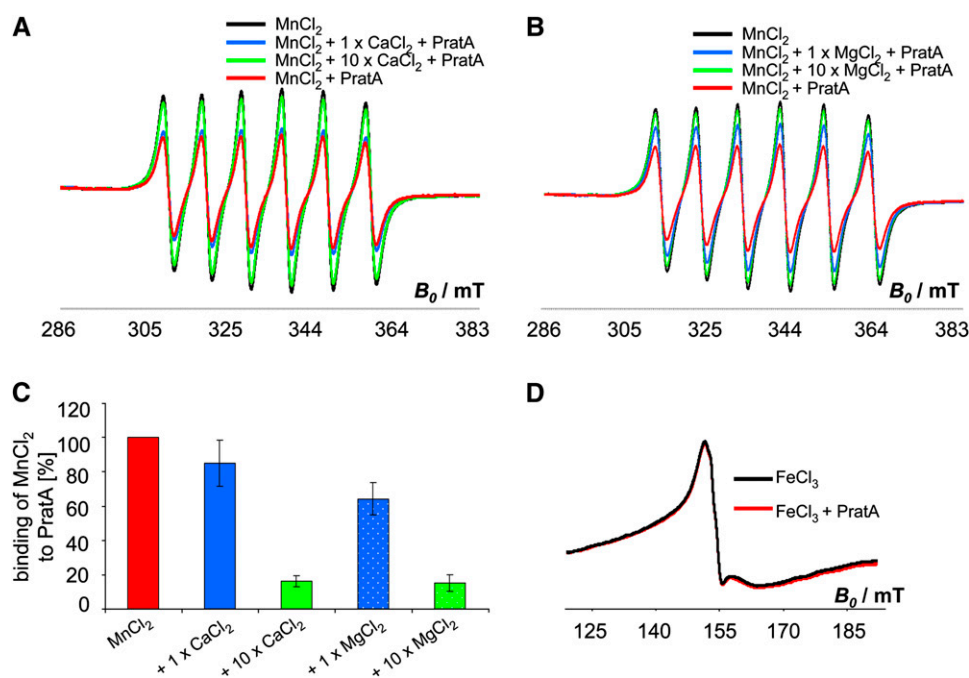


**Figure 4.** Specificity of Mn<sup>2+</sup> Binding to PrtA.

(A) and (B) Competition experiment using EPR analysis of 500 μM MnCl<sub>2</sub> ± 100 μM PrtA in Tris/NaCl + 500 μM (1×) or 5 mM (10×) CaCl<sub>2</sub> (A) and 500 μM MnCl<sub>2</sub> ± 100 μM PrtA in Tris/NaCl + 500 μM (1×) or 5 mM (10×) MgCl<sub>2</sub> (B).

(C) Quantification of MnCl<sub>2</sub> bound to PrtA obtained via EPR spectroscopy. The fraction of bound Mn<sup>2+</sup> was calculated from the amplitudes relative to total Mn<sup>2+</sup> bound without competitor (=100%; red bar).

(D) EPR analysis of 1 mM FeCl<sub>3</sub> before (black curve) and after (red curve) the addition of 100 μM PrtA.

whether other PSII assembly mutants show similar effects in Mn<sup>2+</sup> incorporation into PSII. To this end, we analyzed Mn<sup>2+</sup> transport and uptake into *ycf48*<sup>-</sup>, a mutant deficient in YCF48, a factor that had been shown to be involved in early PSII assembly steps and that, like PrtA, is a direct D1 interaction partner (Komenda et al., 2008). However, we detected only a minor reduction in both transport and uptake of Mn<sup>2+</sup> (1.3- and 1.2-fold decrease after 3 h incubation with <sup>54</sup>Mn<sup>2+</sup>, respectively) in *ycf48*<sup>-</sup>, indicating a specific role of PrtA for Mn<sup>2+</sup> delivery to PSII (Figures 6E and 6F).

### PrtA-Dependent Formation of Semicircle-Shaped Structures at the Cell Periphery

The spatial organization of TM biogenesis has been a matter of debate for several years. To gain further insights into the organization of Mn delivery to PSII, we analyzed the ultrastructure of *Synechocystis* 6803 wild-type and *prtA*<sup>-</sup> cells using transmission electron microscopy. Overview images of whole cells depicted clear changes in the overall membrane appearance between the wild type and *prtA*<sup>-</sup> (Figures 7A and 7B). In *prtA*<sup>-</sup>, TMs appeared less compressed and the outer membrane and PM were less smooth and organized. A closer look at TM convergence sites at the periphery of cells using higher magnifications (110,000- to 140,000-fold) revealed structures of ~60 nm in diameter that are filled by a granular matrix coated with

dense material in both wild-type and *prtA*<sup>-</sup> sections (Figures 7C and 7D). Most likely these structures represent cross sections of previously described so-called thylakoid centers (van de Meene et al., 2006). Interestingly, in wild-type cells, in some cases membranous semicircle-like structures surrounding thylakoid centers were observed which appeared to contact especially TMs and PMs (Figure 7C). At least eight of these semicircles located between the arcuated and arranged TM layers were found in 360 wild-type cells analyzed. It has to be considered that this structure was described two-dimensionally, meaning that in general only one section was analyzed per cell. Hence, not all of those regions could be detected. The relatively low number

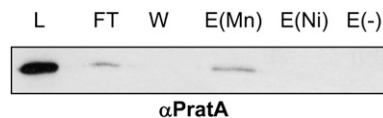


**Figure 5.** Mn<sup>2+</sup> Can Be Bound by Native PrtA.

Metal-ion chromatography of periplasm from *Synechocystis* 6803 wild-type cells. Bound proteins were eluted (see Methods) and subjected to immunoblotting with αPrtA. E(-), 50% of eluate from column not preloaded with cations (25 μL); E(Mn), 50% of eluate from Mn<sup>2+</sup> column (25 μL); E(Ni), 50% of eluate from Ni<sup>2+</sup> column (25 μL); FT, 10% of flow-through (20 μL) from Mn<sup>2+</sup> column; L, load (periplasm, 10 μg protein); W, 10% of final wash (20 μL) from Mn<sup>2+</sup> column.

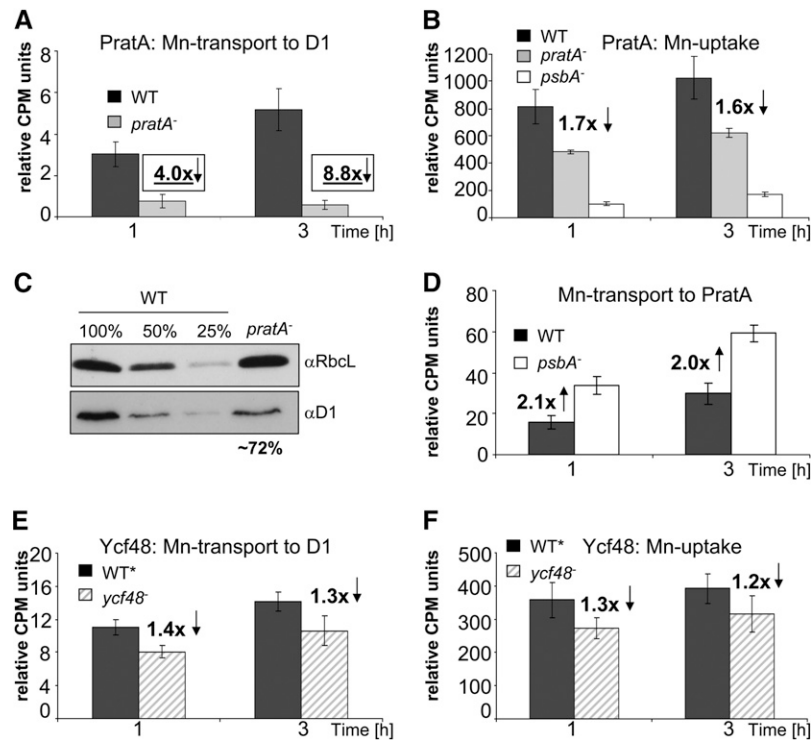


**Figure 6.** Prata Influences Mn Uptake and Transport to PSII in Vivo.

**(A)** Amounts of Mn delivered to D1 in wild-type and *pratA*<sup>-</sup> cells upon incubation of the cells with <sup>54</sup>Mn<sup>2+</sup> for 1 and 3 h, extraction of proteins, and immunoprecipitation with αD1. Radioactivity levels (in counts per minute [CPM]) measured in samples from *psbA*<sup>-</sup> cells (background) were subtracted from values for the wild type (WT) and *pratA*<sup>-</sup>.

**(B)** Uptake of <sup>54</sup>Mn<sup>2+</sup> into wild-type, *pratA*<sup>-</sup>, and *psbA*<sup>-</sup> cells. For this, cells were used directly for measurement of <sup>54</sup>Mn<sup>2+</sup> with a scintillation counter.

**(C)** Immunoblot using αD1 of total protein extracts from the wild type and *pratA*<sup>-</sup>. For 100% of the wild type and *pratA*<sup>-</sup>, 10 μg proteins were loaded and the amount of D1 in *pratA*<sup>-</sup> was quantified (from three independent experiments) using Aida software (version 3.52.046). The same blot was probed with αRbcL as loading control.

**(D)** Amount of <sup>54</sup>Mn<sup>2+</sup> taken up by Prata in wild-type and *psbA*<sup>-</sup> cells, measured after incubation with <sup>54</sup>Mn<sup>2+</sup> for 1 and 3 h and subsequent protein extraction and immunoprecipitation with αPrata. Counts per minute of samples from *pratA*<sup>-</sup> cells (background) were subtracted from values for the wild type and *psbA*<sup>-</sup>.

**(E)** and **(F)** Transport **(E)** and uptake **(F)** of <sup>54</sup>Mn<sup>2+</sup> in wild-type\* (Komenda et al., 2008) and *ycf48*<sup>-</sup> cells.

In **(A)** to **(F)**, the levels of radioactivity detected after 1 and 3 h of incubation are expressed relative to the value measured immediately after addition of <sup>54</sup>Mn<sup>2+</sup> (0 h). Values shown are means (±SD) of four independent experiments.

indicates that the semicircle-like structures are either located at a central place in the cell and that each cell contains only a few of them or that they are dynamic and form only transiently. However, the semicircles were not detected in any of 1006 analyzed *pratA*<sup>-</sup> cells (Figure 7D). To test further the error probability (i.e., to disclaim the null hypothesis “no difference between observed structures in wild-type and *pratA*<sup>-</sup> cells”), a Pearson’s  $\chi^2$  test was performed (in dependence of  $n = 1$  degrees of freedom; Zöfel, 1988). Comparing the expected ratio of 0.022 (wild-type cells, 8/360; expected for *pratA*<sup>-</sup> cells, 22.35/1006) of structures per cell with the observed ratio of those structures examined in *pratA*<sup>-</sup> cells (*pratA*<sup>-</sup> cells, 0/1006), we found a highly significant difference to that for the wild type ( $\chi^2$  22.35, P value <0.001), indicating a very low error probability. Taken together, our data suggest that the semicircle-shaped structures are drastically reduced, if not lacking, in *pratA*<sup>-</sup>, indicating that they form in a Prata-dependent manner.

### Prata and pD1 Localize to Distinct Structures at the Cell Periphery

As a next step, we localized Prata within the cyanobacterial cell by performing immunogold labeling experiments using a specific αPrata antibody. No or only few randomly localized signals were detected upon incubation of *Synechocystis* 6803 wild-type sections without the primary antibody (followed by treatment with the gold-labeled anti-rabbit IgG only; Figure 8A, Table 1) or when sections of *pratA*<sup>-</sup> cells were treated with αPrata (Figure 8B, Table 1). However, upon incubation of wild-type sections with αPrata antibody, Prata could be localized to distinct clusters of ~100 nm in diameter at the cell periphery (Figures 8C and 8D). These clusters (defined by more than five gold particles) were detected in 79 out of 520 cells (=15.2%; Table 1), but they were almost completely missing in *pratA*<sup>-</sup> sections. Thus, we conclude that they resemble PDMs, and we named these structures “biogenesis centers.”

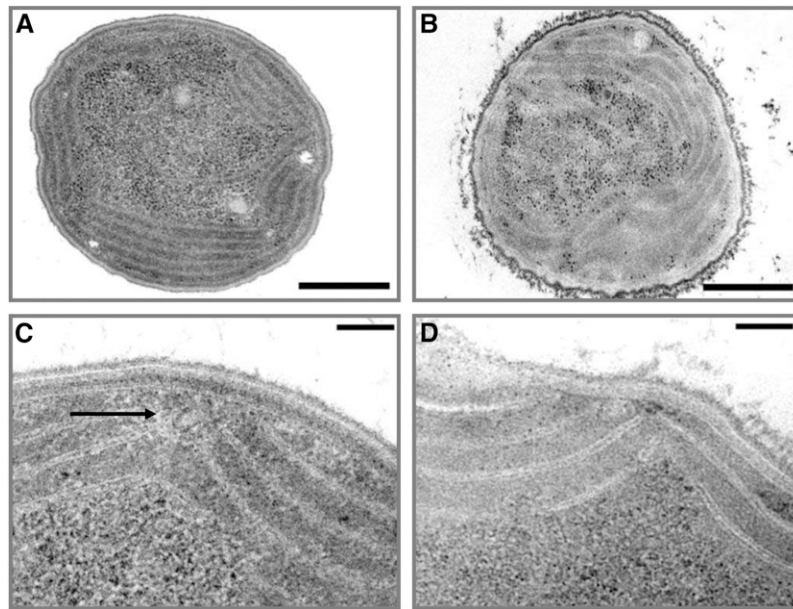


**Figure 7.** Ultrastructural Analyses of Wild-Type and *pratA*<sup>-</sup> Cells.

Electron microscopy pictures of a typical wild-type (**A**) and **C**) and *pratA*<sup>-</sup> (**B**) and **D**) *Synechocystis* cell. (**A**) and (**B**) show an overview with a magnification of 11,000-fold and (**C**) and (**D**) a detailed picture of the PM/TM interface (magnification 110,000-fold). Ultrathin sections (30 to 60 nm) of the cryofixed samples were stained with osmium tetroxide and poststained using lead citrate. The arrow in (**C**) marks the Prata-dependent semicircular structure. Bars = 500 nm (overview) and 100 nm (details), respectively.

To substantiate this hypothesis further, we performed additional immunogold labeling experiments using an antibody against the pD1 precursor protein, which represents the Prata interaction partner and serves as a second marker for initial PSII assembly steps. Whereas the negative controls showed only few signals that were equally distributed throughout the cells (Figures 9A and 9B, Table 1), pD1 was found to localize to distinct clusters in the wild type, similar to Prata. Although a colocalization of Prata and pD1 on the same sample could not be achieved due to the fact that both antibodies require the same secondary antibody (anti-rabbit), the similar sizes of the clusters (diameter of ~100 nm) and the localization at the convergence sites of the cells in the wild type suggest that both proteins accumulate at the same structures (Figures 9C and 9D, Table 1). Interestingly, in *pratA*<sup>-</sup>, pD1 was still detected in clusters at the cell periphery, but their number was found to be approximately twofold diminished (Figures 9E and 9F, Table 1). A thorough analysis of the pD1 clusters in the wild type compared with *pratA*<sup>-</sup> using as parameters (1) the area of the cluster, (2) the cluster perimeter, (3) the length of the minor and major axes of a suggested ellipse, and (4) an estimation value for the circularity or noncircularity (values between 1 = circle and 0 = other structures) revealed no obvious differences (see Supplemental Figure 4 online). The parameter of circularity is a calculated mean value that represents the Gaussian distribution of circularity of clusters in a selection of cells. If this value comes close to 1, this means that the clusters adopt on average a more circle-like structure. By contrast, a value of nearly 0 indicates random cluster shapes. For the cluster, two different definitions were used (i.e., an accumulation of  $n \geq 5$  or  $n \geq 7$  gold particles, respectively;  $n \geq 7$ ,  $n = 11$  for anti pD1-immunolabeled

structures in wild-type cells,  $n = 12$  for those in *pratA*<sup>-</sup> cells), both revealing no obvious changes in *pratA*<sup>-</sup> compared with the wild type. Additionally, two ways of analysis were applied, one connecting the particles forming a single cluster and one where the overall shape of the particles building each cluster was plotted by hand. Again, both variations did not lead to the recognition of alterations in *pratA*<sup>-</sup> compared with the wild type. However, in *pratA*<sup>-</sup>, the gold particles adjacent to the clusters often appeared to form streak-like structures. This observation, together with the reduced overall amount of pD1 organized in clusters (20.0% in wild-type cells and 10.2% in *pratA*<sup>-</sup> cells; Table 1) corresponds to the loss of semicircle-like structures observed in the ultrastructure of *pratA*<sup>-</sup> cells (Figures 7C and 7D), supporting the idea that both Prata and pD1 are colocalizing in these semicircles in the wild type and that this spatial organization is lost in the absence of Prata (Figures 9G and 9H).

## DISCUSSION

### Prata Is a Mn<sup>2+</sup> Binding Protein

In this study, we assigned a yet unidentified function to the periplasmic TPR protein Prata from *Synechocystis* 6803. The data strongly suggest that it works as a Mn<sup>2+</sup> binding and transport protein that delivers Mn<sup>2+</sup> ions directly and efficiently to PSII. Our conclusions are based on the findings that (1) Prata inactivation affects intercellular Mn levels, (2) recombinant as well as native Prata specifically bind Mn<sup>2+</sup> ions, and (3) Mn<sup>2+</sup> incorporation into PSII is reduced in a *pratA*<sup>-</sup> mutant.

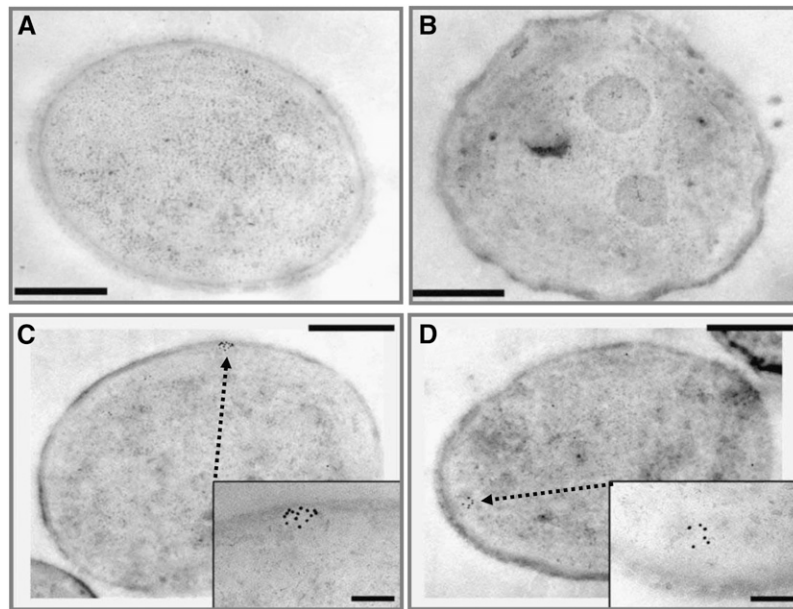


**Figure 8.** PratA Localizes to Distinct Structures at the Cell Periphery.

Ultrathin sections of *Synechocystis* cells were incubated with  $\alpha$ PratA (1:25, rabbit) prior to incubation with gold-conjugated goat anti-rabbit IgG.

(A) Negative control of the wild type without addition of  $\alpha$ PratA.

(B) *Synechocystis pratA*<sup>-</sup> cell incubated with  $\alpha$ PratA.

(C) and (D) Immunogold-labeled sections showing the PratA localization in distinct clusters (marked by arrows). Samples were analyzed without further contrast. Bars = 500 nm (overview) and 100 nm (details), respectively.

EPR measurements and filter binding assays revealed at least one high-affinity  $Mn^{2+}$  binding site within PratA with a binding constant of  $K_{d1} = 73 \mu M$ . Based on titration and competition experiments with  $Ca^{2+}$  and  $Mg^{2+}$  ions, we postulate a stoichiometry of 1  $Mn^{2+}$ :1 PratA at this site (Figures 3 and 4). The observed  $K_{d1}$  value is in the range of affinities of other  $Mn^{2+}$  binding proteins, such as the Mn-dependent catalase MnCat ( $K_d = 40 \mu M$ ) or the oxidative stress protecting protein SsDPS ( $K_d = 48 \mu M$ ) (Meier et al., 1996; Crowley et al., 2000; Pierce et al., 2003; Hayden and Hendrich, 2010). Nevertheless, much higher binding constants for  $Mn^{2+}$  to protein have been reported, for instance, in case of MnSOD and PsbP proteins (Mizuno et al., 2004; Bondarava et al., 2007). It has to be taken into account, however, that metal binding to these proteins is irreversible, in contrast with PratA, for which we postulate a function in  $Mn^{2+}$  transport and, thus, transient  $Mn^{2+}$  binding. Consequently, the

observed binding constant of PratA is in good agreement with its proposed function. We further postulate that the high-affinity  $Mn^{2+}$ -specific binding site cannot be occupied by  $Ca^{2+}$ ,  $Mg^{2+}$ , or  $Fe^{3+}$ , which provides an explanation why changes in the secondary structure of PratA using CD spectroscopy have only been observed in the presence of  $Mn^{2+}$  ions (Figure 2). In addition, low-affinity  $Mn^{2+}$  binding sites were determined ( $K_{d2} > 1 mM$ ), at which  $Mn^{2+}$  is loosely and probably unspecifically attached to the surface of PratA. This is suggested by the above-mentioned competition experiments, which showed that the weakly attached  $Mn^{2+}$  ions could be replaced by  $Ca^{2+}$  or  $Mg^{2+}$ , whereas the tightly bound  $Mn^{2+}$  remained associated with PratA, even in the presence of 10-fold excess of  $Ca^{2+}$  or  $Mg^{2+}$ . Thus, it remains questionable whether  $Mn^{2+}$  is bound to the low-affinity binding sites in vivo under physiological conditions. Interestingly, PratA is rich in Asp and Glu residues and has a pI of  $\sim 5.1$ . As it is known

**Table 1.** Summary of Immunogold Labeling Experiments

Antibody	Strain	Total No. of Cells Analyzed	No. of Cells with Cluster of Gold Particles ( $n > 5$ )	Relative No. of Cluster-Containing Cells (%)
-	Wild type	40	0	0.0
$\alpha$ PratA	Wild type	520	79	15.2
$\alpha$ PratA	<i>pratA</i> <sup>-</sup>	254	1	0.4
$\alpha$ pD1	Wild type	50	10	20.0
$\alpha$ pD1	<i>TD41 (psbA</i> <sup>-</sup> )	214	0	0.0
$\alpha$ pD1	<i>pratA</i> <sup>-</sup>	235	24	10.2

-, No primary antibody was applied in the control.

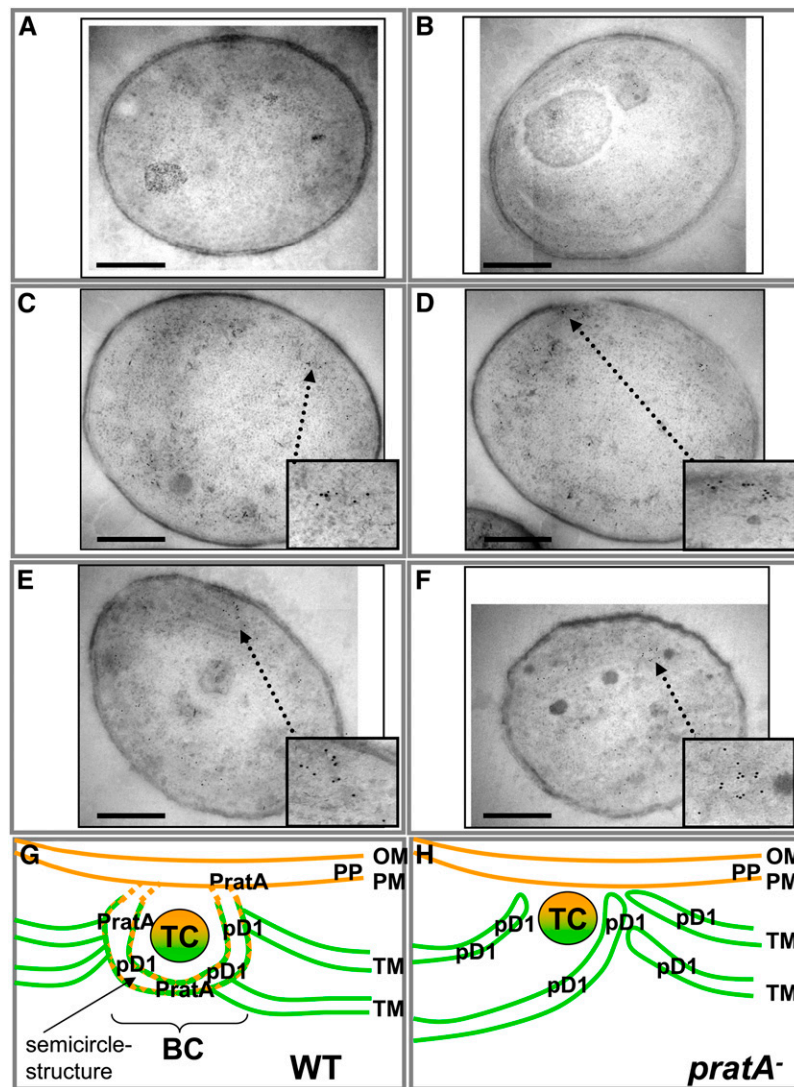


**Figure 9.** Localization of pD1.

Ultrathin sections of *Synechocystis* cells were incubated with  $\alpha$ pD1 (1:50, rabbit) prior to incubation with gold-conjugated goat anti-rabbit IgG.

**(A)** Control of the wild type without  $\alpha$ pD1.

**(B)** *Synechocystis psbA*<sup>-</sup> cell incubated with  $\alpha$ pD1.

**(C)** to **(F)** Immunogold-labeled electron microscopy pictures depicting the pD1 localization in the wild type (**(C)** and **(D)**) and *prata*<sup>-</sup> (**(E)** and **(F)**). Samples were analyzed without further contrast. Bars = 500 nm.

**(G)** and **(H)** Schematic model depicting the structure of TM convergence sites and the localization of PrataA and pD1 in the wild type and *prata*<sup>-</sup>. BC, biogenesis center; OM, outer membrane; PP, periplasm; TC, thylakoid center; WT, wild type. For further details, see text.

[See online article for color version of this figure.]

that  $Mn^{2+}$  prefers such ligands, it seems likely that these residues are involved in loose attachment of  $Mn^{2+}$  to the surface of PrataA. A similar effect has been described for PsbP, for which a stoichiometry of 10  $Mn^{2+}$ :1 PsbP has been found; however, further analyses revealed two different binding modes as well, as most  $Mn^{2+}$  ions were also merely bound with a low affinity to the Asp/Glu-containing surface of PsbP (Bondarava et al., 2007). The exact localization of the high-affinity  $Mn^{2+}$  binding site for PrataA including the amino acids involved has to be determined in

future work. In addition, the relation of PrataA to another recently described periplasmic Mn binding protein, named MncA (Tottey et al., 2008), remains to be further investigated. This cupin-folded protein is the only other Mn binding protein localized in the periplasm described so far. However, the function of this protein remains elusive, and a potential connection to PSII assembly has not been analyzed yet. Taken into account that MncA was suggested to be the principal periplasmic Mn binding protein (Tottey et al., 2008), and knowing that *Synechocystis* 6803 is able

to store Mn very efficiently in high concentrations in the periplasm in a yet unknown manner (Bartsevich and Pakrasi, 1996; Keren et al., 2002), it can be hypothesized that MncA might rather function in Mn storage than in delivery of Mn to PSII.

### Delivery of Mn<sup>2+</sup> to PSII

The radioactive pulse labeling experiments (Figure 6) revealed that the kinetics of Mn<sup>2+</sup> incorporation into PSII are affected in a *pratA*<sup>-</sup> mutant background. Furthermore, the parallel analysis of the PSII assembly mutant *ycf48*<sup>-</sup> verified that inefficient Mn<sup>2+</sup> transport to PSII in *pratA*<sup>-</sup> is not a secondary effect of distorted PSII assembly, but PrtA specific. Hence, the question arises at which stage of PSII assembly Mn<sup>2+</sup> is delivered to PSII by PrtA. Earlier studies revealed that PrtA associates only with very early PSII assembly intermediates, probably already with newly membrane inserted pD1 protein (Schottkowski et al., 2009a; Rengstl et al., 2011). Furthermore, a *pratA*<sup>-</sup> mutant showed defects in C-terminal processing of D1 (Klinkert et al., 2004), which is required for assembly of the Mn<sub>4</sub>Ca cluster in the WOC. Processing occurs at the level of RC complex formation of PSII; thus, this might represent the intermediate PSII assembly stage at which Mn<sup>2+</sup> is delivered by PrtA, resulting in a preloading of D1 with Mn<sup>2+</sup>. After the transfer, PrtA leaves the RC complex, and the inner antennae subunits CP47 and CP43 attach to this intermediate in a stepwise fashion to form RCC1 complexes (Rengstl et al., 2011). At this stage, all ligands for complexing the four Mn ions are available and photoactivation of the WOC takes place (Figure 10; Becker et al., 2011).

In *pratA*<sup>-</sup>, the Mn<sup>2+</sup> transport rate to PSII was found to be strongly reduced; nevertheless, Mn<sup>2+</sup> was still incorporated by PSII, allowing photoautotrophic growth of mutant cells although with reduced rates compared with the wild type (Klinkert et al., 2004). Therefore, complementing Mn<sup>2+</sup> delivery systems to PSII apart from the periplasmic PrtA-assisted transport have to exist; alternatively, Mn<sup>2+</sup> might reach D1 without the coupling to

transport proteins. However, PrtA seems to be responsible for a direct Mn<sup>2+</sup> transport to PSII, and it drastically increases the transport efficiency. To date, at least two different systems for cellular Mn uptake have been described (i.e., an ABC transporter [Mnt system] and a yet unidentified system) (Bartsevich and Pakrasi, 1995, 1996). The presence of a Mn transporter system in the PM suggests that Mn is also supplied from the cytoplasmic compartment of the cell in a yet unknown way. PrtA-mediated capture of Mn<sup>2+</sup> by D1 already at the periplasm would, however, be an elegant way to bypass the need for active transport of Mn<sup>2+</sup> across the PM to the thylakoids via the Mnt system. This is likely to be crucial when the cell faces a high demand for Mn, for instance, during/after cell division when substantial amounts of new TMs have to be synthesized. Moreover, periplasmic Mn<sup>2+</sup> loading of PSII would prevent nonspecific oxidation of Mn<sup>2+</sup> during subsequent transfer processes. The exact mechanism of Mn<sup>2+</sup> transfer from PrtA to D1 and the possible involvement of additional factors required for this process have to be determined structurally and biochemically in future studies.

### Spatial Organization of PSII Assembly

PrtA defines the PDM system, an intermediate membrane fraction proposed to be the site for initial steps of PSII biogenesis, which harbors especially the pD1 precursor protein as well as several PSII assembly factors and the chlorophyll precursor chlorophyllide *a* (Schottkowski et al., 2009a; Nickelsen et al., 2011; Rengstl et al., 2011). Our data suggest that the first steps in Mn incorporation into PSII (i.e., binding to D1) also occur in PDMs, whereas further assembly of RC47 and RCC1 complexes and photoactivation of the Mn cluster take place in the TM (Cheniae and Martin, 1971; Hwang and Burnap, 2005). Based on several facts it has been postulated that PDMs connect the PM and the TM system (Nickelsen et al., 2011) and that they function in transport of precomplexes from PM to TM: (1) D1 and D2 are not exclusively present in TMs, but also in PM/PDM fractions of

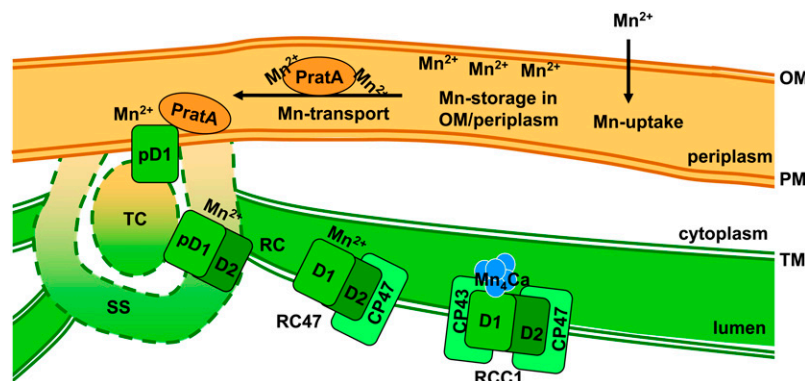


**Figure 10.** Schematic Model of Mn Delivery to PSII.

Mn is first taken up into the periplasm (as Mn<sup>2+</sup>). Subsequently, it can be stored in the periplasm or is transported to PSII via the assistance of PrtA. It is then bound by D1, which is thus preloaded with Mn<sup>2+</sup> to assemble a functional Mn cluster (depicted in blue) during later steps of PSII biogenesis. OM, outer membrane; RC, reaction complex; SS, semicircular structure; TC, thylakoid center. Since the precise architecture of the biogenesis centers (= TC + SS) remains to be resolved at higher resolution, it is depicted with broken lines. For further details, see text.

[See online article for color version of this figure.]

*Synechocystis* 6803 (Smith and Howe, 1993; Zak et al., 2001; Keren et al., 2005; Rengstl et al., 2011); (2) CtpA, the protease required for cleavage of the C-terminal extension of D1, is exclusively found in the PM/PDM (Zak et al., 2001); (3) PrtA is localized in the periplasm and in the PDMs; (4) pD1 accumulates in the PDMs upon knockout of PrtA (Schottkowski et al., 2009a). However, the existence of structures connecting PM and TM being the site of early PSII assembly processes has been discussed controversially (Liberton et al., 2006; Liberton and Pakrasi, 2008; Mullineaux, 2008; Nixon et al., 2010; Nickelsen et al., 2011). Here, we present experimental evidence from ultrastructural analyses that show the existence of PrtA-dependent semicircular structures of ~100 nm in diameter surrounding thylakoid centers at the cellular periphery, which indeed appear to connect TMs and PM (Figure 7) and which we called biogenesis centers (= thylakoid center + semicircular structure; Figure 9G). Although these structures have to be analyzed three-dimensionally in more detail in further studies, it can be hypothesized that the observed semicircles surround the rod-like thylakoid centers detected before (van de Meene et al., 2006). In none of the >1000 *prtA*<sup>-</sup> cells analyzed have these semicircle-shaped structures been found, suggesting that although we cannot exclude that certain prestructures already form PrtA independently, PrtA seems to be required for either the stability of these structures or its fixation at the cell periphery. Furthermore, both PrtA and pD1 signals in immunogold labeling experiments form clusters of similar size close to the PM. The localization of these two markers for initial PSII biogenesis at structures apparently connecting PMs and TMs provides a solution to the long-standing, controversial discussion whether or not the PM is involved in TM biogenesis in cyanobacteria. This is in line with membrane fractionation experiments in *Synechocystis* 6803 that also indicated a crucial role of PrtA for membrane organization (Rengstl et al., 2011). Due to technical limitations in staining of images in gold-labeling assays, we were not able to localize precisely the clusters to the semicircular structures. However, their common localization and size as well as their absence in the *prtA*<sup>-</sup> mutant strongly suggest that these structures at the cell periphery represent biogenesis centers formed by PDMs. Further high-resolution imaging techniques will be required to resolve the structure of the biogenesis centers in more detail and three-dimensionally. Interestingly, similar biogenesis centers have additionally been detected in *C. reinhardtii* (Uniacke and Zerges, 2007). In this case, the biogenesis regions seem to consist of membranes surrounding the pyrenoid structure of the chloroplast. Thus, it can be postulated that the general mechanisms of TM biogenesis are evolutionary conserved from cyanobacteria to algae and possibly also to plants. Taken together, our data allow the proposal of a coherent model for the spatiotemporal organization of TM biogenesis in cyanobacteria, which includes not only biogenesis centers as PM/TM connecting sites responsible for early PSII assembly processes, but which additionally involves Mn<sup>2+</sup> preloading of PSII from the periplasm (Figure 10).

### A Function of PrtA during Repair of PSII?

Our results provide evidence for a function of PrtA in direct and efficient delivery of Mn<sup>2+</sup> to D1 during PSII de novo assembly. It remains unknown if and how PrtA functions in PSII repair, as a

role in this process has not been investigated yet. Although light-induced damage to PSII (photoinhibition) has been studied in great detail in vitro (Adir et al., 2003; Edelman and Mattoo, 2008; Nixon et al., 2010), the in vivo mechanism of PSII photodamage is controversial (Vass and Cser, 2009). Furthermore, it is unclear whether PSII repair in cyanobacteria is spatially separated from PSII de novo assembly like in chloroplasts of green algae (Zak et al., 2001; Komenda et al., 2006; Nixon et al., 2010; Uniacke and Zerges, 2007). Concerning Mn, it has even been suggested that the Mn cluster itself is the initial site of damage (Hakala et al., 2005; Ohnishi et al., 2005), and it can be speculated that Mn is merely recycled during PSII repair; however, direct evidence for this is missing. Hence, future studies have to analyze further PSII repair in general and a potential photodamage-related function of PrtA in particular.

### Evolutionary Aspects of PrtA Function

PrtA is a cyanobacterial protein for which no homologs exist in eukaryotes (Klinkert et al., 2004). However, Lpa1 (for Low PSII Accumulation I) from *Arabidopsis* has recently been shown to possess similar properties: It interacts directly with D1 and belongs to the TPR protein family along with its homolog from *C. reinhardtii* named REP27 (for repair-aberrant mutant 27; Peng et al., 2006; Park et al., 2007). Lpa1 contains two TPR motifs near its N terminus, which are arranged like the first two of the nine TPR domains in PrtA, but it shows no additional sequence similarities to PrtA (see Supplemental Figure 5A online). Interestingly, initial EPR measurements suggest that Lpa1, similar to PrtA, has Mn<sup>2+</sup> binding activity, suggesting that the participation of TPR proteins in Mn<sup>2+</sup> transport to PSII by direct interaction with D1 might be evolutionary conserved from cyanobacteria to vascular plants (see Supplemental Figure 5B online).

Recently, membrane domains with specialized functions have been localized even in the ancient cyanobacterium *Gloeobacter violaceus*, the only known organism performing oxygenic photosynthesis without internal TMs (Rexroth et al., 2011). The cytoplasmic membrane of *G. violaceus* was found to contain a "green fraction" and an "orange fraction," which, regarding protein and lipid content, seem to resemble the TM and PM of other cyanobacteria, respectively. This idea is supported by the observation that components of the photosynthetic and respiratory electron transfer chain are highly enriched in the green fraction (Rexroth et al., 2011). Interestingly, a PrtA homologous protein was detected exclusively in the orange fraction, which allows the proposal that this specialized membrane region might be the evolutionary origin of the later-developed biogenesis centers. Taken together, we hypothesize that PrtA-related proteins function in early PSII assembly steps, including its preloading with Mn<sup>2+</sup> in all photosynthetic organisms from *G. violaceus* to vascular plants.

### METHODS

#### Strains, Growth Conditions, and Sequence Analysis

*Synechocystis* sp PCC 6803 (*Synechocystis* 6803) wild-type and mutant strains (*prtA*<sup>-</sup>, *psbA*<sup>-</sup>, and *ycf48*<sup>-</sup>, including the respective wild type

used; Komenda et al., 2008) were grown on solid or in liquid BG11 medium (Rippka et al., 1979) at 23°C at a continuous photon irradiance of 30  $\mu\text{E m}^{-2} \text{s}^{-1}$ . The mutant strains *prata*<sup>-</sup> and *ycf48*<sup>-</sup> and the *psbA*<sup>-</sup> deletion strain *TD41* were previously constructed as described (Nixon et al., 1992; Klinkert et al., 2004; Komenda et al., 2008). For sequence analysis of PrataA (slr2048) and Lpa1 (At1g02910), the full-length protein sequences were aligned using ClustalX2 (see Supplemental Figure 5A online).

### Isolation of Periplasm and Atomic Absorption Spectrometry

Periplasm was isolated from 9 liters of *Synechocystis* wild-type and *prata*<sup>-</sup> cultures (Fulda et al., 2000) and concentrated to 6 mL by ultrafiltration (Millipore). Fe and Mn levels were measured with a multielement hollow-cathode lamp (slit width, 0.2 nm; lamp current, Fe, 5 mA; Mn, 4 mA) on a Varian AA240 atomic absorption spectrometer at 248.3 and 279.5 nm, respectively. All measurements were performed in an air (13.5 L/min)-acetylene (2 L/min) flame. Single element solutions (Roth) were used for calibration. Experiments were performed in triplicate, and results are expressed in nanograms of metal per milligram of chlorophyll.

### Overexpression and Purification of Proteins

For heterologous expression of N-terminal GST fusion proteins, GST-Lpa1, GST-PrataA, GST-mD1, and GST-pD1 (Schottkowski et al., 2009a) were used. For Lpa1, the coding region, excluding the transit sequence (Peng et al., 2006), was cloned into the *Sall*-*Bam*HI sites of pGEX-4T-1 (GE Healthcare) using the primers Lpa\_for (5'-GATCGGATCCATG-GATGCTCTTGTTCAGTTTG-3') and Lpa\_rev (5'-GATCGTGCAC-GTCTTCTAACTTGCTGAGAA-3'). Overexpression (in *Escherichia coli* BL21 [DE3] cells) was performed at 12°C overnight. Proteins were purified via GST-agarose (Biontix) under native conditions in the presence of 5 mM EDTA and, if required, recovered from the matrix by removing the GST tag by incubation with 1 unit of thrombin (GE Healthcare) per 100  $\mu\text{g}$  of fusion protein for 6 h at room temperature (RT). Thrombin was removed by benzamidine-sepharose (GE Healthcare). Freshly prepared proteins (see Supplemental Figure 1 online) were used for CD or EPR analysis after dialysis against 10 mM Tris/H<sub>2</sub>SO<sub>4</sub>, pH 8.0, or 50 mM Tris/HCl, pH 8.0, and 150 mM NaCl, respectively.

### CD Measurements

CD experiments with PrataA were performed at RT using a Jasco J-810 spectropolarimeter flushed with nitrogen (Stengel et al., 2008). Spectra were collected from 260 to 190 nm using a cylindrical quartz cell (path length of 1 mm). Each spectrum was the average of three scans taken at a scan rate of 50 nm/min with a spectral bandwidth of 1 nm. For the final representation, the baseline was subtracted from the spectrum. The protein concentration varied from 0.080 to 0.122 mg/mL. Where indicated, 1 mM MnCl<sub>2</sub>, FeCl<sub>3</sub>, FeCl<sub>2</sub>, MgCl<sub>2</sub>, or CaCl<sub>2</sub> was added and incubated with the protein for 15 min at RT prior to the measurement. Experiments were performed in triplicate. Data analysis was performed using CDSSTR (reference set 7) from the DichroWeb server (<http://dichroweb.cryst.bbk.ac.uk/html/home.shtml>), and spectra were plotted after subtraction of the baseline.

### EPR Analysis

Continuous-wave EPR spectra were recorded on a Miniscope MS200 X-band spectrometer (microwave frequency  $\approx$  9.4 GHz) equipped with a rectangular TE102 resonator (Magnettech). The temperature was adjusted with a TC H02 control unit (Magnettech). Measurements were performed using 298.15K, 3.162 mW (microwave power), 100 kHz (modulation frequency), and 0.5 mT (modulation amplitude) for Mn(II); and 104K, 15.85 mW, 100 kHz, and 0.5 mT for Fe(III). Prior to the measurements, 500  $\mu\text{M}$  MnCl<sub>2</sub> (or 5 mM MnCl<sub>2</sub> where indicated) or 1 mM FeCl<sub>3</sub>

were incubated for 5 min at RT with PrataA (100  $\mu\text{M}$  if not indicated differently). For the competition experiments, 500  $\mu\text{M}$  (1 $\times$ ) or 5 mM (10 $\times$ ) CaCl<sub>2</sub> or MgCl<sub>2</sub> was incubated together with 500  $\mu\text{M}$  MnCl<sub>2</sub> and PrataA before analysis. For Mn titration experiments, 100  $\mu\text{M}$  PrataA was titrated with 25 to 5000  $\mu\text{M}$  MnCl<sub>2</sub>, and continuous-wave EPR spectra were recorded after incubation for 5 min. The amount of protein-bound Mn<sup>2+</sup> was calculated from the signal amplitude of the lowest-field transition. Thereby, the peak-to-peak height of the lowest-field line of a Mn<sup>2+</sup> standard was plotted against Mn<sup>2+</sup> concentration to obtain a standard curve. The concentration of the free Mn<sup>2+</sup> in solutions containing rPrataA was calculated by comparison to the standard curve, and the amount bound was determined by difference. The stoichiometry of bound Mn<sup>2+</sup> per rPrataA molecule was then obtained by dividing the amount of protein-bound Mn<sup>2+</sup> by the concentration of rPrataA in solution. Data were analyzed by plotting according to Scatchard using SigmaPlot 11 with the Enzyme Kinetics module 1.3.

### Filter Binding Assays

For determination of the PrataA-Mn binding properties, recombinant PrataA (100  $\mu\text{M}$ ; in 50 mM Tris/HCl, pH 8.0, and 150 mM NaCl) was incubated with 10 to 75  $\mu\text{M}$  of <sup>54</sup>Mn<sup>2+</sup> (as MnCl<sub>2</sub>; Hartmann Analytics) for 15 min at RT, loaded on Amicon Ultra-0.5 10 kD columns (Millipore), concentrated, and washed once with Tris/NaCl. Recovered samples were suspended in scintillation mixture (Optiphase Supermix; Perkin-Elmer), and <sup>54</sup>Mn<sup>2+</sup> was measured with a LS 6500 multipurpose scintillation counter (Beckman Coulter). For calculation of the amount of bound Mn<sup>2+</sup> per PrataA, the obtained counts per minute of the control (rPrataA without added <sup>54</sup>Mn<sup>2+</sup>; background) was subtracted from the measured counts per minute of samples that had been incubated with 10 to 75  $\mu\text{M}$  of <sup>54</sup>Mn<sup>2+</sup> and calculated relative to the counts per minute detected for total <sup>54</sup>Mn<sup>2+</sup> used for the experiment. From these values, the concentration of <sup>54</sup>Mn<sup>2+</sup> that was bound by the protein was obtained, and using the known concentration of rPrataA (100  $\mu\text{M}$ ), the amount of bound Mn<sup>2+</sup> per PrataA was calculated. Data were analyzed by plotting according to Scatchard using SigmaPlot 11 with the Enzyme Kinetics module 1.3.

### Affinity Chromatography Using Metal-Loaded Columns

His-Bind Fractogel Matrix (Novagen; 100  $\mu\text{L}$ ) was incubated with 100 mM MnCl<sub>2</sub>, NiSO<sub>4</sub>, or buffer as control (50 mM Tris, pH 8.0, and 200 mM NaCl) for 1 h at RT and washed five times with Tris/NaCl. The beads were subsequently incubated (2 h, RT) with periplasm (200  $\mu\text{g}$  protein) isolated from wild-type *Synechocystis* (Fulda et al., 2000) and washed five times with Tris/NaCl. Proteins were eluted by incubation with 50  $\mu\text{L}$  2 $\times$  Roti-Load 1 (Roth) for 5 min at 95°C. Samples of load, flow-through, wash, and eluate were analyzed by immunoblotting using a  $\alpha$ PrataA antibody (Klinkert et al., 2004). Quantification of signals was performed using AIDA software (version 3.52.046).

### GST Pull-Down Assays

GST fusion proteins (mD1 and pD1; 100  $\mu\text{g}$  each) were bound to GST-agarose (Biontix) for 2 h at RT. The matrix was then incubated for 2 h at RT with periplasm (300  $\mu\text{g}$  protein) from *Synechocystis* wild-type and *prata*<sup>-</sup> cultures (Fulda et al., 2000). As control, wild-type periplasm was incubated with an equivalent amount of GST-agarose matrix without bound mD1/pD1 protein. The beads were washed five times with 50 mM Tris, pH 8.0, and 150 mM NaCl, proteins were eluted by incubation with 50  $\mu\text{L}$  2 $\times$  Roti-Load 1 (Roth) for 5 min at 95°C, and samples were analyzed by immunoblotting using  $\alpha$ PrataA.

### Mn Uptake Assay and Immunoprecipitation with $\alpha$ D1

*Synechocystis* wild-type and mutant strains (*prata*<sup>-</sup>, *psbA*<sup>-</sup> TD41, and *ycf48*<sup>-</sup> with the respective wild type; Komenda et al., 2008) were grown in

50 mL liquid BG11 for 5 to 6 d. Chlorophyll concentrations were measured after extraction with 100% methanol and calculated from the absorbance values at 666 and 720 nm (Wellburn and Lichtenthaler, 1984). Cells were resuspended in BG11 (chlorophyll concentration 5  $\mu\text{g}/\text{mL}$ ), and  $^{54}\text{Mn}^{2+}$  was added for 1 and 3 h at 1  $\mu\text{Ci}/\text{mL}$ . As control, one sample was analyzed immediately after addition of  $^{54}\text{Mn}^{2+}$  (0 h), and values obtained after incubation for 1 and 3 h were calculated relative to it. Samples (10  $\mu\text{g}$  chlorophyll) were washed twice in TMK buffer (10 mM Tris/HCl, pH 6.8, 10 mM  $\text{MgCl}_2$ , and 20 mM KCl). For analysis of Mn uptake, cells were used directly for measurement of  $^{54}\text{Mn}^{2+}$  with a scintillation counter. To monitor the delivery of Mn to PS II (Mn transport), cells were resuspended in 200  $\mu\text{L}$  TMK buffer and broken by shaking with glass beads (0.1 mm diameter) on a vortex for  $2 \times 1$  min separated by 1 min on ice. The suspension was centrifuged for 1 min at 6000g, and the supernatant was solubilized with dodecylmaltoside (1.5%, 10 min on ice). After centrifugation for 10 min at 20,000g, the supernatant was diluted 1:10 with TMK buffer and supplied with 5  $\mu\text{L}$  primary antiserum ( $\alpha\text{D1}$ ; Schottkowsky et al., 2009a). After incubation for 2 h at RT, 25  $\mu\text{L}$  Protein A-Sepharose (Roche) was added, and the suspension was incubated overnight at 4°C. The beads were washed five times in TMK buffer and analyzed with a scintillation counter (Beckman Coulter). For normalization purposes, radioactivity levels (in cpm) measured in samples from *psbA*<sup>-</sup> cells (background) were subtracted from values for the wild type and *pratA*<sup>-</sup>. Experiments were performed four times. Protein extracts for determination of D1 content in wild-type and *pratA*<sup>-</sup> cells were prepared according to Schottkowsky et al. (2009b). Isolated proteins were separated by SDS-PAGE and probed with the indicated antibodies. Quantification of signals was performed using AIDA software (version 3.52.046), and the levels in the *pratA*<sup>-</sup> strain were compared with those in the wild-type strain (set to 100%). Means ( $\pm$ SD) were calculated from three independently inoculated cultures.

### Transmission Electron Microscopy and Immunogold Labeling

*Synechocystis* cells (the wild type, *pratA*<sup>-</sup>, and *psbB*<sup>-</sup>) were harvested and 20  $\mu\text{L}$  of the moist cell pellet was placed into a HPF aluminum platelet (Leica, BAL-TEC, HPM 100 carriers type A and B; 100  $\mu\text{m}$  in depth), high-pressure frozen (Leica EM HPM100) at 2100 bar, and stored in liquid nitrogen. No cryoprotectants were used. For analyzing the ultrastructure, cryofixed samples were freeze-substituted (Leica EM AFS2) at  $-85^\circ\text{C}$  for 72 h in acetone anhydrous with 1% glutaraldehyde and 1% tannic acid according to van de Meene et al. (2006) and washed three times in acetone anhydrous ( $-85^\circ\text{C}$ , 15 min each). Infiltration of cells was achieved using acetone including 1% osmium tetroxide for 3 h at  $-85^\circ\text{C}$ , followed by incubation for 20 h at  $-20^\circ\text{C}$ , 3 h at  $4^\circ\text{C}$ , and 1 h at RT. Cells were washed four times in acetone and infiltrated with Spurr's resin (Spurr, 1969). For immunodetection experiments, cryofixed samples were freeze-substituted in acetone containing 0.5% uranyl acetate (Pfeiffer and Krupinska, 2005) for 20 h at  $-90^\circ\text{C}$ . Dehydration was performed by two infiltration steps with acetone (8 h at  $-70^\circ\text{C}$  and 8 h at  $-50^\circ\text{C}$ ). Afterwards, cells were infiltrated with HM-20 (Lowicryl HM-20; Polysciences) by washing 30 min with acetone at  $-50^\circ\text{C}$ , infiltrated with 30% HM-20/70% acetone overnight, followed by 70% HM-20/30% acetone for 2 h, finally three times in 100% HM-20 for 2 h at  $-50^\circ\text{C}$ . Polymerization was performed under UV light at  $-50^\circ\text{C}$  for 48 h and at RT for 24 h. Ultrathin sections (30 to 60 nm) were cut with a diamond knife (Ultramicrotome Leica EM UC6). For ultrastructural analysis, they were poststained with lead citrate (Reynolds, 1963). For immunogold labeling, the sections were collected on coated Ni grids, incubated twice with glycine (50 mM in PBS, pH 7.4), once in blocking buffer (FCS 10% inactivated at  $56^\circ\text{C}$  for 30 min, 0.01% gelatin, 0.05% Tween 20 in PBS, pH 7.4) for 5 min, and twice in blocking buffer for 60 min. Sections were incubated for 18 h at  $4^\circ\text{C}$  with  $\alpha\text{PratA}$  1:25 (rabbit) or  $\alpha\text{pD1}$  1:50 (rabbit). The sections were washed six times for 5 min and incubated with gold-conjugated goat anti-rabbit IgG (BBInternational; 5 nm, 1:50) for 90 min at

RT before washing three times in blocking buffer, twice with 50 mM glycine in PBS, pH 7.4, twice with PBS, pH 7.4, and twice with double-distilled water. Samples were analyzed without further contrast. Micrographs were taken at 80 kV on a Fei Morgagni 268 electron microscope;  $\times 1800$  and 11,000-fold (overviews), 44,000-fold and 110,000-fold (details). As negative control, *Synechocystis* wild-type sections were incubated without the primary antibody, followed by treatment with the gold-labeled anti-rabbit IgG. The cluster analysis (determination of cluster area, perimeter, major axis, minor axis, and circularity) was performed with ImageJ (<http://rsb.info.nih.gov/ij/>; see Supplemental Figure 4 online).

### Accession Numbers

Sequence data from this article can be found in the Arabidopsis Genome Initiative or GenBank/EMBL databases under the following accession numbers: slr2048 (*PratA*), slr2034 (*Ycf48*), and At1g02910 (*Lpa1*). The three-dimensional structure of D1 is derived from the Protein Data Bank file 3BZ1.

### Supplemental Data

The following materials are available in the online version of this article.

**Supplemental Figure 1.** Purification of Recombinant *PratA*.

**Supplemental Figure 2.** Competition of  $\text{Mn}^{2+}$  Binding to *PratA* Using 5 mM  $\text{MnCl}_2$ .

**Supplemental Figure 3.** Recovery of  $\text{Mn}^{2+}$  Signal and Dependency of  $\text{Mn}^{2+}$  Binding on *PratA* Concentration.

**Supplemental Figure 4.** Determination of Parameters Used for Analysis of Gold Clusters in Immunogold Labeling Experiments with  $\alpha\text{pD1}$ .

**Supplemental Figure 5.** Evolutionary Investigation of *PratA* Function.

### ACKNOWLEDGMENTS

We thank Christian Schwarz for generation of the three-dimensional illustration of D1, Norio Murata for providing the pD1 antibody, and Gunnar Jeschke and Jürgen Soll for helpful discussions and suggestions. This work is supported by grants from the Deutsche Forschungsgemeinschaft (SFB TR1 TPC10 to J.N.; Ju333/4-3 to H.J.) and by the Bayerische Gleichstellungsförderung Scholarship of Ludwig-Maximilians-Universität Munich (A.S.).

### AUTHOR CONTRIBUTIONS

A.S. and J.N. designed the research. A.S., I.L.G., D.H., and B.R. performed research. A.S., I.L.G., H.J., and J.N. analyzed data. A.S. and J.N. wrote the article.

Received November 17, 2011; revised January 12, 2012; accepted January 23, 2012; published February 7, 2012.

### REFERENCES

**Abramowicz, D.A., and Dismukes, G.C.** (1984). Manganese proteins isolated from spinach thylakoid membranes and their role in O<sub>2</sub> evolution. II. A binuclear manganese-containing 34 kilodalton protein, a probable component of the water dehydrogenase enzyme. *Biochim. Biophys. Acta* **765**: 318–328.

- Adir, N., Zer, H., Shochat, S., and Ohad, I.** (2003). Photoinhibition - A historical perspective. *Photosynth. Res.* **76**: 343–370.
- Barber, J.** (2008). Crystal structure of the oxygen-evolving complex of photosystem II. *Inorg. Chem.* **47**: 1700–1710.
- Bartsevich, V.V., and Pakrasi, H.B.** (1995). Molecular identification of an ABC transporter complex for manganese: Analysis of a cyanobacterial mutant strain impaired in the photosynthetic oxygen evolution process. *EMBO J.* **14**: 1845–1853.
- Bartsevich, V.V., and Pakrasi, H.B.** (1996). Manganese transport in the cyanobacterium *Synechocystis* sp. PCC 6803. *J. Biol. Chem.* **271**: 26057–26061.
- Becker, K., Cormann, K.U., and Nowaczyk, M.M.** (2011). Assembly of the water-oxidizing complex in photosystem II. *J. Photochem. Photobiol. B* **104**: 204–211.
- Blatch, G.L., and Lässle, M.** (1999). The tetratricopeptide repeat: A structural motif mediating protein-protein interactions. *Bioessays* **21**: 932–939.
- Bondarava, N., Un, S., and Krieger-Liszkay, A.** (2007). Manganese binding to the 23 kDa extrinsic protein of photosystem II. *Biochim. Biophys. Acta* **1767**: 583–588.
- Chenai, G.M., and Martin, I.F.** (1971). Photoactivation of the manganese catalyst of O<sub>2</sub> evolution. I. Biochemical and kinetic aspects. *Biochim. Biophys. Acta* **253**: 167–181.
- Crowley, J.D., Traynor, D.A., and Weatherburn, D.C.** (2000). Enzymes and proteins containing manganese: An overview. In *Metal Ions in Biological Systems*, A. Sigel and H. Sigel, eds (New York: Marcel Dekker, Inc.), pp. 211–261.
- Edelman, M., and Mattoo, A.K.** (2008). D1-protein dynamics in photosystem II: The lingering enigma. *Photosynth. Res.* **98**: 609–620.
- Ferreira, K.N., Iverson, T.M., Maghlaoui, K., Barber, J., and Iwata, S.** (2004). Architecture of the photosynthetic oxygen-evolving center. *Science* **303**: 1831–1838.
- Fulda, S., Huang, F., Nilsson, F., Hagemann, M., and Norling, B.** (2000). Proteomics of *Synechocystis* sp. strain PCC 6803. Identification of periplasmic proteins in cells grown at low and high salt concentrations. *Eur. J. Biochem.* **267**: 5900–5907.
- Guskov, A., Kern, J., Gabdulkhakov, A., Broser, M., Zouni, A., and Saenger, W.** (2009). Cyanobacterial photosystem II at 2.9-Å resolution and the role of quinones, lipids, channels and chloride. *Nat. Struct. Mol. Biol.* **16**: 334–342.
- Hakala, M., Tuominen, I., Keränen, M., Tyystjärvi, T., and Tyystjärvi, E.** (2005). Evidence for the role of the oxygen-evolving manganese complex in photoinhibition of photosystem II. *Biochim. Biophys. Acta* **1706**: 68–80.
- Hayden, J.A., and Hendrich, M.P.** (2010). EPR spectroscopy and catalase activity of manganese-bound DNA-binding protein from nutrient starved cells. *J. Biol. Inorg. Chem.* **15**: 729–736.
- Hinterstoisser, B., Chichna, M., Kuntner, O., and Peschek, G.A.** (1993). Cooperation of plasma and thylakoid membranes for the biosynthesis of chlorophyll in cyanobacteria: The role of the thylakoid centers. *J. Plant Physiol.* **142**: 407–413.
- Hwang, H.J., and Burnap, R.L.** (2005). Multiflash experiments reveal a new kinetic phase of photosystem II manganese cluster assembly in *Synechocystis* sp. PCC6803 in vivo. *Biochemistry* **44**: 9766–9774.
- Keren, N., Kidd, M.J., Penner-Hahn, J.E., and Pakrasi, H.B.** (2002). A light-dependent mechanism for massive accumulation of manganese in the photosynthetic bacterium *Synechocystis* sp. PCC 6803. *Biochemistry* **41**: 15085–15092.
- Keren, N., Liberton, M., and Pakrasi, H.B.** (2005). Photochemical competence of assembled photosystem II core complex in cyanobacterial plasma membrane. *J. Biol. Chem.* **280**: 6548–6553.
- Kern, J., Biesiadka, J., Loll, B., Saenger, W., and Zouni, A.** (2007). Structure of the Mn<sub>4</sub>-Ca cluster as derived from X-ray diffraction. *Photosynth. Res.* **92**: 389–405.
- Klinkert, B., Ossenbühl, F., Sikorski, M., Berry, S., Eichacker, L., and Nickelsen, J.** (2004). PrtA, a periplasmic tetratricopeptide repeat protein involved in biogenesis of photosystem II in *Synechocystis* sp. PCC 6803. *J. Biol. Chem.* **279**: 44639–44644.
- Komenda, J., Barker, M., Kuviková, S., de Vries, R., Mullineaux, C.W., Tichy, M., and Nixon, P.J.** (2006). The FtsH protease slr0228 is important for quality control of photosystem II in the thylakoid membrane of *Synechocystis* sp. PCC 6803. *J. Biol. Chem.* **281**: 1145–1151.
- Komenda, J., Nickelsen, J., Tichý, M., Prásil, O., Eichacker, L.A., and Nixon, P.J.** (2008). The cyanobacterial homologue of HCF136/YCF48 is a component of an early photosystem II assembly complex and is important for both the efficient assembly and repair of photosystem II in *Synechocystis* sp. PCC 6803. *J. Biol. Chem.* **283**: 22390–22399.
- Liberton, M., Howard Berg, R., Heuser, J., Roth, R., and Pakrasi, H.B.** (2006). Ultrastructure of the membrane systems in the unicellular cyanobacterium *Synechocystis* sp. strain PCC 6803. *Protoplasma* **227**: 129–138.
- Liberton, M., and Pakrasi, H.B.** (2008). Membrane systems in cyanobacteria. In *The Cyanobacteria*, A. Herrero and E. Flores, eds (Norfolk, UK: Caister Academic Press), pp. 271–288.
- Main, E.R., Stott, K., Jackson, S.E., and Regan, L.** (2005). Local and long-range stability in tandemly arrayed tetratricopeptide repeats. *Proc. Natl. Acad. Sci. USA* **102**: 5721–5726.
- Meier, A.E., Whittaker, M.M., and Whittaker, J.W.** (1996). EPR polarization studies on Mn catalase from *Lactobacillus plantarum*. *Biochemistry* **35**: 348–360.
- Mizuno, K., Whittaker, M.M., Bächinger, H.P., and Whittaker, J.W.** (2004). Calorimetric studies on the tight binding metal interactions of *Escherichia coli* manganese superoxide dismutase. *J. Biol. Chem.* **279**: 27339–27344.
- Mullineaux, C.W.** (2008). Biogenesis and dynamics of thylakoid membranes and the photosynthetic apparatus. In *The Cyanobacteria*, A. Herrero and E. Flores, eds (Norfolk, UK: Caister Academic Press), pp. 289–304.
- Mulo, P., Sirpiö, S., Suorsa, M., and Aro, E.M.** (2008). Auxiliary proteins involved in the assembly and sustenance of photosystem II. *Photosynth. Res.* **98**: 489–501.
- Nickelsen, J., Nowaczyk, M.M., and Klinkert, B.** (2007). Assembly factors of the photosynthetic machinery in cyanobacteria. *Prog. Bot.* **68**: 57–79.
- Nickelsen, J., Rengstl, B., Stengel, A., Schottkowski, M., Soll, J., and Ankele, E.** (2011). Biogenesis of the cyanobacterial thylakoid membrane system—An update. *FEMS Microbiol. Lett.* **315**: 1–5.
- Nixon, P.J., Michoux, F., Yu, J., Boehm, M., and Komenda, J.** (2010). Recent advances in understanding the assembly and repair of photosystem II. *Ann. Bot. (Lond.)* **106**: 1–16.
- Nixon, P.J., Trost, J.T., and Diner, B.A.** (1992). Role of the carboxy terminus of polypeptide D1 in the assembly of a functional water-oxidizing manganese cluster in photosystem II of the cyanobacterium *Synechocystis* sp. PCC 6803: Assembly requires a free carboxyl group at C-terminal position 344. *Biochemistry* **31**: 10859–10871.
- Ohnishi, N., Allakhverdiev, S.I., Takahashi, S., Higashi, S., Watanabe, M., Nishiyama, Y., and Murata, N.** (2005). Two-step mechanism of photodamage to photosystem II: Step 1 occurs at the oxygen-evolving complex and step 2 occurs at the photochemical reaction center. *Biochemistry* **44**: 8494–8499.
- Park, S., Khamai, P., Garcia-Cerdan, J.G., and Melis, A.** (2007). REP27, a tetratricopeptide repeat nuclear-encoded and chloroplast-localized protein, functions in D1/32-kD reaction center protein turnover and photosystem II repair from photodamage. *Plant Physiol.* **143**: 1547–1560.

- Peng, L., Ma, J., Chi, W., Guo, J., Zhu, S., Lu, Q., Lu, C., and Zhang, L.** (2006). LOW PSII ACCUMULATION1 is involved in efficient assembly of photosystem II in *Arabidopsis thaliana*. *Plant Cell* **18**: 955–969.
- Pfeiffer, S., and Krupinska, K.** (2005). New insights in thylakoid membrane organization. *Plant Cell Physiol.* **46**: 1443–1451.
- Pierce, B.S., Elgren, T.E., and Hendrich, M.P.** (2003). Mechanistic implications for the formation of the diiron cluster in ribonucleotide reductase provided by quantitative EPR spectroscopy. *J. Am. Chem. Soc.* **125**: 8748–8759.
- Plücker, H., Müller, B., Grohmann, D., Westhoff, P., and Eichacker, L.A.** (2002). The HCF136 protein is essential for assembly of the photosystem II reaction center in *Arabidopsis thaliana*. *FEBS Lett.* **532**: 85–90.
- Reaney, S.H., Kwik-Urbe, C.L., and Smith, D.R.** (2002). Manganese oxidation state and its implications for toxicity. *Chem. Res. Toxicol.* **15**: 1119–1126.
- Reed, G.H., and Cohn, M.** (1970). Electron paramagnetic resonance spectra of manganese (II)-protein complexes. Manganese (II)-concanavalin A. *J. Biol. Chem.* **245**: 662–664.
- Reed, G.H., and Markham, G.D.** (1984). EPR of Mn(II) complexes with enzymes and other proteins. In *Biological Magnetic Resonance*, L.J. Berliner and J. Reuben, eds (New York: Plenum Press), pp. 73–142.
- Rengstl, B., Oster, U., Stengel, A., and Nickelsen, J.** (2011). An intermediate membrane subfraction in cyanobacteria is involved in an assembly network for photosystem II biogenesis. *J. Biol. Chem.* **286**: 21944–21951.
- Rexroth, S., Mullineaux, C.W., Ellinger, D., Sendtko, E., Rögner, M., and Koenig, F.** (2011). The plasma membrane of the cyanobacterium *Gloeobacter violaceus* contains segregated bioenergetic domains. *Plant Cell* **23**: 2379–2390.
- Reynolds, E.S.** (1963). The use of lead citrate at high pH as an electron-opaque stain in electron microscopy. *J. Cell Biol.* **17**: 208–212.
- Rippka, R., Deruelles, J., Waterbury, J.B., Herdmann, M., and Stanier, R.** (1979). Generic assignments, strain histories and properties of pure cultures of cyanobacteria. *J. Gen. Microbiol.* **111**: 1–61.
- Roose, J.L., Wegener, K.M., and Pakrasi, H.B.** (2007). The extrinsic proteins of photosystem II. *Photosynth. Res.* **92**: 369–387.
- Schneider, D., Fuhrmann, E., Scholz, I., Hess, W.R., and Graumann, P.L.** (2007). Fluorescence staining of live cyanobacterial cells suggest non-stringent chromosome segregation and absence of a connection between cytoplasmic and thylakoid membranes. *BMC Cell Biol.* **8**: 39.
- Schottkowski, M., Gkalypoudis, S., Tzekova, N., Stelljes, C., Schünemann, D., Ankele, E., and Nickelsen, J.** (2009a). Interaction of the periplasmic PrtA factor and the PsbA (D1) protein during biogenesis of photosystem II in *Synechocystis* sp. PCC 6803. *J. Biol. Chem.* **284**: 1813–1819.
- Schottkowski, M., Ratke, J., Oster, U., Nowaczyk, M., and Nickelsen, J.** (2009b). Pitt, a novel tetratricopeptide repeat protein involved in light-dependent chlorophyll biosynthesis and thylakoid membrane biogenesis in *Synechocystis* sp. PCC 6803. *Mol. Plant* **2**: 1289–1297.
- Sen, K.I., Sienkiewicz, A., Love, J.F., vanderSpek, J.C., Fajer, P.G., and Logan, T.M.** (2006). Mn(II) binding by the anthracis repressor from *Bacillus anthracis*. *Biochemistry* **45**: 4295–4303.
- Smith, D., and Howe, C.J.** (1993). The distribution of photosystem-I and photosystem-II polypeptides between the cytoplasmic and thylakoid membranes of cyanobacteria. *FEMS Microbiol. Lett.* **110**: 341–347.
- Spurr, A.R.** (1969). A low-viscosity epoxy resin embedding medium for electron microscopy. *J. Ultrastruct. Res.* **26**: 31–43.
- Stengel, A., Benz, P., Balsera, M., Soll, J., and Bölder, B.** (2008). TIC62 redox-regulated translocon composition and dynamics. *J. Biol. Chem.* **283**: 6656–6667.
- Tamura, N., and Cheniae, G.** (1987). Photoactivation of the water-oxidizing complex in photosystem-II membranes depleted of mn and extrinsic proteins. 1. Biochemical and kinetic characterization. *Biochim. Biophys. Acta* **890**: 179–194.
- Totter, S., Waldron, K.J., Firbank, S.J., Reale, B., Bessant, C., Sato, K., Cheek, T.R., Gray, J., Banfield, M.J., Dennison, C., and Robinson, N.J.** (2008). Protein-folding location can regulate manganese-binding versus copper- or zinc-binding. *Nature* **455**: 1138–1142.
- Umena, Y., Kawakami, K., Shen, J.R., and Kamiya, N.** (2011). Crystal structure of oxygen-evolving photosystem II at a resolution of 1.9 Å. *Nature* **473**: 55–60.
- Uniacke, J., and Zerges, W.** (2007). Photosystem II assembly and repair are differentially localized in *Chlamydomonas*. *Plant Cell* **19**: 3640–3654.
- van de Meene, A.M.L., Hohmann-Marriott, M.F., Vermaas, W.F.J., and Roberson, R.W.** (2006). The three-dimensional structure of the cyanobacterium *Synechocystis* sp. PCC 6803. *Arch. Microbiol.* **184**: 259–270.
- Vass, I., and Cser, K.** (2009). Janus-faced charge recombinations in photosystem II photoinhibition. *Trends Plant Sci.* **14**: 200–205.
- Wellburn, A.R., and Lichtenthaler, H.K.** (1984). Formulae and programme to determine total carotenoids and chlorophyll a and b of leaf extracts in different solvents. In *Advances in Photosynthesis Research*, Vol. II, C. Sybesma, ed (The Hague, Lancaster, Boston: Martinus Nijhoff/Dr. W. Junk Publishers), pp. 9–12.
- Yano, J., Kern, J., Sauer, K., Latimer, M.J., Pushkar, Y., Biesiadka, J., Loll, B., Saenger, W., Messinger, J., Zouni, A., and Yachandra, V.K.** (2006). Where water is oxidized to dioxygen: structure of the photosynthetic Mn<sub>4</sub>Ca cluster. *Science* **314**: 821–825.
- Zak, E., Norling, B., Maitra, R., Huang, F., Andersson, B., and Pakrasi, H.B.** (2001). The initial steps of biogenesis of cyanobacterial photosystems occur in plasma membranes. *Proc. Natl. Acad. Sci. USA* **98**: 13443–13448.
- Zaltsman, L., Ananyev, G.M., Bruntrager, E., and Dismukes, G.C.** (1997). Quantitative kinetic model for photoassembly of the photosynthetic water oxidase from its inorganic constituents: requirements for manganese and calcium in the kinetically resolved steps. *Biochemistry* **36**: 8914–8922.
- Zöfel, P.** (1988). *Statistik in der Praxis*. (Stuttgart, Germany: Gustav Fischer Verlag).

### 3.4 CHARACTERIZATION OF A *SYNECHOCYSTIS* DOUBLE MUTANT LACKING THE PHOTOSYSTEM II ASSEMBLY FACTORS YCF48 AND Sll0933

**Rengstl, B.**, Knoppová, J., Komenda, J., and Nickelsen, J. (2012) *Planta*

By investigation of interrelationships between different PSII assembly factors, an interaction between the two PSII assembly factors YCF48 and Sll0933 was detected (see chapter 3.2). To further examine the function of the YCF48/Sll0933 complex, a *Synechocystis* 6803 double mutant lacking both proteins was constructed. Characterization of *ycf48<sup>-</sup>sll0933<sup>-</sup>* with regard to growth, oxygen evolution, whole cell absorption spectra, 77 K measurements as well as quantification of PSII subunit and assembly factor amounts displayed a phenotype comparable to the *ycf48<sup>-</sup>* single mutant, suggesting that YCF48 acts upstream of Sll0933 during PSII assembly. Additionally, by using a modified protocol for protein isolation for 2D-BN/SDS-PAGE analysis (as compared to *sll0933<sup>-</sup>* characterization in chapter 3.1), it could be shown that lack of Sll0933 causes reduction of newly synthesized CP43 and CP47 proteins, accompanied by accumulation of RC complexes and decrease of PSII monomers. This is in agreement with the phenotype of *A. thaliana pam68* (the Sll0933 homolog) mutant plants, and substantiates a role of Sll0933 in synthesis and assembly of CP47 and CP43. Moreover, direct interaction of Sll0933 with YCF48, CP47, CP43 and with other Sll0933 proteins was depicted by yeast split-ubiquitin experiments. In summary, analysis of the *ycf48<sup>-</sup>sll0933<sup>-</sup>* double mutant as well as further studies of the *sll0933<sup>-</sup>* single mutant confirmed the proposed role of the YCF48/Sll0933 complex in conversion from RC to RC47 and subsequently to PSII [1] complexes.

My contribution to this study was the construction of the *ycf48<sup>-</sup>sll0933<sup>-</sup>* double mutant as well as the performance of the yeast split-ubiquitin experiments. Furthermore, measurements of oxygen evolution, absorption spectra and fluorescence spectra were carried out in the laboratory of J. Komenda by J. Knoppová and me. Radioactive labeling of *Synechocystis* 6803 cells was conducted by J. Komenda; J. Knoppová and I performed the protein analyses. The manuscript was written by me and revised by J. Nickelsen and J. Komenda.

# Characterization of a *Synechocystis* double mutant lacking the photosystem II assembly factors YCF48 and Sll0933

Birgit Rengstl · Jana Knoppová ·  
Josef Komenda · Jörg Nickelsen

Received: 24 May 2012 / Accepted: 13 July 2012  
© Springer-Verlag 2012

**Abstract** The de novo assembly of photosystem II (PSII) depends on a variety of assisting factors. We have previously shown that two of them, namely, YCF48 and Sll0933, mutually interact and form a complex (Rengstl et al. in J Biol Chem 286:21944–21951, 2011). To gain further insights into the importance of the YCF48/Sll0933 interaction, an *ycf48<sup>-</sup>sll0933<sup>-</sup>* double mutant was constructed and its phenotype was compared with the single mutants' phenotypes. Analysis of fluorescence spectra and oxygen evolution revealed high-light sensitivity not only for YCF48 deficient strains but also for *sll0933<sup>-</sup>*, which, in addition, showed reduced synthesis and accumulation of newly synthesized CP43 and CP47 proteins in pulse-labeling experiments. In general, the phenotypic characteristics of *ycf48<sup>-</sup>sll0933<sup>-</sup>* were dominated by the effect of the *ycf48* deletion and additional inactivation of the *sll0933* gene showed only negligible additional impairments with

regard to growth, absorption spectra and accumulation of PSII-related proteins and assembly complexes. In yeast split-ubiquitin analyses, the interaction between YCF48 and Sll0933 was confirmed and, furthermore, support for direct binding of Sll0933 to CP43 and CP47 was obtained. Our data provide important new information which further refines our knowledge about the PSII assembly process and role of accessory protein factors within it.

**Keywords** Complex assembly · Cyanobacteria · Photosynthesis · Thylakoid membranes

## Abbreviations

pD1/iD1	Precursor/intermediate form of D1
PDMs	PratA-defined membranes
POR	Protochlorophyllide oxidoreductase
PSI	Photosystem I
PSII	Photosystem II
RC	PSII reaction center complex
RC47	PSII monomer lacking CP43
RCC1	PSII monomer
RCC2	PSII dimer
RCCS1	Supercomplex containing PSII and PSI proteins

A contribution to the Special Issue on Evolution and Biogenesis of Chloroplasts and Mitochondria.

**Electronic supplementary material** The online version of this article (doi:10.1007/s00425-012-1720-0) contains supplementary material, which is available to authorized users.

B. Rengstl · J. Nickelsen (✉)  
Molekulare Pflanzenwissenschaften, Biozentrum LMU  
München, Großhaderner Str. 2–4, 82152 Planegg-Martinsried,  
Germany  
e-mail: joerg.nickelsen@lrz.uni-muenchen.de

J. Knoppová · J. Komenda  
Faculty of Science, University of South Bohemia,  
Branišovská 31, 370 05 České Budějovice, Czech Republic

J. Knoppová · J. Komenda  
Institute of Microbiology, Academy of Sciences,  
Opatovický mlýn, 379 81 Třeboň, Czech Republic

## Introduction

Photosystem II (PSII) is the initial complex in the photosynthetic electron transfer chain, responsible for oxidation of water and generation of molecular oxygen. In its monomeric form, PSII consists of at least 20 protein subunits and a complex set of different cofactors (Umena et al. 2011). The assembly of the whole complex occurs in a stepwise manner: The reaction center proteins pD1 (precursor form of D1 with

a C-terminal extension of 16 amino acids) and D2 are integrated into the membrane and form pre-complexes with PsbI and cytochrome  $b_{559}$  (PsbEF), respectively (Dobáková et al. 2007; Komenda et al. 2008). Both pre-complexes are then assembled to the so-called reaction center (RC) complex. After subsequent addition of the inner antenna proteins CP47 and CP43, together with some smaller subunits, RC47 complexes (reaction center complex containing CP47) and, finally, PSII monomers are formed (Komenda et al. 2012b). During biogenesis of PSII, the C-terminal extension of pD1 is cleaved off by the specific endoprotease CtpA to enable proper assembly of the manganese cluster at the luminal side of PSII (Nixon et al. 1992; Anbudurai et al. 1994; Roose and Pakrasi 2004).

To assure correct assembly of the whole complex, various additional trans-acting factors are assisting the process (Nixon et al. 2010). Among them, in *Synechocystis* sp. PCC 6803 (hereafter *Synechocystis* 6803) YCF48 was suggested to be involved in stabilization of newly synthesized pD1 and its subsequent binding to a D2-cytochrome  $b_{559}$  pre-complex (Komenda et al. 2008). Recently, our co-immunoprecipitation data have suggested that YCF48 forms a complex with another PSII assembly factor, named Sll0933 (Rengstl et al. 2011). In a *sll0933*<sup>-</sup> mutant, RC complexes do not accumulate to detectable levels under steady-state conditions, whereas accumulation of functional PSII complexes is not affected suggesting that Sll0933 is involved in the process of RC47 and PSII core formation (Armbruster et al. 2010).

In this work, we investigated the importance of the YCF48/Sll0933 interaction during PSII assembly. Both proteins are involved in early stages of the PSII assembly process, but seem to act at successive steps. In addition, they do not show identical distribution among cyanobacterial membranes. In *Synechocystis* 6803 a special membrane subfraction can be isolated by sucrose density gradient centrifugation which is characterized by the presence of the PSII assembly factor PratA and therefore was named PDMs (PratA-defined membranes) (Schottkowski et al. 2009a). These PDMs are suggested to represent PSII biogenesis centers which are located at connection sites between plasma membrane and thylakoid membranes (Schottkowski et al. 2009a; Rengstl et al. 2011; Stengel et al. 2012). Whereas YCF48 could be found in PDMs as well as in thylakoid membranes, Sll0933 was detected exclusively in fractions representing thylakoid membranes (Rengstl et al. 2011). This argues for a role of the YCF48/Sll0933 complex at the interface between RC and RC47 complex formation and the movement of PSII assembly complexes from PDMs to thylakoid membranes. Here, we report on the phenotypical effects observed in an *ycf48*<sup>-</sup>*sll0933*<sup>-</sup> double mutant as well as Sll0933 interaction studies using the yeast split-ubiquitin system.

## Materials and methods

### Construction and cultivation of cyanobacterial strains

The strains used in the study were derived from the non-motile, glucose-tolerant strain of *Synechocystis* sp. PCC 6803 (Williams 1988) referred to as the wild type (WT) and obtained from the laboratory of P. J. Nixon. They were grown on an orbital shaker in liquid BG11 medium at 30 °C under continuous irradiation of 40  $\mu\text{mol photons m}^{-2} \text{s}^{-1}$  (normal light) or 300  $\mu\text{mol photons m}^{-2} \text{s}^{-1}$  (high light), respectively (Rippka et al. 1979). For photoheterotrophic growth conditions, the medium was supplemented with 5 mM glucose. Wild-type cells were always grown under the same conditions as the mutant strains.

The *sll0933*<sup>-</sup> (*ins0933*) and *ycf48*<sup>-</sup> mutant strains have been previously described (Komenda et al. 2008; Armbruster et al. 2010). For generation of the *ycf48*<sup>-</sup>*sll0933*<sup>-</sup> double mutant, *ycf48*<sup>-</sup> cells were transformed with the pKS vector containing the *sll0933* gene interrupted by a kanamycin resistance cassette as described in Armbruster et al. (2010). Full segregation of the mutant was confirmed by PCR.

### Measurement of oxygen evolution, absorption spectra and fluorescence spectra

Light-saturated rate of oxygen evolution was measured at 30 °C in BG11 medium containing 10 mM Hepes/NaOH, pH 7.0 in the presence of artificial electron acceptors 2.5 mM *p*-benzoquinone and 1 mM potassium ferricyanide as described (Tichy et al. 2003). Averages  $\pm$  SD of three measurements were calculated.

Whole cell absorption spectra were measured using a Shimadzu UV3000 spectrophotometer in a compartment close to the photomultiplier with a slit width of 2 nm. The suspensions with the same OD<sub>750</sub> were always used for measurement of each strain in the range 350–750 nm.

77 K fluorescence spectra were obtained using an Aminco Bowman Series 2 luminescence spectrometer (Spectronic Unicam). The same number of cells for each strain was excited at 435 nm (bandwidth 4 nm); spectra were recorded in the range 550–800 nm, subsequently corrected for the sensitivity of the photomultiplier and normalized to the emission maxima of Photosystem I at 728 nm.

### Protein analyses

Isolation of whole cell proteins, separation by SDS-PAGE and immunoblot analysis were carried out as described (Schottkowski et al. 2009a, b; Rengstl et al. 2011). Representative results of at least three independent experiments are shown.

For the two-dimensional (2D) analyses of PSII protein accumulation and synthesis, thylakoid membranes were either isolated and separated by 2D blue native/SDS-PAGE (2D-BN/SDS-PAGE) according to Schottkowski et al. (2009a) or, alternatively, a more gentle method for 2D-BN or clear native (CN)/SDS-PAGE described by Komenda et al. (2012a) was employed. To briefly describe the differences between both methods, the former BN-PAGE (Schägger and von Jagow 1991) was performed in 4.5–12 % polyacrylamide (PAA) gel after 30 min solubilization of the thylakoids resuspended in ACA buffer (50 mM Bis-Tris, pH 7.0 containing 750 mM aminocaproic acid and 0.5 mM EDTA) in 1 % n-dodecyl- $\beta$ -D-maltoside (DM). For the latter, more gentle BN-PAGE, thylakoids were resuspended in the milder B-buffer (25 % (v/v) glycerol; 25 mM Mes/NaOH, pH 6.5; 10 mM MgCl<sub>2</sub>; 10 mM CaCl<sub>2</sub>), solubilized with 1 % DM and immediately analyzed by blue-native electrophoresis at 4 °C in a 4–14 % gradient PAA gel according to Schägger and von Jagow (1991). The CN variant of the method was used for analysis of radioactively labeled thylakoids in which Coomassie blue was omitted from all solutions and upper electrophoretic buffer contained 0.05 % sodium deoxycholate and 0.02 % DM (Wittig and Schägger 2008). The single stripes of the mild BN or CN-gel were then incubated for 20 min in 25 mM Tris/HCl, pH 7.5; 1 % SDS; 1 % DTT and placed on top of a 12–20 % SDS-gel. Gels were either stained with Coomassie, dried and exposed to a phosphor-imager plate (GE Healthcare, Vienna, Austria), or stained with Sypro orange and electroblotted onto PVDF membrane for immunodetection,

#### Radioactive labeling of the cells

For pulse labeling experiments, cells were treated as described in Komenda et al. (2008).

#### Yeast split-ubiquitin analysis

To analyze protein interactions, the yeast split-ubiquitin system was utilized (Pasch et al. 2005). For expression as Cub fusion proteins, the *sll0933*, *cp47* (*str0906*) and *cp43* (*sll0851*) genes were amplified by PCR (primer pairs 0933-TMBV-for/0933-TMBV-rev, CP47-TMBV-for/CP47-TMBV-rev and CP43-TMBV-for/CP43-TMBV-rev, respectively; see Supplemental Table S1), subcloned into pJET 1.2 (Fermentas) and inserted into the *XbaI/StuI* restriction sites of the yeast vector pTMBV4 (Dualsystems Biotech AG). In addition, Sll0933 was expressed fused to NubG after amplification using primer pairs 0933-ADSL-Nx-for/0933-ADSL-Nx-rev (Supplemental Table S1), ligation with pJET 1.2 (Fermentas) and cloning into the *BamHI/EcoRI* restriction sites of pADSL-Nx (Dualsystems

Biotech AG). The pADSL vector containing the *ycf48* coding region has already been described (Komenda et al. 2008). As controls, yeast cells were cotransformed with the plasmids pAlg5-NubI (positive control) and pAlg5-NubG (negative control), respectively. In case of protein interaction, transformed DSY-1 cells can grow on plates lacking leucine, tryptophane and histidine. Furthermore, they show activity of  $\beta$ -galactosidase resulting in blue color when grown on plates containing X-Gal (Pasch et al. 2005).

## Results

### Construction and biophysical characterization of *ycf48*<sup>-</sup>*sll0933*<sup>-</sup>

Recently, YCF48 and Sll0933 were shown to form—at least transiently—part of a common complex, since Sll0933 could be immunoprecipitated using an YCF48 antiserum (Rengstl et al. 2011). To investigate the physiological role of the YCF48/Sll0933 complex, we constructed a mutant lacking Sll0933 in the *ycf48*<sup>-</sup> background. Complete segregation of the double mutant was confirmed by PCR (Supplemental Fig. S1). Measurements of optical densities of cultures grown under photoheterotrophic and photoautotrophic conditions revealed slower growth rates for *ycf48*<sup>-</sup>*sll0933*<sup>-</sup> as compared with the wild type, but there was no additional effect when compared with *ycf48*<sup>-</sup> mutant cells (Fig. 1a, b). Also the whole cell absorption spectrum of photoautotrophically grown cells appeared similar to that of the *ycf48*<sup>-</sup> single mutant with an increased absorption at 440–500 nm, i.e., higher amounts of carotenoids and decreased absorption at 680 nm pointing to a reduction of chlorophyll a accumulation (Fig. 1c). Absorption spectra measured after cell growth under high light conditions (300  $\mu\text{mol m}^{-2} \text{s}^{-1}$ ) were analogous (data not shown). However, high light treatment caused a decrease in levels of functional PSII in all mutants. After 3-h exposure to high light, rates of oxygen evolution calculated on a per chlorophyll basis reached only approximately 10–20 % of wild-type levels in *ycf48*<sup>-</sup>*sll0933*<sup>-</sup> and *ycf48*<sup>-</sup> and 50 % in *sll0933*<sup>-</sup>, whereas under normal light conditions, oxygen evolution values were, due to a lower cellular content of chlorophyll, even higher in *ycf48*<sup>-</sup>*sll0933*<sup>-</sup> and *ycf48*<sup>-</sup> than in the wild-type strain (Fig. 1d). In the presence of the protein synthesis inhibitor lincomycin oxygen evolution of wild-type and *sll0933*<sup>-</sup> cells dropped to 20 % and almost 0 % of the initial activity, respectively, after 90 min of illumination and the drop was faster in the *sll0933*<sup>-</sup> strain during the initial 30 min of illumination (data not shown). Similar results had been obtained for the strain lacking YCF48 (Komenda et al. 2008).

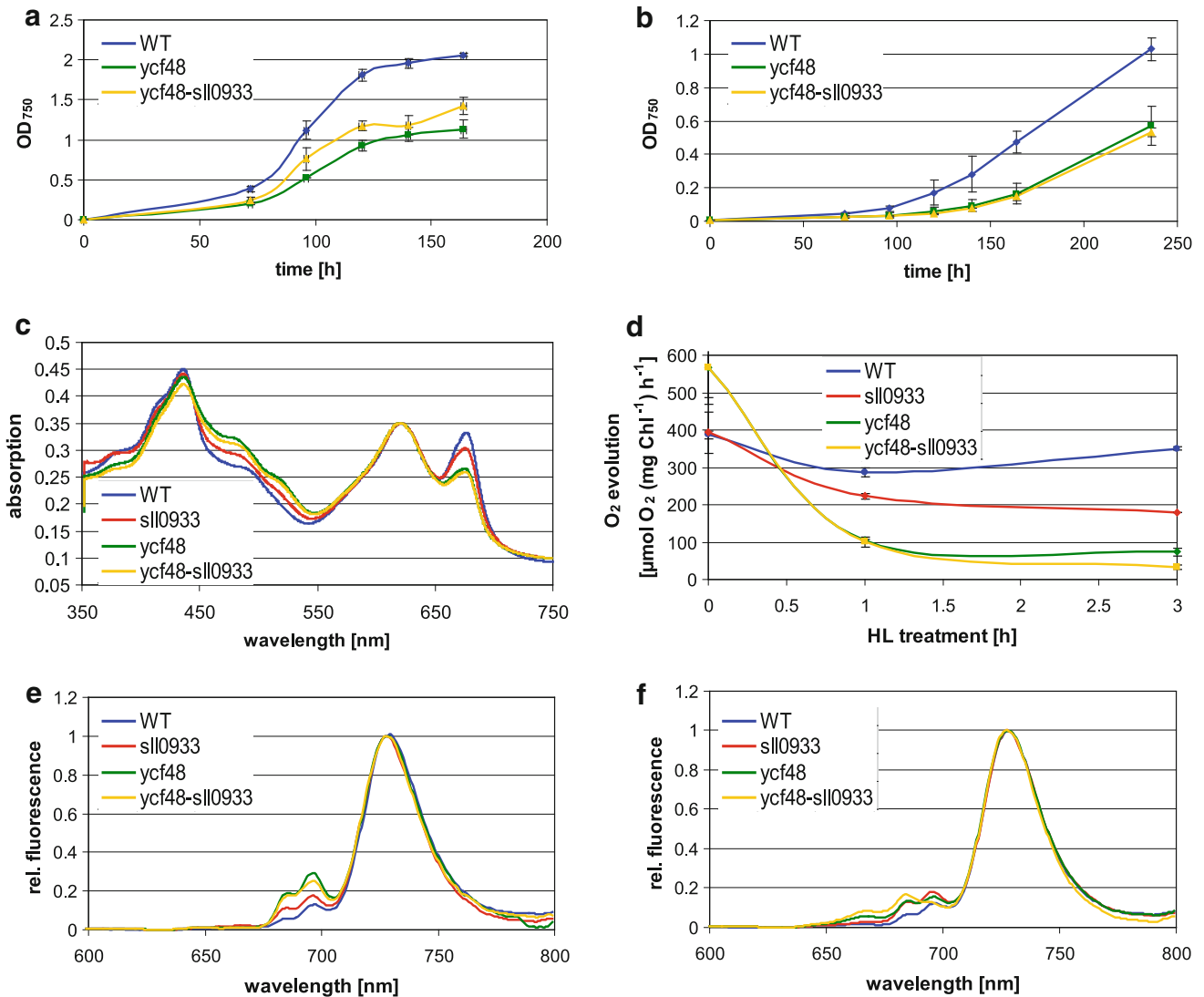


**Fig. 1** Growth curves, absorption/fluorescence spectra and oxygen evolution of *ycf48<sup>-</sup>sll0933<sup>-</sup>* mutant cells. **a, b** Growth of *Synechocystis* 6803 wild type (WT), *ycf48<sup>-</sup>* and *ycf48<sup>-</sup>sll0933<sup>-</sup>* under photoheterotrophic (**a**) and photoautotrophic (**b**) conditions, respectively. Shown are mean values  $\pm$  SD of three independent measurements. **c** Room temperature absorption spectra of photoautotrophically cultivated cells of WT, *sll0933<sup>-</sup>*, *ycf48<sup>-</sup>* and *ycf48<sup>-</sup>sll0933<sup>-</sup>*. Spectra were normalized to their absorption values at 621 nm (phycobilisomes). **d** Effect of high light treatment ( $300 \mu\text{mol m}^{-2} \text{s}^{-1}$ )

on oxygen evolution of the indicated photoautotrophically cultivated strains. Values are averages  $\pm$  SD of three measurements. **e, f** Low-temperature fluorescence emission spectra of whole cells grown photoautotrophically under normal light ( $40 \mu\text{mol m}^{-2} \text{s}^{-1}$ , **e**) and incubated for 3 h at high light ( $300 \mu\text{mol m}^{-2} \text{s}^{-1}$ , **f**) conditions, respectively. Spectra were monitored after excitation of chlorophyll at 435 nm and normalized to the emission maxima at 728 nm

When fluorescence emission spectra were measured at 77 K, all mutants showed a more or less pronounced increase in chlorophyll emission peaks from PSII at 685 and 695 nm reflecting an increased PSII to PSI ratio (Fig. 1e). After incubation of cells in high light, emission at 695 nm arising from photochemically active CP47-containing PSII complexes dropped in *ycf48<sup>-</sup>sll0933<sup>-</sup>* and *ycf48<sup>-</sup>*, again suggesting susceptibility of these mutants to higher irradiances (Fig. 1e, f; Keränen et al. 1999). Altogether, *ycf48<sup>-</sup>sll0933<sup>-</sup>* behaved like the *ycf48<sup>-</sup>* single

mutant with regard to growth, pigment accumulation, oxygen evolution and high light sensitivity.

#### Accumulation of PSII proteins and PSII complex formation in *ycf48<sup>-</sup>sll0933<sup>-</sup>*

Accumulation of PSII proteins was analyzed in cells grown in the presence of glucose. Thus, cells could be harvested after the same time period of growth and results were comparable to the previously reported accumulation of

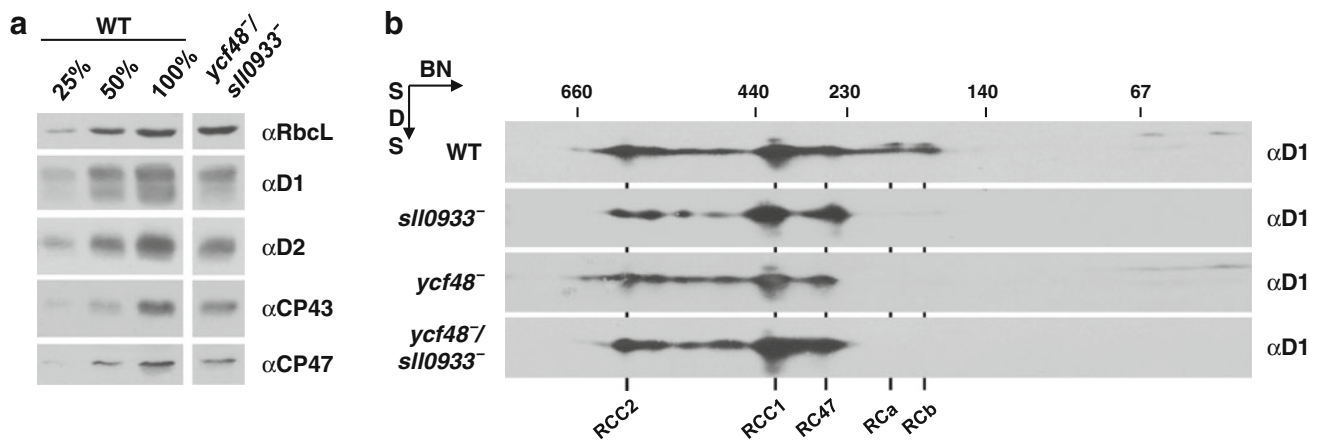


**Fig. 2** Accumulation of PSII proteins and complexes. **a** Accumulation of PSII subunits in *ycf48<sup>-</sup>sll0933<sup>-</sup>*. Whole cell protein extracts of photoheterotrophically grown wild-type and *ycf48<sup>-</sup>sll0933<sup>-</sup>* cells were isolated, separated by SDS-PAGE, blotted onto nitrocellulose and tested with the indicated antibodies. 30 µg protein were loaded for each sample. **b** Two-dimensional BN/SDS-PAGE of membrane extracts from photoheterotrophically grown cells of wild-type (WT), *sll0933<sup>-</sup>*, *ycf48<sup>-</sup>* and *ycf48<sup>-</sup>sll0933<sup>-</sup>* mutants. Membranes were

isolated and analyzed by 2D-BN/SDS-PAGE (Schottkowsky et al. 2009a). After blotting onto nitrocellulose membrane PSII complexes and assembly intermediates were detected using an antiserum raised against D1. Designation of complexes: RCC2, PSII dimer; RCC1, PSII monomer; RC47, PSII monomer lacking CP43; RCa and RCb, reaction center complexes a and b, respectively. 20 µg of chlorophyll were loaded for each sample

PSII-related proteins in the two single mutants (Rengstl et al. 2011). Amounts of the PSII subunits D1, D2, CP43 and CP47 were, unlike as in *sll0933<sup>-</sup>*, reduced in the double mutant, which is consistent with the reported 30–50 % decrease in the PSII level in *ycf48<sup>-</sup>* (Fig. 2a; Komenda et al. 2008; Armbruster et al. 2010). To investigate effects of *ycf48* and *sll0933* double deletion on other PSII assembly factors, the amounts of PrtA (Klinkert et al. 2004), Slr1471 (Ossenbühl et al. 2006), Pitt (Schottkowsky et al. 2009b) and the protochlorophyllide oxidoreductase (POR) (Schoefs and Franck 2003) were assessed in the single and double mutants using Western blot. Only the level of POR was significantly decreased in the double mutant, whereas PrtA, Slr1471 and Pitt accumulated to wild-type levels (Table 1). This pattern, again, resembled the characteristics of the *ycf48<sup>-</sup>* single mutant (Rengstl et al. 2011). Interestingly, for the *sll0933<sup>-</sup>* single mutant, a 1.8-fold increase in Pitt accumulation had been observed (Rengstl et al. 2011), whereas this effect did not appear in *ycf48<sup>-</sup>sll0933<sup>-</sup>*. Thus, the phenotype of *ycf48<sup>-</sup>sll0933<sup>-</sup>* was dominated by the *ycf48* mutation.

Since both proteins, YCF48 and Sll0933, are involved in PSII assembly, we further examined the accumulation of PSII assembly complexes in photoheterotrophically grown cells by 2D-BN/SDS-PAGE. In wild-type cells, five different PSII complexes could be assigned: dimeric and monomeric PSII (RCC2 and RCC1, respectively), the RC47 complex as well as two RC complexes which still contain incompletely processed D1 (Fig. 2b; Komenda et al. 2004). These RC complexes accumulated neither in *sll0933<sup>-</sup>*, nor in *ycf48<sup>-</sup>* and accordingly, were not

detectable in *ycf48<sup>-</sup>sll0933<sup>-</sup>* under these conditions (Fig. 2b; Komenda et al. 2008; Armbruster et al. 2010).

The observed absence of the RC complexes in the *sll0933<sup>-</sup>* mutant was in agreement with previous studies of Armbruster et al. (2010) but contrasted with the phenotype of the *Arabidopsis thaliana pam68* mutant in which RC complexes overaccumulated but the assembly of larger PSII complexes was delayed. In the attempt to reconcile this discrepancy we also analyzed cells of wild-type and the *sll0933<sup>-</sup>* mutant using a modified, more gentle method of membrane preparation, solubilization and native electrophoresis recently described by Komenda et al. (2012a). In addition, we also compared cells grown under photoautotrophic and photoheterotrophic conditions to see whether the presence of glucose could also contribute to the observed discrepancy between *A. thaliana* and *Synechocystis* 6803 mutant analyses (previous analyses of the *Synechocystis* 6803 *sll0933<sup>-</sup>* mutant were performed using cultures grown in the presence of glucose). Surprisingly, the gentler 2D-BN/SDS-PAGE of thylakoids from photoautotrophically grown cells showed differences between the wild-type and the *sll0933<sup>-</sup>* mutant strains which were in agreement with differences seen in *A. thaliana*. Namely, the mutant strain accumulated significantly more RC complexes, in this case the RCa and larger RC\*, as revealed by immunodetection of the D1 protein (Fig. 3a, D1 blot, arrow) and especially of the YCF48 factor, which is the component of both these RC complexes (Komenda et al. 2008). In contrast, the PSII antenna complex CP47 was missing both in the unassembled protein fraction and in the supercomplex RCCS1 which seems to be also

**Table 1** Accumulation of PSII assembly factors in *ycf48<sup>-</sup> sll0933<sup>-</sup>*

	<i>sll0933<sup>-</sup>*</i>	<i>ycf48<sup>-</sup>*</i>	<i>ycf48<sup>-</sup> sll0933<sup>-</sup></i>
PratA	105 ± 22	108 ± 33	111 ± 14
Slr1471	105 ± 10	106 ± 21	110 ± 13
Pitt	178 ± 32	103 ± 21	78 ± 38
POR	104 ± 20	52 ± 16	57 ± 19

Whole cell proteins of photoheterotrophically grown cultures were separated and immunologically detected as in Fig. 2a

Amounts of proteins were calculated in percentage of wild-type levels; values are mean ± SD of three independent experiments

\* From (Rengstl et al. 2011)

involved in PSII biogenesis (Komenda et al. 2012a). The amount of unassembled CP43, especially the smaller of the two resolved complexes (Fig. 3a, Blots, CP43b) that lacks bound PSII small subunits and reflects accumulation of the newly synthesized CP43 (Komenda et al. 2004, 2012a), was also diminished. The differences between strains grown in the presence of glucose were qualitatively similar, but much less pronounced (Fig. 3b). Thus, the new, milder 2D analysis of the *sll0933<sup>-</sup>* mutant supported the role of Sll0933 in the assembly of larger size PSII complexes.

To further support the previous conclusions concerning the role of Sll0933 in the synthesis of CP47 and CP43, we also followed the incorporation of newly synthesized proteins during pulse labeling of the cells of all four studied strains. For this analysis, we used mild, in this case 2D-CN/SDS-PAGE and photoautotrophically grown cells, since under these conditions mutations revealed more pronounced effects (Fig. 4). In agreement with immunodetection in Fig. 3 the radioactive signal corresponding to the iD1 protein in RCa and RC\* complexes was stronger in the *sll0933<sup>-</sup>* mutant as compared with the wild type while less radioactivity was incorporated into CP43 and CP47 (Fig. 4, marked by stars) resulting in reduced accumulation of PSII monomers (Figs. 3, 4). In the double mutant, the pattern of radioactivity resembled that of the *ycf48<sup>-</sup>* single mutant's phenotype with additionally reduced CP43 and CP47 signals (Fig. 4; Komenda et al. 2008). Therefore, protein labeling characteristics of the *ycf48<sup>-</sup> sll0933<sup>-</sup>* mutant represent a combination of those observed in both the *ycf48<sup>-</sup>* and *sll0933<sup>-</sup>* single mutants.

Yeast split-ubiquitin interaction studies

In addition to the phenotypical characterization of the *ycf48<sup>-</sup> sll0933<sup>-</sup>* double mutant, we also examined interaction of YCF48 and Sll0933 using the yeast split-ubiquitin system. Therefore, Sll0933 and YCF48 were expressed as NubG and/or Cub fusion proteins in yeast cells. Only in case of direct protein-protein interaction, NubG and Cub

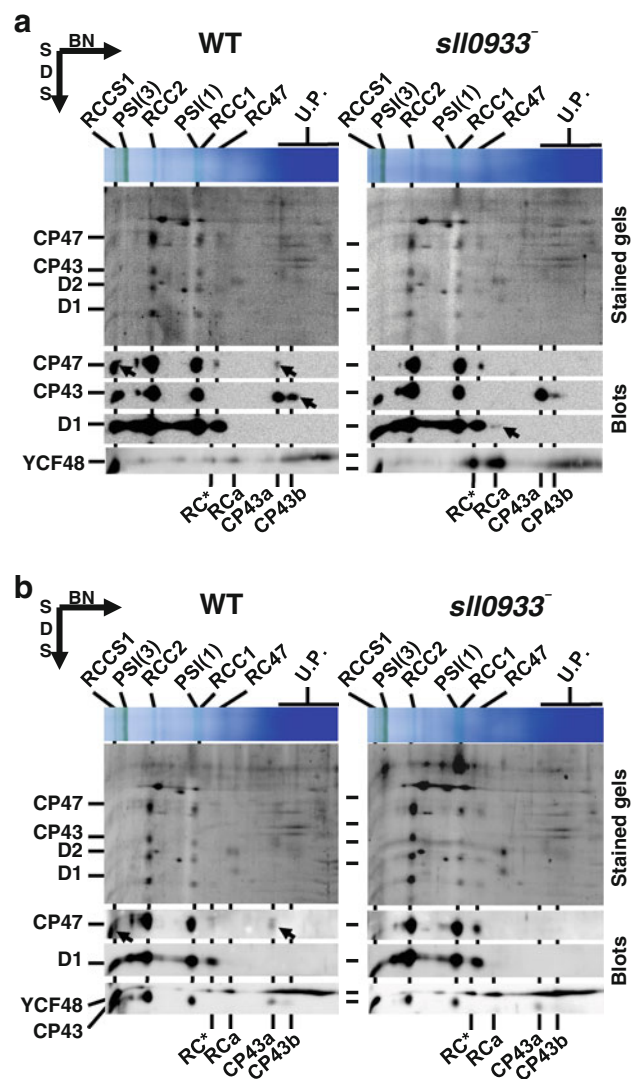


**Fig. 3** Two-dimensional mild BN/SDS-PAGE of membrane proteins from photoautotrophically (a) and photoheterotrophically (b) grown cells of wild type (WT) and *sll0933<sup>-</sup>*. Membranes were analyzed by mild 2D-BN/SDS-PAGE (Komenda et al. 2012a). Gels were stained by Sypro orange (stained gels) and electroblotted to PVDF membrane which was sequentially probed with antibodies against D1, CP43, CP47 and YCF48 (blots). Designations: RCCS1, a supercomplex containing PSII and PSI proteins; PSI(1) and PSI(3), monomeric and trimeric form of PSI; RC\*, the largest form of the RC complex, CP43a and CP43b; two forms of the CP43 subcomplex; arrows designate CP47 in the supercomplex and in the unassembled fraction and increased level of CP43b in WT, and increased level of RCa detected by anti-D1 antibody in the mutant; for other designations of complexes see Fig. 2b; U.P. unbound proteins. 2 µg of chlorophyll was loaded for each sample

are in sufficiently close proximity to allow reconstitution of split-ubiquitin thereby enabling these cells to grow on plates lacking histidine and to show β-galactosidase activity. This was the case when Sll0933-Cub and Nub-YCF48 were coexpressed in yeast DSY-1 cells (Fig. 5).

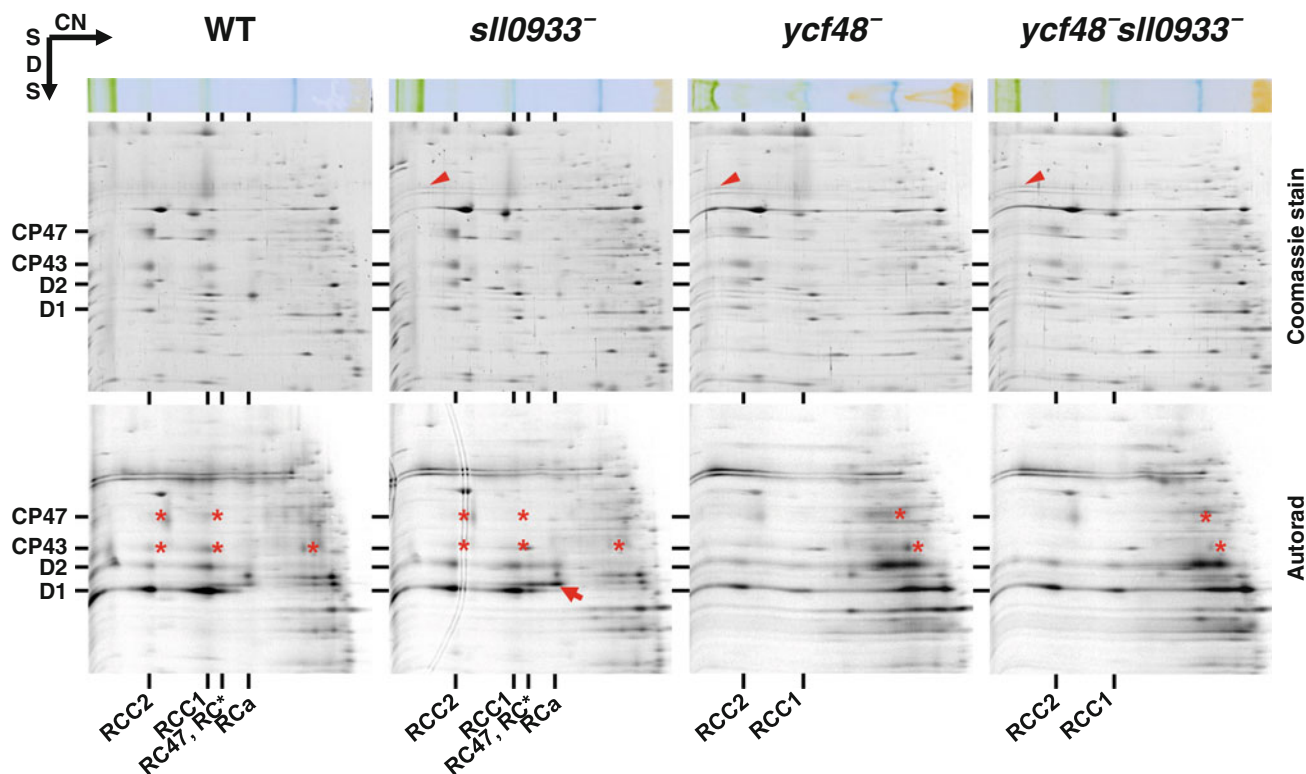


**Fig. 4** Two-dimensional CN/SDS-PAGE of radioactively labeled membrane proteins from photoautotrophically grown cells of wild type (WT), *slI0933*<sup>-</sup>, *ycf48*<sup>-</sup> and *ycf48*<sup>-</sup>*slI0933*<sup>-</sup>. Cells were radiolabeled for 20 min at 500 μmol photons m<sup>-2</sup> s<sup>-1</sup> with a mixture of (<sup>35</sup>S)Met/Cys. Labeled cells were used for thylakoid membrane isolation and proteins were separated by 2D-CN/SDS-PAGE (Komenda et al. 2012a). Upper panels show Coomassie-stained gels (Coomassie stain) and lower panels show autoradiograms (Autorad).

Arrowheads in the upper panels designate an increased level of FtsH2/FtsH3 complexes in the mutants (Zhang et al. 2007). In the lower panels asterisks mark CP47 and CP43 signals which were reduced in *slI0933*<sup>-</sup> and *ycf48*<sup>-</sup>*slI0933*<sup>-</sup>; the increased amount of RC complexes in *slI0933*<sup>-</sup> is indicated by an arrow. 5 μg of chlorophyll were loaded for each sample. For designation of complexes see Fig. 2b

Autoactivation of SII0933–Cub could be excluded since cotransformation with pAlg5–NubG (encoding the endoplasmic reticulum membrane protein Alg5 fused to NubG) did neither result in growth on histidine deficient plates nor in β-galactosidase activity (Fig. 5). Furthermore, expression of SII0933 as Cub- as well as Nub-fusion protein in the same yeast cells revealed the ability of SII0933 to form homodimers/oligomers (Fig. 5).

Previously, a strong relationship between SII0933 and CP47 was suggested based on high reduction of the SII0933 level in a CP47-less strain (Rengstl et al. 2011). This suggestion was supported by a decreased synthesis of CP47 as well as CP43 in *slI0933*<sup>-</sup> as revealed by radioactive labeling (Fig. 4). Therefore, we also tested SII0933 for interaction with these two PSII inner antenna proteins. Indeed, at least in the yeast system, SII0933 was found to directly interact with CP43 and CP47 (Fig. 5). These data were in agreement with results obtained using the split-ubiquitin assay for the SII0933 homolog in *A. thaliana*, PAM68, which has also been shown to interact amongst

others with HCF136 (*A. thaliana* homolog of YCF48), CP43 and CP47 (Armbruster et al. 2010).

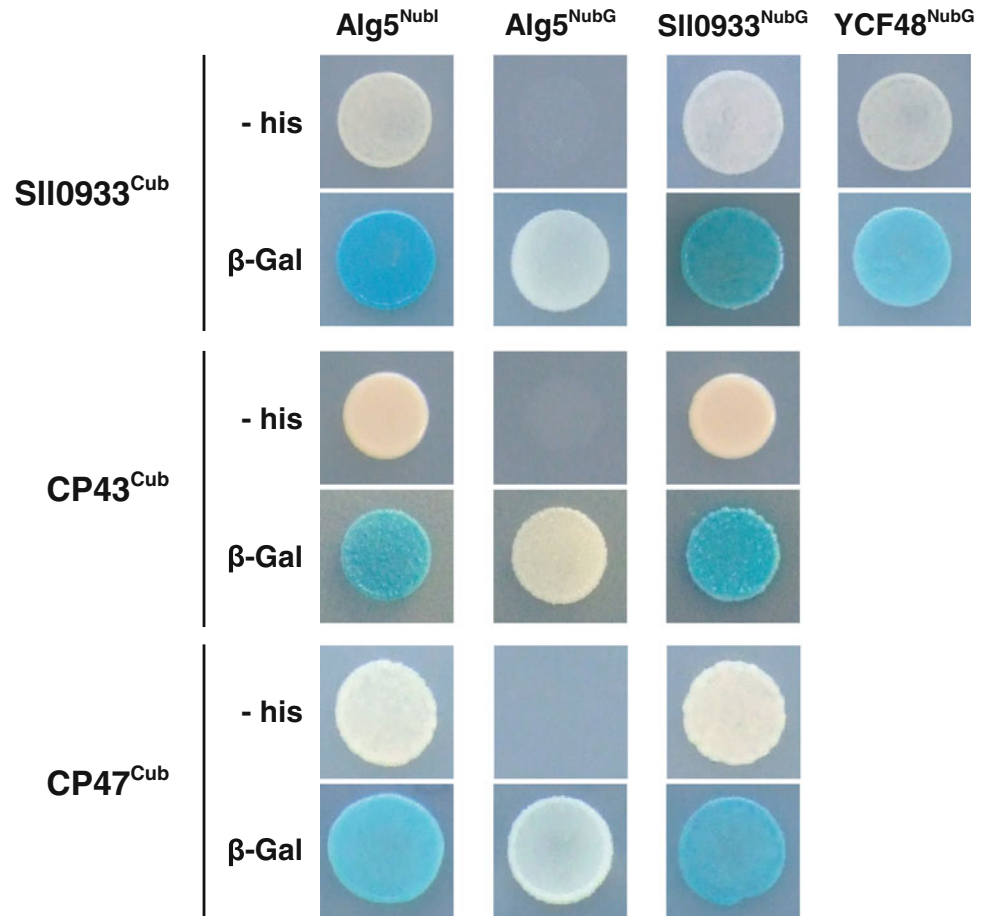
### Discussion

#### Phenotypical characterization of *ycf48*<sup>-</sup>*slI0933*<sup>-</sup>

The biogenesis of PSII is a well-organized process requiring a number of accessory protein factors which bind transiently to certain PSII subunits and/or assembly intermediate complexes and mediate distinct assembly steps (Nixon et al. 2010; Komenda et al. 2012b). However, assembly factors do not only act separately during PSII biogenesis, but they are also part of a complex regulatory network and interfere with each other (Rengstl et al. 2011).

To elucidate the role of the previously described YCF48/SII0933 complex during PSII biogenesis, we constructed and characterized an *ycf48*<sup>-</sup>*slI0933*<sup>-</sup> double mutant. Analysis of growth, pigment content, high light

**Fig. 5** Analysis of protein–protein interactions in the yeast split-ubiquitin system. Growth and  $\beta$ -galactosidase activity of yeast cells expressing different combinations of Cub and NubG fusion proteins. Yeast cells were spotted onto plates lacking leucine, tryptophane and histidine (–his). For the  $\beta$ -galactosidase assay, cells were dropped onto medium lacking leucine and tryptophane but containing X-Gal (X-Gal).  $\text{Alg5}^{\text{NubI}}$  served as positive,  $\text{Alg5}^{\text{NubG}}$  served as negative control



susceptibility and PSII protein accumulation revealed that  $\text{ycf48}^- \text{sll0933}^-$  behaves like the  $\text{ycf48}^-$  single mutant (Figs. 1, 2). At first view, 77 K measurements (Fig. 1e) seem to be in contrast with PSII protein accumulation data (Fig. 2a) since they show an increased PSII/PSI ratio which also goes together with higher oxygen evolution in YCF48 lacking cells measured on a per chlorophyll basis (Fig. 1d). However, Western blot analyses which are based on the same amount of protein revealed a clear decrease in the level of PSII proteins. It has to be considered that the overall chlorophyll content is lowered in  $\text{ycf48}^-$  cells. This preferentially affects the antenna of PSI resulting in this case in an apparent higher relative PSII/PSI ratio in low-temperature fluorescence experiments although accumulation of PSII is reduced.

Interestingly, accumulation of Pitt, an interaction partner of the chlorophyll synthesis enzyme protochlorophyllide oxidoreductase, had been shown to be increased in  $\text{sll0933}^-$ , whereas in  $\text{ycf48}^- \text{sll0933}^-$  cells wild-type levels of this factor were observed (Schottkowski et al. 2009b; Rengstl et al. 2011). Thus, the phenotype caused by the  $\text{ycf48}$  mutation seems to dominate in  $\text{ycf48}^- \text{sll0933}^-$ . This indicates that YCF48 acts upstream of SII0933 during PSII biogenesis, which is in agreement with the suggested

functions of YCF48 and SII0933 in stabilization of newly synthesized pD1 and formation of RC47 complexes, respectively (Komenda et al. 2008; Armbruster et al. 2010). This goes together with the fact that YCF48 is also present in PDMs pointing to a role in early steps of PSII assembly (Rengstl et al. 2011). SII0933, however, was only detected in thylakoid membranes, again suggesting a role in PSII assembly more downstream of YCF48-mediated steps (Rengstl et al. 2011).

#### Involvement of SII0933 in the de novo assembly of PSII

In addition to the described phenotype of the  $\text{sll0933}^-$  mutant in Armbruster et al. (2010), we newly demonstrated an increased reduction of oxygen evolution after high light treatment in the  $\text{sll0933}^-$  strain compared with the wild-type one. Furthermore, 2D protein analysis using a more gentle method (Komenda et al. 2012a) in combination with Western blotting and radioactive pulse labeling indicated an increased accumulation of newly synthesized RC complexes in  $\text{sll0933}^-$  (Figs. 3, 4). This is in agreement with results from an *A. thaliana* mutant lacking the homolog of SII0933, PAM68, which showed a sixfold increase in newly synthesized RC complexes (Armbruster et al. 2010).

The increased level of RC complexes in the *sll0933*<sup>-</sup> mutant was accompanied by a decrease in de novo synthesis of CP47 and CP43 and retardation of PSII monomer formation which is also seen in the *ycf48*<sup>-</sup> mutant after additional loss of Sll0933 (Fig. 4). All these results can be explained by the insufficient availability of newly synthesized CP47 and CP43 which leads to the slower de novo assembly of PSII. The increased susceptibility of the *sll0933*<sup>-</sup> strain to photoinhibition therefore documents that not only the efficient repair but also the fast de novo assembly of PSII is essential for cyanobacteria to successfully cope with high irradiance. Since the synthesis and accumulation of the D1 protein is required for both the PSII repair and PSII de novo assembly, the extreme sensitivity to photoinhibition observed in the single *ycf48*<sup>-</sup> and in the *ycf48*<sup>-</sup>*sll0933*<sup>-</sup> double mutant might be ascribed to the deficiency in both these processes.

A closer inspection of the new gentle 2D protein analyses also revealed an increased abundance of the FtsH2/FtsH3 complex in all three tested mutants in comparison with the wild type (Fig. 4, arrowheads). Since this complex is implicated in removal of incorrectly assembled or unassembled PSII proteins (Komenda et al. 2012b) it could be responsible for the absence of RC assembly complexes in the membranes of the *sll0933*<sup>-</sup> strain when they were assessed by less gentle 2D analysis (Armbruster et al. 2010 and Fig. 2). FtsH-mediated degradation during long solubilization and long-running native PAGE could therefore explain the apparent discrepancy between older and newer 2D analyses.

#### Protein interaction studies

Protein interaction studies using the yeast split-ubiquitin system revealed the ability of Sll0933 to directly interact with YCF48 as well as with CP43 and CP47 enforcing the idea of Sll0933 functioning during PSII inner antenna synthesis/assembly as discussed before (Rengstl et al. 2011). Since YCF48 was shown to be part of and to mediate an earlier assembly step, i.e., formation of RC complexes, YCF48/Sll0933 complexes probably play a role at the later conversion steps from RC to RC47 and the core complexes. In agreement with the proposed successive mode of action of YCF48 and Sll0933 during PSII assembly it is conceivable that the phenotype of the *ycf48*<sup>-</sup>*sll0933*<sup>-</sup> double mutant is similar to that of the *ycf48*<sup>-</sup> single mutant without any pronounced additional effect of the *sll0933* inactivation. The almost complete absence of radioactively labeled bands of unassembled CP43 and CP47 argues for a direct requirement of Sll0933 for CP47 and CP43 synthesis. The protein could bind to CP43 and CP47 nascent chains and stabilize them until the whole proteins are synthesized. Affinity of Sll0933 to

YCF48 bound to RC complexes may then facilitate quick assembly of CP47 and CP43 and formation of the PSII core complex. Less probably, Sll0933 may stabilize just the complete, newly synthesized CP47 and CP43 and without it these proteins are quickly recognized by proteases and removed. Clearly, further study of the Sll0933 protein and its interaction with other PSII assembly factors is required to elucidate the mechanism of its action.

**Acknowledgments** We thank Jürgen Soll (Plant Biochemistry, Department of Biology I, Botany, Ludwig-Maximilians University, Germany) for providing the anti-Slr1471 and anti-POR antibodies and Peter Nixon (Division of Molecular Biosciences, Wolfson Biochemistry Building, Imperial College London, UK) for the *ycf48*<sup>-</sup> strain and the anti-YCF48 antibody. This work was supported by the Deutsche Forschungsgemeinschaft SFB-TR1/C10, the Graduate School Life Science Munich and by projects Algatech (CZ.1.05/2.1.00/03.0110), RVO61388971 and P501/12/G055 of the Grant Agency of the Czech Republic.

#### References

- Anbudurai PR, Mor TS, Ohad I, Shestakov SV, Pakrasi HB (1994) The *ctpA* gene encodes the C-terminal processing protease for the D1 protein of the photosystem II reaction center complex. *Proc Natl Acad Sci USA* 91:8082–8086
- Armbruster U, Zühlke J, Rengstl B, Kreller R, Makarenko E, Rühle T, Schünemann D, Jahns P, Weisshaar B, Nickelsen J, Leister D (2010) The *Arabidopsis* thylakoid protein PAM68 is required for efficient D1 biogenesis and photosystem II assembly. *Plant Cell* 22:3439–3460
- Dobáková M, Tichy M, Komenda J (2007) Role of the PsbI protein in photosystem II assembly and repair in the cyanobacterium *Synechocystis* sp. PCC 6803. *Plant Physiol* 145:1681–1691
- Keränen M, Aro E-M, Tyystjärvi E (1999) Excitation-emission map as a tool in studies of photosynthetic pigment-protein complexes. *Photosynthetica* 37:225–237
- Klinkert B, Ossenbühl F, Sikorski M, Berry S, Eichacker L, Nickelsen J (2004) PrataA, a periplasmic tetratricopeptide repeat protein involved in biogenesis of photosystem II in *Synechocystis* sp. PCC 6803. *J Biol Chem* 279:44639–44644
- Komenda J, Reisinger V, Müller BC, Dobáková M, Granvogl B, Eichacker LA (2004) Accumulation of the D2 protein is a key regulatory step for assembly of the photosystem II reaction center complex in *Synechocystis* PCC 6803. *J Biol Chem* 279:48620–48629
- Komenda J, Nickelsen J, Tichy M, Prasil O, Eichacker LA, Nixon PJ (2008) The cyanobacterial homologue of HCF136/YCF48 is a component of an early photosystem II assembly complex and is important for both the efficient assembly and repair of photosystem II in *Synechocystis* sp. PCC 6803. *J Biol Chem* 283:22390–22399
- Komenda J, Knoppova J, Kopečna J, Sobotka R, Halada P, Yu J, Nickelsen J, Boehm M, Nixon PJ (2012a) The Psb27 assembly factor binds to the CP43 complex of photosystem II in the cyanobacterium *Synechocystis* sp. PCC 6803. *Plant Physiol* 158:476–486
- Komenda J, Sobotka R, Nixon PJ (2012b) Assembling and maintaining the Photosystem II complex in chloroplasts and cyanobacteria. *Curr Opin Plant Biol* 15:245–251
- Nixon PJ, Trost JT, Diner BA (1992) Role of the carboxy terminus of polypeptide D1 in the assembly of a functional water-oxidizing

- manganese cluster in photosystem II of the cyanobacterium *Synechocystis* sp. PCC 6803: assembly requires a free carboxyl group at C-terminal position 344. *Biochemistry* 31:10859–10871
- Nixon PJ, Michoux F, Yu J, Boehm M, Komenda J (2010) Recent advances in understanding the assembly and repair of photosystem II. *Ann Bot* 106:1–16
- Ossenbühl F, Inaba-Sulpice M, Meurer J, Soll J, Eichacker LA (2006) The *Synechocystis* sp PCC 6803 Oxa1 homolog is essential for membrane integration of reaction center precursor protein pD1. *Plant Cell* 18:2236–2246
- Pasch J, Nickelsen J, Schünemann D (2005) The yeast split-ubiquitin system to study chloroplast membrane protein interactions. *Appl Microbiol Biotechnol* 69:440–447
- Rengstl B, Oster U, Stengel A, Nickelsen J (2011) An intermediate membrane subfraction in cyanobacteria is involved in an assembly network for photosystem II biogenesis. *J Biol Chem* 286:21944–21951
- Rippka R, Deruelles J, Waterbury JB, Herdman M, Stanier RY (1979) Generic assignments, strain histories and properties of pure cultures of cyanobacteria. *J Gen Microbiol* 111:1–61
- Roose JL, Pakrasi HB (2004) Evidence that D1 processing is required for manganese binding and extrinsic protein assembly into photosystem II. *J Biol Chem* 279:45417–45422
- Schägger H, von Jagow G (1991) Blue native electrophoresis for isolation of membrane protein complexes in enzymatically active form. *Anal Biochem* 199:223–231
- Schoefs B, Franck F (2003) Protochlorophyllide reduction: mechanisms and evolutions. *Photochem Photobiol* 78:543–557
- Schottkowski M, Gkalympoudis S, Tzekova N, Stelljes C, Schünemann D, Ankele E, Nickelsen J (2009a) Interaction of the periplasmic PrtA factor and the PsbA (D1) protein during biogenesis of photosystem II in *Synechocystis* sp. PCC 6803. *J Biol Chem* 284:1813–1819
- Schottkowski M, Ratke J, Oster U, Nowaczyk M, Nickelsen J (2009b) Pitt, a novel tetratricopeptide repeat protein involved in light-dependent chlorophyll biosynthesis and thylakoid membrane biogenesis in *Synechocystis* sp. PCC 6803. *Mol Plant* 2:1289–1297
- Stengel A, Gügel IL, Hilger D, Rengstl B, Jung H, Nickelsen J (2012) Initial steps of photosystem II de novo assembly and preloading with manganese take place in biogenesis centers in *Synechocystis*. *Plant Cell* 24:660–675
- Tichy M, Lupinkova L, Sicora C, Vass I, Kuvikova S, Prasil O, Komenda J (2003) *Synechocystis* 6803 mutants expressing distinct forms of the Photosystem II D1 protein from *Synechococcus* 7942: relationship between the *psbA* coding region and sensitivity to visible and UV-B radiation. *Biochim Biophys Acta* 1605:55–66
- Umena Y, Kawakami K, Shen JR, Kamiya N (2011) Crystal structure of oxygen-evolving photosystem II at a resolution of 1.9 Å. *Nature* 473:55–60
- Williams JGK (1988) Construction of specific mutations in photosystem II photosynthetic reaction center by genetic engineering methods in *Synechocystis* 6803. *Methods Enzymol* 167:766–778
- Wittig I, Schägger H (2008) Features and applications of blue-native and clear-native electrophoresis. *Proteomics* 8:3974–3990
- Zhang P, Sicora CI, Vorontsova N, Allahverdiyeva Y, Battchikova N, Nixon PJ, Aro EM (2007) FtsH protease is required for induction of inorganic carbon acquisition complexes in *Synechocystis* sp. PCC 6803. *Mol Microbiol* 65:728–740

## 4 DISCUSSION

### 4.1 ROLE OF PRATA-DEFINED MEMBRANES IN ASSEMBLY OF PHOTOSYNTHETIC COMPLEXES

Oxygenic cyanobacteria like *Synechocystis* 6803 possess three different types of membranes, the outer membrane (OM) and the plasma membrane (PM) that encircle the cell, and the internal thylakoid membrane system (TM) that comprises the photosynthetic machineries. Additionally, in 2009, a specific membrane subfraction was isolated that seems to be in close proximity to the TM system, but possesses a distinct density and protein composition. It was defined and characterized by the presence of the PSII assembly factor PrataA and hence named PDMs (PrataA-defined membranes; Schottkowski et al., 2009b). The focus of the present work was the characterization of PDMs in more detail, taking into account various aspects such as their function in assembly of the photosynthetic complexes, their role in synthesis of pigments, as well as their participation in the insertion of cofactors.

#### 4.1.1 Involvement of PDMs in assembly of PSII

As considerable amounts of pD1 were – besides PrataA – additionally detected in the PDM subfraction, it was suggested to be involved in early steps of PSII biogenesis (Schottkowski et al., 2009b). The present study aimed at describing the role of PDMs in more detail by subjecting them to further analyses with regard to their protein, lipid and pigment content. The proposed function in initial PSII biogenesis steps was supported by the detection of not only PrataA, but also substantial amounts of other PSII assembly factors, namely Slr1471 and YCF48, in PDMs (see Figure 2A in section 3.2). Similar to PrataA, both proteins have been shown to be able to interact with D1 and to be involved in early assembly steps, i.e. membrane integration and insertion of D1 into RC complexes (Ossenbühl et al., 2006; Komenda et al., 2008). Interestingly, in a *prataA*<sup>-</sup> mutant, all PSII assembly factors investigated displayed an altered distribution with a more pronounced occurrence in PDM-corresponding fractions underlining a basic function of PrataA in membrane organization in *Synechocystis* 6803 (see Figure 2A, B in section 3.2).

The presence of different domains within one membrane system of *Synechocystis* 6803 was also proposed by other studies: Proteome analyses of *Synechocystis* 6803 revealed that the TM system is not homogeneous, but displays different functional compartments (Agarwal et al., 2010; Agarwal et al., 2012). Similarly, also distinct PM sub-fractions were identified, namely the so-called RSO (right-side-out) and ISO (insight-out) vesicles that possess varying

protein compositions. Photosynthesis-associated proteins were found to accumulate in ISO, hence they were hypothesized to represent the PM membrane regions involved in biogenesis of photosynthetic complexes, similar to the in the present study suggested function of PDMs (Zak et al., 2001; Srivastava et al., 2006).

A spatial separation between PSII biogenesis and the site of its function seems to be already realized in the primordial cyanobacterium *Gloeobacter violaceus*. This species is the only known exception within the cyanobacterial group as it does not contain a TM system and thus harbors the photosynthetic complexes in its PM (Rippka et al., 1974). However, photosynthetic and respiratory complexes are not distributed equally all over the membrane, but rather seem to be concentrated in special bioenergetic domains, which were shown to have a diameter of approx. 140 nm and, in sum, account for ~6% of the total membrane area (Rexroth et al., 2011). These bioenergetically active, chlorophyll containing membrane regions can be separated from the remaining PM by biochemical means and were suggested to represent the starting point for the development of TMs during evolution (Rexroth et al., 2011). Interestingly, a protein homologous to PratA was found to be exclusively located in the photosynthetically non-active membrane fraction arguing for the occurrence of PSII assembly initiation in these domains. Thus, organization of PSII dynamics in different membrane regions probably is conserved throughout the whole cyanobacterial group.

#### **4.1.2 Coordination of protein and pigment synthesis/assembly in PDMs**

Analysis of lipid composition in TMs and PDMs indicated no major differences (see section 3.2). This is not surprising since lipid composition of PM and TM systems in cyanobacteria has been described to be very similar as well (Gombos et al., 1996). However, investigation of pigment distribution throughout PDM and TM fractions revealed a specific accumulation of the chlorophyll *a* precursor chlorophyllide *a* in the more dense PDM fractions (see Figure 1 in section 3.2). This strongly indicates a role of PDMs not only in assembly of PSII protein subunits but also in pigment synthesis and probably their insertion into apoproteins, as it has already been suggested based on detection of Pitt and POR in PDMs (Schottkowski et al., 2009a). These data support earlier studies examining the distribution of chlorophyll and its precursor molecules in cyanobacteria, exhibiting accumulation of chlorophyll *a* in TMs and chlorophyllide *a* in the PM (Peschek et al., 1989). Separation of membranes from *Synechocystis* 6803 by this group resulted in partitioning into even four different membrane subfractions, of which two were assigned as PM, one as TM and the fourth one displayed an intermediate character and contained protochlorophyllide *a*

and chlorophyllide *a*, similar to PDMs (Hinterstoisser et al., 1993). At that time, this intermediate membrane fraction was hypothesized to represent the earlier described TCs (Kunkel, 1982; Hinterstoisser et al., 1993).

Whether accumulation of chlorophyllide *a* in PDMs is the result of a higher production rate, or whether its processing to chlorophyll *a* is retarded compared to TMs is not unambiguously answered to date. Whereas in higher plants the chlorophyll synthase enzyme converting chlorophyllide *a* into chlorophyll *a* has been exclusively detected in TMs (Soll et al., 1983; Eckhardt et al., 2004), chlorophyll synthase activity measurements in *Synechocystis* 6803 suggested its presence in TMs as well as TCs/PDMs (Hinterstoisser et al., 1993). This would argue for a higher production rate of chlorophyllide *a* in PDMs compared to TMs, although on the other hand this appears unlikely since the chlorophyllide *a* producing enzyme POR was predominantly located in TM fractions (Schottkowski et al., 2009a). Nevertheless, it has to be considered that the *Synechocystis* 6803 genome encodes a second, light-independent protochlorophyllide oxidoreductase (LiPOR), of which the cellular localization remains to be investigated (Armstrong, 1998). Due to unspecific binding of an antibody raised against the ChlL subunit of LiPOR, the results regarding its subcellular localization in PDMs and/or TMs were not conclusive. However, chlorophyllide *a* accumulation was strongly decreased in PDM fractions of a *pitt*<sup>-</sup> mutant (see Figure 1C in section 3.2). Since absence of Pitt causes reduced levels of POR, it can be concluded that the chlorophyllide *a* molecules in PDM fractions result from activity of the POR rather than the LiPOR enzyme. Furthermore, recent studies with mutants lacking POR or LiPOR indicated that the POR enzyme is responsible for synthesis of the majority of chlorophyll molecules, even under low light conditions (Kopečná et al., 2012a). To further address the origin of chlorophyllide *a* in PDMs, examination of its accumulation in cells lacking functional LiPOR could shed more light on the origin of the PDM localized chlorophyllide *a* molecules.

The fact that the assembly of PSII is tightly coordinated with pigment synthesis and insertion has become more and more apparent during the last years, supported e.g. by characterization of formerly unknown assembly factors. In 2008, an operon was identified in *Synechocystis* 6803 (*slr0144 – slr0152*) containing nine genes of which six were shown to be associated with PSII (Wegener et al., 2008). Deletion of the whole operon in a wild-type background only displayed slight effects on PSII function. However, based on analyses of domain structures, some of the encoded proteins were speculated to participate in binding of pigment cofactors (chlorophyll, bilins) during PSII dynamics (Wegener et al., 2008).

More recently, Sll0606 was described to constitute an important component participating in

pigment integration during PSII assembly. Loss of this protein specifically inhibited PSII activity and resulted in strong reduction of D1 and CP43 levels and, consequently, also PSII [1] and PSII [2] (Zhang et al., 2010). Nevertheless, although the precise function of Sll0606 remains to be investigated, it was suggested to be involved in transport and/or integration of carotenoids into PSII (Zhang et al., 2010).

The impact of the presence of carotenoids for PSII biogenesis was also studied using a *Synechocystis* 6803 mutant unable to accumulate these pigments. This strain was found to be severely impaired in accumulation of CP47 and especially CP43 and, consequently, no functional PSII complexes can be assembled (Sozer et al., 2010). Further experiments with a *Synechocystis* 6803 strain accumulating non-assembled His-tagged CP47 and CP43 complexes provided evidence that preloading of CP47 and CP43 with pigments already takes place before integration of these subunits into the PSII complex (Boehm et al., 2011).

Although PDMs were found to participate in chlorophyll synthesis, it remains to be addressed in future whether they are additionally involved in the synthesis of carotenoids. However, in higher plant chloroplasts, chlorophyll and carotenoid synthesis do not show the same suborganellar localization (Joyard et al., 2009). Thus, in contrast to the generation of chlorophyll, carotenoid synthesis in *Synechocystis* 6803 might occur in a PDM-independent manner.

#### 4.1.3 Involvement of PDMs in assembly of PSI

As depicted above, PSII biogenesis and chlorophyll synthesis are connected to PDMs. To examine the impact of PDMs on PSI assembly, membrane distribution of PsaA, a core subunit of PSI, as well as the PSI assembly factor Ycf37 was examined (Dühring et al., 2006). Both proteins were located in TM fractions of wild-type cells and did not exhibit changes upon loss of *prata* as it was the case for pD1/D1 and all PSII assembly factors (see Figure 2A, B in section 3.2). Hence, whereas PDMs apparently play an important role in PSII biogenesis, the assembly of PSI seems to follow a different pathway. However, as chlorophyll synthesis, on the other hand, takes place at least partially in PDMs, these structures might influence PSI assembly indirectly by providing pigment molecules necessary for construction of PSI. Moreover, a link between synthesis of the chlorophyll binding proteins CP47 as well as the PSI subunits PsaA and PsaB has been suggested before, since all three protein subunits were affected in their accumulation in a *Synechocystis* 6803 *psb28*<sup>-</sup> mutant (Dobáková et al., 2009). This reduction seems to be caused by an insufficiency of chlorophyll due to a defect in its synthesis pathway at the cyclization step. Interestingly, accumulation of other chlorophyll

binding proteins like D1, D2 and CP43 were not affected in this strain. It was therefore speculated that a branching point at the final stages of chlorophyll synthesis might exist responsible for inserting newly synthesized pigments either into proteins of the CP47/PsaA/PsaB or the D1/D2/CP43 branch, respectively (Dobáková et al., 2009). Results obtained in additional studies propose the existence of a mechanism which can distinguish between PSI and PSII target proteins for newly synthesized chlorophyll molecules (Kopečná et al., 2012a). One could speculate that such a differentiation of chlorophyll targeting might be achieved by a spatial separation of PSI and PSII assembly or probably by binding to different accessory proteins which deliver the pigments to individual PSI and/or PSII apoproteins.

Interestingly, the abovementioned proteins Slr0146, Slr0147, Slr0149 and Slr0151, were not only detected in association with PSII but also with PSI complexes (Kubota et al., 2010). Furthermore, the PSII assembly factor Psb27 and even the PSII subunit CP43 were found to interact with PSI (Komenda et al., 2012b). These findings propose the existence of an interwoven network comprising the assembly of PSII protein subunits, different cofactors and even the biogenesis of other complexes such as PSI. However, the understanding of the various interrelationships is still at the very beginning.

Taken together, the more detailed characterization of PDMs (i) could substantiate their role in especially the PSII assembly process, (ii) underlined the important function of PrtA in spatial organization of PSII biogenesis and (iii) revealed a connection of protein synthesis/assembly and pigment synthesis/insertion in this membrane subcompartment.

#### **4.2 MEDIATION OF PSII ASSEMBLY BY A NETWORK OF FACILITATING FACTORS**

During recent years, a number of assembly factors have been found and characterized that function in regulation of PSII biogenesis. However, relatively little is known about potential interrelations between these proteins, but it is becoming more and more apparent that the different facilitating factors do not act isolated but rather are integrated in an elaborated network of interactions. More detailed characterization of already known factors as well as identification of novel proteins participating in regulation of PSII assembly can provide new insights into the function and coordination of this complex process.

To investigate potential interconnections between different facilitating factors in *Synechocystis* 6803, in this work, their accumulation as well as effects on their membrane distribution in various PSII mutants was studied (see Figures 2 and 3 in section 3.2). The results confirmed that lack of one assembly factor indeed specifically affected localization

and accumulation of others demonstrating that a connected network of facilitating factors exists in cyanobacteria (Figure 9A). Whether these impairments are caused by direct interactions or represent secondary effects due to a disturbed PSII assembly process or distorted membrane structure has to be elucidated in future work. At least for YCF48 and Sll0933 as well as Pitt and POR direct interactions could be confirmed by studies in yeast (see Figure 5 in section 3.4; Schottkowski et al., 2009a). Interaction between the latter two is especially interesting with regard to the connection of protein subunit assembly with pigment synthesis, since Pitt was shown to stabilize the chlorophyll synthesis enzyme POR. The presence of both proteins in PDMs and their altered membrane sublocalization upon inactivation of *prataA* as well as accumulation of pD1 in PDMs of a *pitt*<sup>-</sup> mutant led to the assumption that Pitt is involved in PSII assembly, perhaps by localizing POR to distinct membrane regions thus integrating pigment synthesis and protein assembly (Schottkowski et al., 2009a).

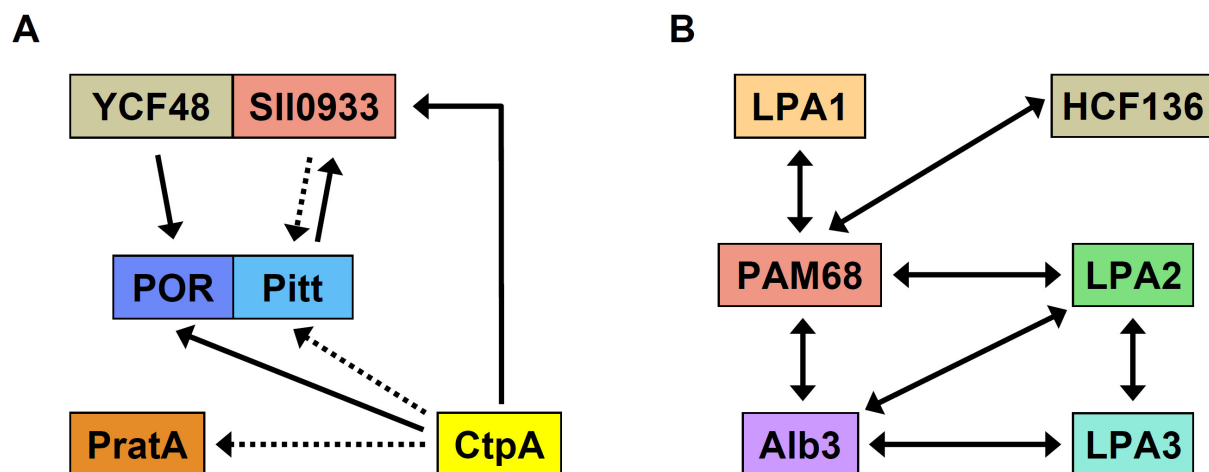


**Figure 9: Interrelationships between different PSII assembly factors in *Synechocystis* 6803 (A) and *A. thaliana* (B).** *Synechocystis* 6803 results (A) are based on protein accumulations in respective mutants (see Table 1 in section 3.2). Solid lines indicate positive, dotted lines negative regulations. Complex formation was confirmed between YCF48 and Sll0933 as well as Pitt and POR (see sections 3.2 and 3.4; Schottkowski et al., 2009a). (B) Known interactions of PSII assembly factors in *A. thaliana* (see section 3.1; Ma et al., 2007; Cai et al., 2010). Homologous proteins in *Synechocystis* 6803 and *A. thaliana* are identically coloured.

Evidence for interaction between YCF48 and Sll0933 in *Synechocystis* 6803 was obtained in this work (see sections 3.2 and section 3.4). This interaction seems to be evolutionary conserved up to chloroplasts of higher plants, since it was also demonstrated for the respective homologous proteins, HCF136 and PAM68, in *A. thaliana* (see Figure 10 in section 3.1). However, in *Synechocystis* 6803, lack of these factors seems to be better substituted by other

proteins, since the observed phenotypes of the respective mutants were not as severe as reported for *A. thaliana* (see section 3.1; Plücker et al., 2002; Komenda et al., 2008). Nevertheless, the main mode of action appears to be similar in *Synechocystis* 6803 and *A. thaliana*.

In membrane fractionation studies, Sll0933 was exclusively detected in TMs whereas YCF48 was also present in PDMs, hence, YCF48 probably acts upstream of Sll0933 during PSII assembly (see Figure 2 in section 3.2). This is in agreement with the finding that Sll0933 assists the attachment of the PSII inner antenna proteins CP47 and CP43 and, thus, is involved in later steps of PSII biogenesis compared to YCF48, which mediates RC assembly (see Figure 4 in section 3.4; Komenda et al., 2008). Interaction between YCF48 and Sll0933 therefore might take place during conversion from RC to RC47 complexes. It can be speculated that the YCF48/Sll0933 complex is involved in distribution of chlorophyll among chlorophyll-binding proteins as it was already suggested for YCF48 and its plant counterpart HCF136 (Plücker et al., 2002; Komenda et al., 2008). Reduced levels of newly synthesized CP47 and CP43 in *sll0933*<sup>-</sup> and *ycf48*<sup>-</sup>*sll0933*<sup>-</sup> could hence be possibly due to a defect in pigment insertion. It furthermore can be hypothesized that YCF48 is indirectly involved in chlorophyll integration by passing on chlorophyll molecules, which are newly synthesized in PDMs, to the TM-localized Sll0933 that subsequently mediates their insertion into PSII inner antenna proteins.

The *A. thaliana* homolog of Sll0933, PAM68, was shown to be able to interact – besides with HCF136 – with a variety of different PSII subunits (D1, D2, CP43, CP47, PsbH, PsbI) and, interestingly, several other assembly factors (Alb3, LPA1, HCF136, LPA2) (Figure 9B; see Figure 10 in section 3.1). Whereas interaction of PAM68 with D1, D2, PsbI, Alb3, LPA1 and HCF136 underlines a function in formation of RC complexes, interaction with CP43, CP47, PsbH and LPA2 points to a role in attachment of the PSII inner antenna proteins as it was also suggested for Sll0933. Due to its interaction with Alb3, which is an integrase involved in membrane integration of light-harvesting chlorophyll binding proteins and potentially of other PSII proteins such as D1, D2 and CP43, PAM68 could indirectly even play a role in the very early steps of the assembly process, i.e. integration of D1 (Moore et al., 2000; Pasch et al., 2005). This is furthermore supported by the interrelationship with LPA1, a chloroplast-specific PSII assembly factor which directly binds to D1 and probably also assists in the correct integration of D1 into the membrane (Peng et al., 2006). Based on analyses of protein complexes in *pam68* and *lpa1* mutants, it was speculated, that LPA1 acts upstream of PAM68 and growing PSII complexes are passed to PAM68 thus displacing LPA1 (see Figure 9 in

section 3.1). These PSII intermediates seem to contain pD1 and D2 but lack CP47 and CP43, therefore arguing for the involvement of PAM68 in steps leading to formation of RC complexes (see Figure 9 in section 3.1). PAM68 additionally interacts with LPA2, substantiating a function of PAM68 in assembly of the inner PSII antennae (see Figure 10 in section 3.1). LPA2 is a facilitating factor only present in higher plants, which acts at the level of CP43 integration into RC47 complexes (Ma et al., 2007). This step is likely assisted by LPA3, an eukaryotic PSII assembly factor which, again, was shown to interact with LPA2 and Alb3 in *A. thaliana* protoplasts (Cai et al., 2010). Alb3, again, was shown to interact with LPA2 and, as mentioned above, with PAM68 (Figure 9B; Ma et al., 2007). However, no homologous proteins to LPA1 or LPA2 can be found in *Synechocystis* 6803, indicating that the regulatory network acting in PSII assembly has undergone several changes during evolution.

In general, the presented data illustrate that different PSII assembly factors act in a tightly regulated network rather than fulfilling their functions separately (Figure 9). Hence, it can be speculated that developing PSII complexes are passed in an assembly line built up by a consecutive machinery of facilitating factors, which is probably also linked to proteins mediating the insertion of newly synthesized pigments and the therein involved enzymes (see also section 4.1).

### 4.3 INVOLVEMENT OF PRATA IN MANGANESE DELIVERY TO PSII

The cyanobacterial protein Prata was described in earlier studies as an important factor for coordinating the early steps of PSII biogenesis (Klinkert et al., 2004; Schottkowski et al., 2009b). However, the precise molecular function of Prata still remained unclear. It was shown before that Prata occurs in two different forms: as part of a soluble complex of ~200 kDa located in the PP, as well as membrane-bound via interaction with D1, which defines the PDM system (see section 4.1; Schottkowski et al., 2009b). To gain further insight into the role of Prata in PSII and TM biogenesis, the function of the soluble form was examined in more detail (see section 3.3). Interestingly, a novel function of Prata was discovered, as results unraveled a specific  $Mn^{2+}$  binding activity for Prata. Taken together, Prata possesses one specific high-affinity  $Mn^{2+}$  binding site with a  $K_d \approx 73 \mu M$  and several low-affinity binding sites, which can easily be substituted by  $Ca^{2+}$  or  $Mg^{2+}$  ions. It could further be shown that  $Mn^{2+}$  is not only bound by Prata but that Prata is required for efficient transport of  $Mn^{2+}$  to the D1 protein, which provides most of the ligands for complexing the

Mn<sub>4</sub>Ca cluster (see Figure 6 in section 3.3). Thus, one function of PrtA is the assistance in direction of Mn<sup>2+</sup> to PSII.

Previous experiments revealed that Mn uptake from the environment into *Synechocystis* 6803 cells occurs in a light-dependent manner and that Mn is stored in high concentrations as Mn(II) in the PP (Figure 10; Keren et al., 2002). This Mn pool ensures the ability to supply the cell with sufficient Mn according to its requirement and, concomitantly, prevents Mn overaccumulation in the cellular interior where transition metals could cause generation of harmful oxygen species by redox reactions (Liochev and Fridovich, 1999; Peña et al., 1999). The components involved in maintenance of this periplasmic Mn pool are still elusive, but there are indications that Mn is stored by attachment to the OM, therefore suggesting the involvement of a protein functioning as membrane anchor (Keren et al., 2002). The main Mn binding protein identified in the PP of *Synechocystis* 6803 is represented by MncA, but its participation in the periplasmic Mn storage still has to be examined (Tottey et al., 2008). Interestingly, the specificity for binding of Mn<sup>2+</sup> to MncA seems to be ensured by a defined folding of MncA in the cytoplasm, which contains other competing metals like Zn<sup>2+</sup> or copper only in a protein-bound form and thus prevented from interfering with the MncA folding process. MncA is subsequently transported in its folded form across the PM to the PP via the Tat export pathway (Fulda et al., 2000; Tottey et al., 2008). The Mn<sup>2+</sup> specificity of PrtA, however, seems to follow a different mechanism, as PrtA was found to contain a transit sequence at its N-terminus pointing to a secretion using the Sec system and, as such, it is transported in an unfolded state followed by its folding in the PP (Klinkert et al., 2004; Albinia et al., 2012). Upon binding of Mn<sup>2+</sup>, PrtA undergoes a change in its secondary structure as measured by circular dichroism experiments (see Figure 2 in section 3.3). This structural alteration could specifically be observed with Mn<sup>2+</sup> and not with Fe<sup>2+</sup>, Fe<sup>3+</sup>, Mg<sup>2+</sup> or Ca<sup>2+</sup>, thus a mode for distinguishing between the different ions has to exist, maybe correlated with the properties of the metals' hydrate shells. The K<sub>d</sub> of the high affinity binding site of PrtA for Mn<sup>2+</sup> (K<sub>d</sub> ≈ 73 μM) is in the range of other reported Mn binding proteins, including e.g. the oxidative stress protecting protein SsDPS and the catalase MnCat (Meier et al., 1996; Hayden and Hendrich, 2010). However, other proteins were described which possess a considerably higher affinity for Mn, like it was shown for PsbP in spinach (Bondarava et al., 2007). In this regard, it has to be considered that Mn<sup>2+</sup> is merely transiently bound to PrtA, as it is destined for transfer to D1 and, therefore, its release from PrtA has to be ensured.

The role of PrtA in preloading of D1 with Mn<sup>2+</sup> is in good agreement with previous studies, which determined the D1 amino acids 314-328 to be predominantly responsible for binding of

PratA (Schottkowski et al., 2009b). Notably, these amino acids form an  $\alpha$ -helical structure and are located in close proximity to the D1 residues His 332, Glu 333, Asp 342 and Ala 344, which are involved in complexing the  $Mn_4Ca$  cluster (see Figure 1C in section 3.3). For a detailed understanding of the molecular mechanisms of the  $Mn^{2+}$ -transfer from PratA to D1, the binding site of D1 as well as of  $Mn^{2+}$  on PratA has to be identified, which will be performed in future experiments by solving the crystal structure of recombinant PratA in the presence of  $Mn^{2+}$  and the respective D1 peptide. As it was found that binding of  $Mn^{2+}$  triggers definite conformational changes within the PratA protein structure, it can be speculated that the binding affinities also underlie certain changes.

Since the soluble form however is part of a complex of  $\sim 200$  kDa and thus several additional proteins might be involved, for a better understanding of the PratA-mediated  $Mn^{2+}$  delivery process, the other components of the periplasmic complex will be identified in future work (Schottkowski et al., 2009b). An interaction of PratA with the periplasmic Mn binding protein MncA has not been detected so far, and additionally the precise function of MncA in Mn-homeostasis remains to be investigated. Hence, newly identified components of the PratA complex could be promising candidates for elucidating the mechanism of Mn transfer from the storage pool to PratA. Moreover, construction and analysis of the respective single mutants as well as strains carrying different combinations of mutations might help to shed more light on the role of the periplasmic PratA complex.

#### 4.4 SPATIAL ORGANIZATION OF INITIAL STEPS OF PSII ASSEMBLY

PDMs have been proposed in earlier studies to represent the site of early steps of PSII biogenesis. In the present work, PDMs were further characterized by biochemical means and it was speculated that this membrane subfraction is identical to the earlier described TCs and in contact to both, the PM and TMs, hence potentially representing the controversially discussed connections between these two membrane types (see section 4.1). Electron microscopic analyses revealed that both, PratA and pD1, were found to localize to distinct clusters at the cell periphery (see Figures 8 and 9 in section 3.3). In *pratA*<sup>-</sup>, pD1 was still detected in such clusters, although their number was twofold diminished, indicating that their formation is at least partially dependent on the presence of PratA. This structure was assigned to so-called biogenesis centers, consisting of a granular matrix assumed to correspond to TCs, which is surrounded by a semicircular structure (Figure 10). These centers are located at sites where TMs converge to the PM and, therefore, seem to link these two membrane systems. However, only a small percentage of examined wild-type cells exhibited these structures;

although it has to be noted that merely a few slices have been analyzed per cell and thus no three-dimensional investigation of the cells has been performed. Nevertheless, the results indicate that either only one or a few biogenesis centers are present per cell, or that they are only formed transiently and dynamically. However, the membrane organization and/or biogenesis was found to be altered in *pratA*<sup>-</sup>, as only the TC structures, but not the semicircle-shaped systems were detected in >1000 analyzed *pratA*<sup>-</sup> cells, underlining that their formation is PrataA-dependent. Determination of the three-dimensional organization of biogenesis centers will be subject of future work, which could also clarify whether they form cylindrical structures as it was previously described for TCs (van de Meene et al., 2006). It can be concluded that these biogenesis centers correspond to PDMs and represent the region where early steps of PSII biogenesis occur. The presented data allow the development of a detailed model of events taking place during these initial assembly steps: Mediated by PrataA, D1 becomes preloaded with Mn<sup>2+</sup> from the PP, thus bypassing an active transport of Mn<sup>2+</sup> across the PM and TMs (Figure 10). In addition, pD1 is processed by CtpA, which has been exclusively detected in PM preparations – probably including PDMs – while PSII assembly proceeds with integration of D2/PsbEF, resulting in formation of RC complexes (Figures 4, 10; Zak et al., 2001). Probably, these RC complexes are located at the transition point from PDMs to TMs and are transferred to the latter for subsequent biogenesis steps, since the next protein assembled, CP47, is found solely in the TM system (Zak et al., 2001; Bergantino et al., 2003). Moreover, the function of the YCF48/Sll0933 complex seems to be connected to this step (see section 4.2). Additionally, chlorophyllide *a* accumulating in PDMs substantiates their function in pigment synthesis and insertion (Figure 10). The whole assembly process is finally completed in the TMs.

It can be speculated that the PM-near localization of initial steps of PSII assembly is due to the necessity of incorporation of metal ions at the luminal side of PSII, as it avoids energy consuming, active metal transport processes across the PM and TM system. This might also explain that PSI-related proteins did not depict changes in their amount or localization upon inactivation of *pratA* (see Figure 2A, B in section 3.2): In contrast to PSII, PSI monomers do not contain inorganic cofactors at their luminal side, therefore, their assembly might be restricted to subcellular regions independent of the cell envelope (Jordan et al., 2001).

A similar organization of PSII assembly has also been suggested for the green alga *Chlamydomonas reinhardtii*. Under conditions triggering *de novo* PSII assembly, ribosomes and mRNAs encoding PSII subunits were shown to localize at distinct regions in the periphery of the pyrenoid, which is formed by semicrystalline concentrations of the CO<sub>2</sub>-

fixing enzyme ribulose-bisphosphate carboxylase/oxygenase (McKay and Gibbs, 1991; Borkhsenius et al., 1998; Uniacke and Zerges, 2007). Furthermore, mutants defective in PSII assembly accumulate early PSII intermediates around the pyrenoid, which further substantiates the importance of this region in PSII biogenesis. Therefore, these regions were named T-zones (translation zones) and suggested to represent the place of early PSII biogenesis with a subsequent transport of newly assembled complexes to the TMs (Uniacke and Zerges, 2007). Taken together, the principle of a centered localization of PSII biogenesis might be evolutionary conserved – at least from cyanobacteria to chloroplasts of unicellular green algae.

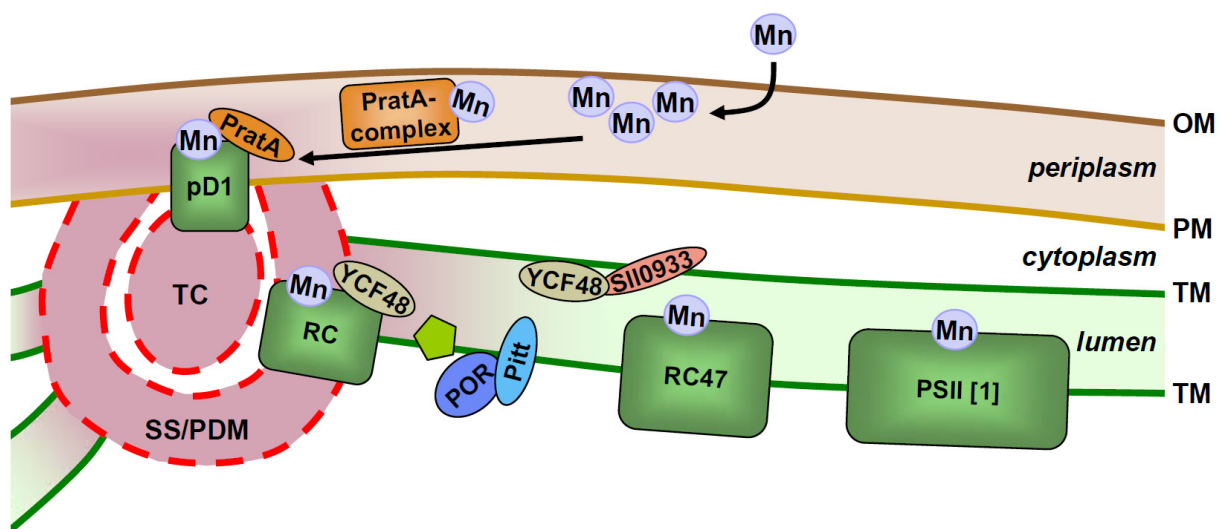


**Figure 10: Model for spatial organization of PSII biogenesis in *Synechocystis* 6803.** PSII assembly starts in biogenesis centers consisting of thylakoid centers (TC) surrounded by semicircular structures (SS), which connect PM and TMs. Mediated by PrataA the D1 precursor is preloaded with manganese ions (Mn) that have been stored in the periplasmic space. PSII complexes are further assembled while they migrate from PDMs to TMs. Chlorophyllide *a* (green pentagon) accumulates in PDM fractions merging with TMs. Pitt and POR as well as YCF48 and SII0933 seem to be involved in pigment synthesis/integration. Assembly of RC47, PSII monomers and dimers (not shown), occurs in TMs. OM, outer membrane; PM, plasma membrane; TM, thylakoid membrane; RC, PSII reaction center complex lacking CP47 and CP43; RC47, PSII reaction center complex lacking CP43; PSII[1], PSII monomer. For further details, see text. According to Nickelsen and Rengstl, submitted (see appendix).

#### 4.5 CORRELATION BETWEEN PSII *DE NOVO* ASSEMBLY AND PSII REPAIR

Based on the results presented above, light has been shed on the subcellular localization of the PSII biogenesis process. However, besides *de novo* synthesis of PSII – which occurs especially in dividing cells – dynamics of this complex also includes its repair that is especially required after photodamage, and even less is known about this process. The repair cycle particularly exchanges D1 subunits, which are dramatically affected by photodamage causing irreversible impairment (Edelman and Mattoo, 2008). For this replacement, the

inactive PSII complex has to be partially disassembled to enable specific degradation of damaged D1, followed by integration of a newly synthesized copy (Figure 11; Nixon et al., 2010). This exchange of D1 is assumed to occur at the level of RC47 complexes, but the subcellular localization of PSII complexes undergoing repair is still unclear (Nixon et al., 2005). In general, this process has to be tightly regulated as well and to date it is unknown whether D1 integration during PSII repair occurs in a similar fashion as during *de novo* assembly of PSII. However, it was suggested that chlorophyll molecules are transiently removed during PSII repair, stored in the TMs and are subsequently reattached to the repaired complexes. This is based on studies showing that the half-life time of chlorophyll molecules associated with PSII is significantly higher than the turnover rate of the major PSII proteins, pointing to a recycle/reusage mechanism of chlorophyll molecules (Vavilin et al., 2005; Yao et al., 2012b). Furthermore, newly synthesized chlorophyll molecules were found to be predominantly directed to PSI complexes whereas PSII subunits are mainly re-synthesized using recycled chlorophyll (Kopečná et al., 2012b). With this regard, so-called SCPs (small CAB-like proteins), which are single helix proteins carrying a conserved motif of residues involved in chlorophyll binding, are thought to transiently bind chlorophyll molecules during replacement of PSII protein subunits (Vavilin et al., 2007; Yao et al., 2012b). Likely, a similar recycling process can be assumed for cofactors like the Mn<sub>4</sub>Ca cluster. A protein which has been discussed to fulfill such a function as Mn storage protein is the PsbP subunit in higher plants (Bondarava et al., 2005). The recycling of Mn would avoid the need of additional transport of Mn<sup>2+</sup> across the cell envelope and TM and, concomitantly, would prevent a regulated and probably energy-requiring removal of “used” Mn.

The site of PSII repair has been a matter of debate and speculations during recent years. If additional cofactors such as Mn<sup>2+</sup> and chlorophylls do not have to be transported to PSII during the repair cycle, it seems likely that D1 repair takes place at the site of damage, i.e. the TMs (Figure 11). In this case, no shuttling of PSII complexes between the TMs and biogenesis centers has to occur. This scenario is supported by the finding that pD1 is not only present in PDMs, but also in TMs (see Figure 2A in section 3.2). Furthermore, FtsH, a protease involved in degradation of damaged D1 protein, has exclusively been detected in TMs, supporting the idea of the TM system as site of PSII repair (Komenda et al., 2006). Moreover, the exclusive localization of CP47 and thus also the RC47 complex, which is thought to represent the D1 integration platform during PSII repair, in TMs strongly argues for an on-site repair of PSII (Figure 11; Zak et al., 2001; Bergantino et al., 2003; Komenda et al., 2004).

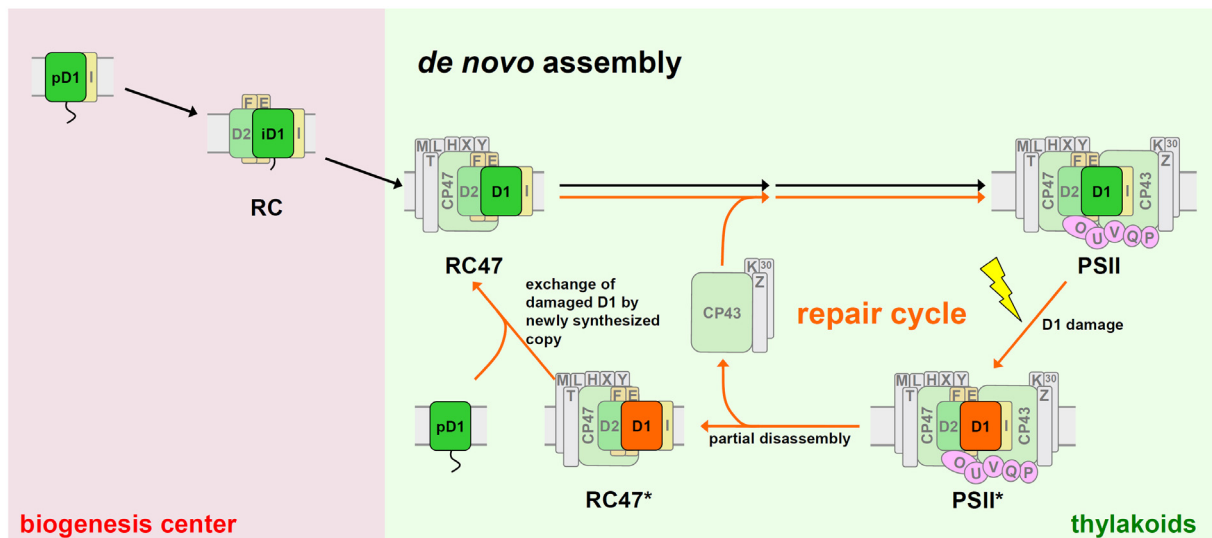


**Figure 11: Subcellular localization of PSII *de novo* and repair assembly.** In *Synechocystis* 6803, early steps of PSII *de novo* assembly (black arrows) take place in biogenesis centers (red). Precomplexes are transferred to the thylakoids (green) where the assembly process is completed. After photodamage by light (yellow flash) the D1 subunit (orange D1) has to be replaced by a newly synthesized copy. During this PSII repair cycle (orange arrows) the inactive PSII complexes (marked by an asterisk) are partially disassembled to allow exchange of D1 at the level of RC47\* complexes. Subsequently, the detached subunits are re-integrated to restore functional PSII. The PSII repair cycle seems to be located completely in the thylakoid membrane system. For clarity, PSII complexes are depicted as monomers and not as supercomplexes. RC, PSII reaction center complex lacking CP47 and CP43; RC47, PSII reaction center complex lacking CP43. According to Nickelsen and Rengstl, submitted (see appendix).

However, contradictory to the idea of a repair cycle located in the TM system is the exclusive detection of the D1 processing protease CtpA in the PM of *Synechocystis* 6803, as maturation of D1 also has to take place during the repair cycle to allow proper reassembly of PSII after integration of a newly synthesized D1 subunit (Zak et al., 2001). Interestingly, whereas the C-terminal extension of D1 is not necessarily required for proper membrane integration of D1 and assembly of PSII *per se*, mutants lacking this extension exhibit declined fitness and a more pronounced susceptibility to photodamage, suggesting its contribution especially during the repair cycle of PSII (Nixon et al., 1992; Ivleva et al., 2000; Kuvikova et al., 2005; Satoh and Yamamoto, 2007). In *Synechocystis* 6803, cleavage of the C-terminal extension was shown to occur in a sequential two-step proteolytic manner, including the intermediate processing form iD1 (Komenda et al., 2007). Since formation of residual amounts of iD1 and D1 is still detectable in a *Synechocystis* 6803 *ctpA*<sup>-</sup> mutant and – to a lesser extent – also in a *ctpA*<sup>-</sup>*ctpB*<sup>-</sup> double mutant, it cannot be excluded that CtpB and probably other additional proteases, like CtpC, can partly substitute for CtpA during this cleavage process (Komenda et al., 2007). CtpB and CtpC represent – besides CtpA – additional carboxyl-terminal endoproteases, which are encoded by the *ctp* genes in *Synechocystis* 6803 (Jansen et al.,

2003). Nonetheless, the marginal residual D1 processing activity of other proteases than CtpA can hardly be sufficient to saturate the high demand of D1 processing under photoinhibitory conditions, since even under growth light intensities ( $75\text{-}100\ \mu\text{mol photons m}^{-2}\ \text{s}^{-1}$ ) the half-life time of D1 is only about 1-2 h (Komenda et al., 2000; Yao et al., 2012a). This argues for an important role of CtpA as main protease not only during *de novo*, but also during repair synthesis of D1. Occurrence of CtpA also in TMs – at least under conditions favoring PSII repair – has been suggested by Jansén et al., since they detected pD1 in TMs, which became readily processed into mature D1 (Jansén, 2002). Hence, more work is required to unambiguously answer the membrane localization of the CtpA protease.

Interestingly, in the microalga *C. reinhardtii*, a strict separation of the sites of PSII *de novo* biogenesis and the PSII repair cycle has been reported. Repair synthesis of D1 occurs directly at TMs all over the chloroplast, whereas synthesis of the D1 subunit for *de novo* PSII assembly was shown to be restricted to the abovementioned T-zones near the pyrenoid (Uniacke and Zerges, 2007). Thus it seems conceivable that a similar regional separation of the two processes of PSII dynamics is found in cyanobacteria as well.

Further data for solving the question concerning the subcellular localization of D1 repair in *Synechocystis* 6803 might be obtained by investigation of the membrane distribution of PSII assembly factors known to function specifically in PSII maintenance. The difficulty of this approach, however, is the fact that most proteins that play a role during PSII repair are additionally involved in the *de novo* pathway. Such dual roles have been reported for e.g. YCF48, Psb27 and Psb28 and the present study suggests a similar function for the newly identified PSII assembly factor Sll0933, since wild-type cells exhibited higher fitness than the *sll0933*<sup>-</sup> mutant when grown under higher light conditions causing photodamage (see Figure 1 in section 3.4; Nowaczyk et al., 2006; Komenda et al., 2008; Roose and Pakrasi, 2008; Nowaczyk et al., 2012). It is therefore questionable whether Slr1768 and Psb32, two proteins which have so far been characterized as maintenance-specific assembly factors in *Synechocystis* 6803, are indeed exclusively involved in PSII repair or whether they also play a yet unidentified role during PSII biogenesis (Bryan et al., 2011; Wegener et al., 2011). As both have been detected in PM preparations, it seems conceivable that they are at least partially located in PDMs, hence participating in the *de novo* assembly steps (Boehm et al., 2009; Wegener et al., 2011).

The determination of the site of PSII repair after photodamage of D1 in *Synechocystis* 6803 will be a task for future work. Additionally, the exact mechanisms mediating PSII repair remain to be resolved, with particular focus on the pathways of storage and reuse of

disassembled subunits and cofactors including the Mn<sub>4</sub>Ca cluster and pigments during the repair cycle. In this regard it would be interesting to examine whether PrtA plays a role during this process as well, as its function in PSII repair has not been analyzed yet.

#### 4.6 PSII ASSEMBLY IN CHLOROPLASTS OF GREEN ALGAE AND PLANTS

The data presented in this work addresses the steps and mechanisms of PSII assembly in the cyanobacterium *Synechocystis* 6803. Chloroplasts of green algae and plants are generally accepted to be the evolutionary result of the engulfment of an ancient relative of nowadays cyanobacteria by an eukaryotic cell, known as the endosymbiotic theory (Gould et al., 2008). Hence, the main features and properties of PSII structure and assembly are conserved from cyanobacteria to higher plants (Figure 12). However, during evolution of nowadays chloroplasts, the majority (>90%) of genes encoded by the endosymbiont has been transferred to the nuclear genome. As a consequence, the respective proteins are synthesized in the cytosol and have to be re-imported into the chloroplast post-translationally. About 50-200 proteins (dependent on the organism) are still encoded for in the chloroplast, resulting in formation of organellar protein complexes with subunits derived from different cell compartments (Barkan, 2011). In the case of PSII, the core subunits D1, D2, cyt b<sub>559</sub>, CP43 and CP47 as well as several low molecular weight subunits are still encoded by the chloroplast genome, whereas other low molecular weight subunits have to be imported from

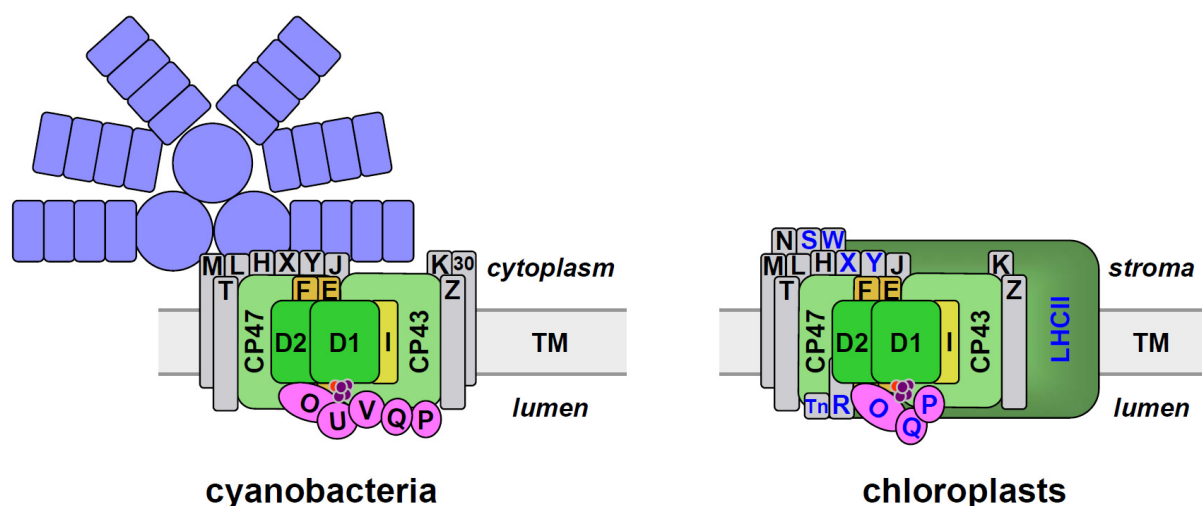


**Figure 12: PSII subunit composition in cyanobacteria and higher plant chloroplasts.** The core of the complex is in both cases built by the D1 and D2 subunits surrounded by the inner antenna proteins CP47 and CP43. Besides the distinct peripheral antennae – soluble phycobilisomes in cyanobacteria (left; in blue) and membrane-intrinsic LHC complexes in plant chloroplasts (right, in dark green) – also differences in the composition of extrinsic proteins (pink) and low molecular mass subunits (grey) can be observed. Proteins encoded by the nuclear genome in plants are indicated by blue lettering. TM, thylakoid membrane. Adapted from Nickelsen and Rengstl, submitted (see appendix).

the cytosol (Figure 12; Allen et al., 2011). Hence, during PSII assembly, tight coordination of chloroplast and nuclear gene expression is necessary to ensure sufficient and reasonable availability of all subunits (Barkan, 2011).

Several PSII assembly factors are conserved throughout the green lineage, for example Alb3/Slr1471 (Moore et al., 2000; Ossenbühl et al., 2004; Göhre et al., 2006; Ossenbühl et al., 2006), HCF136/YCF48 (Meurer et al., 1998; Plücker et al., 2002; Komenda et al., 2008), PAM68/Sll0933 (see section 3.1), Psb28 (Dobáková et al., 2009; Shi et al., 2012) and Psb29/Thf1 (Wang et al., 2004; Keren et al., 2005b; Huang et al., 2006). However, also several exceptions have been described: some PSII assembly factors, e.g. LPA1 and LPA3, are present in chloroplasts of plants and green algae, but have no homologs in cyanobacteria, whereas others including LPA2 and HCF243 – a protein involved in stabilization of D1 in *A. thaliana* – are even restricted to higher plants (see Table 1 in Nickelsen and Rengstl, submitted, see appendix; Peng et al., 2006; Ma et al., 2007; Cai et al., 2010; Zhang et al., 2011). The presence of plant chloroplast-specific facilitating factors might reflect the different evolutionary development of chloroplasts from vascular plants compared to the prokaryotic cyanobacteria, as they had to adapt to other external influences and living conditions: During evolution, plants have developed a predominantly land-based life and thus have to cope with different environmental situations, which could be a reason for development of minor evolutionary changes in PSII composition and regulation of its assembly compared to cyanobacteria.

Interestingly, the existence of specialized PSII assembly proteins is not restricted to chloroplasts, as several factors are exclusively present in cyanobacteria, indicating that they have either been lost in chloroplasts of algae and plants during evolution or that they have been developed in cyanobacteria after the lineages spread (see Table 1 in Nickelsen and Rengstl, submitted, see appendix). The best studied example is the PratA protein, which does not possess any sequence homologs in e.g. *C. reinhardtii* or *A. thaliana*. Due to its important function in cyanobacteria in membrane organization required for PSII assembly, and as Mn<sup>2+</sup> binding and transporting protein, it is likely that its role has been taken over by other proteins in chloroplasts. In this regard, a good candidate is represented by LPA1, which belongs, like PratA, to the family of TPR proteins and was shown to be able to directly bind to D1 as well (Peng et al., 2006). Initial analyses indeed revealed Mn<sup>2+</sup> binding activity for LPA1 – at least *in vitro* (see section 3.3). However, substantial further analyses are required to clarify the mechanism of Mn<sub>4</sub>Ca cluster assembly and membrane organization in general and especially the role of LPA1 in *A. thaliana* during these processes.

Whereas the spatial organization of PSII *de novo* assembly initiation seems to be generally conserved in cyanobacteria and green algae (see section 4.4; Uniacke and Zerges, 2007), it is still unclear whether such an organization also exists in chloroplasts of higher plants. One striking difference is represented by the multicellularity of plants: whereas in unicellular photosynthetic organisms, PSII *de novo* assembly and repair occur (i) in the same cell and (ii) at the same time, these processes are – at least to a great extent – temporarily separated in plants. During plant development, their chloroplasts originate from undifferentiated proplastids at the shoot apex, which do not contain TMs and, thus, represent *de novo* TM/PSII biogenesis (Charuvi et al., 2012). Once the chloroplast TM system is fully developed, membrane and complex organization is largely sustained and – in case of PSII – complex dynamics are predominantly determined by operation of the repair cycle (Mulo et al., 2012). Hence, due to this temporal separation of both processes, a spatial differentiation does not necessarily have to be realized to the same extent in plants as in cyanobacteria, but more work is required to verify or disprove this hypothesis.

The exact site of PSII assembly in chloroplasts of higher plants and the existence of PDM-like biogenesis centers remain elusive; however, there is evidence that their TM system depicts a heterogeneous distribution. In these organisms, TMs appear either in non-appressed lamellar sheets or as appressed grana stacks (Arvidsson and Sundby, 1999). Photosynthetic protein complexes are not distributed evenly throughout this complex TM system, creating a lateral heterogeneity of TMs: Whereas PSII and LHCII (the light-harvesting complex of chloroplast PSII) are found in grana thylakoids, PSI, LHCI (the light-harvesting complex of chloroplast PSI) and ATP synthase are – likely due to steric reasons – located in stroma lamellae. Cyt  $b_6f$  complexes are, on the other hand, present in both membrane types (Dekker and Boekema, 2005). Formation of grana stacks is thought to be mainly caused by electrostatic interactions between LHCII, although minor LHCs and PSII reaction centers may also play a role (Standfuss et al., 2005; Daum et al., 2010). Furthermore, analysis of distribution of PSII complexes, including the assembly intermediates RC and RC47, revealed that 80% of PSII can be found in the grana, especially the grana core fraction, whereas PSII supercomplexes were exclusively detected in grana TMs. The less the membranes are stacked, the lower is the proportion of PSII [2] and, concomitantly, the higher is the percentage of PSII [1], RC47 and RC complexes (Danielsson et al., 2006). Hence, this is a hint that PSII complexes might be assembled in non-appressed TM regions. This assumption of synthesis and assembly of membrane proteins taking place at the stromal lamellae of TMs is supported by the finding that ribosomes bind to the non-stacked membrane regions and proteins are inserted into the

membrane co-translationally (Yamamoto et al., 1981). Whether PSII assembly in higher plants starts at specialized domains within the stroma thylakoids comparable to the situation of biogenesis centers and T-zones in *Synechocystis* 6803 and *C. reinhardtii*, respectively, remains an issue for future work.

Further indications for a spatial organization of pigment/protein complex assembly is given by results on sublocalization of pigment synthesis enzymes in chloroplasts. Whereas early steps of chlorophyll synthesis take place in the chloroplast stroma, subsequent reactions converting protoporphyrinogen IX to chlorophyll *a* were reported to occur at the chloroplast envelope and TMs. The chlorophyll synthase enzyme using phytyl pyrophosphate as substrate for esterification of chlorophyllide *a* to chlorophyll *a* has even been exclusively detected in TMs (Figure 7; Soll et al., 1983; Eckhardt et al., 2004; Czarnecki and Grimm, 2012). Thus, chlorophyll synthesis in plants seems to underlie a strict compartmentalization. On the other hand, carotenoid synthesis in chloroplasts was reported to be almost restricted to envelope membranes, thereby raising the question how transport to the TM system is mediated (Joyard et al., 2009). Nonetheless, whether the organization of pigment synthesis in higher plant chloroplasts is directly linked to spatial sublocalization of PSII assembly, as it seems to be the case in biogenesis centers of *Synechocystis* 6803 (see section 4.1), remains unknown.

Besides synthesis and assembly of proteins and pigments, biogenesis of TMs additionally requires high rates of lipid synthesis, especially for newly synthesized TMs in developing chloroplasts. Interestingly, final steps of biosynthesis of TM lipids have been reported to occur in envelope membranes, thus necessitating either a transport system or a direct connection between the different membranes (Kelly and Dormann, 2004). In *C. reinhardtii*, it was suggested that TMs develop by local expansion and invagination of the inner envelope membrane, although it remains to be clarified whether the membrane systems are directly linked or whether the lipids are transferred to the TMs as vesicles (Hooper et al., 1991). Similar observations have been made in developing proplastids of higher plants, where the inner envelope and the TMs indeed seem to be connected (Mühlethaler and Frey-Wyssing, 1959). In mature chloroplasts, however, such connections are only observed rarely (Shimoni et al., 2005) and lipid transfer from the envelope to TMs rather may occur by a vesicle trafficking system (Garcia et al., 2010; Vothknecht et al., 2012).

#### 4.7 CONCLUSIONS AND FUTURE PROSPECTS

Recent years unraveled the structure of cyanobacterial PSII with high resolution (Umena et al., 2011). Nevertheless, knowledge about the dynamic processes of PSII assembly with

regard to their temporal and spatial organization is still in its beginning. Identification of yet unknown facilitating factors as well as more detailed characterization of already described ones will be required to gain more comprehensive insight into the molecular mechanisms of generating this protein/pigment complex. It will be challenging to identify the components involved in coordinating the integration of cofactors in both, cyanobacteria and chloroplasts, also with regard to the subcellular localization of the events including the interrelationship between PSII biogenesis and repair pathways, as well as in regard to evolutionary similarities/differences. Studying PSII biogenesis and maintenance will help to better understand the common underlying aspects of protein complex formation and dynamics.

Further insights into function and dynamics of the photosynthetic complexes might in future contribute to the development of new types of solar cells, which mimic the process of photosynthesis. Moreover, elucidation of the underlying molecular principles are also the basis for generation of more robust crop plants, which show increased fitness and tolerance of challenging environmental conditions. The achievement of higher biomass yields is of particular importance, since, due to the continuous population growth, the area of cultivable land will decrease whereas the demand of food and crops for biofuel production will grow. Especially studies of unicellular photosynthetic systems like green algae and cyanobacteria might give access to low-cost biological systems which can easily be cultivated, engineered and optimized to directly convert sunlight energy into basic substances for biofuel production.

## 5 REFERENCES

- Adhikari, N.D., Orlor, R., Chory, J., Froehlich, J.E., and Larkin, R.M. (2009). Porphyrins promote the association of GENOMES UNCOUPLED 4 and a Mg-chelatase subunit with chloroplast membranes. *J Biol Chem* **284**, 24783-24796.
- Agarwal, R., Matros, A., Melzer, M., Mock, H.P., and Sainis, J.K. (2010). Heterogeneity in thylakoid membrane proteome of *Synechocystis* 6803. *J Proteomics* **73**, 976-991.
- Agarwal, R., Maralihalli, G., Sudarsan, V., Choudhury, S.D., Vatsa, R.K., Pal, H., Melzer, M., and Sainis, J.K. (2012). Differential distribution of pigment-protein complexes in the thylakoid membranes of *Synechocystis* 6803. *J Bioenerg Biomembr* **44**, 399-409.
- Albiniak, A.M., Baglieri, J., and Robinson, C. (2012). Targeting of luminal proteins across the thylakoid membrane. *J Exp Bot* **63**, 1689-1698.
- Allen, J.F., de Paula, W.B., Puthiyaveetil, S., and Nield, J. (2011). A structural phylogenetic map for chloroplast photosynthesis. *Trends Plant Sci* **16**, 645-655.
- Anbudurai, P.R., Mor, T.S., Ohad, I., Shestakov, S.V., and Pakrasi, H.B. (1994). The *ctpA* gene encodes the C-terminal processing protease for the D1 protein of the photosystem II reaction center complex. *Proc Natl Acad Sci USA* **91**, 8082-8086.
- Armstrong, G.A. (1998). Greening in the dark: light-independent chlorophyll biosynthesis from anoxygenic photosynthetic bacteria to gymnosperms. *J Photochem Photobiol B* **43**, 87-100.
- Aro, E.M., Virgin, I., and Andersson, B. (1993). Photoinhibition of photosystem II. Inactivation, protein damage and turnover. *Biochim Biophys Acta* **1143**, 113-134.
- Arvidsson, P.O., and Sundby, C. (1999). A model for the topology of the chloroplast thylakoid membrane. *Aust J Plant Physiol* **26**, 687-694.
- Baranov, S.V., Ananyev, G.M., Klimov, V.V., and Dismukes, G.C. (2000). Bicarbonate accelerates assembly of the inorganic core of the water-oxidizing complex in manganese-depleted photosystem II: a proposed biogeochemical role for atmospheric carbon dioxide in oxygenic photosynthesis. *Biochemistry* **39**, 6060-6065.
- Baranov, S.V., Tyrshkin, A.M., Katz, D., Dismukes, G.C., Ananyev, G.M., and Klimov, V.V. (2004). Bicarbonate is a native cofactor for assembly of the manganese cluster of the photosynthetic water oxidizing complex. Kinetics of reconstitution of O<sub>2</sub> evolution by photoactivation. *Biochemistry* **43**, 2070-2079.
- Barkan, A. (2011). Expression of plastid genes: organelle-specific elaborations on a prokaryotic scaffold. *Plant Physiol* **155**, 1520-1532.
- Bartsevich, V.V., and Pakrasi, H.B. (1996). Manganese transport in the cyanobacterium *Synechocystis* sp. PCC 6803. *J Biol Chem* **271**, 26057-26061.
- Becker, K., Cormann, K.U., and Nowaczyk, M.M. (2011). Assembly of the water-oxidizing complex in photosystem II. *J Photochem Photobiol B* **104**, 204-211.
- Bergantino, E., Brunetta, A., Touloupakis, E., Segalla, A., Szabo, I., and Giacometti, G.M. (2003). Role of the PSII-H subunit in photoprotection: novel aspects of D1 turnover in *Synechocystis* 6803. *J Biol Chem* **278**, 41820-41829.
- Boehm, M., Nield, J., Zhang, P., Aro, E.M., Komenda, J., and Nixon, P.J. (2009). Structural and mutational analysis of band 7 proteins in the cyanobacterium *Synechocystis* sp. strain PCC 6803. *J Bacteriol* **191**, 6425-6435.
- Boehm, M., Yu, J., Reisinger, V., Beckova, M., Eichacker, L., Schlodder, E., Komenda, J., and Nixon, P.J. Subunit composition of CP43-less photosystem II complexes of *Synechocystis* sp. PCC 6803: implications for the assembly and repair of photosystem II. *Phil Trans B*, in press.
- Boehm, M., Romero, E., Reisinger, V., Yu, J., Komenda, J., Eichacker, L.A., Dekker, J.P., and Nixon, P.J. (2011). Investigating the early stages of photosystem II assembly in *Synechocystis* sp. PCC 6803: isolation of CP47 and CP43 complexes. *J Biol Chem* **286**, 14812-14819.
- Bondarava, N., Beyer, P., and Krieger-Liszkay, A. (2005). Function of the 23 kDa extrinsic protein of photosystem II as a manganese binding protein and its role in photoactivation. *Biochim Biophys Acta* **1708**, 63-70.
- Bondarava, N., Un, S., and Krieger-Liszkay, A. (2007). Manganese binding to the 23 kDa extrinsic protein of photosystem II. *Biochim Biophys Acta* **1767**, 583-588.

- Borkhsenius, O.N., Mason, C.B., and Moroney, J.V.** (1998). The intracellular localization of ribulose-1,5-bisphosphate carboxylase/oxygenase in *Chlamydomonas reinhardtii*. *Plant Physiol* **116**, 1585-1591.
- Brown, S.B., Houghton, J.D., and Vernon, D.I.** (1990). Biosynthesis of phycobilins. Formation of the chromophore of phytochrome, phycocyanin and phycoerythrin. *J Photochem Photobiol B* **5**, 3-23.
- Bryan, S.J., Burroughs, N.J., Evered, C., Sacharz, J., Nenninger, A., Mullineaux, C.W., and Spence, E.M.** (2011). Loss of the SPHF homologue Slr1768 leads to a catastrophic failure in the maintenance of thylakoid membranes in *Synechocystis* sp. PCC 6803. *PLoS One* **6**, e19625.
- Cai, W., Ma, J., Chi, W., Zou, M., Guo, J., Lu, C., and Zhang, L.** (2010). Cooperation of LPA3 and LPA2 is essential for photosystem II assembly in *Arabidopsis*. *Plant Physiol*. **155**, 1493-1500.
- Charuvi, D., Kiss, V., Nevo, R., Shimoni, E., Adam, Z., and Reich, Z.** (2012). Gain and loss of photosynthetic membranes during plastid differentiation in the shoot apex of *Arabidopsis*. *Plant Cell* **24**, 1143-1157.
- Cormann, K.U., Bangert, J.A., Ikeuchi, M., Rogner, M., Stoll, R., and Nowaczyk, M.M.** (2009). Structure of Psb27 in solution: implications for transient binding to photosystem II during biogenesis and repair. *Biochemistry* **48**, 8768-8770.
- Czarnecki, O., and Grimm, B.** (2012). Post-translational control of tetrapyrrole biosynthesis in plants, algae, and cyanobacteria. *J Exp Bot* **63**, 1675-1687.
- D'Andrea, L.D., and Regan, L.** (2003). TPR proteins: the versatile helix. *Trends Biochem Sci* **28**, 655-662.
- Danielsson, R., Suorsa, M., Paakkarinen, V., Albertsson, P.A., Styring, S., Aro, E.M., and Mamedov, F.** (2006). Dimeric and monomeric organization of photosystem II. Distribution of five distinct complexes in the different domains of the thylakoid membrane. *J Biol Chem* **281**, 14241-14249.
- Dasgupta, J., Tyryshkin, A.M., and Dismukes, G.C.** (2007). ESEEM spectroscopy reveals carbonate and an N-donor protein-ligand binding to Mn<sup>2+</sup> in the photoassembly reaction of the Mn<sub>4</sub>Ca cluster in photosystem II. *Angew Chem Int Ed Engl* **46**, 8028-8031.
- Dau, H., Zaharieva, I., and Haumann, M.** (2012). Recent developments in research on water oxidation by photosystem II. *Curr Opin Chem Biol*.
- Daum, B., Nicastro, D., Austin, J., 2nd, McIntosh, J.R., and Kuhlbrandt, W.** (2010). Arrangement of photosystem II and ATP synthase in chloroplast membranes of spinach and pea. *Plant Cell* **22**, 1299-1312.
- Davison, P.A., Schubert, H.L., Reid, J.D., Iorg, C.D., Heroux, A., Hill, C.P., and Hunter, C.N.** (2005). Structural and biochemical characterization of Gun4 suggests a mechanism for its role in chlorophyll biosynthesis. *Biochemistry* **44**, 7603-7612.
- Dekker, J.P., and Boekema, E.J.** (2005). Supramolecular organization of thylakoid membrane proteins in green plants. *Biochim Biophys Acta* **1706**, 12-39.
- Deusch, O., Landan, G., Roettger, M., Gruenheit, N., Kowallik, K.V., Allen, J.F., Martin, W., and Dagan, T.** (2008). Genes of cyanobacterial origin in plant nuclear genomes point to a heterocyst-forming plastid ancestor. *Mol Biol Evol* **25**, 748-761.
- Dobáková, M., Tichy, M., and Komenda, J.** (2007). Role of the PsbI protein in photosystem II assembly and repair in the cyanobacterium *Synechocystis* sp. PCC 6803. *Plant Physiol* **145**, 1681-1691.
- Dobáková, M., Sobotka, R., Tichy, M., and Komenda, J.** (2009). Psb28 protein is involved in the biogenesis of the photosystem II inner antenna CP47 (PsbB) in the cyanobacterium *Synechocystis* sp. PCC 6803. *Plant Physiol* **149**, 1076-1086.
- Domanskii, V., Rassadina, V., Gus-Mayer, S., Wanner, G., Schoch, S., and Rüdiger, W.** (2003). Characterization of two phases of chlorophyll formation during greening of etiolated barley leaves. *Planta* **216**, 475-483.
- Dühring, U., Irrgang, K.D., Lünser, K., Kehr, J., and Wilde, A.** (2006). Analysis of photosynthetic complexes from a cyanobacterial *ycf37* mutant. *Biochim Biophys Acta* **1757**, 3-11.
- Eckhardt, U., Grimm, B., and Hörtensteiner, S.** (2004). Recent advances in chlorophyll biosynthesis and breakdown in higher plants. *Plant Mol Biol* **56**, 1-14.

- Edelman, M., and Mattoo, A.K.** (2008). D1-protein dynamics in photosystem II: the lingering enigma. *Photosynth Res* **98**, 609-620.
- Eichacker, L.A., Helfrich, M., Rüdiger, W., and Müller, B.** (1996). Stabilization of chlorophyll a-binding apoproteins P700, CP47, CP43, D2, and D1 by chlorophyll a or Zn-pheophytin a. *J Biol Chem* **271**, 32174-32179.
- Falcon, L.I., Magallon, S., and Castillo, A.** (2010). Dating the cyanobacterial ancestor of the chloroplast. *ISME J* **4**, 777-783.
- Ferreira, K.N., Iverson, T.M., Maghlaoui, K., Barber, J., and Iwata, S.** (2004). Architecture of the photosynthetic oxygen-evolving center. *Science* **303**, 1831-1838.
- Frank, H.A., and Brudvig, G.W.** (2004). Redox functions of carotenoids in photosynthesis. *Biochemistry* **43**, 8607-8615.
- Fulda, S., Huang, F., Nilsson, F., Hagemann, M., and Norling, B.** (2000). Proteomics of *Synechocystis* sp. strain PCC 6803. Identification of periplasmic proteins in cells grown at low and high salt concentrations. *Eur J Biochem* **267**, 5900-5907.
- Fulgosi, H., Gerdes, L., Westphal, S., Glockmann, C., and Soll, J.** (2002). Cell and chloroplast division requires ARTEMIS. *Proc Natl Acad Sci USA* **99**, 11501-11506.
- Garcia, C., Khan, N.Z., Nannmark, U., and Aronsson, H.** (2010). The chloroplast protein CPSAR1, dually localized in the stroma and the inner envelope membrane, is involved in thylakoid biogenesis. *Plant J* **63**, 73-85.
- Göhre, V., Ossenbühl, F., Crevecoeur, M., Eichacker, L.A., and Rochaix, J.D.** (2006). One of two Alb3 proteins is essential for the assembly of the photosystems and for cell survival in *Chlamydomonas*. *Plant Cell* **18**, 1454-1466.
- Golbeck, J.H.** (2003). The binding of cofactors to photosystem I analyzed by spectroscopic and mutagenic methods. *Annu Rev Biophys Biomol Struct* **32**, 237-256.
- Gombos, Z., Wada, H., Varkonyi, Z., Los, D.A., and Murata, N.** (1996). Characterization of the Fad12 mutant of *Synechocystis* that is defective in  $\Delta 12$  acyl-lipid desaturase activity. *Biochim Biophys Acta* **1299**, 117-123.
- Gould, S.B., Waller, R.F., and McFadden, G.I.** (2008). Plastid evolution. *Annu Rev Plant Biol* **59**, 491-517.
- Grasse, N., Mamedov, F., Becker, K., Styring, S., Rogner, M., and Nowaczyk, M.M.** (2011). Role of novel dimeric photosystem II (PSII)-Psb27 protein complex in PSII repair. *J Biol Chem* **286**, 29548-29555.
- Griese, M., Lange, C., and Soppa, J.** (2011). Ploidy in cyanobacteria. *FEMS Microbiol Lett* **323**, 124-131.
- Guskov, A., Kern, J., Gabdulkhakov, A., Broser, M., Zouni, A., and Saenger, W.** (2009). Cyanobacterial photosystem II at 2.9-Å resolution and the role of quinones, lipids, channels and chloride. *Nat Struct Mol Biol* **16**, 334-342.
- Hankamer, B., Morris, E., Nield, J., Carne, A., and Barber, J.** (2001). Subunit positioning and transmembrane helix organisation in the core dimer of photosystem II. *FEBS Lett* **504**, 142-151.
- Hayden, J.A., and Hendrich, M.P.** (2010). EPR spectroscopy and catalase activity of manganese-bound DNA-binding protein from nutrient starved cells. *J Biol Inorg Chem* **15**, 729-736.
- He, Q., and Vermaas, W.** (1998). Chlorophyll a availability affects *psbA* translation and D1 precursor processing in vivo in *Synechocystis* sp. PCC 6803. *Proc Natl Acad Sci USA* **95**, 5830-5835.
- Hinterstoisser, B., Chichna, M., Kuntner, O., and Peschek, G.A.** (1993). Cooperation of plasma and thylakoid membranes for the biosynthesis of chlorophyll in cyanobacteria: The role of the thylakoid centers. *J Plant Physiol* **142**, 407-413.
- Hooper, J.K., Boyd, C.O., and Paavola, L.G.** (1991). Origin of thylakoid membranes in *Chlamydomonas reinhardtii* y-1 at 38°C. *Plant Physiol* **96**, 1321-1328.
- Huang, J., Taylor, J.P., Chen, J.G., Uhrig, J.F., Schnell, D.J., Nakagawa, T., Korth, K.L., and Jones, A.M.** (2006). The plastid protein THYLAKOID FORMATION1 and the plasma membrane G-protein GPA1 interact in a novel sugar-signaling mechanism in *Arabidopsis*. *Plant Cell* **18**, 1226-1238.
- Hwang, H.J., and Burnap, R.L.** (2005). Multiflash experiments reveal a new kinetic phase of photosystem II manganese cluster assembly in *Synechocystis* sp. PCC 6803 in vivo. *Biochemistry* **44**, 9766-9774.

- Hwang, H.J., Nagarajan, A., McLain, A., and Burnap, R.L.** (2008). Assembly and disassembly of the photosystem II manganese cluster reversibly alters the coupling of the reaction center with the light-harvesting phycobilisome. *Biochemistry* **47**, 9747-9755.
- Ivleva, N.B., Shestakov, S.V., and Pakrasi, H.B.** (2000). The carboxyl-terminal extension of the precursor D1 protein of photosystem II is required for optimal photosynthetic performance of the cyanobacterium *Synechocystis* sp. PCC 6803. *Plant Physiol* **124**, 1403-1412.
- Jansèn, T., Kidron, H., Soitamo, A., Salminen, T., and Mäenpää, P.** (2003). Transcriptional regulation and structural modelling of the *Synechocystis* sp. PCC 6803 carboxyl-terminal endoprotease family. *FEMS Microbiol Lett* **228**, 121-128.
- Jansén, T., Kanervo, E., Aro, E.-A., Mäenpää, P.** (2002). Localisation and processing of the precursor form of photosystem II protein D1 in *Synechocystis* 6803. *J Plant Physiol* **159**, 1205-1211.
- Jordan, P., Fromme, P., Witt, H.T., Klukas, O., Saenger, W., and Krausz, N.** (2001). Three-dimensional structure of cyanobacterial photosystem I at 2.5 Å resolution. *Nature* **411**, 909-917.
- Joyard, J., Ferro, M., Masselon, C., Seigneurin-Berny, D., Salvi, D., Garin, J., and Rolland, N.** (2009). Chloroplast proteomics and the compartmentation of plastidial isoprenoid biosynthetic pathways. *Mol Plant* **2**, 1154-1180.
- Kaneko, T., Sato, S., Kotani, H., Tanaka, A., Asamizu, E., Nakamura, Y., Miyajima, N., Hirosawa, M., Sugiura, M., Sasamoto, S., Kimura, T., Hosouchi, T., Matsuno, A., Muraki, A., Nakazaki, N., Naruo, K., Okumura, S., Shimpo, S., Takeuchi, C., Wada, T., Watanabe, A., Yamada, M., Yasuda, M., and Tabata, S.** (1996). Sequence analysis of the genome of the unicellular cyanobacterium *Synechocystis* sp. strain PCC 6803. II. Sequence determination of the entire genome and assignment of potential protein-coding regions. *DNA Res* **3**, 109-136.
- Kashino, Y., Lauber, W.M., Carroll, J.A., Wang, Q., Whitmarsh, J., Satoh, K., and Pakrasi, H.B.** (2002). Proteomic analysis of a highly active photosystem II preparation from the cyanobacterium *Synechocystis* sp. PCC 6803 reveals the presence of novel polypeptides. *Biochemistry* **41**, 8004-8012.
- Kawakami, K., Umena, Y., Kamiya, N., and Shen, J.R.** (2011). Structure of the catalytic, inorganic core of oxygen-evolving photosystem II at 1.9 Å resolution. *J Photochem Photobiol B* **104**, 9-18.
- Kelly, A.A., and Dormann, P.** (2004). Green light for galactolipid trafficking. *Curr Opin Plant Biol* **7**, 262-269.
- Keren, N., Liberton, M., and Pakrasi, H.B.** (2005a). Photochemical competence of assembled photosystem II core complex in cyanobacterial plasma membrane. *J Biol Chem* **280**, 6548-6553.
- Keren, N., Kidd, M.J., Penner-Hahn, J.E., and Pakrasi, H.B.** (2002). A light-dependent mechanism for massive accumulation of manganese in the photosynthetic bacterium *Synechocystis* sp. PCC 6803. *Biochemistry* **41**, 15085-15092.
- Keren, N., Ohkawa, H., Welsh, E.A., Liberton, M., and Pakrasi, H.B.** (2005b). Psb29, a conserved 22-kD protein, functions in the biogenesis of photosystem II complexes in *Synechocystis* and *Arabidopsis*. *Plant Cell* **17**, 2768-2781.
- Kim, J., Eichacker, L.A., Rudiger, W., and Mullet, J.E.** (1994). Chlorophyll regulates accumulation of the plastid-encoded chlorophyll proteins P700 and D1 by increasing apoprotein stability. *Plant Physiol* **104**, 907-916.
- Klinkert, B., Ossenbühl, F., Sikorski, M., Berry, S., Eichacker, L., and Nickelsen, J.** (2004). PratA, a periplasmic tetratricopeptide repeat protein involved in biogenesis of photosystem II in *Synechocystis* sp. PCC 6803. *J Biol Chem* **279**, 44639-44644.
- Komenda, J., Sobotka, R., and Nixon, P.J.** (2012a). Assembling and maintaining the photosystem II complex in chloroplasts and cyanobacteria. *Curr Opin Plant Biol* **15**, 245-251.
- Komenda, J., Hassan, H.A., Diner, B.A., Debus, R.J., Barber, J., and Nixon, P.J.** (2000). Degradation of the photosystem II D1 and D2 proteins in different strains of the cyanobacterium *Synechocystis* PCC 6803 varying with respect to the type and level of *psbA* transcript. *Plant Mol Biol* **42**, 635-645.

- Komenda, J., Reisinger, V., Müller, B.C., Dobáková, M., Granvogl, B., and Eichacker, L.A.** (2004). Accumulation of the D2 protein is a key regulatory step for assembly of the photosystem II reaction center complex in *Synechocystis* PCC 6803. *J Biol Chem* **279**, 48620-48629.
- Komenda, J., Kuvikova, S., Granvogl, B., Eichacker, L.A., Diner, B.A., and Nixon, P.J.** (2007). Cleavage after residue Ala352 in the C-terminal extension is an early step in the maturation of the D1 subunit of photosystem II in *Synechocystis* PCC 6803. *Biochim Biophys Acta* **1767**, 829-837.
- Komenda, J., Nickelsen, J., Tichy, M., Prasil, O., Eichacker, L.A., and Nixon, P.J.** (2008). The cyanobacterial homologue of HCF136/YCF48 is a component of an early photosystem II assembly complex and is important for both the efficient assembly and repair of photosystem II in *Synechocystis* sp. PCC 6803. *J Biol Chem* **283**, 22390-22399.
- Komenda, J., Barker, M., Kuvikova, S., de Vries, R., Mullineaux, C.W., Tichy, M., and Nixon, P.J.** (2006). The FtsH protease slr0228 is important for quality control of photosystem II in the thylakoid membrane of *Synechocystis* sp. PCC 6803. *J Biol Chem* **281**, 1145-1151.
- Komenda, J., Knoppova, J., Kopečná, J., Sobotka, R., Halada, P., Yu, J., Nickelsen, J., Boehm, M., and Nixon, P.J.** (2012b). The Psb27 assembly factor binds to the CP43 complex of photosystem II in the cyanobacterium *Synechocystis* sp. PCC 6803. *Plant Physiol* **158**, 476-486.
- Kopečná, J., Sobotka, R., and Komenda, J.** (2012a). Inhibition of chlorophyll biosynthesis at the protochlorophyllide reduction step results in the parallel depletion of photosystem I and photosystem II in the cyanobacterium *Synechocystis* PCC 6803. *Planta*.
- Kopečná, J., Komenda, J., Bucinska, L., and Sobotka, R.** (2012b). Long-term acclimation of the cyanobacterium *Synechocystis* PCC 6803 to high light is accompanied by an enhanced production of chlorophyll that is preferentially channeled to trimeric PSI. *Plant Physiol*.
- Krieger-Liszskay, A., Fufezan, C., and Trebst, A.** (2008). Singlet oxygen production in photosystem II and related protection mechanism. *Photosynth Res* **98**, 551-564.
- Kroll, D., Meierhoff, K., Bechtold, N., Kinoshita, M., Westphal, S., Vothknecht, U.C., Soll, J., and Westhoff, P.** (2001). VIPP1, a nuclear gene of *Arabidopsis thaliana* essential for thylakoid membrane formation. *Proc Natl Acad Sci USA* **98**, 4238-4242.
- Kubota, H., Sakurai, I., Katayama, K., Mizusawa, N., Ohashi, S., Kobayashi, M., Zhang, P., Aro, E.M., and Wada, H.** (2010). Purification and characterization of photosystem I complex from *Synechocystis* sp. PCC 6803 by expressing histidine-tagged subunits. *Biochim Biophys Acta* **1797**, 98-105.
- Kufryk, G.I., and Vermaas, W.F.** (2001). A novel protein involved in the functional assembly of the oxygen-evolving complex of photosystem II in *Synechocystis* sp. PCC 6803. *Biochemistry* **40**, 9247-9255.
- Kufryk, G.I., and Vermaas, W.F.** (2003). Slr2013 is a novel protein regulating functional assembly of photosystem II in *Synechocystis* sp. strain PCC 6803. *J Bacteriol* **185**, 6615-6623.
- Kunkel, D.D.** (1982). Thylakoid centers: structures associated with the cyanobacterial photosynthetic membrane system. *Arch Microbiol* **133**, 97-99.
- Kurusu, G., Zhang, H., Smith, J.L., and Cramer, W.A.** (2003). Structure of the cytochrome  $b_6f$  complex of oxygenic photosynthesis: tuning the cavity. *Science* **302**, 1009-1014.
- Kuvikova, S., Tichy, M., and Komenda, J.** (2005). A role of the C-terminal extension of the photosystem II D1 protein in sensitivity of the cyanobacterium *Synechocystis* PCC 6803 to photoinhibition. *Photochem Photobiol Sci* **4**, 1044-1048.
- Larkin, R.M., Alonso, J.M., Ecker, J.R., and Chory, J.** (2003). GUN4, a regulator of chlorophyll synthesis and intracellular signaling. *Science* **299**, 902-906.
- Lehtimäki, N., Lintala, M., Allahverdiyeva, Y., Aro, E.-M., and Mulo, P.** (2010). Drought stress-induced upregulation of components involved in ferredoxin-dependent cyclic electron transfer. *J Plant Physiol* **167**, 1018-1022.
- Liberton, M., and Pakrasi, H.B.** (2008). Membrane systems in cyanobacteria. In *The cyanobacteria: Molecular biology, genomics and evolution*, A. Herrero and E. Flores, eds (Norfolk, UK: Caister Academic Press).

- Liberton, M., Howard Berg, R., Heuser, J., Roth, R., and Pakrasi, H.B.** (2006). Ultrastructure of the membrane systems in the unicellular cyanobacterium *Synechocystis* sp. strain PCC 6803. *Protoplasma* **227**, 129-138.
- Liochev, S.I., and Fridovich, I.** (1999). Superoxide and iron: Partners in crime. *IUBMB Life* **48**, 157-161.
- Liu, H., Roose, J.L., Cameron, J.C., and Pakrasi, H.B.** (2011a). A genetically tagged Psb27 protein allows purification of two consecutive photosystem II (PSII) assembly intermediates in *Synechocystis* 6803, a cyanobacterium. *J Biol Chem* **286**, 24865-24871.
- Liu, H., Huang, R.Y., Chen, J., Gross, M.L., and Pakrasi, H.B.** (2011b). Psb27, a transiently associated protein, binds to the chlorophyll binding protein CP43 in photosystem II assembly intermediates. *Proc Natl Acad Sci USA* **108**, 18536-18541.
- Loll, B., Kern, J., Saenger, W., Zouni, A., and Biesiadka, J.** (2005). Towards complete cofactor arrangement in the 3.0 Å resolution structure of photosystem II. *Nature* **438**, 1040-1044.
- Ma, J., Peng, L., Guo, J., Lu, Q., Lu, C., and Zhang, L.** (2007). LPA2 is required for efficient assembly of photosystem II in *Arabidopsis thaliana*. *Plant Cell* **19**, 1980-1993.
- Mabbitt, P.D., Rautureau, G.J., Day, C.L., Wilbanks, S.M., Eaton-Rye, J.J., and Hinds, M.G.** (2009). Solution structure of Psb27 from cyanobacterial photosystem II. *Biochemistry* **48**, 8771-8773.
- Manna, P., and Vermaas, W.** (1997). Mutational studies on conserved histidine residues in the chlorophyll-binding protein CP43 of photosystem II. *Eur J Biochem* **247**, 666-672.
- Maresca, J.A., Graham, J.E., and Bryant, D.A.** (2008). The biochemical basis for structural diversity in the carotenoids of chlorophototrophic bacteria. *Photosynth Res* **97**, 121-140.
- Masuda, T.** (2008). Recent overview of the Mg branch of the tetrapyrrole biosynthesis leading to chlorophylls. *Photosynth Res* **96**, 121-143.
- McKay, R.M.L., and Gibbs, S.P.** (1991). Composition and function of pyrenoids: cytochemical and immunocytochemical approaches. *Can J Bot* **69**, 1040-1052.
- Meier, A.E., Whittaker, M.M., and Whittaker, J.W.** (1996). EPR polarization studies on Mn catalase from *Lactobacillus plantarum*. *Biochemistry* **35**, 348-360.
- Meurer, J., Plücker, H., Kowalik, K.V., and Westhoff, P.** (1998). A nuclear-encoded protein of prokaryotic origin is essential for the stability of photosystem II in *Arabidopsis thaliana*. *EMBO J* **17**, 5286-5297.
- Michoux, F., Takasaka, K., Boehm, M., Komenda, J., Nixon, P.J., and Murray, J.W.** (2012). Crystal structure of the Psb27 assembly factor at 1.6 Å: implications for binding to photosystem II. *Photosynth Res* **110**, 169-175.
- Moore, M., Harrison, M.S., Peterson, E.C., and Henry, R.** (2000). Chloroplast Oxa1p homolog Albino3 is required for post-translational integration of the light harvesting chlorophyll-binding protein into thylakoid membranes. *J Biol Chem* **275**, 1529-1532.
- Mühlethaler, K., and Frey-Wyssing, A.** (1959). Entwicklung und Struktur der Proplastiden. *J Biophys Biochem Cytol* **6**, 507-512.
- Mullineaux, C.W.** (1992). Excitation energy transfer from phycobilisomes to photosystem I in a cyanobacterium. *Biochim Biophys Acta* **1100**, 285-292.
- Mullineaux, C.W., and Allen, C.F.** (1990). State 1-State 2 transitions in the cyanobacterium *Synechococcus* 6301 are controlled by the redox state of electron carriers between photosystems I and II. *Photosynth Res* **23**, 297-311.
- Mulo, P., Sakurai, I., and Aro, E.M.** (2012). Strategies for *psbA* gene expression in cyanobacteria, green algae and higher plants: from transcription to PSII repair. *Biochim Biophys Acta* **1817**, 247-257.
- Mulo, P., Sirpiö, S., Suorsa, M., and Aro, E.M.** (2008). Auxiliary proteins involved in the assembly and sustenance of photosystem II. *Photosynth Res* **98**, 489-501.
- Najafpour, M.M., Moghaddam, A.N., Yang, Y.N., Aro, E.M., Carpentier, R., Eaton-Rye, J.J., Lee, C.H., and Allakhverdiev, S.I.** (2012). Biological water-oxidizing complex: a nano-sized manganese-calcium oxide in a protein environment. *Photosynth Res* **114**, 1-13.
- Nelson, N.** (2011). Photosystems and global effects of oxygenic photosynthesis. *Biochim Biophys Acta* **1807**, 856-863.
- Nelson, N., and Ben-Shem, A.** (2004). The complex architecture of oxygenic photosynthesis. *Nat Rev Mol Cell Biol* **5**, 971-982.

- Nelson, N., and Yocum, C.F. (2006). Structure and function of photosystems I and II. *Annu Rev Plant Biol* **57**, 521-565.
- Nevo, R., Charuvi, D., Shimon, E., Schwarz, R., Kaplan, A., Ohad, I., and Reich, Z. (2007). Thylakoid membrane perforations and connectivity enable intracellular traffic in cyanobacteria. *EMBO J* **26**, 1467-1473.
- Nixon, P.J., Trost, J.T., and Diner, B.A. (1992). Role of the carboxy terminus of polypeptide D1 in the assembly of a functional water-oxidizing manganese cluster in photosystem II of the cyanobacterium *Synechocystis* sp. PCC 6803: assembly requires a free carboxyl group at C-terminal position 344. *Biochemistry* **31**, 10859-10871.
- Nixon, P.J., Barker, M., Boehm, M., de Vries, R., and Komenda, J. (2005). FtsH-mediated repair of the photosystem II complex in response to light stress. *J Exp Bot* **56**, 357-363.
- Nixon, P.J., Michoux, F., Yu, J., Boehm, M., and Komenda, J. (2010). Recent advances in understanding the assembly and repair of photosystem II. *Ann Bot* **106**, 1-16.
- Nowaczyk, M.M., Hebeler, R., Schlodder, E., Meyer, H.E., Warscheid, B., and Rögner, M. (2006). Psb27, a cyanobacterial lipoprotein, is involved in the repair cycle of photosystem II. *Plant Cell* **18**, 3121-3131.
- Nowaczyk, M.M., Krause, K., Mieseler, M., Sczibilanski, A., Ikeuchi, M., and Rögner, M. (2012). Deletion of *psbJ* leads to accumulation of Psb27-Psb28 photosystem II complexes in *Thermosynechococcus elongatus*. *Biochim Biophys Acta* **1817**, 1339-1345.
- Ogawa, T., Bao, D.H., Katoh, H., Shibata, M., Pakrasi, H.B., and Bhattacharyya-Pakrasi, M. (2002). A two-component signal transduction pathway regulates manganese homeostasis in *Synechocystis* 6803, a photosynthetic organism. *J Biol Chem* **277**, 28981-28986.
- Ossenbühl, F., Inaba-Sulpice, M., Meurer, J., Soll, J., and Eichacker, L.A. (2006). The *Synechocystis* sp PCC 6803 Oxa1 homolog is essential for membrane integration of reaction center precursor protein pD1. *Plant Cell* **18**, 2236-2246.
- Ossenbühl, F., Göhre, V., Meurer, J., Krieger-Liszkay, A., Rochaix, J.D., and Eichacker, L.A. (2004). Efficient assembly of photosystem II in *Chlamydomonas reinhardtii* requires Alb3.1p, a homolog of *Arabidopsis* ALBINO3. *Plant Cell* **16**, 1790-1800.
- Pasch, J., Nickelsen, J., and Schünemann, D. (2005). The yeast split-ubiquitin system to study chloroplast membrane protein interactions. *Appl Microbiol Biotechnol* **69**, 440-447.
- Peña, M.M.O., Lee, J., and Thiele, D.J. (1999). A delicate balance: homeostatic control of copper uptake and distribution. *J Nutr* **129**, 1251-1260.
- Peng, L., Ma, J., Chi, W., Guo, J., Zhu, S., Lu, Q., Lu, C., and Zhang, L. (2006). LOW PSII ACCUMULATION1 is involved in efficient assembly of photosystem II in *Arabidopsis thaliana*. *Plant Cell* **18**, 955-969.
- Peschek, G.A., Obinger, C., and Paumann, M. (2004). The respiratory chain of blue-green algae (cyanobacteria). *Physiol Plant* **120**, 358-369.
- Peschek, G.A., Hinterstoisser, B., Wastyn, M., Kuntner, O., Pineau, B., Missbichler, A., and Lang, J. (1989). Chlorophyll precursors in the plasma membrane of a cyanobacterium, *Anacystis nidulans*. Characterization of protochlorophyllide and chlorophyllide by spectrophotometry, spectrofluorimetry, solvent partition, and high performance liquid chromatography. *J Biol Chem* **264**, 11827-11832.
- Pisareva, T., Kwon, J., Oh, J., Kim, S., Ge, C., Wieslander, A., Choi, J.S., and Norling, B. (2011). Model for membrane organization and protein sorting in the cyanobacterium *Synechocystis* sp. PCC 6803 inferred from proteomics and multivariate sequence analyses. *J Proteome Res* **10**, 3617-3631.
- Plücken, H., Müller, B., Grohmann, D., Westhoff, P., and Eichacker, L.A. (2002). The HCF136 protein is essential for assembly of the photosystem II reaction center in *Arabidopsis thaliana*. *FEBS Lett* **532**, 85-90.
- Reinbothe, C., El Bakkouri, M., Buhr, F., Muraki, N., Nomata, J., Kurisu, G., Fujita, Y., and Reinbothe, S. (2010). Chlorophyll biosynthesis: spotlight on protochlorophyllide reduction. *Trends Plant Sci* **15**, 614-624.
- Rexroth, S., Mullineaux, C.W., Ellinger, D., Sendtko, E., Rögner, M., and Koenig, F. (2011). The plasma membrane of the cyanobacterium *Gloeobacter violaceus* contains segregated bioenergetic domains. *Plant Cell* **23**, 2379-2390.

- Rippka, R., Waterbury, J., and Cohenbazire, G.** (1974). A cyanobacterium which lacks thylakoids. *Arch Microbiol* **100**, 419-436.
- Rokka, A., Suorsa, M., Saleem, A., Battchikova, N., and Aro, E.M.** (2005). Synthesis and assembly of thylakoid protein complexes: multiple assembly steps of photosystem II. *Biochem J* **388**, 159-168.
- Roose, J.L., and Pakrasi, H.B.** (2004). Evidence that D1 processing is required for manganese binding and extrinsic protein assembly into photosystem II. *J Biol Chem* **279**, 45417-45422.
- Roose, J.L., and Pakrasi, H.B.** (2008). The Psb27 protein facilitates manganese cluster assembly in photosystem II. *J Biol Chem* **283**, 4044-4050.
- Saenger, W., Jordan, P., and Krauß, N.** (2002). The assembly of protein subunits and cofactors in photosystem I. *Curr Opin Struct Biol* **12**, 244-254.
- Samsonoff, W.A., and MacColl, R.** (2001). Biliproteins and phycobilisomes from cyanobacteria and red algae at the extremes of habitat. *Arch Microbiol* **176**, 400-405.
- Satoh, K., and Yamamoto, Y.** (2007). The carboxyl-terminal processing of precursor D1 protein of the photosystem II reaction center. *Photosynth Res* **94**, 203-215.
- Schneider, D., Fuhrmann, E., Scholz, I., Hess, W.R., and Graumann, P.L.** (2007). Fluorescence staining of live cyanobacterial cells suggest non-stringent chromosome segregation and absence of a connection between cytoplasmic and thylakoid membranes. *BMC Cell Biol* **8**, 39.
- Schoefs, B., and Franck, F.** (2003). Protochlorophyllide reduction: mechanisms and evolutions. *Photochem Photobiol* **78**, 543-557.
- Schottkowski, M., Ratke, J., Oster, U., Nowaczyk, M., and Nickelsen, J.** (2009a). Pitt, a novel tetratricopeptide repeat protein involved in light-dependent chlorophyll biosynthesis and thylakoid membrane biogenesis in *Synechocystis* sp. PCC 6803. *Mol Plant* **2**, 1289-1297.
- Schottkowski, M., Gkalypoudis, S., Tzekova, N., Stelljes, C., Schünemann, D., Ankele, E., and Nickelsen, J.** (2009b). Interaction of the periplasmic PrtA factor and the PsbA (D1) protein during biogenesis of photosystem II in *Synechocystis* sp. PCC 6803. *J Biol Chem* **284**, 1813-1819.
- Shen, G., and Vermaas, W.F.** (1994). Mutation of chlorophyll ligands in the chlorophyll-binding CP47 protein as studied in a *Synechocystis* sp. PCC 6803 photosystem I-less background. *Biochemistry* **33**, 7379-7388.
- Shestakov, S.V., Anbudurai, P.R., Stanbekova, G.E., Gadzhiev, A., Lind, L.K., and Pakrasi, H.B.** (1994). Molecular cloning and characterization of the *ctpA* gene encoding a carboxyl-terminal processing protease. Analysis of a spontaneous photosystem II-deficient mutant strain of the cyanobacterium *Synechocystis* sp. PCC 6803. *J Biol Chem* **269**, 19354-19359.
- Shi, L.X., Hall, M., Funk, C., and Schroder, W.P.** (2012). Photosystem II, a growing complex: updates on newly discovered components and low molecular mass proteins. *Biochim Biophys Acta* **1817**, 13-25.
- Shimoni, E., Rav-Hon, O., Ohad, I., Brumfeld, V., and Reich, Z.** (2005). Three-dimensional organization of higher-plant chloroplast thylakoid membranes revealed by electron tomography. *Plant Cell* **17**, 2580-2586.
- Smith, D., and Howe, C.J.** (1993). The distribution of photosystem I and photosystem II polypeptides between the cytoplasmic and thylakoid membranes of cyanobacteria. *FEMS Microbiol Lett* **110**, 341-347.
- Sobotka, R., Komenda, J., Bumba, L., and Tichy, M.** (2005). Photosystem II assembly in *cp47* mutant of *Synechocystis* sp. PCC 6803 is dependent on the level of chlorophyll precursors regulated by ferrochelatase. *J Biol Chem* **280**, 31595-31602.
- Sobotka, R., Dühring, U., Komenda, J., Peter, E., Gardian, Z., Tichy, M., Grimm, B., and Wilde, A.** (2008). Importance of the cyanobacterial Gun4 protein for chlorophyll metabolism and assembly of photosynthetic complexes. *J Biol Chem* **283**, 25794-25802.
- Soll, J., Schultz, G., Rüdiger, W., and Benz, J.** (1983). Hydrogenation of geranylgeraniol: Two pathways exist in spinach chloroplasts. *Plant Physiol* **71**, 849-854.
- Sozer, O., Komenda, J., Ughy, B., Domonkos, I., Laczko-Dobos, H., Malec, P., Gombos, Z., and Kis, M.** (2010). Involvement of carotenoids in the synthesis and assembly of protein subunits of photosynthetic reaction centers of *Synechocystis* sp. PCC 6803. *Plant Cell Physiol* **51**, 823-835.

- Spence, E., Bailey, S., Nenninger, A., Moller, S.G., and Robinson, C. (2004). A homolog of Albino3/Oxa1 is essential for thylakoid biogenesis in the cyanobacterium *Synechocystis* sp. PCC6803. *J Biol Chem* **279**, 55792-55800.
- Srivastava, R., Battchikova, N., Norling, B., and Aro, E.M. (2006). Plasma membrane of *Synechocystis* PCC 6803: a heterogeneous distribution of membrane proteins. *Arch Microbiol* **185**, 238-243.
- Standfuss, J., Terwisscha van Scheltinga, A.C., Lamborghini, M., and Kuhlbrandt, W. (2005). Mechanisms of photoprotection and nonphotochemical quenching in pea light-harvesting complex at 2.5 Å resolution. *EMBO J* **24**, 919-928.
- Stroebel, D., Choquet, Y., Popot, J.L., and Picot, D. (2003). An atypical haem in the cytochrome  $b_6/f$  complex. *Nature* **426**, 413-418.
- Takahashi, T., Inoue-Kashino, N., Ozawa, S., Takahashi, Y., Kashino, Y., and Satoh, K. (2009). Photosystem II complex in vivo is a monomer. *J Biol Chem* **284**, 15598-15606.
- Tottey, S., Waldron, K.J., Firbank, S.J., Reale, B., Bessant, C., Sato, K., Cheek, T.R., Gray, J., Banfield, M.J., Dennison, C., and Robinson, N.J. (2008). Protein-folding location can regulate manganese-binding versus copper- or zinc-binding. *Nature* **455**, 1138-1142.
- Umena, Y., Kawakami, K., Shen, J.R., and Kamiya, N. (2011). Crystal structure of oxygen-evolving photosystem II at a resolution of 1.9 Å. *Nature* **473**, 55-60.
- Uniacke, J., and Zerges, W. (2007). Photosystem II assembly and repair are differentially localized in *Chlamydomonas*. *Plant Cell* **19**, 3640-3654.
- van de Meene, A., Hohmann-Marriott, M., Vermaas, W., and Roberson, R. (2006). The three-dimensional structure of the cyanobacterium *Synechocystis* sp. PCC 6803. *Arch Microbiol* **184**, 259-270.
- van de Meene, A.M., Sharp, W.P., McDaniel, J.H., Friedrich, H., Vermaas, W.F., and Roberson, R.W. (2012). Gross morphological changes in thylakoid membrane structure are associated with photosystem I deletion in *Synechocystis* sp. PCC 6803. *Biochim Biophys Acta* **1818**, 1427-1434.
- Vavilin, D., Brune, D.C., and Vermaas, W. (2005).  $^{15}\text{N}$ -labeling to determine chlorophyll synthesis and degradation in *Synechocystis* sp. PCC 6803 strains lacking one or both photosystems. *Biochim Biophys Acta* **1708**, 91-101.
- Vavilin, D., Yao, D., and Vermaas, W. (2007). Small Cab-like proteins retard degradation of photosystem II-associated chlorophyll in *Synechocystis* sp. PCC 6803: kinetic analysis of pigment labeling with  $^{15}\text{N}$  and  $^{13}\text{C}$ . *J Biol Chem* **282**, 37660-37668.
- Vermaas, W.F.J. (1994). Molecular-genetic approaches to study photosynthetic and respiratory electron transport in thylakoids from cyanobacteria. *Biochim Biophys Acta* **1187**, 181-186.
- Vothknecht, U.C., Otters, S., Hennig, R., and Schneider, D. (2012). Vipp1: a very important protein in plastids?! *J Exp Bot* **63**, 1699-1712.
- Wang, Q., Sullivan, R.W., Kight, A., Henry, R.L., Huang, J., Jones, A.M., and Korth, K.L. (2004). Deletion of the chloroplast-localized Thylakoid formation1 gene product in *Arabidopsis* leads to deficient thylakoid formation and variegated leaves. *Plant Physiol* **136**, 3594-3604.
- Wegener, K.M., Bennewitz, S., Oelmüller, R., and Pakrasi, H.B. (2011). The Psb32 protein aids in repairing photodamaged photosystem II in the cyanobacterium *Synechocystis* 6803. *Mol Plant* **4**, 1052-1061.
- Wegener, K.M., Welsh, E.A., Thornton, L.E., Keren, N., Jacobs, J.M., Hixson, K.K., Monroe, M.E., Camp, D.G., 2nd, Smith, R.D., and Pakrasi, H.B. (2008). High sensitivity proteomics assisted discovery of a novel operon involved in the assembly of photosystem II, a membrane protein complex. *J Biol Chem* **283**, 27829-27837.
- Westphal, S., Heins, L., Soll, J., and Vothknecht, U.C. (2001). Vipp1 deletion mutant of *Synechocystis*: a connection between bacterial phage shock and thylakoid biogenesis? *Proc Natl Acad Sci USA* **98**, 4243-4248.
- Yamamoto, T., Burke, J., Autz, G., and Jagendorf, A.T. (1981). Bound ribosomes of pea chloroplast thylakoid membranes: Location and release in vitro by high salt, puromycin, and RNase. *Plant Physiol* **67**, 940-949.
- Yao, D.C., Brune, D.C., and Vermaas, W.F. (2012a). Lifetimes of photosystem I and II proteins in the cyanobacterium *Synechocystis* sp. PCC 6803. *FEBS Lett* **586**, 169-173.

- Yao, D.C., Brune, D.C., Vavilin, D., and Vermaas, W.F.** (2012b). Photosystem II component lifetimes in the cyanobacterium *Synechocystis* sp. strain PCC 6803: small Cab-like proteins stabilize biosynthesis intermediates and affect early steps in chlorophyll synthesis. *J Biol Chem* **287**, 682-692.
- Zak, E., Norling, B., Maitra, R., Huang, F., Andersson, B., and Pakrasi, H.B.** (2001). The initial steps of biogenesis of cyanobacterial photosystems occur in plasma membranes. *Proc Natl Acad Sci USA* **98**, 13443-13448.
- Zaltsman, L., Ananyev, G.M., Bruntrager, E., and Dismukes, G.C.** (1997). Quantitative kinetic model for photoassembly of the photosynthetic water oxidase from its inorganic constituents: requirements for manganese and calcium in the kinetically resolved steps. *Biochemistry* **36**, 8914-8922.
- Zhang, D., Zhou, G., Liu, B., Kong, Y., Chen, N., Qiu, Q., Yin, H., An, J., Zhang, F., and Chen, F.** (2011). *HCF243* encodes a chloroplast-localized protein involved in the D1 protein stability of the *Arabidopsis* photosystem II complex. *Plant Physiol* **157**, 608-619.
- Zhang, L., Li, Y., Wang, Z., Xia, Y., Chen, W., and Tang, K.** (2007). Recent developments and future prospects of *Vitreoscilla* hemoglobin application in metabolic engineering. *Biotechnol Adv* **25**, 123-136.
- Zhang, S., Frankel, L.K., and Bricker, T.M.** (2010). The Sll0606 protein is required for photosystem II assembly/stability in the cyanobacterium *Synechocystis* sp. PCC 6803. *J Biol Chem* **285**, 32047-32054.
- Zhu, Y., Graham, J.E., Ludwig, M., Xiong, W., Alvey, R.M., Shen, G., and Bryant, D.A.** (2010). Roles of xanthophyll carotenoids in protection against photoinhibition and oxidative stress in the cyanobacterium *Synechococcus* sp. strain PCC 7002. *Arch Biochem Biophys* **504**, 86-99.

## 6 APPENDIX

### MANUSCRIPT: PHOTOSYSTEM II ASSEMBLY: FROM CYANOBACTERIA TO PLANTS

Nickelsen, J., and Rengstl, B. (submitted) *Annu Rev Plant Biol*

#### Abstract

Photosystem II (PSII) is an integral membrane, multisubunit complex which initiates electron flow in oxygenic photosynthesis. The biogenesis of this complex machine involves the concerted assembly of at least twenty different polypeptides as well as the incorporation of a variety of inorganic and organic cofactors. Many factors have recently been identified which constitute an integrative network mediating the stepwise assembly of PSII components. One reoccurring theme is the subcellular organization of the assembly process in specialized membranes forming distinct biogenesis centers. Here, we provide a review on our current knowledge of the molecular components and events involved in PSII assembly and their high degree of evolutionary conservation.

#### Introduction

The invention of oxygenic photosynthesis by cyanobacteria 2.4 billion years ago triggered dramatic changes in the Earth's physiognomy and biosphere. The most momentous was the resulting rise in the level of molecular oxygen in the atmosphere. By enabling energy production via respiration, O<sub>2</sub> provided the basis for the development of aerobic complex life forms and of almost all biomass on Earth (43). The initial chemical reaction is the extraction of electrons from water; these are then used to fuel the photosynthetic electron transport (PET) chain, generating the chemical energy carriers NADPH and ATP. The constituents of PET include small, mobile electron carriers like plastoquinone and plastocyanin, as well as the multisubunit protein/pigment complexes photosystems I and II (PSI, PSII) and the cytochrome b<sub>6</sub>f complex, all of which are associated with a specialized membrane system known as the thylakoids (30).

During the course of evolution from early prokaryotic cyanobacteria to modern vascular plants containing chloroplasts of endosymbiotic origin (see sidebar), the core machinery for PET has been conserved (5). The only exception is among the peripheral components of the photosynthetic apparatus, the bulky extrinsic phycobilisomes of cyanobacteria and red algae

were replaced by membrane-intrinsic light-harvesting complexes (LHCs) in green algae and plants (Figure 1A; 5).

Independently of its role in the evolutionary context, PSII represents the heart of photosynthesis. By serving as a light-driven water plastoquinone oxidoreductase, it mediates initial charge separation to generate the high-energy electrons for PET. Apart from minor differences in subunit composition, the PSII core with a molecular weight of ca. 350 kDa is conserved from cyanobacteria to plants. It consists of at least 20 protein subunits, 35 chlorophylls, 2 pheophytins, 11  $\beta$ -carotenes, 2 plastoquinones, 2 hemes, 1 non-heme iron and the  $Mn_4CaO_5$  cluster that catalyzes the splitting of water and  $O_2$  production (Figure 1A; 5; 128). Recently, the structure of cyanobacterial PSII was solved at close to atomic resolution, revealing fine details of the  $Mn_4CaO_5$  cluster (128). A comprehensive overview of the structural organization of PSII is provided by Shen et al. in this volume.

Although our current knowledge of the structure/function of PSII is quite extensive, comparatively little is known about how it is put together during development of the TM system. However, recent genetic and biochemical work has provided initial insights into the process of PSII biogenesis. Two major findings have emerged: (i) PSII assembly is a highly ordered process, and (ii) large numbers of accessory factors are involved in formation of the multiprotein complex and the incorporation of the various cofactors. How then do these factors work? A second question that arises is how the assembly of photosynthetic complexes is coordinated spatially within the context of the biogenesis of the TM system. Where in the cell does PSII assembly take place, and – why there and not elsewhere? A third issue concerns one special feature of PSII – its sensitivity to photodamage, which is manifested in the high turnover rate of its D1 subunit. Replacement of damaged D1 involves partial disassembly and subsequent rebuilding of PSII. Consequently, two fundamentally different PSII assembly pathways must be considered: one for the *de novo* assembly of all its subunits and cofactors, and one for the repair of its D1 subunit alone (Figure 1B). – And this immediately raises the question of the interrelationship between the two pathways.

Here, we will address these three problems by summarizing recent advances in our knowledge of the molecular details of PSII assembly, from cyanobacteria to plants.

## **PSII assembly is a highly ordered process**

### Principal steps in PSII assembly

Pioneering work by Eichacker and Komenda established the basic steps in PSII assembly. These occur in a sequential manner and are highly coordinated in the model cyanobacterium

*Synechocystis* sp. PCC 6803 (hereafter *Synechocystis* 6803) (61; 91). A combination of 2D BN/SDS PAGE and radioisotopic pulse-labeling of proteins in different mutant backgrounds has allowed visualization of distinct PSII assembly intermediates, which indicated that PSII basically grows outwards from the reaction center (Figure 2A). It was later shown that a similar pathway exists in the chloroplasts of eukaryotic algae and plants, suggesting that both the core subunits of PSII and their mode of assembly are highly conserved (Figure 2B; 95; 106).

The first transiently accumulating intermediate subcomplex of PSII is the so-called reaction center (RC) complex consisting of the D1, D2, cyt  $b_{559}$  and PsbI subunits (Figure 2). Its formation represents the endpoint of an “early” phase of PSII biogenesis which is initiated by the synthesis of cyt  $b_{559}$  as a precondition for the accumulation of D2 via formation of a D2-cyt  $b_{559}$  subcomplex (61). This complex then serves as a platform for the incorporation of a dimer comprising the D1 precursor (pD1) and PsbI, which was independently formed upon integration of D1 into the membrane (29). During formation of the RC complex pD1 is processed at its C-terminus by the CtpA protease, yielding mature D1 (see sidebar).

The RC complex is then converted into an RC47 complex containing the inner antenna protein CP47 but not CP43 (Figure 2). Like D2 and D1, CP47 is first integrated into the membrane separately, and forms a precomplex with several low molecular mass (LMM) PSII subunits. In cyanobacteria, these include PsbH, PsbT and PsbL, whereas in spinach chloroplasts, PsbH is thought to join the RC complex after CP47 (13; 106). In the next step, RC47 incorporates a preformed complex comprising the second inner antenna protein CP43 and PsbK, Psb30 and PsbZ in the case of cyanobacteria, and at least PsbK in case of chloroplasts from the green alga *Chlamydomonas reinhardtii* (12; 124). Subsequently, monomeric PSII (PSII [1]) is generated after formation of a transient intermediate consisting of PSII and an assembly factor called Psb27 in cyanobacteria and LPA19 in chloroplasts (Figure 2A, B; see below).

Upon attachment of CP43, PSII [1] can provide all amino acid residues required for the light-driven assembly of the oxygen-evolving  $Mn_4CaO_5$  cluster, a process known as “photoactivation” (25). Furthermore, the extrinsic subunits PsbO, PsbV, PsbU, PsbP and PsbQ that stabilize the  $Mn_4CaO_5$  cluster are attached at the luminal side of cyanobacterial PSII. In chloroplasts, this shielding cap is formed by PsbO, PsbP and PsbQ (15). When the remaining LMM proteins of PSII are integrated into the complex is not known.

The accepted view is that active PSII located in TMs then forms dimers (PSII [2]; 63), and a function in this dimerization process has been ascribed to some of the LMM subunits, such as

PsbW, PsbI and PsbM (116). Finally, the peripheral antennae are attached to the core complex and PSII supercomplexes are formed (63).

Generally speaking, then, PSII is assembled in essentially the same order in cyanobacteria and chloroplasts. This reflects the conservation of the subunits involved and the need for careful coordination of the process.

#### Networks of facilitating assembly factors

Concomitantly with the discovery of the PSII assembly pathway, a combination of genetic and biochemical approaches identified several facilitating factors. These do not form part of functional PSII but interact transiently with distinct assembly intermediates (Table 1; 86; 91). Not surprisingly, in light of the conserved nature of the process as a whole, many – but not all – of the assembly factors are represented by orthologous proteins found in all photoautotrophic organisms (Table 1). In eukaryotes, all are encoded by the nuclear genome and have to be imported into the chloroplast. In the following, the factors identified so far are described. Their molecular functions and interrelationships imply that a network of assembly factors monitors the building of PSII from beginning to end (103).

##### *a) Factors involved in RC complex formation – the early phase*

It is widely accepted that synthesis of at least the large PSII core subunits takes place directly at the membrane, where nascent polypeptide chains integrate into the lipid bilayer in a co-translational manner (149). During translation, nascent D1 polypeptides interact with components of the general signal recognition particle (SRP) and secretory (Sec) TM protein transport systems for chloroplast proteins substantiating this idea (90; 148). Furthermore, D1-interacting general insertases belonging to the Alb3/Oxa1/YidC family have been shown to support the integration, folding and/or assembly of pD1 in *Synechocystis* 6803 and chloroplasts of *C. reinhardtii* (95; 96).

Upon insertion of pD1 into the membrane, one of the first PSII-specific assembly factors to act in cyanobacteria is probably the soluble PrataA protein, which belongs to the TPR family (see sidebar, Table 1; 56). A *prataA*<sup>-</sup> mutant accumulates less active PSII and is defective in RC complex formation; e.g. C-terminal processing of D1 is retarded (56). The PrataA factor interacts directly with an  $\alpha$ -helical structure at the D1 C-terminus, which forms close to the amino acids involved in complexation of the Mn<sub>4</sub>CaO<sub>5</sub> cluster (113; 128). Intriguingly, PrataA binds Mn<sup>2+</sup> with high affinity, and radioisotope uptake experiments revealed that transport of Mn<sup>2+</sup> to PSII is affected in a *prataA*<sup>-</sup> mutant background (122). This led to the hypothesis that PrataA loads early PSII precomplexes with Mn<sup>2+</sup> (122).

No obvious Prata homologs have been identified by bioinformational means, but two factors named LPA1 in *Arabidopsis thaliana* and REP27 in *C. reinhardtii* share some features with Prata (Table 1, Figure 2B; 97; 98). Like Prata, both belong to the TPR family and interact directly with D1 (97; 98). In *lpa1* mutants, accumulation and synthesis of D1 and D2 is particularly affected, probably due to delayed assembly of PSII complexes (98). Intriguingly, recombinant LPA1 also binds  $Mn^{2+}$ , supporting the idea that LPA1 fulfills a Prata-related function in plants (122).

REP27 is the LPA1 homolog in *C. reinhardtii* and D1 levels are affected in *rep27* mutants (97). Unlike LPA1, however, REP27 was postulated to be involved specifically in the synthesis of D1 during the PSII repair cycle. Despite this apparent difference, the modes of action of REP27 and LPA1 appear to be closely related, since a role in facilitating integration of nascent D1 into PSII precomplexes has been ascribed to both (97). More detailed studies suggest that REP27 mediates cotranslational insertion of D1 via its C-terminal domain. Moreover, newly synthesized D1 appears to be functionally activated via the TPR motifs of REP27 (27). It remains to be demonstrated whether this activation includes the delivery of  $Mn^{2+}$  ions.

In the late 1990s, the very first PSII assembly factor was discovered by Westhoff and co-workers based on the analysis of a nuclear *A. thaliana* mutant named *hcf136* for its high chlorophyll fluorescence phenotype (Table 1; 78). This mutant exhibited severe reductions in levels of all PSII subunits due to their instability. Soluble HCF136 protein is located in the thylakoid lumen and mediates formation of RC complexes (Figure 2B; 101). Its homolog in *Synechocystis* 6803, YCF48, participates in stabilization of newly synthesized pD1 and its subsequent binding to the D2-cyt  $b_{559}$  receptor complex (Figure 2A; 60). In agreement with the idea that YCF48 acts during the early PSII assembly phase, it was shown to interact with pD1 but not with mature D1 or D2 by yeast two-hybrid analysis (60). In *Synechocystis* 6803, YCF48 also seems to participate in selective replacement of damaged D1 during PSII repair (60). Another D1-interacting factor from *A. thaliana*, HCF243, was recently described which, unlike HCF136, is an integral membrane protein, but it is also involved in stabilizing D1 upon membrane integration and RC complex formation (Table 1, Figure 2B; 147). Interestingly, homologs of HCF243 are found in angiosperms but not in lower plants or cyanobacteria, indicating that this factor is a recent evolutionary addition to the PSII biogenesis machinery.

The precise relationship between the factors that associate with D1 remains unresolved. However, the available data suggest that in cyanobacteria Prata first loads pD1 with  $Mn^{2+}$  and then YCF48 takes over to mediate RC complex formation (Figure 2A). In chloroplasts, a

similar sequence of events is conceivable, involving LPA1 and HCF136 and perhaps HCF243 (Figure 2B).

In contrast to initial D1 assembly, no assembly factors are known to participate in D2 precomplex formation. Only two *Synechocystis* 6803-specific proteins, Slr0286 and Slr2013, were implicated in folding of D2. (Table 1; 65; 66). But their precise role remains elusive since their targeted inactivation in a wild-type background did not yield interpretable phenotypes (65; 66). Whether this apparent lack of D2-related factors reflects a functional autonomy of D2 or is a result of gaps in our current knowledge remains to be seen.

A particularly interesting PSII assembly factor is represented by the recently identified PAM68 protein from *A. thaliana* TMs and its homolog Sll0933 in *Synechocystis* 6803 (Figure 2A, B; 7). Mutation of PAM68 and Sll0933 perturbs conversion of the RC complex into larger PSII complexes (7). It was speculated that PAM68 displaces LPA1 during early steps of PSII biogenesis, taking over at the RC complex stage (7). Moreover, PAM68/Sll0933 was shown to interact with several PSII core proteins, as well as known assembly factors such as HCF136/YCF48 (7; 102). The currently available data support the idea that PAM68/Sll0933 might provide the bridge between RC and PSII [1] complex formation, and therefore mark the transition between “early” and “later” phases of PSII assembly.

#### *b) Factors involved in PSII monomer formation – the later phase*

Formation of monomeric PSII (PSII [1]) from RC complexes includes the sequential attachment of the two inner antenna proteins CP47 and CP43 as well as assembly of the extrinsic subunits that shield the  $Mn_4CaO_5$  cluster (Figure 2). Starting from genetically engineered strains of *Synechocystis* 6803, three proteins, Psb27, Psb28 and Psb29, were identified as substoichiometric components of His-tagged CP47 preparations (50; 116).

A variety of functions has been attributed to Psb29 and its homolog in *A. thaliana*, Thf1, including the control of D1 degradation during PSII repair, and PSII supercomplex formation (116). Psb28 was shown to associate with RC47, PSII [1] and non-assembled CP47 (13; 28). Deletion of the *psb28* gene in *Synechocystis* 6803 reduces levels of CP47 and the PSI subunits PsaA/PsaB as well as amounts of chlorophyll *a*. It was therefore proposed that Psb28 has a broader function in chlorophyll synthesis and biogenesis of the chlorophyll-binding proteins CP47, PsaA and PsaB (28). An NMR structure of Psb28 is available, but it is not clear exactly how it binds to CP47 and/or the PSII core (142). Eukaryotic homologs of Psb28 are found in green algae and in vascular plants, but no functional studies have been done on them (116).

More information is available concerning the subsequent binding of CP43 to the RC complex. In this context, one of the best-studied PSII biogenesis factors is represented by Psb27. Cyanobacterial Psb27 was first identified as a luminal lipoprotein that binds transiently to PSII intermediates during both repair and *de novo* assembly (Figure 2A; 94; 108). It has been proposed that Psb27 prevents premature binding of the extrinsic PSII subunits and thereby enables proper processing of D1 and subsequent assembly of the Mn<sub>4</sub>CaO<sub>5</sub> cluster (108). The structure of Psb27 from *T. elongatus* and *Synechocystis* 6803 has been resolved by NMR spectroscopy and recently also by X-ray crystallography (21; 75; 79). It forms a four-helix bundle and its binding site lies close to the PsbV binding region on the CP43 side of PSII (58; 71; 75; 79). Moreover, Psb27 interacts with non-assembled CP43 as well as PSII [1] and even PSII [2] supercomplexes, probably via binding to CP43 (58; 71; 72). This suggests that Psb27 stabilizes non-assembled CP43 and assists in its integration into RC47 complexes. Like Psb28, both CP43 and Psb27, were, surprisingly, found to interact with PSI. This led to speculations that Psb27 represents a more general stabilization factor for photosynthetic complexes and might coordinate their assembly during TM biogenesis (58; 62).

The *A. thaliana* genome encodes two Psb27 homologs. One of them, LPA19 (Psb27-H2; *At1g05385*), is involved in *de novo* biogenesis of PSII. Loss of this protein impairs the synthesis and C-terminal processing of pD1 in particular and, indeed, LPA19 interacts with the C-terminus of D1 (138). However, the second Psb27 homolog, Psb27-H1 (*At1g03600*), is required for efficient recovery of PSII activity after photoinhibition (19). Therefore, the functions of cyanobacterial Psb27 appear to be divided between two homologous factors in plants.

An additional factor necessary for CP43 attachment to RC47 in *Synechocystis* 6803 is Sll0606 (150). Furthermore, Sll0606 might be linked to a defect in carotenoid transport and/or insertion into apoproteins, since carotenoid levels were drastically increased in a *sll0606* mutant (150). While *C. reinhardtii* contains a Sll0606 homolog, plants do not, suggesting that Sll0606 function is either dispensable or is supplied by other assembly factors (Table 1; 150). Two candidate substitutes are the TM protein LPA2 and the stromal protein LPA3 from *A. thaliana*, which are not structurally related to Sll0606. Both are required for insertion of CP43 into RC47 complexes but share no homology with cyanobacterial proteins (Table 1; 17; 74). Interaction studies in yeast and *in planta* provided evidence for a direct interaction between LPA2/LPA3 and CP43, as well as between LPA2 and LPA3 themselves (Figure 2B; 17).

After attachment of CP43, the extrinsic proteins shielding the  $Mn_4CaO_5$  cluster bind at the luminal side of PSII. To date, two factors from *A. thaliana* have been implicated in this step, namely CYP38 and LTO1 (Figure 2B, Table 1; 34; 49). CYP38 belongs to the immunophilin family and its inactivation leads to defects in folding of D1, and probably also of CP43 (119). As a consequence, binding of PsbO, P and Q and susceptibility to photoinhibition are abnormal (Figure 2B). Recently, the crystal structure of CYP38 was solved, revealing two distinct domains (133). A four helix-bundle in the N-terminus is structurally related to the PsbQ protein from spinach and is involved in an autoinhibitory activity that regulates accessibility of the C-terminal cyclophilin-like domain which appears to interact with the E-loop of CP47 (133). This strongly supports a function of CYP38 during PSII [1] formation. LTO1 is a luminal thiol oxidoreductase that catalyzes the formation of intramolecular disulfide bonds in PsbO (49).

*c) Factors involved in dimerization of PSII and attachment of the peripheral antennae – the final phase*

The final steps in PSII biogenesis include dimerization of PSII monomers and the attachment of the peripheral antennae. To date, few factors have been described which are specifically implicated in the formation of PSII [2] supercomplexes. These include the above-mentioned Alb3 insertase, FKBP20-2 in *A. thaliana* (another luminal member of the immunophilin family) and, strikingly, the TM protease Deg1 (Table1, Figure 2B; 70; 82; 125). Earlier studies had revealed that Deg1 participates in degradation of the D1 protein during repair after photoinhibition (48). However, Deg1RNAi plants accumulate increased amounts of RC47 and PSII [1] complexes, indicating that their conversion into PSII [2] and PSII [2] supercomplexes, respectively, is perturbed (125). Hence, besides its protease activity, Deg1 appears to possess chaperone function, which may be part of a quality control mechanism that monitors the assembly process.

Integration of cofactors

Most of the assembly factors discussed so far are involved in mediating protein-protein interactions. However, many inorganic and organic cofactors have to be incorporated into PSII before it can function, but far fewer data are available on these processes. For instance, with the exception of the aforementioned PrtA system for  $Mn^{2+}$  delivery in cyanobacteria, we know virtually nothing about when and how essential ions, including non-heme  $Fe^{2+}$  as well as  $Ca^{2+}$  and  $Cl^-$  for the water-splitting apparatus, are inserted into PSII (10). The recent identification of a Fe-containing rubredoxin-like factor required for PSII assembly in

*C. reinhardtii* will hopefully shed more light on this rather black box in PSII assembly (R. Calderon and K. Niyogi, unpublished data).

Similarly, the integration of organic molecules, especially pigments, remains largely unexplored. However, it seems likely that cofactor synthesis and integration must accompany protein synthesis and assembly, as the accumulation of free pigments would cause photooxidative damage to cells (62). Analysis of carotenoid biosynthesis mutants in various organisms provided evidence that not only the function but also the assembly of PSII is dependent on the availability of carotenoids (120). Apparently carotenoids are mainly important for synthesis and integration of CP47 and – particularly – CP43 (120). The latter effect on CP43 would be compatible with the above-mentioned function of Sll0606 during carotenoid integration into PSII (Figure 2A, Table 1; 150).

The integration of chlorophylls into PSII subcomplexes has received much more attention. Light-absorbing chlorophyll molecules are bound to the integral PSII subunits D1, D2, CP47 and CP43, as well as to the proteins of LHC complexes (Figure 1A). In cyanobacteria, eukaryotic algae and gymnosperms, two chlorophyll synthesis pathways exist, which differ in the light requirements of their protochlorophyllide oxidoreductase (POR) enzymes (see sidebar).

Previous work in both *Synechocystis* 6803 and *C. reinhardtii* cells defective in LiPOR demonstrated that they are unable to synthesize and accumulate PSII in the dark (40; 76). However, in barley chloroplasts, light-induced accumulation of chlorophyll-binding proteins is not regulated at the level of synthesis; instead chlorophyll seems to protect freshly synthesized apoproteins from immediate degradation (32). So at what point in PSII assembly, and in what form, are pigments attached to their apoproteins? It has been demonstrated for cyanobacteria that RC complexes are already capable of light-induced charge separation, indicating that pigments have been inserted into the D1/D2 proteins by this early stage (53).

The recent isolation of His-tagged CP47 and CP43 complexes from *Synechocystis* 6803 cells lacking D1 provided clear evidence that non-assembled CP47-His and CP43-His complexes already contain bound chlorophyll *a* and  $\beta$ -carotene molecules (12). This suggests that pigment binding occurs very early – probably co-translationally – during PSII assembly, and thus serves to stabilize the intermediate PSII precomplexes (12). The Psb28 factor described above represents a possible link between synthesis of pigments and their integration into apoproteins (28). Furthermore, in *Synechocystis* 6803 a type IV pilin-like protein, Sll1694, has been postulated to be involved in delivering chlorophyll to apoproteins (41).

Recent data suggest that POR might also be involved in linking chlorophyll synthesis to PSII assembly via the so-called Pitt factor, a membrane-bound TPR protein that binds and stabilizes POR (114). It was speculated that Pitt specifically positions POR to enable proper insertion of pigments into apoproteins during their assembly into PSII. This idea is supported by the fact that Pitt levels are significantly increased in various mutants affected in PSII assembly (103). Hence, dynamic interactions within a PSII assembly factor network apparently operate to integrate chlorophyll biosynthesis with PSII formation (103).

In cyanobacteria, a group of small Cab-like proteins (SCPs) has been described that bind carotenoids as well as chlorophyll molecules (123; 140), and are involved in stabilizing PSII intermediates (143). It has therefore been postulated that SCPs serve as transient carriers of chlorophylls, especially during the PSII repair cycle (134). In accordance with this idea, SCPs interact with PSII via CP47 (13). In plants, SCP-related functions are probably carried out by so-called LHC-like proteins (33).

#### Evolution of assembly factors

Inspection of the inventory of *trans*-acting factors that facilitate PSII assembly reveals that most have been conserved throughout evolution from cyanobacteria to plants (Table 1). This is perhaps not surprising when one considers that the subunits of PSII and their assembly order exhibit high levels of conservation. Moreover, apparent deviations from this principle often relate to plant-specific factors that might have evolved as functional substitutes for cyanobacterial equivalents, e.g. the PratA-related LPA1/REP27 protein. For other plant-specific factors like HCF243, and especially those involved in PSII repair (LQY1, PPL1, see below), novel – as yet unknown – functions might be considered. Such functions could have arisen in response to the exigencies of a land-based lifestyle and the need to cope with varying environmental conditions. Intriguingly, most of the assembly factors appear to be present in the primordial cyanobacterium *Gloeobacter violaceus*, which is the only organism capable of oxygenic photosynthesis that lacks internal membrane systems (Figure 3A; 80; 105). *G. violaceus* is able to perform photosynthesis because its photosynthetic protein complexes are embedded in the PM (105). This further underlines the fact that the PSII assembly process is extremely conservative and can take place even in the absence of a TM system raising questions regarding the spatial organization of the assembly process.

### **Spatial organization of PSII assembly – the concept of biogenesis centers**

The emerging picture of a highly ordered network for PSII biogenesis made up of facilitating factors that connect several biosynthesis pathways raises the problem of how the process is coordinated in space. In principle, three different scenarios for TM, and hence PSII biogenesis, can be envisaged. In the first, PSII assembly takes place all along thylakoids as a randomly distributed process. Secondly, specialized TM regions might exist where the PSII components are synthesized and assembled before moving to their final destination in photosynthetically active TMs. And finally, initial steps in complex assembly might occur at other membranes, with precomplexes being transferred to TMs via lateral fusions or vesicles. Recent data from two different organisms provides evidence that a mixture of scenarios two and three is likely to have been realized during evolution (89; 146).

#### Localization of PSII assembly in cyanobacteria

Most cyanobacteria contain three major membrane systems: the outer membrane (OM), the inner plasma membrane (PM) and the internal TM system (Figure 3F). TMs form shells of three to ten parallel sheets which follow the periphery of the cells and converge on the PM at various sites (Figure 3B; 131). Whether these are sites of direct contact with the PM has been controversially discussed (see below; 69; 111; 131). However, TMs in cyanobacteria are organized in a connected network related to those of higher plant chloroplasts (87).

A more complex picture of cyanobacterial TMs than might be expected also emerges from proteomic studies in *Synechocystis* 6803, which reveal that TM subfractions are compositionally heterogeneous with respect to their photosynthetic complexes (3; 4). Similarly, a non-homogenous protein distribution has been observed for PMs (100; 121), suggesting the existence of distinct membrane subdomains even in cyanobacterial systems.

#### *a) Synechocystis 6803*

Most of the initial work on the spatial organization of PSII assembly was carried out in *Synechocystis* 6803. In particular, the immunological detection of PSII subunits D1, D2 and cyt  $b_{559}$  in PMs by Pakrasi and co-workers provoked speculation about a possible spatial separation of PSII biogenesis from photosynthetically active PSII (145). In the PM RC complexes are formed that are capable of light-induced charge separation (53; 145). In contrast, the inner antenna proteins CP47 and CP43 were absent from PMs and exclusively localized to TMs (145). This implied that the transition from RC to RC47 complexes requires the transfer of PSII precomplexes from the PM to the TM system, where PSII assembly is then completed (145). However, how this transfer is accomplished remained moot.

More recent cell fractionation studies have identified a special membrane subfraction that displays a mixture of PM and TM properties (113). This is characterized by the D1-dependent accumulation of a membrane-associated form of the  $Mn^{2+}$  transporter PrataA, and was therefore named the PrataA-defined membrane fraction or PDM (113). Strikingly, pD1 also accumulates in PDMs in a PrataA-dependent manner. The presence of these two marker proteins for the initial steps of PSII assembly in PDMs led to the hypothesis that the latter represent a biogenesis-related membrane subcompartment (113). Interestingly, inactivation of PrataA alters the membrane sublocalization of several PSII assembly factors, e.g. YCF48 and Slr1471 (Table 1), indicating that PrataA – apart from its aforementioned role in  $Mn^{2+}$  delivery to PSII – is required for proper formation of this membrane region (103). Furthermore, the enzyme POR and its interaction partner Pitt, as well as the product of the POR reaction, chlorophyllide *a*, accumulate in PDMs, indicating that PDMs are also important for synthesis of chlorophyll, and probably for its insertion into apoproteins in early PSII intermediates (42; 103; 114). This is in line with recent suggestions predicting that the machinery for chlorophyll synthesis is coupled to early PSII precomplexes via the D2/cytb<sub>559</sub> subcomplex (Figure 2; 62). Seen in this light, this PDM-localized complex would represent both a nucleation site for PSII assembly and an anchor for the chlorophyll synthesis apparatus, thereby tightly connecting both biogenesis pathways.

Ultrastructural studies of wild-type and *prataA*<sup>-</sup> cells revealed a PrataA-dependent, cup-shaped structure close to the periphery of the cell at TM convergence sites, further substantiating the postulated role of PDMs (Figure 3; 122). This structure appears to partially surround electron-dense particles approximately 50 nm in diameter which have previously been termed “thylakoid centers” (see sidebar) (67). Most intriguingly, both PrataA and pD1 preferentially localize to these structures at TM convergence sites, strongly suggesting that they correspond to the biochemically isolated PDM fractions (122). Thus, they appear to mark subcellular biogenesis centers at which the initial steps in PSII assembly, including preloading of PSII with  $Mn^{2+}$ , and probably pigment insertion, take place (Figure 3; 122). Based on the available data, our current view of the sequence, and subcellular location, of molecular events during the early phase of PSII assembly in *Synechocystis* 6803 is depicted in Figure 3F. At biogenesis centers in direct contact with the PM, which are formed by a central thylakoid rod and the surrounding PDMs,  $Mn^{2+}$  is delivered to pD1 from a  $Mn^{2+}$  pool at the OM via the PrataA factor (52; 122).  $Mn^{2+}$  delivery from the periplasm would avoid the time- and energy-consuming transport of this essential transition metal into the thylakoid lumen across the PM and the TM. This is probably especially important after cell division, when new TMs

including PSII have to be rapidly synthesized. Following formation of the RC complex and the concomitant insertion of chlorophyll molecules, the complex can be transferred into the developing thylakoid lamellae. There the inner antenna is attached and the  $Mn_4CaO_5$  cluster is photoactivated, giving rise to PSII monomers (Figure 3F).

#### b) *Gloeobacter violaceus*

While the above model describes the situation for PSII assembly in *Synechocystis* 6803, it is not known whether it also holds for other cyanobacteria. However, thylakoid centers have previously been detected in several of them and the accumulation of chlorophyllide *a* in special membrane fractions has been reported for *Synechococcus elongatus* (67; 99). This suggests that the use of dedicated centers for PSII biogenesis is probably more widespread.

As mentioned above, one particularly interesting case concerns the cyanobacterium *G. violaceus*, which integrates PSII into its PM. The lipid composition of the PM seems to be relatively homogeneous, but distinct distributions of proteins and pigments define two different domains within it: an “orange” fraction that resembles the PM of other cyanobacteria and a “green” fraction whose composition is reminiscent of TMs.

Interestingly, a PratA homolog from *G. violaceus* (Glr1902) was found exclusively in orange membrane fractions containing non-assembled PSII subunits (104). It was concluded that the carotenoid-rich “orange” fraction includes areas that are involved in the biogenesis of membrane protein complexes. In contrast, functional components of photosynthetic and respiratory electron transfer chains are restricted to bioenergetically active, chlorophyll-containing, green patches, which are approximately 140 nm in diameter (Figure 3A; 104). Thus PSII assembly and PSII activity are already spatially separated in *G. violaceus* cells that lack TMs, and the green patches are likely to represent the evolutionary starting point for the development of an internal TM system (104).

#### Spatial organization of PSII assembly in chloroplasts

The membrane systems of chloroplasts include outer and inner envelopes, which represent the evolutionary remnants of the OM and PM of the former cyanobacterial endosymbiont (14). In particular the internal chloroplast TM system is more complex than its cyanobacterial counterpart, since it is organized into non-appressed lamellar sheets as well as appressed grana stacks. Photosynthetic protein complexes are unevenly distributed over the whole system, such that TMs exhibit lateral heterogeneity (88). PSII and LHCII are restricted to grana thylakoids and are segregated from PSI, LHCI and ATP synthase which – for steric reasons – are located in stroma lamellae only (26).

Analogously to the situation in cyanobacteria, several lines of evidence suggest that direct physical contacts or mobile vesicles connect the chloroplast's inner envelope to the TM system (1). First, pigment and lipid synthesis are highly ordered spatially. Whereas early steps in chlorophyll synthesis take place in the stroma, later reactions leading to chlorophyll *a* are reported to occur at the chloroplast envelope and finally on the TMs (22). On the other hand, carotenoid synthesis in chloroplasts is apparently localized to the inner envelope membrane (47). Furthermore, biosynthesis of thylakoid lipids is completed at the chloroplast envelope. Thus lipids/pigments must somehow be transported from the inner envelope to TMs (47; 51). In algal chloroplasts and in developing proplastids, it was suggested that TMs develop by local expansion and invagination of the inner envelope membrane (Figure 3D; 44; 83). In mature plant chloroplasts, vesicle trafficking seems to be involved in the transfer of TM constituents from the envelope to developing TMs (135). However, EM tomography has revealed that – at least in rare cases – connections between stromal TMs and the inner chloroplast envelope are still formed in mature chloroplasts (Figure 3E; 117). Candidates for factors mediating a transfer of lipid material between the inner envelope and TMs include VIPP1 (see sidebar), Thf (thylakoid formation 1) and CPSAR1, as inactivation of any of these leads to aberrant TM development (1; 36; 136; 139). If and how these processes are linked to PSII assembly remains largely unresolved.

#### *a) Chlamydomonas reinhardtii*

The green alga *C. reinhardtii* possesses a single cup-shaped chloroplast whose membrane organization is basically similar to that in vascular plants (Figure 3C). Unlike a plant chloroplast, however, its basal region contains a pyrenoid, formed by semicrystalline concentrations of the CO<sub>2</sub>-fixing enzyme ribulose-bisphosphate carboxylase/oxygenase (77). The pyrenoid is itself surrounded by TMs, some of which protrude into its interior. Interestingly, the region around the pyrenoid also appears to serve as an organization site for PSII biogenesis. Work by Zerges and co-workers has shown that, in cultures exposed to moderate light levels favoring *de novo* assembly of PSII, ribosomes and mRNAs encoding PSII subunits localize to distinct punctate regions in the periphery of the pyrenoid (129; 130). These regions are approximately 600 nm in diameter and have been named T-(translation) zones (Figure 3C; 129). Based on immunofluorescence and RNA studies, a specific function in the early steps of PSII, but not PSI, synthesis/assembly has been assigned to the T-zones (129). Interestingly, analysis of PSII mutants impaired in PSII assembly revealed an accumulation of early PSII intermediates at the pyrenoid in close proximity to T-zones. This

substantiates the idea that synthesis and assembly of PSII core subunits are initiated at T-zones in *C. reinhardtii*, with assembled precomplexes moving into adjoining TMs surrounding the pyrenoid (129). All subsequent steps in PSII assembly, including the attachment of the light-harvesting outer antenna, then take place there (Schottkowski and Zerges, personal communication).

This scenario is very reminiscent of the organization of biogenesis centers in *Synechocystis* 6803, suggesting that spatially localized PSII biogenesis represents an evolutionarily conserved concept (Figure 3). In principle, the spatial separation of the assembly process from sites of active photosynthesis has two major advantages. It provides for substrate channeling, which reduces diffusion-dependent dilution effects and allows nearly simultaneous insertion of different components. In addition, the local concentrations of cofactors like ions and pigments are increased, thereby accelerating assembly by shifting the chemical equilibrium of assembly reactions. Secondly, a multienzyme/assembly factor complex should minimize the release of toxic intermediate complexes containing redox-active chlorophylls.

#### *b) Plants*

Less is known about the subcellular organization of PSII biogenesis in vascular plants than in cyanobacteria and eukaryotic microalgae. It is generally assumed that synthesis of membrane proteins takes place at stromal TMs, since ribosomes bind to these non-stacked membrane regions (Figure 3E; 141). Furthermore, analysis of the distribution of PSII subcomplexes revealed that the ratio of PSII supercomplexes and dimers to PSII monomers, RC47 and RC complexes is directly correlated with the height of the membrane stack, supporting the idea that PSII complexes are assembled in non-appressed TM regions (24).

To date, no structures similar or related to cyanobacterial thylakoid centers or algal T-zones have been described in plant chloroplasts. One possible reason for this may lie in a fundamental developmental difference between plants and the unicellular systems. Microorganisms like *Synechocystis* 6803 or *C. reinhardtii* do not differentiate into multiple cell types or possess different chloroplast types. Moreover, they divide frequently. Thus, even in non-synchronous cultures, a high percentage of cells undergoes cell division, which is accompanied by the rapid synthesis of new TM material in the two daughter cells. In contrast, the chloroplasts of vascular plants develop from undifferentiated proplastids in meristem tissues, which account for only a minor fraction of the whole plant biomass (Figure 3D). It is likely that the bulk of TM biogenesis, including *de novo* PSII assembly, takes place during

differentiation of the meristems (18). Once a TM system is formed in chloroplasts of mature leaves, it is relatively stable, as indicated by the fact that gene expression in developed chloroplasts is mainly dedicated to maintenance functions, especially the repair of PSII. Therefore, more detailed analyses focusing on the transition phase from proplastids to chloroplasts are required to address the issue of photosynthetic complex assembly more specifically (Figure 3D, E).

Alternatively, the physiological constraints that led to the establishment and conservation of spatially localized PSII assembly in microorganisms might not hold for chloroplasts. In microorganisms, biogenesis and maintenance of PSII probably take place contemporaneously in the same cell. Thus spatial separation of the two processes might be necessary to avoid competition between *de novo* assembly and repair of PSII (see below). In contrast, the proplastid to chloroplast transition in plants might already ensure that the two processes are separated temporally, reducing the need to dissociate them spatially.

### **The relationship between PSII assembly and PSII repair**

One intrinsic feature of PSII, from cyanobacteria to plants, is its sensitivity to light-mediated damage or photoinhibition (31). The precise molecular events that lead to photodamage are the subject of intense debate (126; 132). However, it is clear that the main target is the D1 subunit, which has an unusually high turnover rate that reflects the rapid replacement of photodamaged D1 in PSII by newly synthesized D1 (85). This entire process, the so-called PSII repair cycle, includes the disassembly of photodamaged PSII down to the level of RC47\* complexes (Figure 4). In chloroplasts – but not in cyanobacteria – the disassembly process is facilitated by phosphorylation of PSII core and antenna proteins (127). At the RC47\* stage, damaged D1 is removed by FtsH metalloproteases localized in the TMs in both cyanobacteria and chloroplasts (62; 91). In addition, serine proteases of the Deg/HtrA family have been implicated in D1 degradation (55; 109). However, immediately after proteolytic removal of damaged D1, newly synthesized pD1 is integrated in its place. This coordinated mode of D1 exchange minimizes destabilization of the RC47\* complex, which then appears to follow the usual PSII assembly pathway involving C-terminal processing of D1, subsequent reattachment of CP43 and finally dimerization of PSII (Figure 4; 91).

Some factors have been described whose inactivation affects the repair cycle after PSII photodamage. These include the cyanobacterial proteins Slr1768 and Psb32, REP27 from *C. reinhardtii*, and the Psb32 homolog TLP18.3, the zinc-finger protein LQY1 and the PsbP-like PPL1 from *A. thaliana* (Table 1; 16; 45; 73; 118; 137). However, with the exception of

REP27 described above, and TLP18.3, their precise modes of action remain obscure. TLP18.3 appears to have a dual function in the turnover of photodamaged D1 and dimerization of PSII complexes, probably mediated by its phosphatase activity (118).

In addition to these repair-related proteins, some PSII assembly factors, such as Psb27 or YCF48, appear to act during both PSII assembly and repair (Table 1). This may be related to the observation that all the assembly steps subsequent to the repair of the RC47 complex are apparently common to both processes (Table 1; Figure 4).

If shared, these steps would be expected to have the same spatial organization. To date, relatively little is known about the subcellular localization of the PSII repair cycle in cyanobacteria. However, RC47 marks the transition point from the early to the later phase of PSII *de novo* assembly, and is the first complex in the assembly pathway to be localized in TMs, while RC complexes form in PDMs (Figures 3F, 4). Furthermore, the finding that the FtsH protease (Slr0228) involved in D1 removal is located in TMs suggests that RC47\* is also localized there (Figure 4; 57). This would imply that the repair cycle takes place at TMs, probably in close vicinity to PDMs (62). One crucial question related to the localization of the repair cycle is whether the newly synthesized D1 protein for PSII repair is also synthesized and integrated into the membrane in biogenesis centers at PDMs and subsequently moves to RC47\* at TMs, or is synthesized and integrated directly at TMs where RC47\* is situated. The latter possibility would account for the tight coupling between the removal of damaged D1 and insertion of the new protein, and postulates two different, spatially separated D1 assembly pathways, one in PDMs and one in TMs (Figure 4). Though the available information on this point is rather limited, analysis of cyanobacterial membrane fractions has revealed that pD1 is detectable in both PDMs and TMs, which supports the idea of two separate D1 assembly pathways, at least in *Synechocystis* 6803 (Figure 4; 113). Two different molecular mechanisms for D1 incorporation must be considered in any event, since the acceptors of pD1 are obviously different, i.e., the D2, PsbE, PsbF complex in the case of PSII *de novo* assembly and a much larger RC47\* complex in case of PSII repair.

In algal and plant chloroplasts, repair has been shown to involve the movement of damaged PSII from grana regions to margins and/or stromal thylakoids (2; 38; 144). For sterical reasons, FtsH-mediated removal of D1 and ribosome access for synthesis/insertion of new D1 is only possible at these stroma-exposed regions. Intriguingly, in *C. reinhardtii*, it has been demonstrated that D1 repair synthesis in high light occurs all over the chloroplast TM system, in contrast to the early steps of PSII *de novo* assembly which – as mentioned above – are restricted to T-zones (Figures 3C, 4; 129). Hence, a strict spatial separation between D1

synthesis for repair and for *de novo* assembly most likely exists in eukaryotic microalgae. A clear distinction between these two systems is further substantiated by the fact that synthesis of D1 for *de novo* assembly is regulated at the level of translation initiation, following the so-called CES principle (see sidebar), in *C. reinhardtii*. In contrast, D1 repair synthesis is independent of CES and most likely regulated at the level of elongation (81).

Altogether, this suggests that, at least in eukaryotic microorganisms, distinct D1 synthesis and assembly systems exist which are spatially separated. In plants with distinct plastid forms like proplastids and mature chloroplasts, such spatial separation has yet to be described, and might not actually exist, since a temporal separation of PSII *de novo* assembly from repair is guaranteed during plant development as outlined above.

The fact that many, if not all, photoautotrophic organisms have apparently established distinct D1 synthesis/integration systems, poses the question of the selective advantage of this separation of PSII assembly and repair. Localized biogenesis allows efficient ordering of assembly, especially cofactor insertion, while active photosynthesis requires superstructures that are less accessible to the complicated assembly machinery. During repair, all subunits except D1, and probably most of the cofactors, are recycled, allowing on-site repair by a less complex apparatus (91). Alternatively, extensive movement of damaged PSII to biogenesis centers for repair might be envisaged, but appears less likely because extensive trafficking would be required within the TM system (84).

### **Concluding remarks and perspectives**

Recent years have seen tremendous progress in understanding the assembly of photosynthetic complexes, especially PSII. Its highly ordered nature, and the growing number of facilitating factors involved, reflect the complexity of the process, which requires the coordination of protein synthesis, membrane insertion and assembly, as well as integration of various cofactors and, finally, supercomplex formation. This complexity has apparently precluded substantial variation of the assembly machinery, which is highly conserved from cyanobacteria to plant chloroplasts. This is in sharp contrast to the apparatus controlling the synthesis of individual PSII subunits. Since the consequences of endosymbiosis led to a redistribution of PSII genes between the nuclear and chloroplast genomes in eukaryotes, gene expression and the facilitating factors involved differ in cyanobacteria and plants (9). Nevertheless, although the need for import of gene products by the chloroplast makes the process more complex than in cyanobacteria, their final assembly largely follows the ancient molecular principles invented by the prokaryotes.

We are now beginning to understand individual assembly steps and the contribution of transiently acting assembly factors at the molecular level. In the near future, the combined use of mutant lines that accumulate particular assembly intermediates and tag-based affinity purification will allow us to resolve even the ultrastructure of distinct PSII precomplexes. Furthermore, study of the subcellular localization of the assembly process has just begun, suggesting that PSII biogenesis occurs not only in a strict temporal sequence, but is also spatially ordered. With identified assembly factors serving as markers, the assignment of distinct assembly steps to subcellular structures or membrane subdomains will be feasible. Understanding the organization of this production line at the ultrastructural level will greatly enhance our knowledge of how different cellular biosynthesis pathways can be coordinated, and might even provide a blueprint for the generation of artificial photosystems.

### Summary points

- The principal steps in PSII assembly are conserved among oxygenic photosynthetic organisms and are mediated by a network of facilitating factors.
- The synthesis/assembly of PSII protein subunits is tightly connected with cofactor synthesis/insertion
- At least in unicellular photosynthetic organisms, initiation of PSII *de novo* assembly is spatially localized.
- PSII repair appears to be spatially separated from PSII *de novo* assembly

### Future issues

- What is the conformational dynamics of the different PSII subunits during the assembly process?
- How and when are the inorganic and organic cofactors inserted into PSII complexes?
- Does assembly of other photosynthetic protein/pigment complexes like PSI follow the same molecular principles and subcellular structures?
- What is the ultrastructure of PSII biogenesis centers and are they also present in plants?
- Where does PSII repair take place?

### Acknowledgments

We apologize to any authors whose work may not have been cited due to length restrictions. We want to thank P. Nixon, W. Zerges and K. Niyogi for providing unpublished results,

J. Soll for valuable discussions, and A. Bohne, P. Hardy and W. Zerges for critical reading of the manuscript. This work was supported by the Deutsche Forschungsgemeinschaft in the context of projects Ni390/5-1 and SFB-TR1.

## References

1. Adam Z, Charuvi D, Tsabari O, Knopf RR, Reich Z. 2011. Biogenesis of thylakoid networks in angiosperms: knowns and unknowns. *Plant Mol Biol* 76:221-34
2. Adir N, Shochat S, Ohad I. 1990. Light-dependent D1 protein synthesis and translocation is regulated by reaction center II. Reaction center II serves as an acceptor for the D1 precursor. *J Biol Chem* 265:12563-8
3. Agarwal R, Maralihalli G, Sudarsan V, Choudhury SD, Vatsa RK, et al. 2012. Differential distribution of pigment-protein complexes in the thylakoid membranes of *Synechocystis* 6803. *J Bioenerg Biomembr* 44:399-409
4. Agarwal R, Matros A, Melzer M, Mock HP, Sainis JK. 2010. Heterogeneity in thylakoid membrane proteome of *Synechocystis* 6803. *J Proteomics* 73:976-91
5. Allen JF, de Paula WB, Puthiyaveetil S, Nield J. 2011. A structural phylogenetic map for chloroplast photosynthesis. *Trends Plant Sci* 16:645-55
6. Anbudurai PR, Mor TS, Ohad I, Shestakov SV, Pakrasi HB. 1994. The *ctpA* gene encodes the C-terminal processing protease for the D1 protein of the photosystem II reaction center complex. *Proc Natl Acad Sci USA* 91:8082-6
7. Armbruster U, Zühlke J, Rengstl B, Kreller R, Makarenko E, et al. 2010. The *Arabidopsis* thylakoid protein PAM68 is required for efficient D1 biogenesis and photosystem II assembly. *Plant Cell* 22:3439-60
8. Armstrong GA. 1998. Greening in the dark: light-independent chlorophyll biosynthesis from anoxygenic photosynthetic bacteria to gymnosperms. *J Photochem Photobiol B* 43:87-100
9. Barkan A. 2011. Expression of plastid genes: organelle-specific elaborations on a prokaryotic scaffold. *Plant Physiol* 155:1520-32
10. Becker K, Cormann KU, Nowaczyk MM. 2011. Assembly of the water-oxidizing complex in photosystem II. *J Photochem Photobiol B* 104:204-11
11. Bellafiore S, Ferris P, Naver H, Gohre V, Rochaix JD. 2002. Loss of Albino3 leads to the specific depletion of the light-harvesting system. *Plant Cell* 14:2303-14
12. Boehm M, Romero E, Reisinger V, Yu J, Komenda J, et al. 2011. Investigating the early stages of photosystem II assembly in *Synechocystis* sp. PCC 6803: isolation of CP47 and CP43 complexes. *J Biol Chem* 286:14812-9
13. Boehm M, Yu J, Reisinger V, Beckova M, Eichacker L, et al. Subunit composition of CP43-less photosystem II complexes of *Synechocystis* sp. PCC 6803: implications for the assembly and repair of photosystem II. *Phil Trans B*: in press
14. Bölter B, Soll J, Schulz A, Hinnah S, Wagner R. 1998. Origin of a chloroplast protein importer. *Proc Natl Acad Sci USA* 95:15831-6
15. Bricker TM, Roose JL, Fagerlund RD, Frankel LK, Eaton-Rye JJ. 2012. The extrinsic proteins of photosystem II. *Biochim Biophys Acta* 1817:121-42
16. Bryan SJ, Burroughs NJ, Evered C, Sacharz J, Nennering A, et al. 2011. Loss of the SPHF homologue Slr1768 leads to a catastrophic failure in the maintenance of thylakoid membranes in *Synechocystis* sp. PCC 6803. *PLoS One* 6:e19625
17. Cai W, Ma J, Chi W, Zou M, Guo J, et al. 2010. Cooperation of LPA3 and LPA2 is essential for photosystem II assembly in *Arabidopsis*. *Plant Physiol.* 155:1493-500
18. Charuvi D, Kiss V, Nevo R, Shimoni E, Adam Z, Reich Z. 2012. Gain and loss of photosynthetic membranes during plastid differentiation in the shoot apex of *Arabidopsis*. *Plant Cell* 24:1143-57
19. Chen H, Zhang D, Guo J, Wu H, Jin M, et al. 2006. A Psb27 homologue in *Arabidopsis thaliana* is required for efficient repair of photodamaged photosystem II. *Plant Mol Biol* 61:567-75

20. Choquet Y, Wollman FA. 2002. Translational regulations as specific traits of chloroplast gene expression. *FEBS Lett* 529:39-42
21. Cormann KU, Bangert JA, Ikeuchi M, Rogner M, Stoll R, Nowaczyk MM. 2009. Structure of Psb27 in solution: implications for transient binding to photosystem II during biogenesis and repair. *Biochemistry* 48:8768-70
22. Czarnecki O, Grimm B. 2012. Post-translational control of tetrapyrrole biosynthesis in plants, algae, and cyanobacteria. *J Exp Bot* 63:1675-87
23. D'Andrea LD, Regan L. 2003. TPR proteins: the versatile helix. *Trends Biochem Sci* 28:655-62
24. Danielsson R, Suorsa M, Paakkarinen V, Albertsson PA, Styring S, et al. 2006. Dimeric and monomeric organization of photosystem II. Distribution of five distinct complexes in the different domains of the thylakoid membrane. *J Biol Chem* 281:14241-9
25. Dasgupta J, Ananyev GM, Dismukes GC. 2008. Photoassembly of the water-oxidizing complex in photosystem II. *Coord Chem Rev* 252:347-60
26. Dekker JP, Boekema EJ. 2005. Supramolecular organization of thylakoid membrane proteins in green plants. *Biochim Biophys Acta* 1706:12-39
27. Dewez D, Park S, Garcia-Cerdan JG, Lindberg P, Melis A. 2009. Mechanism of REP27 protein action in the D1 protein turnover and photosystem II repair from photodamage. *Plant Physiol* 151:88-99
28. Dobáková M, Sobotka R, Tichy M, Komenda J. 2009. Psb28 protein is involved in the biogenesis of the photosystem II inner antenna CP47 (PsbB) in the cyanobacterium *Synechocystis* sp. PCC 6803. *Plant Physiol* 149:1076-86
29. Dobáková M, Tichy M, Komenda J. 2007. Role of the PsbI protein in photosystem II assembly and repair in the cyanobacterium *Synechocystis* sp. PCC 6803. *Plant Physiol* 145:1681-91
30. Eberhard S, Finazzi G, Wollman FA. 2008. The dynamics of photosynthesis. *Annu Rev Genet* 42:463-515
31. Edelman M, Mattoo AK. 2008. D1-protein dynamics in photosystem II: the lingering enigma. *Photosynth Res* 98:609-20
32. Eichacker LA, Helfrich M, Rüdiger W, Müller B. 1996. Stabilization of chlorophyll a-binding apoproteins P700, CP47, CP43, D2, and D1 by chlorophyll a or Zn-pheophytin a. *J Biol Chem* 271:32174-9
33. Engelken J, Brinkmann H, Adamska I. 2010. Taxonomic distribution and origins of the extended LHC (light-harvesting complex) antenna protein superfamily. *BMC Evol Biol* 10:233
34. Fu A, He Z, Cho HS, Lima A, Buchanan BB, Luan S. 2007. A chloroplast cyclophilin functions in the assembly and maintenance of photosystem II in *Arabidopsis thaliana*. *Proc Natl Acad Sci U S A* 104:15947-52
35. Gao H, Xu X. 2009. Depletion of Vipp1 in *Synechocystis* sp. PCC 6803 affects photosynthetic activity before the loss of thylakoid membranes. *FEMS Microbiol Lett* 292:63-70
36. Garcia C, Khan NZ, Nannmark U, Aronsson H. 2010. The chloroplast protein CPSAR1, dually localized in the stroma and the inner envelope membrane, is involved in thylakoid biogenesis. *Plant J* 63:73-85
37. Göhre V, Ossenbühl F, Crevecoeur M, Eichacker LA, Rochaix JD. 2006. One of two Alb3 proteins is essential for the assembly of the photosystems and for cell survival in *Chlamydomonas*. *Plant Cell* 18:1454-66
38. Goral TK, Johnson MP, Brain AP, Kirchhoff H, Ruban AV, Mullineaux CW. 2010. Visualizing the mobility and distribution of chlorophyll proteins in higher plant thylakoid membranes: effects of photoinhibition and protein phosphorylation. *Plant J* 62:948-59
39. Gould SB, Waller RF, McFadden GI. 2008. Plastid evolution. *Annu Rev Plant Biol* 59:491-517
40. He Q, Vermaas W. 1998. Chlorophyll a availability affects *psbA* translation and D1 precursor processing in vivo in *Synechocystis* sp. PCC 6803. *Proc Natl Acad Sci USA* 95:5830-5
41. He Q, Vermaas W. 1999. Genetic deletion of proteins resembling Type IV pilins in *Synechocystis* sp. PCC 6803: their role in binding or transfer of newly synthesized chlorophyll. *Plant Mol Biol* 39:1175-88

42. Hinterstoisser B, Chichna M, Kuntner O, Peschek GA. 1993. Cooperation of plasma and thylakoid membranes for the biosynthesis of chlorophyll in cyanobacteria: The role of the thylakoid centers. *J Plant Physiol* 142:407-13
43. Hohmann-Marriott MF, Blankenship RE. 2011. Evolution of photosynthesis. *Annu Rev Plant Biol* 62:515-48
44. Hooper JK, Boyd CO, Paavola LG. 1991. Origin of thylakoid membranes in *Chlamydomonas reinhardtii* y-1 at 38°C. *Plant Physiol* 96:1321-8
45. Ishihara S, Takabayashi A, Ido K, Endo T, Ifuku K, Sato F. 2007. Distinct functions for the two PsbP-like proteins PPL1 and PPL2 in the chloroplast thylakoid lumen of *Arabidopsis*. *Plant Physiol* 145:668-79
46. Ivleva NB, Shestakov SV, Pakrasi HB. 2000. The carboxyl-terminal extension of the precursor D1 protein of photosystem II is required for optimal photosynthetic performance of the cyanobacterium *Synechocystis* sp. PCC 6803. *Plant Physiol* 124:1403-12
47. Joyard J, Ferro M, Masselon C, Seigneurin-Berny D, Salvi D, et al. 2009. Chloroplast proteomics and the compartmentation of plastidial isoprenoid biosynthetic pathways. *Mol Plant* 2:1154-80
48. Kapri-Pardes E, Naveh L, Adam Z. 2007. The thylakoid lumen protease Deg1 is involved in the repair of photosystem II from photoinhibition in *Arabidopsis*. *Plant Cell* 19:1039-47
49. Karamoko M, Cline S, Redding K, Ruiz N, Hamel PP. 2011. Lumen Thiol Oxidoreductase1, a disulfide bond-forming catalyst, is required for the assembly of photosystem II in *Arabidopsis*. *Plant Cell* 23:4462-75
50. Kashino Y, Lauber WM, Carroll JA, Wang Q, Whitmarsh J, et al. 2002. Proteomic analysis of a highly active photosystem II preparation from the cyanobacterium *Synechocystis* sp. PCC 6803 reveals the presence of novel polypeptides. *Biochemistry* 41:8004-12
51. Kelly AA, Dormann P. 2004. Green light for galactolipid trafficking. *Curr Opin Plant Biol* 7:262-9
52. Keren N, Kidd MJ, Penner-Hahn JE, Pakrasi HB. 2002. A light-dependent mechanism for massive accumulation of manganese in the photosynthetic bacterium *Synechocystis* sp. PCC 6803. *Biochemistry* 41:15085-92
53. Keren N, Liberton M, Pakrasi HB. 2005. Photochemical competence of assembled photosystem II core complex in cyanobacterial plasma membrane. *J Biol Chem* 280:6548-53
54. Keren N, Ohkawa H, Welsh EA, Liberton M, Pakrasi HB. 2005. Psb29, a conserved 22-kD protein, functions in the biogenesis of photosystem II complexes in *Synechocystis* and *Arabidopsis*. *Plant Cell* 17:2768-81
55. Kley J, Schmidt B, Boyanov B, Stolt-Bergner PC, Kirk R, et al. 2011. Structural adaptation of the plant protease Deg1 to repair photosystem II during light exposure. *Nat Struct Mol Biol* 18:728-31
56. Klinkert B, Ossenbühl F, Sikorski M, Berry S, Eichacker L, Nickelsen J. 2004. Prata, a periplasmic tetratricopeptide repeat protein involved in biogenesis of photosystem II in *Synechocystis* sp. PCC 6803. *J Biol Chem* 279:44639-44
57. Komenda J, Barker M, Kuvikova S, de Vries R, Mullineaux CW, et al. 2006. The FtsH protease slr0228 is important for quality control of photosystem II in the thylakoid membrane of *Synechocystis* sp. PCC 6803. *J Biol Chem* 281:1145-51
58. Komenda J, Knoppova J, Kopečná J, Sobotka R, Halada P, et al. 2012. The Psb27 assembly factor binds to the CP43 complex of photosystem II in the cyanobacterium *Synechocystis* sp. PCC 6803. *Plant Physiol* 158:476-86
59. Komenda J, Kuvikova S, Granvogl B, Eichacker LA, Diner BA, Nixon PJ. 2007. Cleavage after residue Ala352 in the C-terminal extension is an early step in the maturation of the D1 subunit of photosystem II in *Synechocystis* PCC 6803. *Biochim Biophys Acta* 1767:829-37
60. Komenda J, Nickelsen J, Tichy M, Prasil O, Eichacker LA, Nixon PJ. 2008. The cyanobacterial homologue of HCF136/YCF48 is a component of an early photosystem II assembly complex and is important for both the efficient assembly and repair of photosystem II in *Synechocystis* sp. PCC 6803. *J Biol Chem* 283:22390-9
61. Komenda J, Reisinger V, Müller BC, Dobáková M, Granvogl B, Eichacker LA. 2004. Accumulation of the D2 protein is a key regulatory step for assembly of the photosystem II reaction center complex in *Synechocystis* PCC 6803. *J Biol Chem* 279:48620-9

62. Komenda J, Sobotka R, Nixon PJ. 2012. Assembling and maintaining the photosystem II complex in chloroplasts and cyanobacteria. *Curr Opin Plant Biol* 15:245-51
63. Kouril R, Dekker JP, Boekema EJ. 2012. Supramolecular organization of photosystem II in green plants. *Biochim Biophys Acta* 1817:2-12
64. Kroll D, Meierhoff K, Bechtold N, Kinoshita M, Westphal S, et al. 2001. VIPP1, a nuclear gene of *Arabidopsis thaliana* essential for thylakoid membrane formation. *Proc Natl Acad Sci USA* 98:4238-42
65. Kufryk GI, Vermaas WF. 2001. A novel protein involved in the functional assembly of the oxygen-evolving complex of photosystem II in *Synechocystis* sp. PCC 6803. *Biochemistry* 40:9247-55
66. Kufryk GI, Vermaas WF. 2003. Slr2013 is a novel protein regulating functional assembly of photosystem II in *Synechocystis* sp. strain PCC 6803. *J Bacteriol* 185:6615-23
67. Kunkel DD. 1982. Thylakoid centers: structures associated with the cyanobacterial photosynthetic membrane system. *Arch Microbiol* 133:97-9
68. Kuvikova S, Tichy M, Komenda J. 2005. A role of the C-terminal extension of the photosystem II D1 protein in sensitivity of the cyanobacterium *Synechocystis* PCC 6803 to photoinhibition. *Photochem Photobiol Sci* 4:1044-8
69. Liberton M, Howard Berg R, Heuser J, Roth R, Pakrasi HB. 2006. Ultrastructure of the membrane systems in the unicellular cyanobacterium *Synechocystis* sp. strain PCC 6803. *Protoplasma* 227:129-38
70. Lima A, Lima S, Wong JH, Phillips RS, Buchanan BB, Luan S. 2006. A redox-active FKBP-type immunophilin functions in accumulation of the photosystem II supercomplex in *Arabidopsis thaliana*. *Proc Natl Acad Sci USA* 103:12631-6
71. Liu H, Huang RY, Chen J, Gross ML, Pakrasi HB. 2011. Psb27, a transiently associated protein, binds to the chlorophyll binding protein CP43 in photosystem II assembly intermediates. *Proc Natl Acad Sci USA* 108:18536-41
72. Liu H, Roose JL, Cameron JC, Pakrasi HB. 2011. A genetically tagged Psb27 protein allows purification of two consecutive photosystem II (PSII) assembly intermediates in *Synechocystis* 6803, a cyanobacterium. *J Biol Chem* 286:24865-71
73. Lu Y, Hall DA, Last RL. 2011. A small zinc finger thylakoid protein plays a role in maintenance of photosystem II in *Arabidopsis thaliana*. *Plant Cell* 23:1861-75
74. Ma J, Peng L, Guo J, Lu Q, Lu C, Zhang L. 2007. LPA2 is required for efficient assembly of photosystem II in *Arabidopsis thaliana*. *Plant Cell* 19:1980-93
75. Mabbitt PD, Rautureau GJ, Day CL, Wilbanks SM, Eaton-Rye JJ, Hinds MG. 2009. Solution structure of Psb27 from cyanobacterial photosystem II. *Biochemistry* 48:8771-3
76. Malnoe P, Mayfield SP, Rochaix JD. 1988. Comparative analysis of the biogenesis of photosystem II in the wild-type and y-1 mutant of *Chlamydomonas reinhardtii*. *J Cell Biol* 106:609-16
77. McKay RML, Gibbs SP. 1991. Composition and function of pyrenoids: cytochemical and immunocytochemical approaches. *Can J Bot* 69:1040-52
78. Meurer J, Plücker H, Kowallik KV, Westhoff P. 1998. A nuclear-encoded protein of prokaryotic origin is essential for the stability of photosystem II in *Arabidopsis thaliana*. *EMBO J* 17:5286-97
79. Michoux F, Takasaka K, Boehm M, Komenda J, Nixon PJ, Murray JW. 2012. Crystal structure of the Psb27 assembly factor at 1.6 Å: implications for binding to photosystem II. *Photosynth Res* 110:169-75
80. Mimuro M, Tomo T, Tsuchiya T. 2008. Two unique cyanobacteria lead to a traceable approach of the first appearance of oxygenic photosynthesis. *Photosynth Res* 97:167-76
81. Minai L, Wostrikoff K, Wollman FA, Choquet Y. 2006. Chloroplast biogenesis of photosystem II cores involves a series of assembly-controlled steps that regulate translation. *Plant Cell* 18:159-75
82. Moore M, Harrison MS, Peterson EC, Henry R. 2000. Chloroplast Oxa1p homolog Albino3 is required for post-translational integration of the light harvesting chlorophyll-binding protein into thylakoid membranes. *J Biol Chem* 275:1529-32
83. Mühlthaler K, Frey-Wyssing A. 1959. Entwicklung und Struktur der Proplastiden. *J Biophys Biochem Cytol* 6:507-12.

84. Mullineaux CW. 2008. Factors controlling the mobility of photosynthetic proteins. *Photochem Photobiol* 84:1310-6
85. Mulo P, Sakurai I, Aro EM. 2012. Strategies for *psbA* gene expression in cyanobacteria, green algae and higher plants: from transcription to PSII repair. *Biochim Biophys Acta* 1817:247-57
86. Mulo P, Sirpiö S, Suorsa M, Aro EM. 2008. Auxiliary proteins involved in the assembly and sustenance of photosystem II. *Photosynth Res* 98:489-501
87. Nevo R, Charuvi D, Shimoni E, Schwarz R, Kaplan A, et al. 2007. Thylakoid membrane perforations and connectivity enable intracellular traffic in cyanobacteria. *EMBO J* 26:1467-73
88. Nevo R, Charuvi D, Tsabari O, Reich Z. 2012. Composition, architecture and dynamics of the photosynthetic apparatus in higher plants. *Plant J* 70:157-76
89. Nickelsen J, Rengstl B, Stengel A, Schottkowski M, Soll J, Ankele E. 2011. Biogenesis of the cyanobacterial thylakoid membrane system - an update. *FEMS Microbiol Lett* 315:1-5
90. Nilsson R, Brunner J, Hoffman NE, van Wijk KJ. 1999. Interactions of ribosome nascent chain complexes of the chloroplast-encoded D1 thylakoid membrane protein with cpSRP54. *EMBO J* 18:733-42
91. Nixon PJ, Michoux F, Yu J, Boehm M, Komenda J. 2010. Recent advances in understanding the assembly and repair of photosystem II. *Ann Bot* 106:1-16
92. Nixon PJ, Trost JT, Diner BA. 1992. Role of the carboxy terminus of polypeptide D1 in the assembly of a functional water-oxidizing manganese cluster in photosystem II of the cyanobacterium *Synechocystis* sp. PCC 6803: assembly requires a free carboxyl group at C-terminal position 344. *Biochemistry* 31:10859-71
93. Nordhues A, Schöttler MA, Unger AK, Geimer S, Schönfelder S, et al. 2012. Evidence for a role of VIPP1 in the structural organization of the photosynthetic apparatus in *Chlamydomonas*. *Plant Cell* 24:637-59
94. Nowaczyk MM, Hebel R, Schlodder E, Meyer HE, Warscheid B, Rögner M. 2006. Psb27, a cyanobacterial lipoprotein, is involved in the repair cycle of photosystem II. *Plant Cell* 18:3121-31
95. Ossenbühl F, Göhre V, Meurer J, Krieger-Liszkay A, Rochaix JD, Eichacker LA. 2004. Efficient assembly of photosystem II in *Chlamydomonas reinhardtii* requires Alb3.1p, a homolog of *Arabidopsis* ALBINO3. *Plant Cell* 16:1790-800
96. Ossenbühl F, Inaba-Sulpice M, Meurer J, Soll J, Eichacker LA. 2006. The *Synechocystis* sp PCC 6803 Oxa1 homolog is essential for membrane integration of reaction center precursor protein pD1. *Plant Cell* 18:2236-46
97. Park S, Khamai P, Garcia-Cerdan JG, Melis A. 2007. REP27, a tetratricopeptide repeat nuclear-encoded and chloroplast-localized protein, functions in D1/32-kD reaction center protein turnover and photosystem II repair from photodamage. *Plant Physiol* 143:1547-60
98. Peng L, Ma J, Chi W, Guo J, Zhu S, et al. 2006. LOW PSII ACCUMULATION1 is involved in efficient assembly of photosystem II in *Arabidopsis thaliana*. *Plant Cell* 18:955-69
99. Peschek GA, Hinterstoisser B, Wastyn M, Kuntner O, Pineau B, et al. 1989. Chlorophyll precursors in the plasma membrane of a cyanobacterium, *Anacystis nidulans*. Characterization of protochlorophyllide and chlorophyllide by spectrophotometry, spectrofluorimetry, solvent partition, and high performance liquid chromatography. *J Biol Chem* 264:11827-32
100. Pisareva T, Kwon J, Oh J, Kim S, Ge C, et al. 2011. Model for membrane organization and protein sorting in the cyanobacterium *Synechocystis* sp. PCC 6803 inferred from proteomics and multivariate sequence analyses. *J Proteome Res* 10:3617-31
101. Plücker H, Müller B, Grohmann D, Westhoff P, Eichacker LA. 2002. The HCF136 protein is essential for assembly of the photosystem II reaction center in *Arabidopsis thaliana*. *FEBS Lett* 532:85-90
102. Rengstl B, Knoppová J, Komenda J, Nickelsen J. 2012. Characterization of a *Synechocystis* double mutant lacking the photosystem II assembly factors YCF48 and SII0933. *Planta*
103. Rengstl B, Oster U, Stengel A, Nickelsen J. 2011. An intermediate membrane subfraction in cyanobacteria is involved in an assembly network for photosystem II biogenesis. *J Biol Chem* 286:21944-51

104. Rexroth S, Mullineaux CW, Ellinger D, Sendtko E, Rögner M, Koenig F. 2011. The plasma membrane of the cyanobacterium *Gloeobacter violaceus* contains segregated bioenergetic domains. *Plant Cell* 23:2379-90
105. Rippka R, Waterbury J, Cohenbazire G. 1974. A cyanobacterium which lacks thylakoids. *Arch Microbiol* 100:419-36
106. Rokka A, Suorsa M, Saleem A, Battchikova N, Aro EM. 2005. Synthesis and assembly of thylakoid protein complexes: multiple assembly steps of photosystem II. *Biochem J* 388:159-68
107. Roose JL, Pakrasi HB. 2004. Evidence that D1 processing is required for manganese binding and extrinsic protein assembly into photosystem II. *J Biol Chem* 279:45417-22
108. Roose JL, Pakrasi HB. 2008. The Psb27 protein facilitates manganese cluster assembly in photosystem II. *J Biol Chem* 283:4044-50
109. Sakamoto W. 2006. Protein degradation machineries in plastids. *Annu Rev Plant Biol* 57:599-621
110. Satoh K, Yamamoto Y. 2007. The carboxyl-terminal processing of precursor D1 protein of the photosystem II reaction center. *Photosynth Res* 94:203-15
111. Schneider D, Fuhrmann E, Scholz I, Hess WR, Graumann PL. 2007. Fluorescence staining of live cyanobacterial cells suggest non-stringent chromosome segregation and absence of a connection between cytoplasmic and thylakoid membranes. *BMC Cell Biol* 8:39
112. Schoefs B, Franck F. 2003. Protochlorophyllide reduction: mechanisms and evolutions. *Photochem Photobiol* 78:543-57
113. Schottkowski M, Gkalympoudis S, Tzekova N, Stelljes C, Schünemann D, et al. 2009. Interaction of the periplasmic PrtA factor and the PsbA (D1) protein during biogenesis of photosystem II in *Synechocystis* sp. PCC 6803. *J Biol Chem* 284:1813-9
114. Schottkowski M, Ratke J, Oster U, Nowaczyk M, Nickelsen J. 2009. Pitt, a novel tetratricopeptide repeat protein involved in light-dependent chlorophyll biosynthesis and thylakoid membrane biogenesis in *Synechocystis* sp. PCC 6803. *Mol Plant* 2:1289-97
115. Schöttler MA, Albus CA, Bock R. 2011. Photosystem I: its biogenesis and function in higher plants. *J Plant Physiol* 168:1452-61
116. Shi LX, Hall M, Funk C, Schroder WP. 2012. Photosystem II, a growing complex: updates on newly discovered components and low molecular mass proteins. *Biochim Biophys Acta* 1817:13-25
117. Shimoni E, Rav-Hon O, Ohad I, Brumfeld V, Reich Z. 2005. Three-dimensional organization of higher-plant chloroplast thylakoid membranes revealed by electron tomography. *Plant Cell* 17:2580-6
118. Sirpiö S, Allahverdiyeva Y, Suorsa M, Paakkarinen V, Vainonen J, et al. 2007. TLP18.3, a novel thylakoid lumen protein regulating photosystem II repair cycle. *Biochem J* 406:415-25
119. Sirpiö S, Khrouchtchova A, Allahverdiyeva Y, Hansson M, Fristedt R, et al. 2008. AtCYP38 ensures early biogenesis, correct assembly and sustenance of photosystem II. *Plant J* 55:639-51
120. Sozer O, Komenda J, Ughy B, Domonkos I, Laczko-Dobos H, et al. 2010. Involvement of carotenoids in the synthesis and assembly of protein subunits of photosynthetic reaction centers of *Synechocystis* sp. PCC 6803. *Plant Cell Physiol* 51:823-35
121. Srivastava R, Battchikova N, Norling B, Aro EM. 2006. Plasma membrane of *Synechocystis* PCC 6803: a heterogeneous distribution of membrane proteins. *Arch Microbiol* 185:238-43
122. Stengel A, Gügel IL, Hilger D, Rengstl B, Jung H, Nickelsen J. 2012. Initial steps of photosystem II de novo assembly and preloading with manganese take place in biogenesis centers in *Synechocystis*. *Plant Cell* 24:660-75
123. Storm P, Hernandez-Prieto MA, Eggink LL, Hooper JK, Funk C. 2008. The small CAB-like proteins of *Synechocystis* sp. PCC 6803 bind chlorophyll. In vitro pigment reconstitution studies on one-helix light-harvesting-like proteins. *Photosynth Res* 98:479-88
124. Sugimoto I, Takahashi Y. 2003. Evidence that the PsbK polypeptide is associated with the photosystem II core antenna complex CP43. *J Biol Chem* 278:45004-10
125. Sun X, Ouyang M, Guo J, Ma J, Lu C, et al. 2010. The thylakoid protease Deg1 is involved in photosystem-II assembly in *Arabidopsis thaliana*. *Plant J* 62:240-9

126. Takahashi S, Badger MR. 2011. Photoprotection in plants: a new light on photosystem II damage. *Trends Plant Sci* 16:53-60
127. Tikkanen M, Nurmi M, Kangasjarvi S, Aro EM. 2008. Core protein phosphorylation facilitates the repair of photodamaged photosystem II at high light. *Biochim Biophys Acta* 1777:1432-7
128. Umena Y, Kawakami K, Shen JR, Kamiya N. 2011. Crystal structure of oxygen-evolving photosystem II at a resolution of 1.9 Å. *Nature* 473:55-60
129. Uniacke J, Zerges W. 2007. Photosystem II assembly and repair are differentially localized in *Chlamydomonas*. *Plant Cell* 19:3640-54
130. Uniacke J, Zerges W. 2009. Chloroplast protein targeting involves localized translation in *Chlamydomonas*. *Proc Natl Acad Sci U S A* 106:1439-44
131. van de Meene A, Hohmann-Marriott M, Vermaas W, Roberson R. 2006. The three-dimensional structure of the cyanobacterium *Synechocystis* sp. PCC 6803. *Arch Microbiol* 184:259-70
132. Vass I, Cser K. 2009. Janus-faced charge recombinations in photosystem II photoinhibition. *Trends Plant Sci* 14:200-5
133. Vasudevan D, Fu A, Luan S, Swaminathan K. 2012. Crystal structure of *Arabidopsis* Cyclophilin38 reveals a previously uncharacterized immunophilin fold and a possible autoinhibitory mechanism. *Plant Cell*
134. Vavilin D, Yao D, Vermaas W. 2007. Small Cab-like proteins retard degradation of photosystem II-associated chlorophyll in *Synechocystis* sp. PCC 6803: kinetic analysis of pigment labeling with <sup>15</sup>N and <sup>13</sup>C. *J Biol Chem* 282:37660-8
135. Vothknecht UC, Otters S, Hennig R, Schneider D. 2012. Vipp1: a very important protein in plastids?! *J Exp Bot* 63:1699-712
136. Wang Q, Sullivan RW, Kight A, Henry RL, Huang J, et al. 2004. Deletion of the chloroplast-localized Thylakoid formation1 gene product in *Arabidopsis* leads to deficient thylakoid formation and variegated leaves. *Plant Physiol* 136:3594-604
137. Wegener KM, Bennewitz S, Oelmüller R, Pakrasi HB. 2011. The Psb32 protein aids in repairing photodamaged photosystem II in the cyanobacterium *Synechocystis* 6803. *Mol Plant* 4:1052-61
138. Wei L, Guo J, Ouyang M, Sun X, Ma J, et al. 2010. LPA19, a Psb27 homolog in *Arabidopsis thaliana*, facilitates D1 protein precursor processing during PSII biogenesis. *J Biol Chem* 285:21391-8
139. Westphal S, Heins L, Soll J, Vothknecht UC. 2001. Vipp1 deletion mutant of *Synechocystis*: a connection between bacterial phage shock and thylakoid biogenesis? *Proc Natl Acad Sci USA* 98:4243-8
140. Xu H, Vavilin D, Funk C, Vermaas W. 2004. Multiple deletions of small Cab-like proteins in the cyanobacterium *Synechocystis* sp. PCC 6803: consequences for pigment biosynthesis and accumulation. *J Biol Chem* 279:27971-9
141. Yamamoto T, Burke J, Autz G, Jagendorf AT. 1981. Bound ribosomes of pea chloroplast thylakoid membranes: Location and release in vitro by high salt, puromycin, and RNase. *Plant Physiol* 67:940-9
142. Yang Y, Ramelot TA, Cort JR, Wang D, Ciccosanti C, et al. 2011. Solution NMR structure of photosystem II reaction center protein Psb28 from *Synechocystis* sp. Strain PCC 6803. *Proteins* 79:340-4
143. Yao DC, Brune DC, Vavilin D, Vermaas WF. 2012. Photosystem II component lifetimes in the cyanobacterium *Synechocystis* sp. strain PCC 6803: small Cab-like proteins stabilize biosynthesis intermediates and affect early steps in chlorophyll synthesis. *J Biol Chem* 287:682-92
144. Yoshioka M, Nakayama Y, Yoshida M, Ohashi K, Morita N, et al. 2010. Quality control of photosystem II: FtsH hexamers are localized near photosystem II at grana for the swift repair of damage. *J Biol Chem* 285:41972-81
145. Zak E, Norling B, Maitra R, Huang F, Andersson B, Pakrasi HB. 2001. The initial steps of biogenesis of cyanobacterial photosystems occur in plasma membranes. *Proc Natl Acad Sci USA* 98:13443-8
146. Zerges W. 2000. Translation in chloroplasts. *Biochimie* 82:583-601

147. Zhang D, Zhou G, Liu B, Kong Y, Chen N, et al. 2011. *HCF243* encodes a chloroplast-localized protein involved in the D1 protein stability of the *Arabidopsis* photosystem II complex. *Plant Physiol* 157:608-19
148. Zhang L, Paakkarinen V, Suorsa M, Aro EM. 2001. A SecY homologue is involved in chloroplast-encoded D1 protein biogenesis. *J Biol Chem* 276:37809-14
149. Zhang L, Paakkarinen V, van Wijk KJ, Aro EM. 1999. Co-translational assembly of the D1 protein into photosystem II. *J Biol Chem* 274:16062-7
150. Zhang S, Frankel LK, Bricker TM. 2010. The Sll0606 protein is required for photosystem II assembly/stability in the cyanobacterium *Synechocystis* sp. PCC 6803. *J Biol Chem* 285:32047-54

## Sidebars

### Endosymbiotic origin of chloroplasts (insert near “Introduction”)

The chloroplasts of eukaryotic cells developed from an ancient endosymbiont that was related to cyanobacteria and conferred upon plants the capacity for oxygenic photosynthesis (39). During the evolution of the organelle, large numbers of the original endosymbiont's genes have been transferred to the nucleus. The products of these genes are now synthesized in the cytosol and have to be re-imported into the organelle. Since the chloroplast itself has retained some genes, different subunits of organellar protein complexes are derived from different genetic systems. This also holds true for PSII, whose core subunits are synthesized in the chloroplast while some smaller subunits have to be imported from the cytosol. Therefore, an elaborate system of gene regulation has evolved to coordinate PSII subunit availability in eukaryotic organisms (9).

### D1 processing (insert near section “Principal steps in PSII protein subunit assembly”)

In almost all known cases, the D1 protein is synthesized in a precursor form (pD1) with a C-terminal extension. The length and sequence of this extension varies among different organisms (46). For instance, in *Synechocystis* 6803 it consists of 16 amino acids, whereas in plants it comprises nine residues (110). During the “early” PSII assembly phase, this C-terminal extension is removed by the specific endoprotease CtpA (carboxyl-terminal processing protease; 6). Whereas in plants the extension is excised in a single proteolytic step, cleavage in *Synechocystis* 6803 was shown to occur in a two-step manner, giving rise to an intermediate form of D1 (iD1) mainly detectable at the level of RC complexes (59). Maturation of D1 is a prerequisite for proper assembly of the  $Mn_4CaO_5$  cluster and binding of the extrinsic PSII proteins (107). The C-terminal extension is not required for proper assembly of PSII *per se* (92; 110), but *Synechocystis* mutants lacking the C-terminal D1 extension exhibit decreased fitness and are more susceptible to photodamage (46; 68).

TPR proteins (insert near section “a) Factors involved in RC complex formation – the early phase”)

TPR (tetratricopeptide repeat) proteins belong to the superfamily of helical repeat proteins and are characterized by the presence of multiple repeats of a 34-amino acid unit containing a degenerate common motif. The TPR domain folds into a superhelical structure which serves as a platform for protein-protein interactions (23). Therefore, TPR proteins seem likely to form molecular scaffolds for assembly processes (23). Evidence for the importance of TPR proteins during assembly of the photosynthetic complexes comes from the identification of two photosystem I assembly factors (Ycf3 and Ycf37/Pyg7) and the PSII assembly factors PrtA and Pitt (56; 114; 115).

Protochlorophyllide oxidoreductase (insert near section “Integration of cofactors”)

Two different enzymes exist that can mediate the conversion of protochlorophyllide *a* into chlorophyllide *a*, the immediate precursor of chlorophyll *a*. One is a light-independent form of the protochlorophyllide oxidoreductase (LiPOR) whose subunits are evolutionarily related to the eubacterial nitrogenase enzyme complex, and which catalyzes chlorophyll synthesis even in the dark (8). The other is a structurally unrelated light-dependent form (POR). Whereas LiPOR is absent in angiosperms, POR is found in all organisms capable of oxygenic photosynthesis (112). Since cyanobacteria, algae and gymnosperms contain both enzyme forms, they can use both pathways for chlorophyllide *a* synthesis, depending on the light conditions (8).

Thylakoid center (insert near section “Localization of PSII assembly in cyanobacteria – *Synechocystis* 6803”)

Initially, cyanobacterial thylakoid centers were characterized as cylindrical structures with a 14-fold symmetry, located at the cell periphery and attached to TMs (67). This idea was revisited by van de Meene et al., who showed that thylakoid centers represent rod-like structures approximately 1  $\mu\text{m}$  in length whose ends are connected to the PM in *Synechocystis* 6803 (131). Based on structural similarities, it has recently been speculated that these thylakoid centers might be formed by assemblies of the VIPP1 protein; however, this idea still awaits experimental validation (93).

VIPP1 (insert near box “Thylakoid center”)

The VIPP1 protein was originally postulated to be involved in TM maintenance, probably by mediating vesicle formation (64; 139). However, later experiments indicate that VIPP1 acts

not in membrane biogenesis directly, but participates in assembly of the protein complexes, probably by facilitating lipid insertion into photosynthetic complexes (35; 93). Interestingly, VIPP1 can form large homo-oligomeric rings with molecular masses of > 1 MD (135), and in *C. reinhardtii* chloroplasts, some VIPP1 was detected in dot-like structures which sometimes extended into rods (93). Loss of VIPP1 resulted in formation of abnormal structures which were observed at regions from which TMs protruded. These structures were often, but not exclusively, found around the pyrenoid, i.e. the area comprising the T-zones (93). A VIPP1 homolog has been found in *Synechocystis*, but, intriguingly, not in the cyanobacterium *G. violaceus*, which lacks a TM system, indicating that the VIPP1 function may indeed be connected to TM formation (135).

CES principle (insert near section on PSII repair)

Unlike cyanobacteria, algal chloroplasts (and yeast mitochondria) utilize a regulatory mechanism which is referred to as CES (control by epistasy of synthesis). CES consists in the assembly-dependent regulation of the translation of subunits destined for protein complexes (20). In the case of PSII in *C. reinhardtii*, it has been demonstrated that the absence of its D2 subunit leads to reduced synthesis of D1 and CP47 via feedback control mechanisms that sense non-assembled D1 and CP47 subunits. Following the strict hierarchy of PSII assembly outlined in Figure 2, this allows the adjustment of subunit synthesis to the amount of assembly-competent precomplexes available, which is in principle defined by the actual level of D2 (81). As a consequence, D2 synthesis serves as a pacemaker for the synthesis of the entire PSII. It is not clear whether CES operates in plant chloroplasts.

## **Definitions**

Immunophilins mediate immune suppression and include cyclophilins (CYPs) and FK509-binding proteins (FKBPs)

**Table 1** Summary and occurrence of described PSII assembly factors. Factors involved in *de novo* assembly are highlighted in green, repair specific factors in orange and factors which were shown to be involved in both processes in yellow.

Assembly factor	<i>G. violaceus</i> PCC7421	<i>Synechocystis</i> <sup>a</sup>	<i>C. reinhardtii</i> <sup>a</sup>	<i>A. thaliana</i> <sup>a</sup>	Size (kDa) <sup>b</sup>	Localization <sup>f</sup>	Proposed functions in PSII assembly	References
Alb3/Alb3.1, Alb3.2/Slr1471	<i>glr2231</i>	<i>slr1471</i> m	<i>Cre06.g251900</i> m <i>Cre17.g729800</i> m	<i>At2g28800</i>	40-45	in; PDM; TM	integration, folding and/or assembly of pD1; integration of LHCII	(11; 37; 82; 95; 96)
CtpA	<i>gll0067</i>	<i>slr0008</i> m	<i>Cre10.g420550</i>	<i>At4g17740</i>	39-47	ex; PM	C-terminal processing of pD1	(6; 145)
CYP38	<i>gll3308</i>	<i>sll0408</i>	<i>Cre03.g3930</i>	<i>At3g01480</i> m	38-40	ex; L	assembly of PSII [1]	(34; 86; 119; 133)
Deg1	<i>gll2097</i>	<i>sll1679</i>	<i>Cre12.g498500</i>	<i>At3g27925</i> m	35	ex; L; TM	assembly of PSII [2] and supercomplexes	(48; 125)
FKBP20-2	<i>glr0841</i>	<i>slr1761</i>	<i>Cre13.g14198</i>	<i>At3g60370</i> m	17	ex; L	assembly of PSII supercomplexes	(70)
HCF136/YCF48	<i>glr0855</i>	<i>slr2034</i> m	<i>Cre06.g273700</i>	<i>At5g23120</i> m	37	ex; L; PDM; TM	stabilization of D1; assembly of RC complexes	(60; 78; 101)
HCF243	-	-	-	<i>At3g15095</i> m	76	in	stabilization of D1; assembly of RC complexes	(147)
LPA1/REP27	<i>glr1902*</i>	<i>slr2048*</i>	<i>Cre10.g430150</i> m	<i>At1g02910</i> m	46-47	in	integration of D1	(27; 97; 98)
LPA2	-	-	-	<i>At5g51545</i> m	~20	in	integration of CP43	(74)
LPA3	-	-	<i>Cre03.g184550</i>	<i>At1g73060</i> m	40 <sup>c</sup>	ex; S; TM	integration of CP43	(17)
LQY1	-	-	-	<i>At1g75690</i> m	12	in; TM	PSII repair	(73)
LTO1	<i>glr2112</i>	<i>slr0565</i>	<i>Cre12.g493150</i>	<i>At4g35760</i> m	40	in	disulfide bond formation in PsbO	(49)
PAM68/Sll0933	<i>glr1740</i>	<i>sll0933</i> m	<i>Cre07.g329000</i>	<i>At4g19100</i> m	18-20	in; TM	conversion of RC to PSII [1]	(7; 102)
Pitt	<i>glr4262</i>	<i>slr1644</i> m	<i>Cre12.g13816</i>	<i>At4g39470</i> <i>At1g78915</i>	32	in; PDM; TM	stabilization and localization of POR	(114)
PPL1	-	-	-	<i>At3g55330</i> m	18	ex; L	PSII repair	(45)
PratA	<i>glr1902</i>	<i>slr2048</i> m	<i>Cre10.g430150*</i>	<i>At1g02910*</i>	36	ex; PP; PDM	Mn <sup>2+</sup> transport to D1; spatial organization of early steps of PSII assembly	(56; 113; 122)
Psb27/LPA19	-	<i>slr1645</i> m	<i>Cre05.g243800</i> <i>Cre02.g073850</i>	<i>At1g03600</i> m <i>At1g05385</i> m	12-15	ex; L; TM	assembly of CP43 and luminal side of PSII; PSII repair	(19; 71; 94; 108; 116; 138)

Psb28	<i>gsl0928</i>	<i>sll1398</i> m	<i>Cre10.g440450</i>	<i>At4g28660</i>	13-15	ex; C; TM	biogenesis of chlorophyll binding proteins	(28; 116)
Psb29/Thf1	<i>glr1400</i>	<i>sll1414</i> m	<i>Cre13.g562850</i>	<i>At2g20890</i> m	27	ex; S and in; OM, TM	PSII repair; assembly of PSII supercomplexes	(50; 54; 116; 136)
SCPs/LHC-like	+ <sup>d</sup>	+ <sup>d</sup>	+ <sup>d</sup>	+ <sup>d</sup>	varying <sup>d</sup>	in, TM	pigment binding; PSII repair	(33; 123; 134; 140)
Sll0606	<i>glr2353</i>	<i>sll0606</i> m	<i>Cre01.g003300</i>	-	51 <sup>e</sup>	ex or in; PM; PP	assembly of CP43; carotenoid transport	(150)
Sll1694	<i>gll2255</i>	<i>sll1694</i> m	-	-	20	in	delivery of chlorophyll	(41)
Slr0286	-	<i>slr0286</i> m	-	-	50 <sup>c</sup>	in	folding of D2	(65)
Slr1768	<i>gll1845</i>	<i>slr1768</i> m	<i>Cre12.g519350</i>	<i>At5g51570</i>	33	in; PM	PSII repair	(16)
Slr2013	-	<i>slr2013</i> m	-	-	49	in	folding of D2	(66)
TLP18.3/Psb32	-	<i>sll1390</i> m	<i>Cre03.g3775</i>	<i>At1g54780</i> m	18-27	in; TM; PM	PSII repair: turnover of damaged D1; assembly of PSII [2]	(118; 137)

<sup>a</sup> m = mutant available

<sup>b</sup> predicted or verified size of proteins

<sup>c</sup> including predicted transit peptide

<sup>d</sup> no gene loci and sizes are indicated since SCPs/LHC-like proteins comprise several different members

<sup>e</sup> including sequence predicted as either transmembrane domain or *sec* transit peptide

<sup>f</sup> in = intrinsic; ex = extrinsic; PDM = PratA-defined membrane; TM = thylakoid membrane; PM = plasma membrane; OM = outer membrane;

E = envelope membranes; iE = inner envelope; PP = periplasm; L = lumen; C = cytoplasm

\* LPA1/REP27 and PratA are regarded as functional homologs despite their sequences being not closely related

## Figure legends

### Figure 1

(A) Subunit composition of PSII in cyanobacteria (*left*) and chloroplasts (*right*). The D1-D2 heterodimer forms the reaction center, which is surrounded by cyt  $b_{559}$  (PsbE, PsbF), PsbI, and the inner antenna proteins CP47 and CP43. On the luminal side, the  $Mn_4CaO_5$  cluster (colored circles) is shielded by the extrinsic proteins of PSII (pink). In cyanobacteria, these include the O, U, V, P and Q subunits, whereas higher plants only have O, P and Q. The set of additional low molecular mass (LMM) subunits (grey) is only partially conserved between cyanobacteria and chloroplasts. Cyanobacteria possess a peripheral antenna system made of phycobilisomes (blue) which are attached to the cytoplasmic side of PSII; in chloroplasts, integral membrane complexes (LHCII) fulfill this role. Chlorophyll-binding proteins are depicted in green. PSII subunits are indicated by the capital letter of their genetic nomenclature, but its chlorophyll-binding subunits are designated by their common names D1, D2, CP47 and CP43, respectively. Subunits encoded by nuclear genes are indicated by blue lettering. TM, thylakoid membrane. (B) Two different pathways exist for integration of D1 into PSII: the *de novo* assembly of all subunits and cofactors (black arrow) during TM biogenesis and the replacement of photodamaged D1 (orange arrow) by a newly synthesized copy, followed by partial reassembly of PSII.

### Figure 2

*De novo* assembly of PSII in cyanobacteria (A) and chloroplasts (B). Biogenesis of PSII occurs in a stepwise manner via a sequential series of intermediates. In addition, a number of transiently interacting factors (ovals) is required to mediate distinct steps in assembly (compare Table 1). Homologous proteins in cyanobacteria and chloroplasts are identically colored (Figure 1A). Only those LMM subunits are depicted for which data on their integration into PSII is available. Dotted arrows mark established interactions suggestive of an assembly network. D1 processing takes place at the level of RC complex formation. The bar indicates the definition of “early”, “later” and “final” phases of the assembly process. For detailed explanation of the order of events see text.

pD1, precursor form of D1; RC, reaction center complex lacking CP47 and CP43; RC47, reaction center complex lacking CP43; PSII-Psb27/LPA19, monomeric PSII complex characterized by the presence of Psb27 and LPA19, respectively, but lacking the extrinsic proteins; PSII [1], monomeric PSII complex; PSII [2], dimeric PSII complex.

### Figure 3

Subcellular organization of PSII assembly in *G. violaceus* (A); *Synechocystis* 6803 (B, F); *C. reinhardtii* chloroplast (C); plant proplastid (D) and plant chloroplast (E). Thylakoid membranes or – in the case of *G. violaceus* – photosynthetically active patches in the plasma membrane – are colored in green. Regions of initial PSII assembly are highlighted in red and represent biogenesis centers (B), T-zones (C), membrane invaginations (D) and stromal thylakoid membranes (E), respectively. In (F) a more detailed schematic model for the spatial organization of TM biogenesis in *Synechocystis* 6803 is shown.  $Mn^{2+}$  (Mn) is taken up into the periplasmic space and stored at the outer membrane (OM). Further transport to PSII is facilitated by the periplasmic PrtA complex, resulting in pre-loading of D1 with  $Mn^{2+}$  at biogenesis centers. The membrane-bound form of PrtA, as well as the pD1 protein, mark the PDMs that harbor these biogenesis centers (red), which are located at TM convergence sites close to the PM. They consist of a thylakoid center (TC) surrounded by a semicircular structure (SS), but their precise architecture remains to be resolved (as indicated by broken lines). Growing PSII complexes are progressively transferred to the thylakoid membrane system (see Figure 2). At the interconnection site, chlorophyll synthesis (green pentagon) and probably its integration into apoproteins occur. The known localization of PSII assembly factors based on membrane fractionation experiments has been integrated into the scheme (103). T, T-zone; P, pyrenoid; for further abbreviations see Figure 2 and text.

### Figure 4

Localization of PSII *de novo* assembly and PSII repair. *De novo* assembly of PSII (black arrows) starts in specialized membrane regions (red) represented by biogenesis centers in *Synechocystis* or T-zones in *C. reinhardtii*. Developing RC47 complexes are transferred to the thylakoids (green), where their assembly is completed. After photodamage to D1 (orange D1), it is exchanged for a newly synthesized copy in the course of the PSII repair cycle (orange arrows). Therefore, inactive PSII complexes (PSII\*) must be partially disassembled to allow for the degradation of damaged D1 and its replacement by a *de novo* synthesized copy at the level of RC47\* complexes. Subsequently, the CP43 complex is reattached to restore functional PSII. The whole PSII repair cycle, including D1 insertion, is suggested to be restricted to TMs. For simplicity, only PSII subunits of the cyanobacterial system are shown. RC, PSII reaction center complex lacking CP47 and CP43; RC47, PSII reaction center complex lacking CP43; RC47\*, RC47 complex containing damaged D1. For clarity, PSII

---

complexes are shown as monomers and not as supercomplexes. For abbreviations see Figure 2.

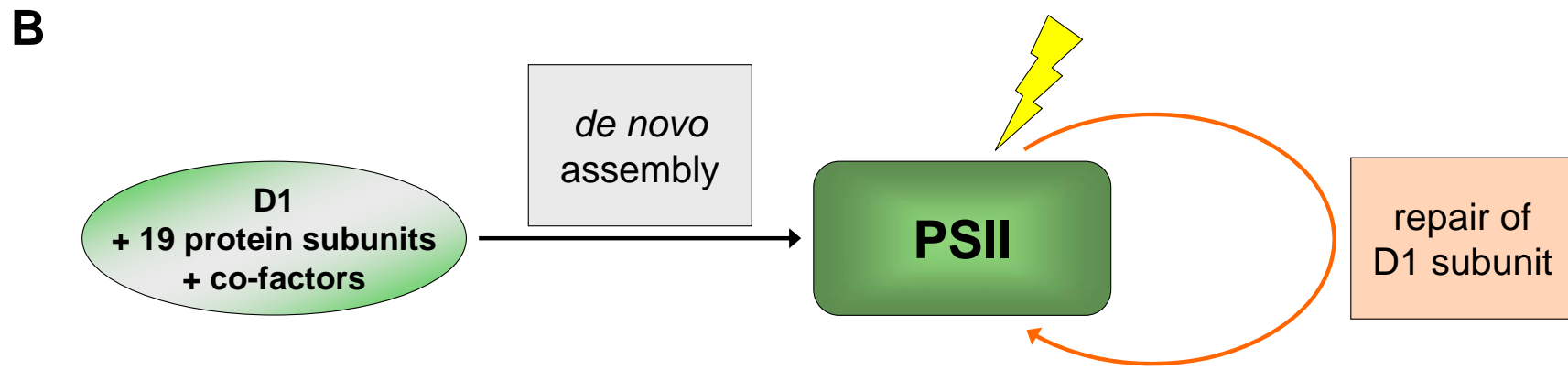
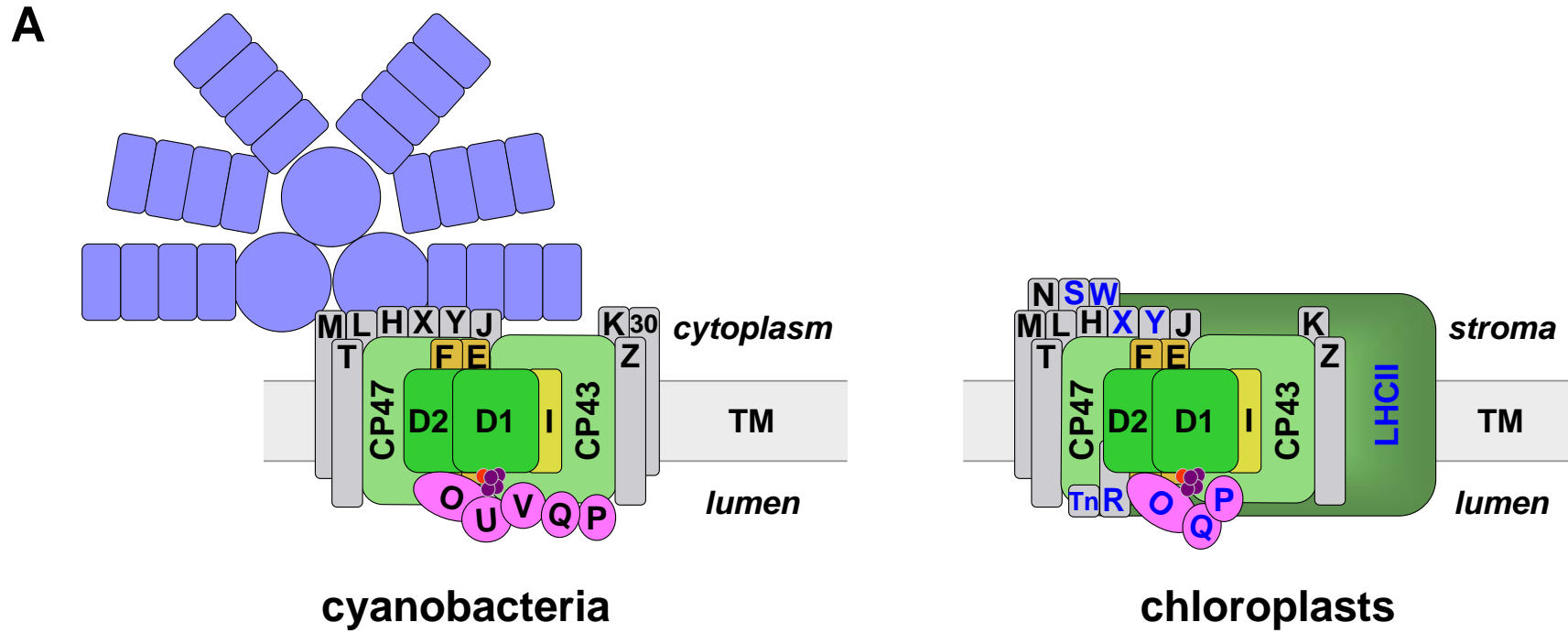


**Figure 1**







**LIST OF ABBREVIATIONS**

2D-PAGE	two dimensional polyacrylamide gel electrophoresis
ATP	adenosine triphosphate
BN	blue native
CN	colorless native
CP43	PSII inner antenna protein CP43
CP47	PSII inner antenna protein CP47
C-terminus	carboxyl terminus
CtpA	carboxyl-terminal processing protease
cyt b <sub>559</sub>	cytochrome b <sub>559</sub> ; subunits PsbE and PsbF of PSII
cyt b <sub>6f</sub>	cytochrome b <sub>6f</sub> complex
D1	PSII reaction center protein D1; PsbA
D2	PSII reaction center protein D2; PsbD
GUN	genome uncoupled
HCF	high chlorophyll fluorescence
iD1	intermediate form of D1
kDa	kilodalton
LHC	light-harvesting complex
LiPOR	light-independent protochlorophyllide oxidoreductase
Mn	manganese
Mn <sub>4</sub> Ca cluster	water-splitting manganese cluster of PSII
NADP	nicotinamide adenine dinucleotide phosphate
OM	outer membrane
PCC	pasteur culture collection
pD1	precursor form of D1
PDM	PratA-defined membrane
Pitt	POR-interacting TPR protein
PM	plasma membrane
POR	light-dependent protochlorophyllide oxidoreductase
PP	periplasm
PratA	processing-associated TPR protein
PSI	photosystem I
PSII	photosystem II
PSII [1]	PSII monomer
PSII [2]	PSII dimer
Q <sub>B</sub>	plastoquinone B
RC	PSII reaction center complex lacking CP47 and CP43
RC47	PSII reaction center complex lacking CP43
TC	thylakoid center
TM	thylakoid membrane
TPR	tetratricopeptide repeat
T-zones	translation zones
VIPP	vesicle-inducing protein in plastids

**LIST OF PUBLICATIONS**

- Nickelsen, J., and **Rengstl, B.** (submitted) Photosystem II assembly: from cyanobacteria to plants. *Annu Rev Plant Biol.*
- Rengstl, B.**, Knoppová, J., Komenda, J., and Nickelsen, J. (2012). Characterization of a *Synechocystis* double mutant lacking the photosystem II assembly factors YCF48 and Sll0933. *Planta.*
- Rengstl, B.**, Stengel, A., Gügel, I., Schottkowski, M., and Nickelsen, J. (2012). Biogenesis of thylakoid membranes in *Synechocystis* sp. PCC 6803. *Endocytobiosis Cell Res* **23**, 86-90.
- Stengel, A., Gügel, I.L., Hilger, D., **Rengstl, B.**, Jung, H., and Nickelsen, J. (2012). Initial steps of photosystem II *de novo* assembly and preloading with manganese take place in biogenesis centers in *Synechocystis*. *Plant Cell* **24**, 660-675.
- Rengstl, B.**, Oster, U., Stengel, A., and Nickelsen, J. (2011). An intermediate membrane subfraction in cyanobacteria is involved in an assembly network for photosystem II biogenesis. *J Biol Chem* **286**, 21944-21951.
- Nickelsen, J., **Rengstl, B.**, Stengel, A., Schottkowski, M., Soll, J., and Ankele, E. (2011). Biogenesis of the cyanobacterial thylakoid membrane system – an update. *FEMS Microbiol Lett* **315**, 1-5.
- Armbruster, U., Zühlke, J., **Rengstl, B.**, Kreller, R., Makarenko, E., Rühle, T., Schünemann, D., Jahns, P., Weisshaar, B., Nickelsen, J., and Leister, D. (2010). The *Arabidopsis* thylakoid protein PAM68 is required for efficient D1 biogenesis and photosystem II assembly. *Plant Cell* **22**, 3439-3460.

## DANKSAGUNG

An erster Stelle möchte ich mich bei Prof. Dr. Jörg Nickelsen bedanken – für das interessante Forschungsthema mit faszinierenden, einzelligen, oxygen photosynthetischen Organismen, bei denen es sich nicht um *Chlamydomonas* handelt! Insbesondere möchte ich mich aber auch für sein Vertrauen und seine Geduld bedanken, vor allem in Situationen, in denen nicht immer alles einfach war.

Prof. Jürgen Soll und Prof. Kirsten Jung danke ich für ihre Unterstützung im Rahmen des LSM Thesis Advisory Committees.

Besonderer Dank gilt Josef Komenda für die herzliche Aufnahme in sein Büro und Labor sowie die fruchtbare Zusammenarbeit und Diskussion von Ergebnissen. In diesem Zusammenhang auch vielen Dank an seine Mitarbeiterinnen Vendula Krynická und Jana Knoppová für die schöne Zeit in Třeboň.

Ulrike Oster möchte ich für die Durchführung und Auswertung der HPLC-Experimente und Irene Gügel für die elektronenmikroskopischen Analysen danken.

Herzlichen Dank auch an die früheren und aktuellen Mitarbeiter der AG Nickelsen, insbesondere Karin Findeisen und Christian Schwarz, für ihre Hilfe im Labor. Außerdem vor allem Anna Stengel für das Korrekturlesen dieser Arbeit.

Danke auch an AG Koop für das häufige Ausleihen des Bead-Beaters und Christian Stelljes für seine stete Hilfsbereitschaft und gute Laune.

Besonders lieben Dank außerdem an Sophie, Daniela und Frank für Kaffeeklatsch, viele interessante Gespräche, schöne Abende und eure wertvolle Unterstützung. Durch euch hab ich die Zeit München lieben gelernt!

Mein allergrößter Dank gebührt meiner Mama, für ihren Uni-Geburtstagsfeier-Partyservice, den häufigen Taxidienst vom und zum Bahnhof, das Gießen meiner Blumen und Füttern meiner Schafe; ihre Zuverlässigkeit, ihr Verständnis, Vertrauen und stets offenes Ohr, ihre bewundernswerte, unendliche Geduld... Einfach für alles – und vor allem dafür, dass du immer für mich da bist, wenn man dich braucht!

**EIDESSTATTLICHE ERKLÄRUNG**

Ich versichere hiermit an Eides statt, dass die vorgelegte Dissertation von mir selbstständig und ohne unerlaubte Hilfe angefertigt wurde. Außerdem erkläre ich, dass die Dissertation nicht ganz oder in wesentlichen Teilen einer anderen Prüfungskommission vorgelegt worden ist und dass ich mich **nicht** anderweitig einer Doktorprüfung ohne Erfolg unterzogen habe.

München, den 13.12.2012

Birgit Rengstl